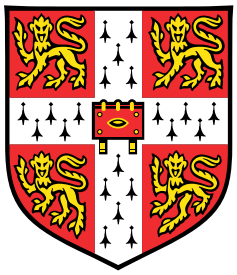

In-vitro Modelling of Stromal and Immune Cell Interactions Following Surgical Bone Marrow Stimulation

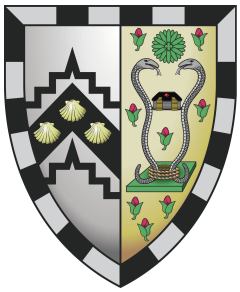

Sophie Louise Frankham-Wells

Prof. A.W. McCaskie
Dr. M.A. Birch

Division of Trauma and Orthopaedic Surgery, Department of Surgery
University of Cambridge

This dissertation is submitted for the degree of
Doctor of Philosophy

Gonville and Caius College

September 2018

Declaration

This thesis is the result of my own work and includes nothing which is the outcome of work done in collaboration except as declared in the Preface and specified in the text.

It is not substantially the same as any that I have submitted, or, is being concurrently submitted for a degree or diploma or other qualification at the University of Cambridge or any other University or similar institution except as declared in the Preface and specified in the text. I further state that no substantial part of my thesis has already been submitted, or, is being concurrently submitted for any such degree, diploma or other qualification at the University of Cambridge or any other University or similar institution except as declared in the Preface and specified in the text.

It does not exceed the prescribed word limit for the Graduate School of Life Sciences (60 000 words not including bibliography, figures, or appendices).

Collaborators:

- Karim Fekir designed, optimised, and assisted with the staining and running of the human Bone Marrow Stromal Cell characterisation flow cytometry panel
- Andrew Hotchen performed monocyte isolation from Leukocyte Reduction System cones under full supervision for two experiments
- Anna Albeiro provided protocols for the isolation, culture, and chondrogenic differentiation of human bone marrow stromal cells under normoxic conditions
- Anna Albeiro, Francesca Beaton, Sarah Lindsay, Andrew Hotchen, Virginia Piombo, and Karim Fekir assisted with medium and reagent preparation, and provided occasional support in maintaining human Bone Marrow Stromal Cell strains or experimental co-cultures during my absences from the laboratory
- Galuh Wenning (summer student) assisted in routine maintenance of human Bone Marrow Stromal Cell strains, performed isolation of Natural Killer cells, and set up experimental co-cultures of Natural Killer cells and human Bone Marrow Stromal Cells under full supervision during the period of the studentship (4 weeks)

Part of this work has been presented as follows:

- Poster and lightning talk: Arthritis Research UK Annual Meeting 2016

  Title: Short-term interactions between PBMC subpopulations and bone marrow stromal cells: a role in tissue repair?

  Authors: Sophie Frankham-Wells, Mark Birch, and Andrew McCaskie

- Poster: Cambridge Stem Cell Institute Meeting 2017

  Title: Functional Significance of Stem and Progenitor Cells in Osteochondral Repair

  Authors: Anna Albeiro[1], Francesca Beaton[1] , Sophie Frankham-Wells[1] , Mark Birch, and Andrew McCaskie

- Poster and lightning talk: Biology of Regenerative Medicine Conference 2017

  Title: Short-term interactions between a peripheral blood subpopulation and bone marrow stromal cells in hypoxia result in a pro-inflammatory environment

  Authors: Sophie Frankham-Wells, Mark Birch, and Andrew McCaskie

- Poster: European Orthopaedic Research Society Conference 2017

  Title: Drilling down: haematopoietic and stromal cell interactions influence microfracture repair

  Authors: Sophie Frankham-Wells, Mark Birch, and Andrew McCaskie

Sophie Louise Frankham-Wells
September 2018

[1] equal contributors

Abstract

In-vitro Modelling of Stromal and Immune Cell Interactions Following Surgical Bone Marrow Stimulation

Sophie Louise Frankham-Wells

Osteoarthritis (OA) results in degeneration of cartilage and bone within a joint, leading to pain and loss-of-function. While effective treatments exist for end-stage OA, earlier disease stages lack treatment options. Micro-fracture and micro-drilling, often termed bone marrow stimulation techniques, offer an early-stage repair and regenerative strategy. These techniques result in the formation of a haematoma containing Bone Marrow Stomal Cell (BMSC) and immune cells at the joint surface, leading to repair. However, the quality of repair after marrow stimulation is, at present, sub-optimal. BMSC are known to interact with immune subpopulations during repair, although the consequences of these interactions for repair outcomes are not fully understood. This thesis aims to further the current understanding of how interactions between immune subpopulations and BMSCs in the environment of a haematoma may influence repair outcomes following surgical bone marrow stimulation techniques.

In order to understand the influence of hypoxia on BMSC, strains of Human Bone Marrow Stromal Cells (hBMSCs) were isolated and cultured under normoxic (18.9 % oxygen) and hypoxic (3.0 % oxygen) conditions. Characterisation demonstrated that hypoxic culture had functional consequences on BMSC phenotype and behaviour. To explore the effect of BMSC-immune cell interactions on BMSC migration, immuno-regulation, and cell phenotypes, parallel experiments were performed under normoxic and hypoxic conditions. A unique approach was taken to identify an immune subpopulation resulting in BMSC migration, which was used as an indicator of potential co-localisation and interaction. BMSC were exposed to paired enriched and depleted populations of peripheral blood mononuclear cells, which had been sequentially fractionated using specific markers. The migration stimulated in the BMSC by the enriched and depleted fractions was compared. A Natural Killer (NK) cell population was found to have induced the greatest BMSC migration relative to its paired fraction. Co-cultures indicated that the influence of NK cells on BMSC, particularly NK cell-mediated cytotoxicity, were heavily dependent on culture conditions, including NK cell number and oxygen

levels. In a further study, co-cultures of BMSC and monocytes, which interact with BMSC and have a potential role in fibrosis, were co-cultured under normoxic and hypoxic conditions. A pro-angiogenic, immunomodulatory phenotype developed in normoxic co-cultures, which was significantly reduced in hypoxic co-cultures.

In conclusion, these data suggest that BMSC and immune subpopulations have diverse interactions which are strongly influenced by the local oxygen tension and cellular environment. These findings demonstrate the importance of the microenvironment formed by bone marrow stimulation techniques on cellular interactions, with potential consequences for the outcome of the repair. Furthermore, this work indicates that manipulation of the haematoma and surrounding environment following bone marrow stimulation could improve repair and regenerative outcomes.

For all those who asked me, 'when?',

I hope one day to answer, 'now'.

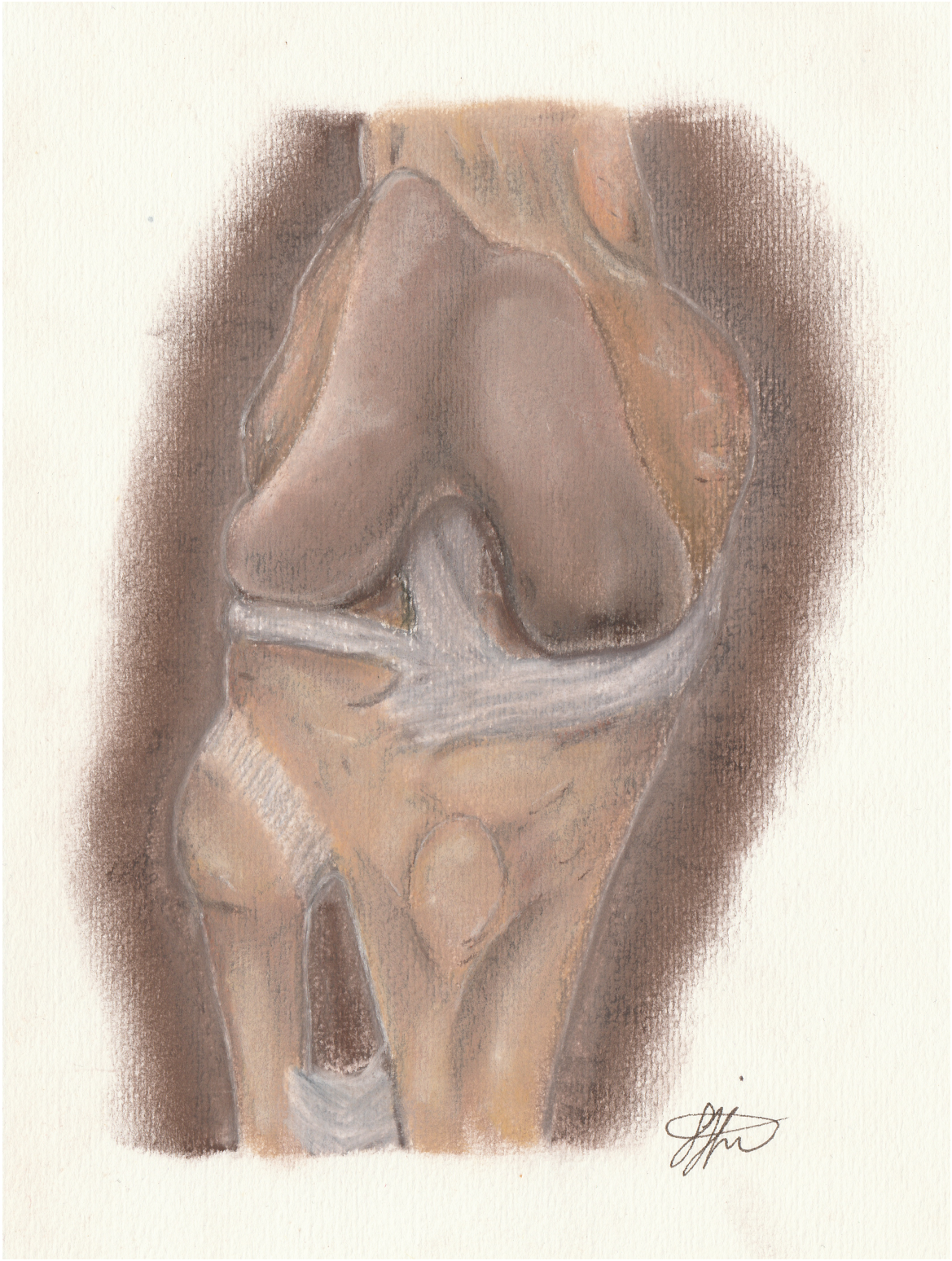

Acknowledgements

‘No man is an island, entire of itself; every man is a piece of the continent, a part of the main.’ John Donne (1572-1631)

This thesis was only possible through the combined efforts and contributions of many people. They have inspired and supported, challenged and encouraged me, for which I am very appreciative.

I would like to thank Professor Andrew McCaskie and Dr. Mark Birch, my supervisors at the University of Cambridge, and Arthritis Research UK for providing the opportunity and the funding for me to do this PhD.

I would like to extend particular thanks to Dr. Nigel Loverage and Dr. Roger Brookes for their constant encouragement, advice, and challenging questioning. Many thanks also to Dr. Frances Henson and Dr. John Wardale for discussions and suggestions which led to new directions in my work. In addition, I am grateful to Christine Coulson and the administrative staff in the Department of Surgery, especially Alison Warrington, Linda Butler, Alison Sawalhi, and Lila Tran for their guidance and support.

This work was made possible by tissue donations from the patients of the Addenbrooke’s Hospital Orthopaedic Unit, and the blood donors at the NIH Blood and Transplant Centre, as well as the work of the medical and administrative staff in both centres. Thank you to Mr Stephen McDonnell and Mr Wasim Khan for their work in the surgical teams, as well as constructive discussions regarding my work.

This research was supported by the Cambridge NIHR BRC Cell Phenotyping Hub. I am thankful for the advice, training and support provided by Esther Perez, Valeria Radjabova, Simon McCallum, and Professor Anna Petrunika-Harrison during my time using the hub facility.

I’d like to express my appreciation to everyone in the Level 4 team, both past and present, for your encouragement and camaraderie. I have been privileged to have worked with you all, and I wish all of you the very best in the future. In particular, I’d like to thank Francesca Beaton, for company on the long days and friendship throughout. Sarah Lindsay provided dreadful jokes, and fantastic

writing advice, while Andrew Hotchen has been a great person to call on for de-stressing sessions, and ludicrous amounts of coffee and sugary treats.

I am very grateful to my family and friends for all their help and support before, during, and after my PhD. A huge thank you to my parents, for incredible editing skills and in-depth discussions, my sister Helena for much-needed R and R, my brother Justin, for introducing me to Imhotep, and to all for their enthusiasm and interest in my work. I am very grateful to Demi and Frankie for providing creative outlets and listening to my science ramblings, and all my lovely friends for keeping my morale up.

Finally, I would like to give my most heartfelt thanks to my husband Ian, who has been a constant, unwavering source of encouragement throughout my research. His support has enabled me to pursue my research and make this thesis a reality. I am indebted to him for all the time and energy he has put into helping me throughout the past four years.

Lay Summary

Osteoarthritis is an extremely common joint condition, affecting many people around the world. During osteoarthritis, the smooth cartilage covering the bone ends in the joint is damaged or lost, leading to stiffness and pain. Osteoarthritis can affect any moving joint, such as the knee, hip, wrist, and spine. Although many sufferers of osteoarthritis are elderly, it does not exclusively affect older people. The chances of developing osteoarthritis can be increased by injury, infection, obesity, smoking, and inherited disease. For example, cruciate ligament injuries, which are very common amongst football players, increase the odds of getting knee osteoarthritis. At the moment, the best treatment for knee osteoarthritis is a knee replacement. However, this is only done once the joint is completely worn-out, which means that people must live with increasingly painful, stiff knees for many years.

Some facts about osteoarthritis:

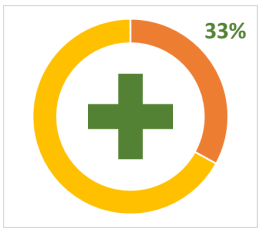

In the UK. 33 % of people over 45 have visited their GP about osteoarthritis

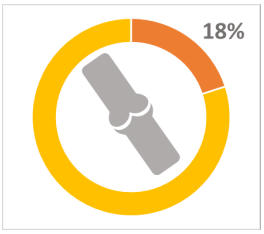

In the UK, 18 % of people over 45 have knee osteoarthritis

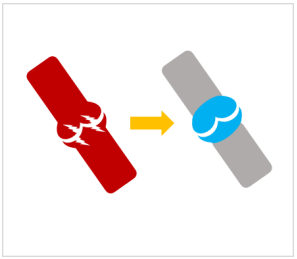

85 000 knee replacements are performed by the NHS every year

This body of work looks at a new group of treatments for knee osteoarthritis, sometimes called bone marrow stimulation techniques. These can be used in the early stages of osteoarthritis to halt the damage to the cartilage, therefore preventing the knee wearing out. There are multiple ways of stimulating the bone marrow to repair the cartilage. For example, during the bone marrow stimulation technique called micro-drilling, a surgeon drills tiny holes between the bone end (where the damaged cartilage is) and the bone marrow, while during micro-fracture an awl is used to create the holes. Bone marrow contains cells with regenerative potential, which means they can repair damage, while cartilage does not contain these cells, so it cannot heal itself. The drill holes allow the bone marrow

cells to reach the cartilage and help it to heal. However, instead of making smooth, strong cartilage, a scar forms, which is rough and weak and does not protect the knee joint. If we understand why the scar forms, we can improve these techniques to make healthy cartilage.

One suggestion as to why these techniques fail is that immune cells from the blood also reach the cartilage and interfere with the regenerative cells, perhaps by killing them or blocking their contributions so that instead of healing, a scar forms. During my research, I studied how different immune cells and the regenerative bone marrow cells interact in different conditions, and how this could influence the healing process. I did this by isolating the regenerative cells from bone marrow samples donated by patients having knee replacement surgery, and immune cells from the waste product produced during platelet donations. These cells were mixed together to form *in vitro* co-cultures, meaning that the cells were grown with each other in the lab and act as a model of what is happening in the body. By varying the conditions I grew the co-cultures in, I was able to study how these cells interact, and what the consequences of these interactions might be. One condition I was interested in was the level of oxygen present. Most experiments are done at atmospheric oxygen, the normal level in the air, or normoxia. However, after bone marrow stimulation techniques are performed, there is no blood supply to the treated area, meaning that there is very little oxygen present, which is called hypoxia. While other people have studied similar interactions before, the work has been done in normoxia. I believed that the low oxygen level, or hypoxia, would have an influence on how these cells interact.

What I found is that the interactions between regenerative bone marrow cells and immune cells are affected by oxygen level. I looked at two types of immune cells: Natural Killer Cells, and Monocytes. These cells are both attracted to wounds, such as bone marrow stimulation, where they have roles in repairing the damage. As the name suggests, Natural Killer Cells kill unhealthy cells, for example tumour cells or cells infected with bacteria. Monocytes have many roles, including phagocytosis where they engulf and digest debris, waste, and bacteria to clear up infections or wounds. In normal oxygen conditions, Natural Killer Cells attract the regenerative cells, which move towards them and are then killed by the Natural Killer Cells. However, under low oxygen conditions, the Natural Killer Cells are less good at attracting the regenerative cells, and are only able to kill them if they are given a signal. Like the Natural Killer Cells, the Monocytes attracted the regenerative bone marrow cells more strongly in normal rather than low oxygen conditions. Instead of then killing the regenerative cells, in normal oxygen levels the two different cell types worked together to increase the growth of blood vessels and reduce inflammation. By contrast, low oxygen levels prevented this.

This means that both the oxygen level and the type of immune cells present can influence the behaviour of the regenerative bone marrow cells, which might influence how well bone marrow stimulation works. Future studies could take this further and look at how this information could be applied to improve bone marrow stimulation techniques for treating osteoarthritis. Eventually, this could lead to improved techniques to treat OA.

Ethical Statement Regarding Use of Human Tissues

All experiments were carried out in strict accordance with local procedures and national ethical regulation.

Bone marrow

Human bone marrow was obtained from patients undergoing total knee replacement as treatment for osteoarthritis with full ethical consent in writing in accordance with the Human Tissue Act 2004 and approved by the local Research Ethics Committee (Cambridge Local Research Ethics Committee No. 06/Q0108/213).

Leukocyte Reduction System Cones

Leukocyte reduction system cones, from platelet donations by healthy donors, were supplied by NHS Blood and Transplant, Addenbrooke's Hospital, in accordance with the Human Tissue Act 2004 and subject to a Material Transfer Agreement and the aforementioned Ethics Committee.

Table of contents

List of figures

List of tables

Chapter 1

Introduction

Osteoarthritis (OA) is a chronic, degenerative condition affecting articulated joints that results in pain and loss of function. The Global Burden of Disease Study 2013 ranked OA 13th on a global scale of Years Lost to Disability (YLD), an increase of 3 places since 1990 with around 250 million or 3 % of the global population now affected (Vos et al. 2015). Furthermore, musculoskeletal conditions including OA were ranked fourth behind neoplasms, cardiovascular disease, and mental health disorders in global causes of mortality. Although OA itself is not directly fatal, the restricted mobility and motility resulting from pain and loss of joint function can contribute to other co-morbidities such as obesity, mental health issues, cardiovascular disease, or diabetes. While all forms of OA are showing increasing global prevalence, cases of knee OA in particular are increasing rapidly. In the United Kingdom, 8.75 million people have consulted a doctor regarding OA, and 18 % of over 45 year olds have been diagnosed with knee OA (ARUK 2013).

Therapies for early-stage OA and focal cartilage lesions, such as Autologous Cartilage Implantation (ACI) or scaffolds, provide a level of regeneration but do not currently represent a definitive, long-term solution. At present, the sole therapy offering a significant period of restored joint function and associated pain reduction is arthroplasty in the end-stage of OA. Therefore, effective, long-term interventions are required for early-stage OA where cartilage deterioration is focal and disability could therefore be minimised.

One such family of interventions are bone marrow stimulation techniques, which introduce bone marrow to the joint surface through abrasion, drilling, or fracturing of the subchondral bone. As a result, a bone marrow clot forms at the defect site. While cartilage has very weak regenerative potential, the bone marrow contains cells capable of regeneration with the potential to differentiate into chondrocytes, called Bone Marrow Stomal Cell (BMSC) (Jiang and Tuan 2015). The identity and role of these cells in repair and regeneration will be discussed later in section 1.5. By introducing the bone marrow to the joint surface in the form of a clot, the BMSC are able to regenerate the lost

cartilage and damaged subchondral bone, and restore functionality to the joint. Furthermore, the presence of the haematoma introduces nutrients, immune cells, and oxygen to the defect site enabling repair.

In practice, bone marrow stimulation techniques have potential to regenerate the osteochondral defects seen in OA, but require significant development. The ideal clinical outcome is regeneration of healthy hyaline cartilage with the requisite biomechanical properties, clearly defined tidemark (the interface between calcified and non-calcified cartilage), and correct extracellular matrix composition. However, studies have shown that while the defects treated with bone marrow stimulating techniques have some infill with hyaline cartilage, the majority of the repair tissue is fibrocartilage (Saw 2011, 2013; Saw et al. 2009). Although this does cover the exposed surface of the bone and restore a level of functionality, fibrocartilage is more prone to abrasion and therefore the repair lacks longevity. Studies have shown that alteration of the cellular environment within the clot formed following bone marrow stimulation resulted in improved clinical outcomes (Broyles 2017b; L. Gao et al. 2017; K. Lee et al. 2007; Murphy et al. 2018; Saw 2013). The interventions used included administration of autologous BMSC, Peripheral Blood Mononuclear Cell (PBMC), bone marrow aspirate, or immunomodulatory compounds such as Hyaluronic Acid (HA). These findings indicate the importance of both BMSC and immune populations during repair. In order to identify methods of improving bone marrow stimulation outcomes, it is important to understand which immune subpopulations present within the haematoma interact with BMSC, and how these interactions may influence the clinical outcome of the repair.

1.1 Osteoarthritis: past and present knowledge

OA is an ancient condition, dating back perhaps 125 million years, and has been described as 'impervious to evolution' (Massicotte 2011). The section below will present a brief history of some of the milestones in OA treatment and research, culminating in the Charnley Hip Replacement and the first successful total knee replacement in the 20th Century.

1.1.1 Osteoarthritis in prehistory

Researchers claim to have found evidence of OA in 30 % of *Caudipteryx* fossils, an oviraptor from the Aptian Age of the Early Cretaceous Period, dating from around 125 million years ago, and also in an *Iguanodon* ankle joint dating from 85 million years ago in the Late Cretaceous Period (Farlow and Brett-Surman 1999; Paul 2016; Rothschild et al. 2012). This last is compelling as osteophyte development is clear on the joint periphery. However, diagnosis of OA from fossilised remains is contentious, being based solely on presence of osteophytes, changes in bone density, and presence of

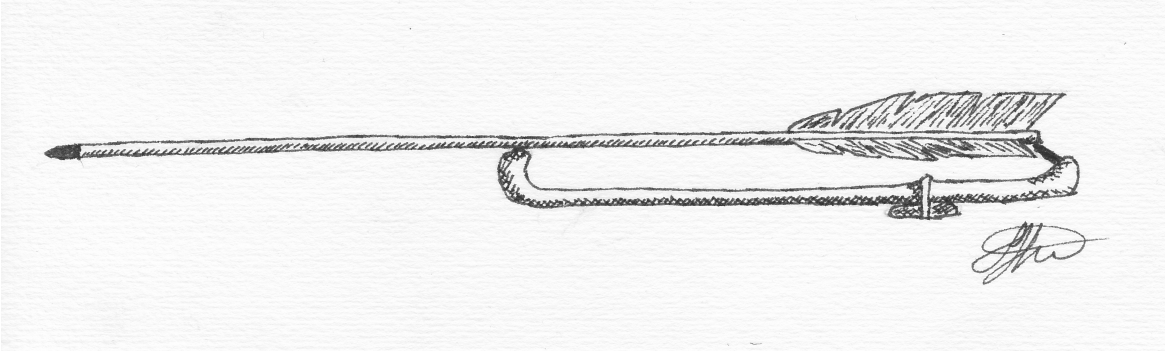

Fig. 1.1 Atlatl and spear

Sketch showing a modern atlatl and spear based on designs from Mesoamerican artefacts. The atlatl, which pre-dates the bow and arrow, acted as an extension of the arm, increasing the leverage and therefore the speed and power of the thrown spear. Original work based on drawing from life.

bone cysts due to the lack of soft tissue, and therefore risks some confusion with other degenerative joint conditions (Farlow and Brett-Surman 1999).

The earliest evidence of OA in hominid species comes from *Homo neanderthalis* remains dated to around 30 000 years ago, while that in modern humans (*Homo sapiens sapiens*) dates to 4500 B.C. in Native American remains found in modern-day Tennessee and Kansas (Bridges 1992). OA in humans appears to have been relatively common in the Neolithic period, affecting the elbows of adults males so often that the condition has been termed 'atlatl elbow' by one paleopathologist, a reference to the atlatl or spear-thrower, depicted in fig. 1.1, which was in widespread use among hunter-gatherer communities at the time and the extensive use of which has been postulated to cause OA (Bridges 1992).

Perhaps the most famous Neolithic sufferer of OA was Ötzi, the Iceman, who died around 3000 B.C. Osteoarthritic changes, namely subchondral sclerosis and joint space narrowing, can be seen in X-rays of his right hip joint (Kean et al. 2013). Due to the excellent preservation of Ötzi's soft tissue, diagnosis of OA can be made with confidence. Further examination of his body may indicate some of the earliest treatment methods for OA in Europe: medicinal tattooing. At the time of his death, Ötzi had 61 tattoos whose locations appear to correspond to regions of his body showing signs of damage or wear, including one tattoo on his right, lower lumbar region which may have corresponded to the perceived location of pain from his advanced hip OA (Samadelli et al. 2015).

References to joint pain and popular treatments thereof begin to appear in the literature in about 2500 B.C. around 500 years after the death of Ötzi. At this point, OA, Rheumatoid Arthritis (RA), septic arthritis, and gout were all treated and referred to as the same condition, termed arthritis deformans, a state of affairs which would continue until the 19th century. However, it is clear that joint pain was a common condition, particularly among the elderly. One of the Ptahhotep Maxims, attributed

to the Egyptian vizier Ptahhotep in 2400 B.C. , reads 'old age descendeth. . . The bones are painful throughout the body; good turneth into evil' indicating an awareness of increasing joint degeneration with age (Ptahhotep translated by (Kagemna and Ptahhotep 2009)). Indeed, mummified remains from Egypt show that OA was very common among the elite classes, particularly in the spine (Fritsch et al. 2015).

The earliest written record of proposed therapy for joint pain appears to be the 'Nei Ching', or 'The Yellow Emperor's Classic of Internal Medicine', rumoured to date to 2500 B.C. , suggesting a combination of acupuncture, and tea made from poplar and willow bark, which was also prescribed for joint pain in a Sumerian tablet dating from 2000 B.C. (Ni 1995). The famous Egyptian medical scroll, the Papyrus Ebers, attributed to the scribe Imhotep in 1550 B.C. , suggested application of a topical ointment made from fat, honey, herbs, and bone marrow to ease painful joints (Halioua and Ziskind 2005). Joint pain and OA appear to have been relatively neglected by the Greek physicians; Hippocrates makes very little mention of either in his Aphorisms dating to 400 B.C. , with only two alluding to the subject. These are the 31st Aphorism of Section III listing the diseases of the elderly, which include vertigo, cataracts, and pains in the joints, and the 25th Aphorism of Section V, where the application of cold water was suggested to soothe painful joints (Hippocrates, translated by (Adams and Hippocrates 2000)). In the first century A.D. , Dioscorides proposed the use of ivy berries for joint pain, a practice which continued to be popular into 19th Century England, where it is proposed in John Hill's 'The Family Herbal' (Hill 1812).

1.1.2 Key stages in the understanding and treatment of osteoarthritis

In 1741, the anatomist Morgagni was the first to produce a written description of osteoarthritic cartilage (Benedek 2006). William Heberden then initiated the process of distinguishing OA from rheumatoid arthritis when in 1782 he described digitorum nodi, 'hard little knobs, about the size of a small pea', on the hands of OA sufferers (Heberden 1818). Nowadays, these are referred to as Heberden's Nodes and, along with Bouchard's Nodes, described by Charles Bouchard in 1887, allow clear discrimination between OA and rheumatoid arthritis of the hand, due to their strong association with OA and relative scarcity in rheumatoid arthritis (Alexander 1999; Tan Ai Lyn et al. 2005). The further differentiation of OA from gout was performed by William Garrod in the early 1850s, although use of the name 'Osteoarthritis' wasn't recorded until 1886 when it was first used by Dr John Kent Spender, an English physician (Garrod 1859; Spender 1888). In this paper, Spender wrote eloquently of the lack of knowledge surrounding the condition, saying that 'Few things are so apt to cause a feeling of drowsy despair. . . as the prospect of an academic discussion on the aetiology of osteoarthritis'. The combination of lack of knowledge about OA and lack of effective treatment ultimately led to the formation of the Empire Rheumatism Council in 1936, which eventually became

Arthritis Research United Kingdom (ARUK) (ARUK 2017). ARUK and Arthritis Care merged in 2017 to form Versus Arthritis (*Versus Arthritis* 2017).

A hugely significant step in the treatment of OA occurred in 1961, when John Charnley perfected the low-friction arthroplasty for OA which represented the first effective treatment for the condition (Charnley 1961). Although arthroplasty had been performed prior to this date, with the earliest recorded procedure performed by Anthony White in 1822, the Charnley method represented the first successful, long-term, reproducible procedure and, with some modification, remains the best solution for end-stage OA (Charnley 1961; Trebše and Mihelič 2012). The first successful total knee arthroplasty, for knee OA, was performed 13 years later in 1974 (Trebše and Mihelič 2012).

1.2 Current understanding of osteoarthritis

1.2.1 Anatomy of the knee

To understand the disease process and treatment methods involved in OA, it is important to first understand the anatomy of the affected tissue. This thesis is primarily concerned with the knee, so this section will discuss key points of relevant anatomy within the knee. Hyaline, derived from the Greek for crystal or transparent (ὑάλινος or ὕαλος), describes cartilage with a smooth, glassy, bluish appearance most commonly found on the articulating surfaces of joints (Martin 2015). In the knee, these surfaces are the patellofemoral, between patella and femur, and lateral and medial tibiofemoral, between the tibia and the lateral or medial condyles of the femur respectively, as shown in fig. 1.2. Articular hyaline cartilage lubricates and provides shock protection to the articulating joint surfaces. Additional protection of the joint is provided by the menisci, articular discs of fibrocartilage, and the bursae, synovial membranous sacs containing synovial fluid. The menisci are located between the tibia and femur, and prevent rubbing of the bone ends as well as providing shock absorption and deepening the tibial sockets. Synovial fluid is a viscous, non-Newtonian, transcellular liquid formed by weeping lubrication from the intracellular fluid of articular cartilage during movement, as well as secretion by the synovial membrane. Synovial fluid contains hyaluronan and lubricin, and provides both lubricant and some shock absorption in the joint, as well as transfer of nutrients, waste, and gas exchange for the cartilage (Gray and Lewis 1918; Margo et al. 2010).

Hyaline cartilage itself is avascular, aneural and alymphatic with very low cellularity, around 2 % chondrocytes by volume, being mainly composed of a highly ordered collagen-proteoglycan matrix (Fox et al. 2009). These components contribute to the macromolecular structure of the cartilage, and the chondrocytes embedded within this matrix are responsible for its maintenance. This matrix has a zonal organisation, made up of the superficial, middle, and deep zones fig. 1.3. Each zone has a distinct organisation of matrix fibre composition and orientation, and chondrocyte location and shape

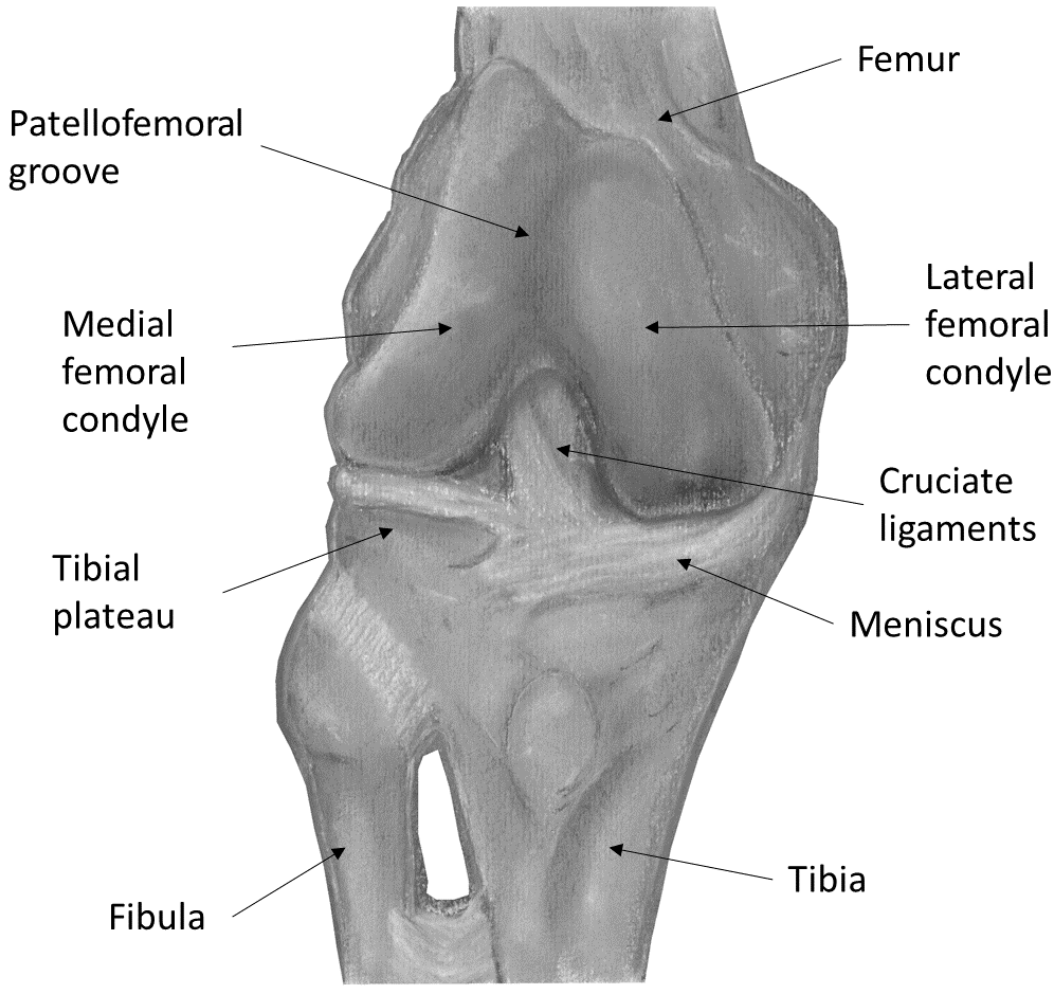

Fig. 1.2 The knee joint

Anatomical drawing of the human knee joint, with key structures labelled. Derivative work by SLFW based on Gray's Anatomy Original Edition (Gray and Lewis 1918).

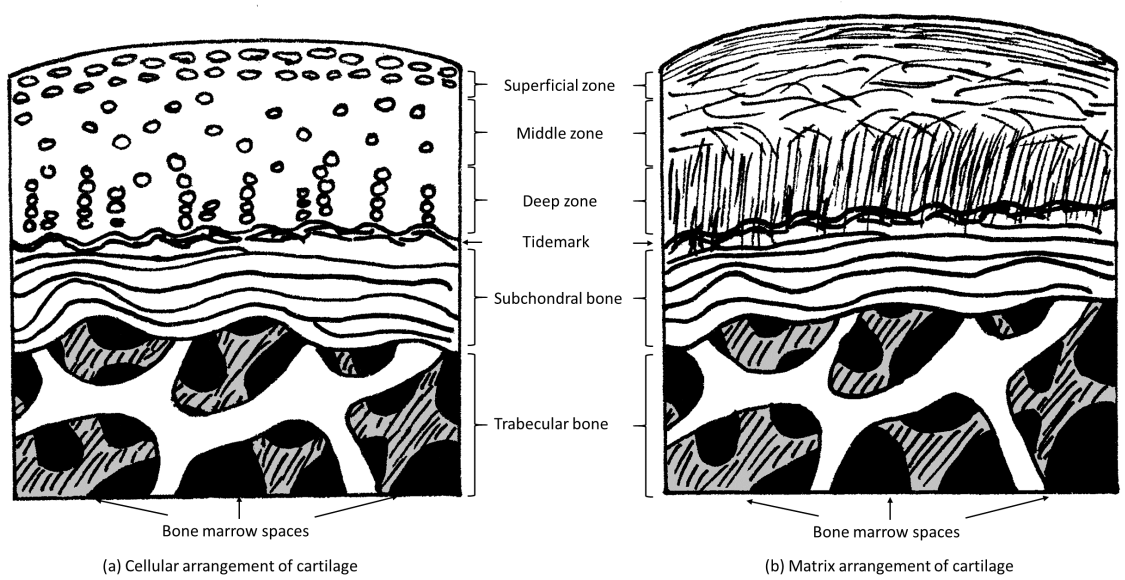

Fig. 1.3 Structure of articular hyaline cartilage

Diagram showing the zonal composition of articular hyaline cartilage in terms of both cellular (fig. 1.3a) and matrix (fig. 1.3b) composition. Original work.

with correspondingly different biomechanical properties (Fox et al. 2009). Below the deep zone of cartilage lies a calcified tidemark zone formed of hypertrophic chondrocytes, marking the transition from cartilage to subchondral bone. This subchondral region is around 10 times more deformable than cortical bone, with a critical role in reducing peak loading and distributing force across the joint surface (Millis 2014).

Damage to the cartilage can occur as a result of congenital abnormality, biomechanical instability and misalignment, trauma, or disease processes including infection and diabetes (Abramson and Attur 2009). In many mammalian species, such as mice, rabbits, sheep, pigs, and goats, articular hyaline cartilage lesions below a critical threshold in size heal completely, but in humans, articular hyaline cartilage has low self-repair potential, making it vulnerable to damage and degradation which may then progress into OA (Chu et al. 2010).

1.2.2 Current understanding of disease processes within osteoarthritis

OA is characterised by damage to, and loss of, articular cartilage, along with meniscal damage, joint space narrowing, proliferation of the synovium (synovitis), osteophytic growth, subchondral sclerosis and bone marrow lesions, indicating that OA is not solely a condition of the cartilage, but the whole joint (Abramson and Attur 2009; Brandt et al. 2006). Originally, lack of inflammation was thought to be a key distinguishing feature between OA and RA or gout, but recent studies have demonstrated

that inflammatory processes may in fact play a role in OA (Goldring and Otero 2011). OA lacks a standard disease progression, so stages of the disease with commonly associated symptoms are grouped together, as outlined in the figure below (fig. 1.4f). The Kellgren-Lawrence scale, first developed in the 1940s, is commonly used to categorise the disease progression, although other grading schemes do exist (Beck et al. 2005; Konan et al. 2011).

1.2.3 Diagnosis of osteoarthritis

Diagnosis of OA is usually made through a combination of reported symptoms, examination, and radiographic evidence, although blood tests and Magnetic Resonance Imaging (MRI) may be used to rule out other conditions such as septic arthritis or damage to soft tissues supporting the knee (ARUK 2013; NICE 2014). Pain correlates poorly to disease progression in OA, and so is used to determine treatment requirements for individual patients rather than as an indicator for disease stage (Pritzker et al. 2006). OA can be either primary, or secondary in cause. Primary or idiopathic OA has in the past commonly been associated with ageing and therefore was termed "wear-and-tear OA". However, while age is a strong risk factor, OA is not necessarily an intrinsic feature of the ageing process, making this term obsolete. Genetic predisposition, sex, lifestyle factors (including occupation and smoking), obesity, and co-morbidites (including diabetes) are also all key risk factors for development of OA, although the impact of each depends on the joint in question: obesity is a key predisposing factor for knee OA, while hip OA is more strongly linked to genetic factors (Abramson and Attur 2009; Buckwalter 2003; Magnusson et al. 2017; Sellam and Berenbaum 2013; Zengini et al. 2018; Zhai et al. 2007). Secondary OA results from a clearly identifiable cause, which may be the aforementioned cartilage trauma, joint infection, inflammatory arthritis, biomechanical and misalignment issues or congenital disease. However, cartilage trauma does not necessarily progress to OA: a retrospective analysis of 4121 knee arthroscopies demonstrated that there was no difference in progression or severity of OA between those with large cartilage defects and those without, indicating that the disease processes are more complex than simple degradation due to cartilage damage (Widuchowski et al. 2011).

Nevertheless, cartilage defects and progressive erosion are a unifying feature of OA and can advance to the point where the exposed subchondral bone is itself eroded, leading to progressively worsening joint misalignment, and disability. Understanding the biology of articular hyaline cartilage can aid understanding of both the disease process and the inherent difficulties faced when considering repair and regenerative strategies for OA.

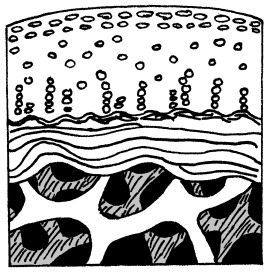

(a) Healthy osteochondral section showing cellular arrangement in hyaline cartilage

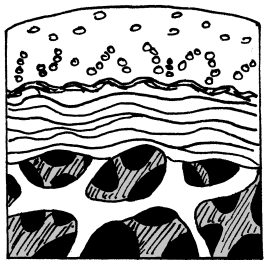

(b) Very early OA: loss of superficial zone of cartlage

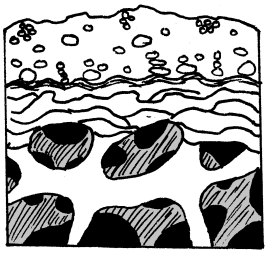

(c) Early OA: zonal structure of cartilage lost

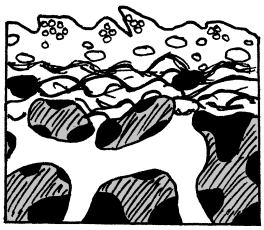

(d) Moderate OA: cartilage loss continues, bone marrow lesions and subchondral sclerosis evident

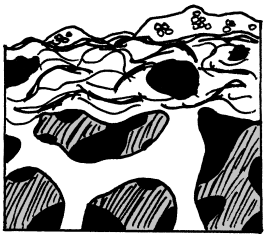

(e) Late OA: pathological changes mature, near-complete loss of cartilage

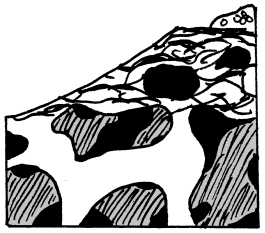

(f) End stage OA: full loss of cartilage, eburnation of subchondral bone, pathological changes highly evident

Fig. 1.4 Stages in the development of Osteoarthritis

In the healthy joint, hyaline cartilage has a highly ordered zonal stucture overlying the subchondral bone (fig. 1.4a). During the initial stages of the disease, the superficial layer of cartilage is lost (fig. 1.4b). As disease progresses, there is further loss of cartilage accompanied by subchondral sclerosis, disorganisation in the cellular structure of the remaining cartilage and development of bone marrow lesions and osteophytes (figs. 1.4c to 1.4e). In the end stage, all cartilage is lost from the joint surface leading to eburnation and erosion of the subchondral bone (fig. 1.4f). Original work based on descriptions of disease progression and histological slide examination.

1.3 Treatment strategies for osteoarthritis

1.3.1 Current techniques

Non-surgical techniques

Non-surgical techniques are employed in the early stages of OA where no definitive cause can be identified and disease has not yet progressed to result in significant impact on a patient's quality of life. These methods are also used in conjunction with surgical techniques in later stages of OA to improve treatment outcomes, and can be classed into symptomatic management techniques, and physiotherapy. Symptomatic management includes the use of painkillers, ranging from over-the-counter medications such as paracetamol through to steroid injections or opioids in more severe cases. Lifestyle modifications, such as weight loss to reduce joint loading, are also covered by this term. Physiotherapy may be employed to improve biomechanical alignment, also achieved through orthotics, or to strengthen the supporting muscles and ligaments to protect the joint from insult, or to assist in recovery from surgical procedures.

Surgical techniques

Resolving underlying biomechanical issues by repairing damaged supporting tissues such as anterior cruciate ligament or meniscus, or by correcting joint misalignment can significantly delay the progression of OA, preventing deterioration. Misalignment can be corrected through use of orthotics and physiotherapy for mild cases, but in severe cases or congenital malformation of the joint, surgical intervention such as wedge osteotomy can be used. Wedge osteotomy is also commonly used in conjunction with techniques to repair the cartilage defect, such as mosaicplasty, Autologous Cartilage Implantation (ACI) or Matrix-induced Autologous Chondrocyte Implantation (MACI). These techniques aim to repair defects by infilling with healthy cartilage or cells taken from non-load-bearing sites (Brittberg et al. 1994). Although the specifics of the techniques vary between the different therapies, the underlying principle is similar: autologous tissue from non-load-bearing regions is taken and used to infill the defect and promote repair, either as intact osteochondral or cartilage plugs (mosaicplasty, sometimes called Osteochondral Autograft Transfer System (OATS)), embedded in a gel (MACI), or sealed under a patch (ACI) (Bartlett et al. 2005; Ebert et al. 2017; NICE 2018). All of these techniques result in damage to the harvest site, are only suitable for defects below a critical size, result in fibrocartilage infill, and delay, rather than prevent, disease progression. For example, ACI showed high engraftment in only 35 % of cases after one year, and success was heavily dependent on site and size of defect. However, use of ACI has been approved by National Institute of Clinical Excellence (NICE) in the UK as the sole effective therapy for individuals with early-stage OA of the

knee and cartilage defects greater than 2 cm^2 in size where symptomatic management has failed, but joint replacement is not indicated (NICE 2017).

Instead of using autologous explants or cells, scaffolds made from biocompatible materials can be implanted into the defect to provide a structure for cellular regeneration. These scaffolds can be made from ceramics, composites or alloys, and advances in biomimetic material design, 3-dimensional printing, and laser sintering have enabled more complex scaffold design . For example, biphasic scaffolds with a hydroxyapatite base and gel top to mimic the biomechanical properties of bone and cartilage respectively are under development (Rodrigues et al. 2016). Other strategies showing promise include embedding scaffolds with regenerative factors such as Bone Morphogenic Protein 2 (BMP-2), stem cells, or chondrocytes (Quinlan et al. 2015; Shimomura et al. 2017). However, the success of these scaffolds is very mixed with poor scaffold-tissue integration, defect collapse, and problems with implantation being seen.

As a result, current and even developing treatment strategies ultimately delay disease progression. However, once the disease has reached end-stage, there are highly effective treatments available: arthrodesis and arthroplasty. Arthrodesis, where the joint is fixed to prevent rubbing, is used in non-replaceable joints such as the vertebral, ankle, manubriosternal, and carpometacarpal joints (Al-Dahiri and Pallister 2006; Hartigan et al. 2001; Takakura et al. 1999). While this does prevent further pain, joint functionality is removed. Arthroplasty, common in large joints such as the hip, knee, or shoulder, replaces the damaged joint with a prosthetic and is considered the gold-standard treatment for end-stage OA in these joints. This treatment prevents pain and restores functionality to the joint, improving both mobility and motility, albeit with some limitations. The surgery occurs in end-stage, when the patient has experienced multiple years of increasing pain and disability with associated personal and economic impacts. Additionally, the prosthetics have limited lifespans; around 20 years for a knee replacement is considered optimal, but many require replacement after fewer than 5 years due to infection, loosening or mechanical wear, resulting in revision surgeries in increasingly elderly patients or, in severe cases, amputation of the affected limb or even, in rare cases, death (Labek et al. 2011; Son et al. 2017; Tay et al. 2013). Furthermore, prosthetic lifespan is influenced by the age of the recipient, with those implanted in more elderly patients showing much greater lifespans than those implanted in younger recipients (Boulos and Jolles-Haeberli 2008). As a result, while an elderly patient may require a single revision procedure, a younger patient may require multiple revisions with the associated increased risks of adverse effects and disability. Therefore, although joint replacement offers an effective solution to end-stage OA in the elderly, it is less ideal in younger patients where an earlier intervention with greater longevity is required.

1.3.2 Potential therapy: Bone marrow stimulation

In OA, the hyaline cartilage covering the articular surface is damaged or lost, along with other pathological changes. Focal cartilage defects, which may progress to OA, also involve loss of hyaline cartilage. Current treatments for early-stage OA either manage the disease, or result in low-level regeneration of the damaged tissue. A more ideal strategy would be a regenerative technique resulting in the re-coverage of the joint surface with hyaline cartilage, complete with the correct zonal structure and biomechanical properties. Such a strategy requires a cell population within the defect site which is capable chondrogenesis and producing articular hyaline cartilage to replace that which was lost.

Human articular hyaline cartilage has low instrinsic repair potential, unlike that found in many other mammalian species (Chu et al. 2010). As a result, any damage sustained by articular hyaline cartilage in humans will resolve poorly, if at all (Widuchowski et al. 2011). The extent and type of repair tissue formed following trauma depends in part on the severity of the injury. A partial-thickness defect, which does not penetrate to the subchondral bone, shows a different level of repair to a full-thickness defect which penetrates to, and may involve damage to, the subchondral bone itself (Fellows et al. 2016). A partial-thickness defect shows little to no cellular recruitment, meaning that cellular involvement is restricted to chondrocytes, which show low and transient proliferation in response to the damage (Hunziker 1999; Hunziker and Rosenberg 1996). By contrast, greater cellular recruitment is seen in the case of full-thickness defects, especially with subchondral involvement, and the cellular response is comprised of cells with higher proliferative and regenerative potential such as bone marrow stromal cells or macrophages (Kreuz et al. 2006). Infill tissue is produced in both defect types, but the nature of this tissue varies with the extent of the cellular response. Partial-thickness defects show infill with an acellular fibrous tissue, while the infill tissue in a full-thickness defect is comparatively more robust, being an unstructured mix of hyaline cartilage and fibrocartilage (Hunziker 1999; Kreuz et al. 2006; L. Zhang et al. 2009). However both repair tissues are considerably less biomechanically stable than healthy articular hyaline cartilage and are highly prone to degradation. In either case, infill of the defect is partial at best leaving an uneven depression in the coverage at the joint surface.

As a result, intrinsic repair processes are insufficient to fully resolve cartilage defects. The repair tissue formed is transient, providing temporary infill but not restoring functionality. Indeed, the uneven joint surface resulting from the partial infill can lead to further degradation of the surrounding cartilage; the rim of a cartilage defect experiences high levels of shear forces, leading to decreases in matrix proteins and cells in surrounding tissue, propagating the trauma and increasing the risk of secondary OA developing (Zevenbergen et al. 2018). The relatively superior repair seen in full-thickness defects with subchondral involvement indicates that there is at the least the potential for formation of articular hyaline cartilage as the infill tissue. The mixed hyaline and fibrocartilage repair tissue is presumably a result of the presence of cells from the bone marrow with higher regenerative potential in the defect in

combination with a fibrin clot. These cells are capable of regenerating hyaline cartilage, but are unable to fully recapitulate the developmental pathways resulting in healthy articular hyaline cartilage.

Articular hyaline cartilage development is a process which begins in utero and finishes post-natally, although it is not yet fully understood. In the earliest stage, joint formation begins with interzone condensation of flattened Collagen 2-positive mesenchymal progenitor cells at presumptive joint sites within the cartilage anlage under the control of Gdf5, Wnt family genes and Erg, among others (Decker, Koyama, et al. 2015; Decker, Um, et al. 2017). Cavitation follows interzone condensation, with the development of the joint space, although the exact mechanism is unknown (Bari et al. 2010; Chijimatsu and Saito 2019). The synergistic effects of multiple transcription factors, including but not limited to bone morphogenic proteins, growth / differentiation factors, Sox and Wnt family members, induce secondary joint structure development which in turn leads to chondrogenic commitment and differentiation at the articular surface (Bari et al. 2010). At this point, the articular cartilage is matrix-poor, highly cellular and isotropic, unlike the matrix-rich, low cellularity and strict zonal organisation of mature cartilage as shown in fig. 1.3 (Decker, Um, et al. 2017). Final development and maturation of the cartilage occurs post-natally, under control of Prg (coding for Lubricin), transforming growth factors, fibroblast growth factors and parathyroid hormone-related peptide, as well as biomechanical forces (Caldwell and J. Wang 2015; Chijimatsu and Saito 2019). Matrix secretion increases leading to increased thickness of the articular cartilage and a corresponding decrease in cellularity. As the cartilage matures, zonal organisation occurs, in part under control of the canonical Wnt pathway.

While full recapitulation of the cartilage developmental pathway to regenerate damaged cartilage is currently out of reach, elements could be manipulated to encourage repair and regeneration. In the context of these thesis the most pertinent is the presence of precursor cells with chondrogenic potential at the joint surface. During cartilage development these cells initiate joint formation in the condensation phase and subsequently differentiate to form the various cell types found within a joint, including chondrocytes as discussed above. However, they are not present in mature articular hyaline cartilage. Adult BMSC are thought to be descendents of these mesenchymal precursor cells and are capable of expressing similar factors, such as Col-2, as well as replicating some of their behaviours, such as chondrogenesis (Caplan 1991; Pittenger et al. 1999; Sheng 2015). In addition, the presence of some hyaline cartilage within the repair tissue formed after cartilage damage with subchondral involvement indicates that they are capable of forming hyaline cartilage in the adult. Therefore, introducing bone marrow cells to the joint surface in a controlled manner could stimulate intrinsic pathways leading to formation of superior repair tissue at sites of cartilage trauma. Furthermore, studies have shown that decreasing immune involvement in regions of trauma may favour a more complete regenerative reponse, possibly closer to tissue formation or fetal repair (Julier et al. 2017; Shi et al. 1997; Toben et al. 2011).

Bone marrow stimulation techniques, which exploit the intrinsic regenerative potential of bone marrow (as shown in fig. 1.5) have been proposed as therapies for osteochondral repair for many years (Pridie

and G. Gordon 1959). During bone marrow stimulation, bone marrow is introduced to the defect site through various techniques, such as abrasion, Micro-Drilling (MD), or Micro-Fracture (MF) of the bone surface exposed by cartilage loss. This marrow forms a marrow clot which contains cells with regenerative potential: hyaline articular cartilage itself is believed to have very few cells with regenerative potential and hence has weak intrinsic repair potential (Jiang and Tuan 2015). These regenerative cells may directly contribute to infill of the defect by undergoing chondrogenic differentiation and producing hyaline cartilage themselves, or may recruit or support other cell types to undergo the same process. Furthermore, articular hyaline cartilage is avascular and hence has low nutrient and oxygen levels and restricted waste exchange, but it is suggested that repair has a greater metabolic requirement than that typically provided at the joint surface (Abramson and Attur 2009). The surgically induced trauma at the defect site increases nutrient, gas, and waste exchange which supports the repair and regeneration, including angiogenesis, occurring during the healing cascade, as well as recruitment of cells with regenerative potential responding to the trauma.

These therapies have shown promise in treating focal cartilage loss and early-stage OA, but this has never been fully realised. This may be due to incomplete understanding of the mechanisms underlying the technique, preventing optimisation. As a result, although there is partial re-covering of the joint surface and infill of defect sites following treatment with bone marrow stimulation techniques, much of the regenerated tissue is fibrocartilage, which is an improvement, but not as desirable or long-lived an outcome as hyaline cartilage (Bae et al. 2006). Therefore, although chondrogenesis can be stimulated using this technique, and some hyaline cartilage is produced, the type and extent of the chondrogenic response is currently sub-optimal. Understanding how the early interactions between cell types within the marrow clot influence chondrogenesis and eventual resolution of the repair could enable the techniques to be improved, resulting in a repair tissue comprised entirely of hyaline cartilage.

1.3.3 Techniques used in bone marrow stimulation

Abrasion arthroplasty

During abrasion arthroplasty, damaged cartilage and subchondral bone is debrided. No direct large diameter conduits between the joint surface and marrow cavity are formed and so the clot forms through bleeding from damaged blood vessels within the subchondral bone. This technique is generally considered palliative and will not be considered in further detail here.

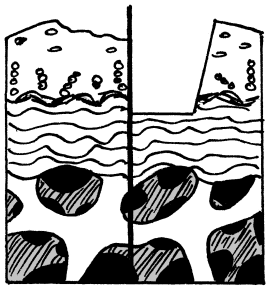

(a) Left side: damaged cartilage. Right side: Damaged cartilage is debrided to expose the subchondral bone. At this stage, the debrided region can be left to repair (Abrasion arthroplasty) or further treatments can be applied

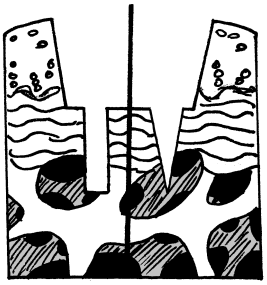

(b) Channels are created between the debrided defect site and bone marrow by drilling (MD, left side) or fracturing with an awl (MF, right side)

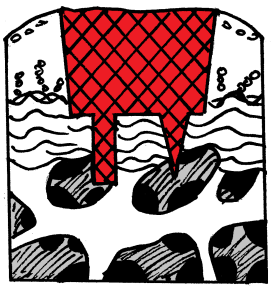

(c) Following creation of the channels, a marrow clot forms within the defect site

Fig. 1.5 Bone marrow stimulation techniques

Figure showing the various bone marrow stimulation techniques: abrasion arthroplasty, MF, and MD. Original work.

Micro-drilling and Micro-fracture

Micro-drilling (MD) was first introduced by Pridie in 1959 (Pridie and G. Gordon 1959). During MD, damaged cartilage is debrided to the level of the subchondral bone, and a drill is used to bore through the subchondral bone to the marrow cavity. Marrow and blood from the marrow cavity are extruded into the defect site by hydraulic pressures to form a marrow clot. Modern MD techniques use irrigation to prevent heat necrosis. Micro-fracture (MF) was originally introduced by Steadman in the late 1990s (Steadman et al. 1997). In principle, MF is similar to MD, although the holes between marrow cavity and joint surface are created using an awl, rather than a drill. This procedure often leads to bone compaction and potentially increased osteocyte necrosis around the holes. MD/MF have potential as a therapy for focal cartilage defects, with multiple long-term studies showing that the techniques reduce development of OA in over 50 % of cases with greater success in non-smoking, younger patients with normal Body Mass Index (BMI), smaller, early-stage defects, and good biomechanical alignment (Gracitelli et al. 2016; Knutsen et al. 2016; Ulstein et al. 2014). Furthermore, the combination of MD/MF with wedge osteotomy or Anterior Cruciate Ligament (ACL) repair (if required) to correct alignment is highly recommended and indeed shows significantly improved results compared to MD/MF alone. The ideal outcome of MD is regeneration of healthy hyaline cartilage with correct zonal structure of the tissue, clearly defined tidemark, correct Extracellular Matrix (ECM) composition and requisite biomechanical properties. However, in those patients where the treatment fails, this occurs within 2 to 5 years of surgery. Regardless of the eventual outcome, in the majority of cases the regenerated tissue is composed mainly of fibrocartilage and lacks the highly organised structure and biomechanical properties of healthy hyaline articular cartilage, leaving the repair tissue vulnerable to erosion as shown in fig. 1.6 (Steadman et al. 1997). Studies have shown that defects treated with MD/MF have some infill with hyaline cartilage, although the proportions within the repair tissue vary (Bae et al. 2006; K. B. L. Lee et al. 2012; Saw 2013). Furthermore, the infill of the defects is often partial or incomplete, leaving a clear indentation on the cartilage surface, which risks collapse of the edges of the defect leading to further erosion. While this does protect the bone from being further damaged by abrasion and provides a level of coverage/joint lubrication the poor biomechanical properties of fibrocartilage means that this acts more as a stop-gap than a true repair. In addition, over-debridement of the calcified cartilage within the defect can lead to bone overgrowth, increasing failure rate (Mithoefer et al. 2016). However, delaying the age of joint replacement through achieving best functional repair is beneficial in younger patients by preventing the need for earlier joint replacement surgery, and potentially multiple revisions. It has been suggested that the influence of MD on the subchondral bone is responsible, at least in part, for the success of the technique, perhaps by creating an environment more conducive to hyaline cartilage formation (de Vries–van Melle et al. 2014).

More recent studies have examined various ways of manipulating MD to improve repair outcomes. These include exogenous administration of Bone Marrow Aspirate Concentrate (BMAC), isolated autologous bone marrow progenitors, or Platelet-Rich Plasma (PRP) and HA (Broyles 2017a,b; K.

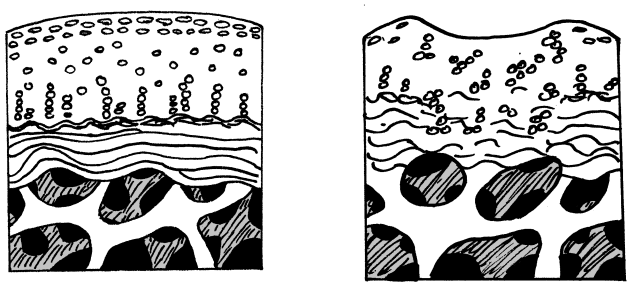

(a) Ideal outcome: reformation of articular hyaline cartilage with correct zonal patterning

(b) Example outcome: disordered repair composed mainly of fibrocartilage, lacking correct zonal patterning or defined tidemark and with an uneven surface

Fig. 1.6 Comparison of the desired and actual outcomes of bone marrow stimulation techniques for cartilage repair. Original work

Diagram showing the desired outcome of bone marrow stimulation techniques and an example of the outcome seen in reality.

Lee et al. 2007; Saw 2011). Outcomes were improved compared to MD alone, suggesting that the positive effects of the treatment are due to the presence of bone marrow progenitors combined with HA, which has immuno-modulatory properties, or PRP, which is thought to have immuno-modulatory and chondroprotective properties through enhancing autophagy and supressing inflammation and apoptosis (Moussa et al. 2017).

However, the patients within these studies were exposed to multiple intra-articular procedures; in one study, patients required 12 separate bone marrow aspiration procedures and intra-articular injections of BMAC, PRP, and HA over a twelve-month period to achieve measurable benefit (Broyles 2017a). This represents a huge burden on the patient and health provider, as well as significant risk of adverse events and patient drop-out. Therefore, since the positive effects of many of these therapies are believed to be mediated through innate immune system effects a greater understanding of the BMSC-immune interactions within the MD clot may yield points of intervention which could be therapeutically exploited using, for example, small molecule therapies administered in less invasive ways. Greater understanding could also indicate the optimum timepoint for interventions such as exogenous cell administration based on the progression of the repair and inflammatory response. This thesis aims to explore some of the interactions between BMSC and immune cells to further this understanding and support development of future interventions.

1.4 Wound healing and fracture repair

1.4.1 Differences between fracture repair and MF / MD

Fracture repair in bone will be considered as a model for the repair occurring following MD therapy, to provide context and insight into the cell biology that underpins these events. It must be noted that the repair occurring following bone fracture and MD is not identical, nor are the desired outcomes. The best outcome in bone repair is one where the cartilage produced within the fracture callus has been fully mineralised and remodelled to restore biomechanical strength. However, following MD the desired outcome is a stratified repair with subchondral bone covered by a highly organised layer of hyaline cartilage. After the currently employed bone marrow stimulation procedure, there is a level of cartilage regeneration which covers the bone end but this is mainly comprised of fibrocartilage with a small amount of hyaline-like cartilage (Bae et al. 2006). In fact, this repair tissue bears similarities to that seen within a pseudarthrosis where the non-union fracture forms a false joint which is lined with a mixture of fibrocartilage and hyaline-like cartilage (Milgram 1991; Panteli et al. 2015; Urist et al. 2017). This would suggest that the healing in a MD/MF repair could be considered a disordered or disrupted version of fracture repair. The MD/MF repair is also small in size compared to a fracture, which may alter the microenvironment and biodynamics within the repair. The repair will also have some contribution from the cartilage and synovium which may produce factors, such as cytokines or proteoglycans which alter repair pathways. The synovium may additionally contribute inflammatory or fibroblastic cell populations, while the contribution of the remaining cartilage within the joint to the repair is less clear cut. There is growing consensus that hyaline cartilage does contain progenitors, but their activity and contribution to repair is currently unknown (Jiang and Tuan 2015). That being said, the same cell types will be present in both scenarios, with contributions from the blood, bone marrow, bone and periosteum of immune cells and stem / progenitor populations. This assessment only considers repair in the context of sterile repair and assumes no infectious component. Presence of infection within repair significantly alters both the physical and cellular environment as well as pathways involved and has profound consequences for the resolution of the injury. This section will consider the descriptive steps in early fracture repair; specific cellular conditions will be considered separately.

1.4.2 Key stages of fracture repair

Fracture repair can be considered a developmental process occurring post-natally, comprising the same pathways and features as skeletal development (Gerstenfeld et al. 2003). Bone is one of the few tissues in the adult body capable of scarless injury resolution. Fracture sites can be nigh indistinguishable from the original bone following complete resolution, with repair tissue displaying the same biomechanical

properties, cellular composition, and organisation as the undamaged tissue (Einhorn and Gerstenfeld 2015). There are five key stages in fracture repair: haemostasis, inflammation, soft callus, hard callus (in general wound repair these are jointly referred to as proliferation), and maturation or remodelling. These phases are not discrete and may overlap temporally with other phases, although they are characterised by specific events, as indicated in fig. 1.7.

1.4.3 Early fracture repair

Formation of the haematoma

My work is primarily concerned with interactions between cells occurring during haemostasis and the first seven days of repair. During haemostasis, a haematoma forms to stop the bleeding from damaged blood vessels and to provide a matrix for the repair. The haematoma is a dynamic environment and has a crucial role in the outcome of the repair: removal of the early haematoma delays repair, increases inflammation and compromises the resolution of the repair (Hoff, Maschmeyer, et al. 2013; Kolar et al. 2011). My work does not consider the role of biomechanical forces, but perturbation of the repair by biomechanical instability also negatively influences repair outcomes. This stage begins with the traumatic insult and continues for the first hours following damage. Platelets degranulate in response to the damage, initiating the clotting cascade and resulting in the production of a haematoma, or clot. The haematoma is a hydrogel, containing fibrin polypeptide chains formed by proteolytic cleavage of terminal glycine residues from fibrinogen by thrombin (Bailey et al. 1951; Doolittle 2010). Thrombin also activates Factor XIII which crosslinks fibrin protofibrils, formed from the polypeptide chains, into a matrix (Doolittle 2010). This matrix is stabilised by platelets which influence both the structure and the mechanical properties of the haematoma (Tocantins 1936). Contained within this matrix are cells from the peripheral blood and bone marrow. Following haemostasis, the release of Damage Associated Molecular Patterns (DAMPs) and cytokines results in infiltration by immune and other cell types, which initiate the inflammatory phase and start clearing debris and remodelling the matrix to form the soft callus.

Physical environment of early fracture

Following haemostasis, the haematoma has no regular blood supply until neovascularisation occurs at around day 5 post-fracture so, during this time, nutrient, waste, and gas exchange is achieved by diffusion from surrounding tissues. In a sheep fracture model, oxygen content was elevated immediately after fracture due to the influx of oxygenated blood prior to haemostasis, followed by a rapid decline as a result of increased metabolic activity in the damaged region consuming residual oxygen (Epari et al. 2008). The haematoma is profoundly hypoxic, with a measured partial pressure

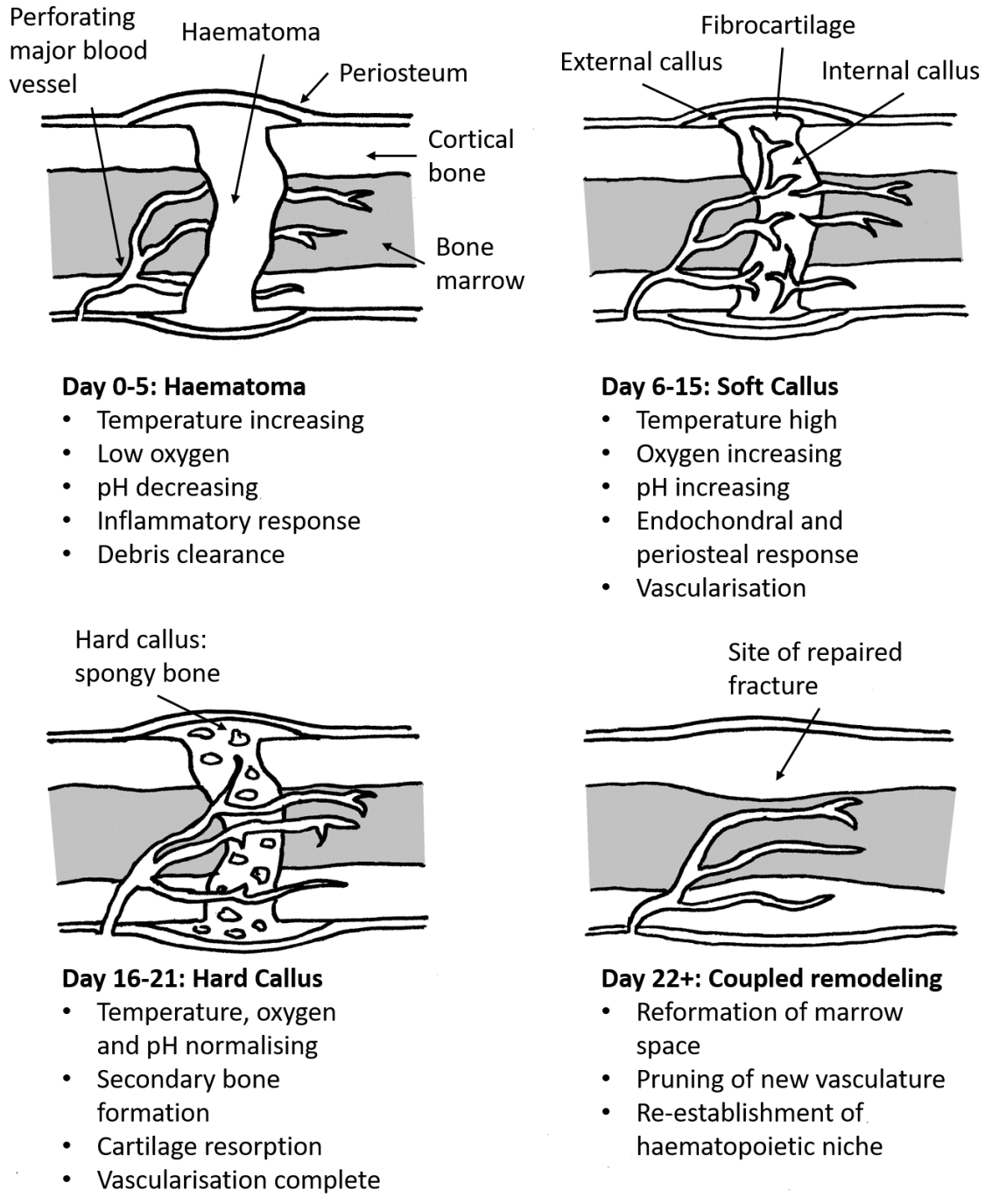

Fig. 1.7 Stages of fracture repair

Diagram showing outline of stages during fracture repair. Original work based on (Einhorn and Gerstenfeld 2015).

of oxygen below 1 %, compared to the usual physiological level of 5 to 12.5 % (physoxia) (Hirao et al. 2006). However, this is similar to the environment found within bone marrow: direct *in vivo* measurements in mice have shown a gradient in oxygen levels within the bone marrow, ranging from 2.8 % in endosteal regions down to 0.6 % in peri-sinusoidal regions (Spencer et al. 2014).

Accompanying the changes in oxygen tension within the haematoma are changes in potential of hydrogen (pH). Following injury, acidification occurs resulting in a decrease in pH relative to physiological conditions (pH 7.35 to 7.45). This acidification has been recorded as lowering haematoma pH to as low as pH 4.7, although is more commonly found to be around 7.2 (Chakkalakal et al. 1994; Newman et al. 1987; Steen, Kay H. et al. 1995). Acidification is followed by alkalinisation, an increase in pH relative to physiological conditions, which peaks 20 days post-fracture. Acidification coincides with the start of the inflammatory response as a result of increased lactic acid concentration within the haematoma due to secretion from infiltrating neutrophils through anaerobic respiration, while alkalisation corresponds to calcification (Lardner 2001; Newman et al. 1987; Swenson and Claff 1946). Disruption of these pH changes has deleterious effects on repair outcomes.

The local temperature of the haematoma also rises as part of the inflammatory response. In a sheep fracture study, knee intra-articular temperature was found to increase from 34.8 °C pre-fracture, to 38.5 °C 4 days post fracture, comparable to sheep core temperature of 38 to 40 °C (Epari et al. 2008). Although studies have not measured the thermal profile of a human haematoma, qualitative observation indicates that local tissue temperature increases following fracture. Human knee intra-articular temperature at rest is 31 to 33 °C, lower than core temperature of 37 °C and similar to the difference between sheep lower limb and core temperature, although temperature changes during exercise do occur (Becher et al. 2008; Harris and McCroskery 1974).

Therefore, in the early stage of repair, the haematoma has a low oxygen tension and pH, high lactate, and a disorganised 3D structure (Kolar et al. 2011; Schmidt-Bleek et al. 2011). This environment is strongly pro-inflammatory, resulting in the recruitment and infiltration of immune cells from the peripheral blood and surrounding tissues. This inflammatory phase peaks 24 hours post-fracture and continues for 5 to 10 days post-fracture when resolution occurs (Einhorn and Gerstenfeld 2015; Mountziaris and Mikos 2008; Pence and Woods 2014).

Biochemical environment of early fracture

During haemostasis and inflammation, cytokines are major biochemical components of the response. Morphogens, proteases and pro-angiogenic factors are secreted by several different cell types later in healing (Gerstenfeld et al. 2003). In early inflammation, the profile is dominated by Interleukin 6 (IL-6), Interleukin 8 (IL-8), Interferon Gamma (IFNγ), and Tumour Necrosis Factor Alpha (TNFα) from the damaged bone and surrounding soft tissue. Interleukin 1 beta (IL-1β) is also increased in the

haematoma, and appears to have a role in controlling endochondral ossification. In response to the pro-inflammatory cytokines, anti-inflammatory cytokine production occurs, characterised by production of Interleukin 1 Receptor Antagonist (IL-1RA), Interleukin 4 (IL-4) and Interleukin 10 (IL-10) and represents a counter-regulatory response (Hoff, Gaber, et al. 2016). Receptor Activator of Nuclear factor $\varkappa$ B Ligand (RANKL) and Osteoprotegerin (OPG), whose relative levels are important in the regulation of bone resorption and formation, are also upregulated at this point (Gerstenfeld et al. 2003). The overall balance of all of these cytokines and growth factors is critical to the success of the healing. For example, both over and under-expression of IFNγ and TNFα have profound consequences for resolution (H. Schell et al. 2017). IL-6, IL-8, IFNγ and TNFα are potent chemokines for neutrophils, the first cells recruited to the haematoma, which rapidly infiltrate the site of trauma within an hour of injury and peak at around 24 hours post-trauma (Edderkaoui 2017; Loi et al. 2016). Neutrophils secrete chemokines such as C-C Motif Chemokine Ligand 2 (CCL2) and C-X-C motif chemokine Ligand 8 (CXCL8) which initiate neoangiogenesis and recruit monocytes to the site of damage (Edderkaoui 2017). Bone marrow cells and Haematopoietic Stem and Progenitor Cells (HSPCs) are recruited during this phase from surrounding bone marrow, muscle tissue and blood, in addition to those captured within the clot during haemostasis (Gerstenfeld et al. 2003; Hoff, Maschmeyer, et al. 2013; Schmidt-Bleek et al. 2011). As a result, the cytokine and cellular profile of the haematoma is dynamic, highly complex and has a significant impact on the eventual repair outcome.

The inflammatory response in fracture repair

A balanced inflammatory response is extremely important to successful repair; the strength and duration of this inflammatory phase is critical to the outcome of the repair, hence the importance of immunoregulatory pathways during the anti-inflammatory phase are clear. The initial pro-inflammatory response appears to have a detrimental effect on healing which is later countered by the anti-inflammatory response, shown in the improved healing seen in immune-deficient mice (Claes et al. 2012; Toben et al. 2011). Further evidence for the important of a correctly regulated pro-inflammatory phase comes from studies on fracture healing in human patients with immune disorders such as Systemic Lupus Erythematosus (SLE) or diabetes mellitus. These patients develop chronic inflammation which prolongs the repair and results in compromised outcomes (Claes et al. 2012).

There is some evidence that lack of an inflammatory response can improve healing where highly organised repair with minimal scarring is required. In a study on wound regeneration after lens surgery in the eye, an immune privileged site, it was found that careful creation of a small incision to minimise inflammatory infiltrate resulted in complete regeneration of the lens (Haotian Lin et al. 2016). The lens has a highly organised cellular and matrix structure, broadly similar to hyaline cartilage, and is able to functionally regenerate in the absence of immune cells. By contrast, when inflammation

occurs the cellular organisation of the lens is disrupted resulting in sub-optimal repair. A similar result was seen when comparing repair in dermal and oral wounding. Oral wounds have lower infiltration of immune cells such as neutrophils, macrophages and T-cells, and show improved healing with decreased scarring compared to dermal wounds (Szpaderska et al. 2003).

1.5 Bone Marrow Stromal Cells

1.5.1 Discovery of Bone Marrow Stromal Cells

In his 1867 paper 'Ueber entzündung und eiterung' (On Sepsis and Inflammation) Julius Friedrich Cohnheim observed dyed cells with a fibroblastic appearance migrating to regions of tissue damage from the bone marrow (as described in Rodríguez-Merchán and Liddle 2016). A year later, L'Academie de France in Paris awarded Emile Goujon a prize of 500 Francs for his work showing that bone marrow transplantation into muscle caused ectopic ossification in chickens and rabbits (Goujon 1869) as summarised in (Bolontrade and García 2016). Despite these early advances, nearly one century would pass before Tavassoli and Crosby enlarged on this work and demonstrated that bone marrow has inherent osteogenic potential (Tavassoli and Crosby 1968). This early work paved the way for the seminal work by Friedenstein and Owen, who first defined an adherent subpopulation of the bone marrow, with a fibroblastic appearance, trilineage potential (osteo-, adipo- and chondro-genic), and colony forming behaviour (Friedenstein, Chailakhjan, et al. 1970; Friedenstein, Chailakhyan, and Gerasimov 1987; Friedenstein, Chailakhyan, Latsinik, et al. 1974). In 1991, Caplan denominated this population the 'Mesenchymal Stem Cell' or 'MSC' (Caplan 1991). Later work by Pittenger demonstrated trilineage potential after clonogenic expansion, as well as the importance of 'MSC' in supporting haematopoiesis (Pittenger et al. 1999). These discoveries showed that these cells had potential applications in the nascent field of regenerative medicine. Since that time, the field has grown immensely. Moreover, analogues of these cells with similar properties have been extracted from multiple tissues within the human, such as adipose, umbilical cord, pancreas, and menstrual blood as well as from diverse mammalian species, including mouse, dog, sheep, whale, and pig (Bornes et al. 2015; Hoogduijn et al. 2013; K. Lee et al. 2007; Russell et al. 2016). These cells appear to be ubiquitous within the body in mammalian species, being distributed throughout the tissues, although the influence of tissue source on cell properties is incompletely understood.

1.5.2 Nomenclature

Throughout this thesis, these cells will be referred to as Bone Marrow Stromal Cells, or BMSCs. As can be seen from fig. 1.8, the nomenclature of these cells is complex, with a range of interpretations in

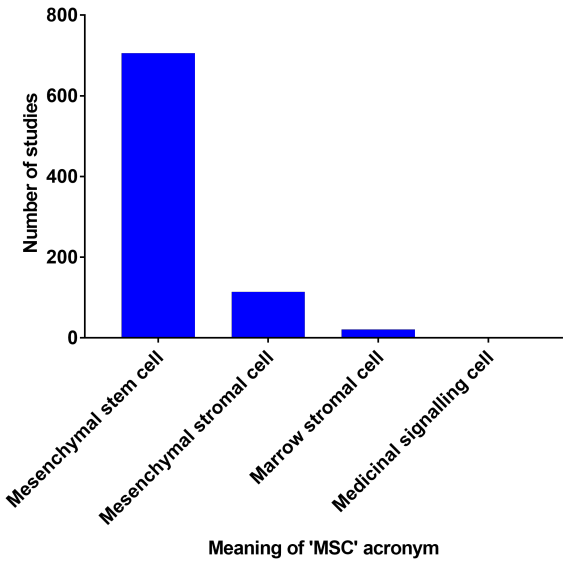

Fig. 1.8 Distribution of ‘MSC’ acronym usage within US clinical trials

The various interpretations of the ‘MSC’ acronym were assessed in a sample of clinical trials from the US in July 2018 and are presented here as a chart (*ClinicalTrials.Gov* 2018).

use. In this section, I will discuss other terms and explain why these cells will be referred to as BMSC throughout my thesis. An exception will be made when discussing research using cell analogues derived from other tissues.

Mesenchymal stem cell

This is the most commonly used term, and was championed by Caplan in his 1991 paper (Caplan 1991). However, the implication of the term ‘stem’ is that of a self-renewing population, and while BMSC are capable of differentiating to other cell types, they are not capable of indefinite self-propagation (DiMarino et al. 2013). Additionally, ‘stem’ is used in an imprecise manner, covering cells ranging from the totipotent blastocyst, to multipotent tissue-specific cell types, and implies a homogeneous, well-characterised population (Tajbakhsh 2009). Indeed, in recent years, Caplan himself has argued against the use of this term, such as at the 2017 International Cartilage Research Society conference.

Mesenchymal stromal cell

This second interpretation avoids the controversy of the word ‘stem’ by replacing it with ‘stromal’. While this is an improvement, the term itself is somewhat of a tautology. ‘Stromal’ refers to the cells supporting the parenchyma, such as blood vessels or connective tissues, which do not have an organ-

or tissue- specific function. In the adult, 'mesenchymal' refers to cells derived from the embryonic mesodermal lineage. This is a very broad term, encompassing the soft, connective tissues derived from the mesenchyme, which provide structure and support to organs. Additionally, this term does not make any distinction between cells derived from different tissue sources; it implies that tissue source is irrelevant. This is clearly not the case, as there are clear differences between MSC from adipose tissue and from bone marrow (Sung et al. 2008). A common practice now is to add an indicator of tissue of origin to the acronym, for example A-MSC for Adipose-derived Mesenchymal Stem/Stromal Cell. This term does acknowledge the heterogeneity of the population, which is an improvement over mesenchymal stem cell (DiMarino et al. 2013).

Medicinal signalling cell

This term is the newest and has been proposed by Caplan as replacement for Mesenchymal Stem Cell (Caplan 2017). The logic is that MSC contribute to regeneration more through immunomodulation than through differentiation. There is also no use of the terms 'mesenchymal' or 'stromal' since Caplan claims that MSC are in fact pericytes (Caplan and Correa 2011). The term is slightly awkward, since the idea of the 'MSC' is well known, and it was believed that changing the acronym would simply be confusing. Further, it is a clinical term, suggesting the cells should be considered as a drug or delivery system, rather than intrinsic components of a biological system and, once again, does not identify tissue of origin or heterogeneity.

Bone Marrow stromal cell

This final term avoids the tautology of mesenchymal stromal cell, and is specific about the tissue of origin. The term BMSC may also be used to further distinguish the tissue of origin and avoid the confusion of the 'MSC' acronym. This term has recently been challenged based on the existence of a marrow stroma: Caplan argues that there is no stroma in bone marrow, and therefore referring to these cells as marrow stromal cells is incorrect (Caplan 2017). However, if the previously discussed definition of stroma (cells which do not perform the specific function of the organ or tissue) is used, then this argument is questionable. The function of the bone marrow is haematopoiesis, which is performed by the resident HSPC within the tissue. The BMSC do not perform haematopoiesis, but instead form part of the HSPC niche in a supportive, or stromal, role. Therefore, in my opinion, the term Bone Marrow Stromal Cell (BMSC) provides the optimal balance between acknowledgement of tissue of origin, cellular function within the niche, population heterogeneity, and cellular identity and will be used throughout this thesis. The acronym is also similar to the well-established 'MSC', and the modified 'B-MSC' used to denote tissue origin, allowing the work to be considered in the broader context of the field while minimising confusion over nomenclature.

1.5.3 *In vitro* isolation and characterisation of Bone Marrow Stromal Cells

Given the confusion surrounding the nomenclature of the BMSC, it should be of no surprise that the scientific definition is equally contentious. While some basic attributes of the BMSC are widely agreed upon, there is no definitive consensus on phenotyping criteria. This means that when the term 'MSC' or 'BMSC' is found in a study, it is always necessary to identify how the individual research groups have defined the population. The basic definition of a Human Bone Marrow Stromal Cell (hBMSC) is based on the work by Friedenstein and Owens, Caplan, and Pittenger as described above and was proposed by the International Society for Cell Therapy (ISCT) in 2006 (Dominici et al. 2006). Their criteria were:

1. The population must be plastic adherent under standard tissue culture conditions
2. The population must have the expression of surface markers defined in table 1.1, as determined by single stain flow cytometry (see table A.1 in Appendix A for a description of markers used)
3. The population must be capable of tri-lineage differentiation. In the context of BMSC / mesenchymal stromal cell (MSC) this refers to osteogenic, adipogenic, and chondrogenic differentiation (see section 1.5.4).

Table 1.1 Surface Marker Expression of hBMSC

Positive ($\geq$95 % expression)	**Negative ($\leq$2 % expression)**
Cluster of differentiation (CD) CD73, CD90, CD105	CD45, CD34, CD14 (or CD11b), CD79α (or CD19), Human Leukocyte Antigen – D Related (HLA-DR)

It is immediately clear that cell populations isolated and characterised using these conditions will be highly heterogeneous, due to the looseness of the guidelines. This is acknowledged by the ISCT, and in the paper, they discuss how these guidelines represent the bare minimum to define a BMSC. To further complicate the definition, a 'Skeletal Stem Cell' which expresses similar markers to BMSC, but does not undergo adipogenic differentiation has been described (Chan et al. 2015; Worthley et al. 2015). Multicolour analysis, additional markers and more stringent thresholds are suggested to improve characterisation of the BMSC (Dominici et al. 2006). The underlying heterogeneity of the population is especially highlighted by work from the Genever group (James et al. 2015). This group has created four human telomerase reverse transcriptase (hTERT) immortalised lines of BMSC, each derived from a single cell and all isolated from the same donor sample, named Y101, Y102, Y201, and Y202. Characterisation of these lines by flow cytometry has shown similar expression of ISCT markers (Positive: CD105, CD90, CD73, and negative: CD34 and CD45), along with extra markers identified by the group (CD29, CD44 and CD166). However, characterisation by tripotential differentiation, proliferation and migratory phenotype demonstrated that the lines can be split into two

groups with starkly differing phenotypes. Critically, while the Y101 and Y201 lines were tripotent, the Y102 and Y202 lines had weak differentiation abilities (with possible immunomodulatory behaviour) despite all having similar marker expression profiles (James et al. 2015). This suggests that BMSC have heterogeneous behaviours despite similar marker profiles. This could be due to a spectrum of behaviour, determined spatially or temporally *in vivo*, which has been fixed by the immortalisation process. Either way, only two of these lines would be considered BMSC by the ISCT, despite their markers and population of origin. A consideration of 9 papers published since the ISCT guidelines were proposed, although a small subset of the available literature, firstly show that none of these papers used these exact criteria as stated, nor were any of the characterisation methods used the same between papers (Adesida et al. 2012; W. Chen et al. 2018; James et al. 2015; J. Kim and Hematti 2009; Poggi et al. 2005; Prasanna et al. 2010; Sacchetti et al. 2007; Sotiropoulou et al. 2006; Wagegg et al. 2012). The use of plastic adherence was the sole consistent criteria in all methods, as shown in fig. 1.9.

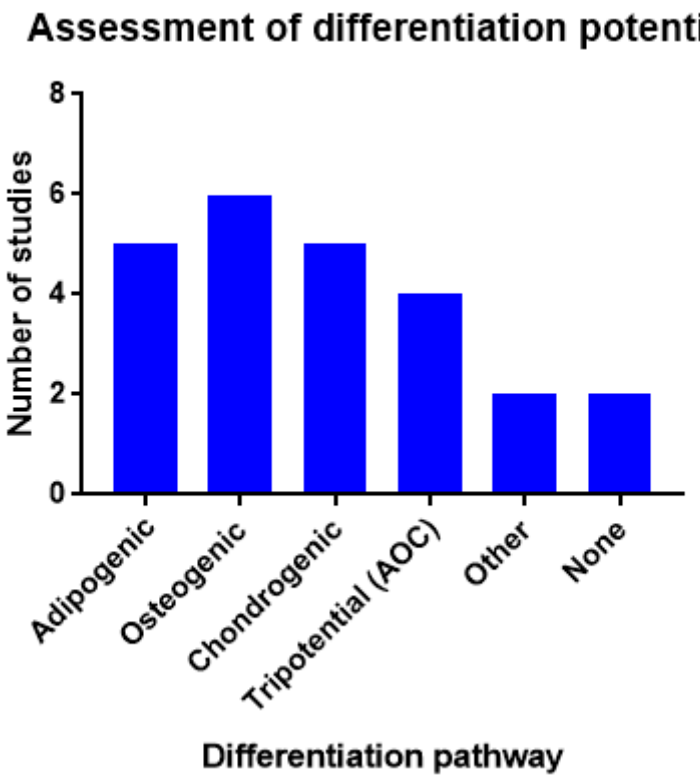

Fig. 1.9 Differentiation ability criteria used for hBMSC identification

Assessment of *in vitro* differentiation ability used to characterise hBMSC in a subsection of published papers (Adesida et al. 2012; W. Chen et al. 2018; James et al. 2015; J. Kim and Hematti 2009; Poggi et al. 2005; Prasanna et al. 2010; Sacchetti et al. 2007; Sotiropoulou et al. 2006; Wagegg et al. 2012).

In terms of both differentiation potential and cell surface marker expression, it is clear that while the ISCT guidelines act as inspiration, and were even referenced as the characterisation method for the study, individual research groups have developed their own methods of characterising BMSC (fig. 1.9 fig. 1.10). CD44 in particular is commonly used, possibly due to its upregulation on cells during *in vitro* culture although its expression is of questionable relevance *in vivo* (Le Blanc and Davies 2018). Further, the expression of these markers is not unique to BMSC: fibroblasts also express many of these markers at similar levels. The divergence in thought is clear if the age of the ISCT guidelines are considered: these have not been updated since 2006, which is most likely due to lack of consensus among key researchers. As a result, comparisons between BMSC / MSC studies are challenging. In my study, the basic ISCT guidelines will be adopted and used for hBMSC characterisation. While other markers are proposed, such as CD44, the guidelines provide a baseline which is widely acknowledged, if not universally accepted, and provide a useful entry-point when developing hBMSC research.

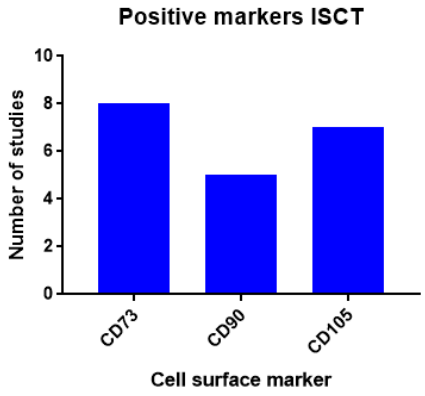

(a) Number of uses of ISCT proposed hBMSC positive cell surface markers

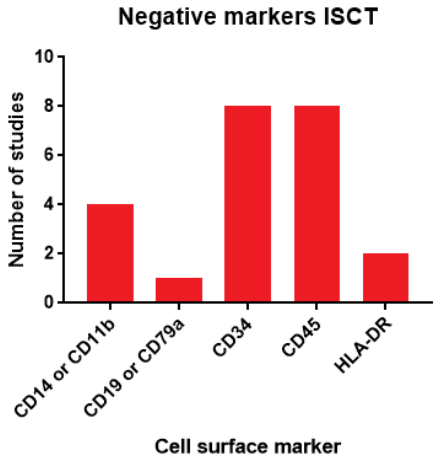

(b) Number of uses of ISCT proposed hBMSC negative cell surface markers

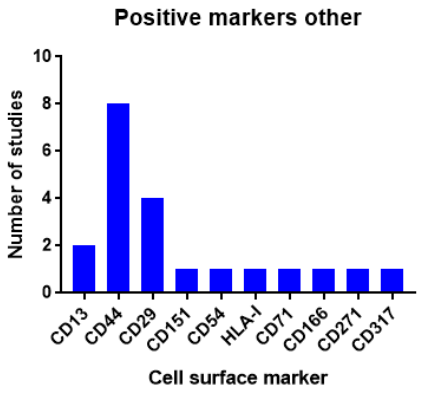

(c) Number of uses of non-ISCT proposed hBMSC positive cell surface markers

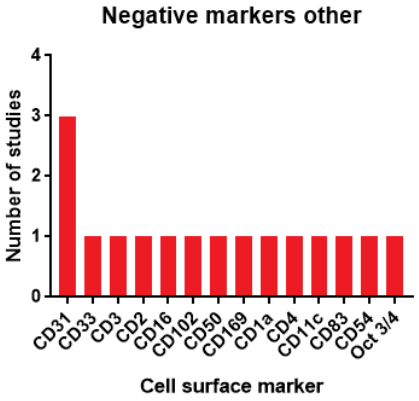

(d) Number of uses of non-ISCT proposed hBMSC negative cell surface markers

Fig. 1.10 Cell surface markers used for hBMSC identification by flow cytometry

Cell surface markers used for the flow cytometric characterisation of hBMSC in papers published since announcement of the ISCT guidelines. (Adesida et al. 2012; W. Chen et al. 2018; James et al. 2015; J. Kim and Hematti 2009; Poggi et al. 2005; Prasanna et al. 2010; Sacchetti et al. 2007; Sotiropoulou et al. 2006; Wagegg et al. 2012).

1.5.4 Pathways and culture conditions for *in vitro* tri-lineage differentiation of BMSCs

During this thesis, the terms 'osteogenesis', 'chondrogenesis', and 'adipogenesis' will be used to refer to specific BMSC differentiation pathways. To clarify exactly what is meant by these terms, there follows a brief discussion of the differentiation pathways and associated culture conditions each refers to.

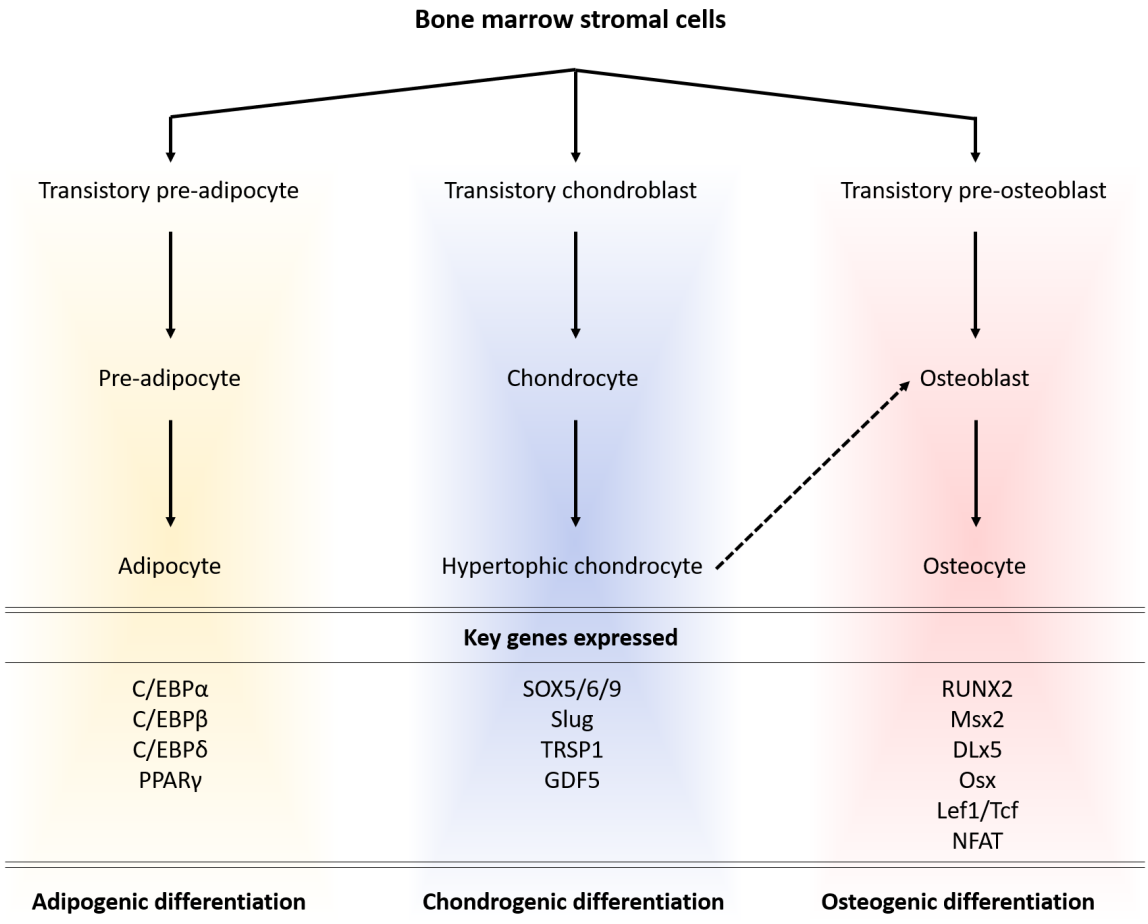

Fig. 1.11 Adipogenic, chondrogenic, and osteogenic differentiation pathways

Outline of differentiation pathways induced by *in-vitro* stimulation of BMSC (Bateman et al. 2016; Green et al. 2015; Karahuseyinoglu et al. 2008).

Chondrogenic differentiation

During chondrogenic differentiation, BMSC become chondrocytes, matrix-secreting cells responsible for the production of cartilage, as shown in fig. 1.11. In the context of osteochondral repair, chondrocytes are a highly desirable cell type at the joint surface, where, ideally, they would produce articular

hyaline cartilage to contribute to the infill of chondral defects. Chondrogenic differentiation of BMSC takes around 14 days.

Chondrogenic differentiation *in-vitro* is stimulated by the addition of proline, Transforming Growth Factor β1 (TGFβ1), Ascorbic Acid Phosphatase Ascorbic Acid Phosphate (AAP), ITS supplement, and dexamethasone to serum-free medium. The key component of the supplement which initiates the chondrogenic response is the TGFβ1. TGFβ1 stimulates the MAP kinase and Wnt pathways through upregulation of p38, ERK-1, and JNK, resulting in the modulation of N-Cadherin and N-CAM (Franceschi and Iyer 1992; Xiao et al. 2009). N-Cadherin initiates, and N-CAM stabilises, the condensation of BMSC which begins the commitment of the cells to the chondrogenic lineage (Tavella et al. 1994). TGFβ1 also increases expression of chondrocyte-related genes, particularly collagen II and aggrecan, and its effects on chondrogenesis are potentiated by the addition of the glucocorticoid dexamethasone to the medium (Shintani and Hunziker 2011; W. Wang et al. 2014). The amino acid proline is added due to its necessity for collagen synthesis, since proline and hydroxyproline account for around 23 % of collagen by mass; AAP is crucial for the hydroxylation of proline to form hydroxyproline, without which the correct helical structure of the collagen strand cannot form (Barbul 2008; Franceschi and Iyer 1992). ITS supplement contains Insulin, Transferrin, and Sodium Selenite, and is a common supplement in differentiation media, which has been shown to have effects on chondrogenic differentiation through interaction with p38, ERK-1, and JNK /glsWatanabe2001.

In addition to the biochemical environment, the physical cellular environment is also important for chondrogenic differentiation. Low oxygen tension, or hypoxic, conditions have been shown to enhance chondrogenesis as a result of increased proliferation, inhibition of osteogenesis, and greater upregulation of chondrogenic genes such as Collagen II (Sheehy et al. 2012). Furthermore, a 3D culture environment, such as pellet cultures, is required for chondrogenesis to ensure that the BMSC develop and maintain the rounded morphology which is a key feature of condensation during early chondrogenic lineage commitment (Johnstone et al. 1998).

Osteogenic differentiation

Bone is a dynamic tissue which is remodelled through finely balanced anabolic and catabolic cell activities. In a highly simplified model, osteoclasts, break down the bone matrix, while osteoblasts secrete the calcified matrix. Unlike osteoclasts, which are derived from myeloid progenitor cells, cells of the osteoblastic lineage, including osteoblasts and osteocytes, are derived from osteochondral progenitor cells: BMSC (fig. 1.11). Due to this shared heritage with chondrocytes, there are similarities in the media used for differentiation. Indeed, hypertrophic chondrocytes are capable of differentiating into osteogenic lineage cells (Bateman et al. 2016).

During osteochondral repair following MF/MD, osteogenic differentiation is not desirable at the joint surface. However, the subchondral bone is perforated during the surgery, and this must be repaired to provide a stable base for the regenerated cartilage. Indeed, it has been suggested that some of the success of MF/MD is due to the stimulation of repair processes within the subchondral bone (de Vries–van Melle et al. 2014).

In-vitro, osteogenic differentiation is stimulated using medium supplemented with dexamethasone, AAP, and β-glycerophosphate, and takes around 21 days. dexamethasone contributes to positive regulation of Runt-related Transcription Factor 2 (RUNX-2), a transcription factor widely regarded as a master regulator of function, gene expression, and differentiation in osteoblasts (Bruderer et al. 2014). This regulation is accomplished through increased transcription of FHL2, TAZ and MKP1 (Langenbach and Handschel 2013; Thiagarajan et al. 2017). FHL2 stimulates translocation of β-catenin to the nucleus, leading to increased transcription of RUNX-2, TAZ regulates the activity of RUNX-2 while also inhibiting adipogenesis, and MKP1 regulates RUNX-2 phosphorylation. AAP and β-glycerophosphate also enhance RUNX-2 activity through activation and phosphorylation of ERK1/2, which translocates to the nucleus, binds RUNX-2 and leads to upregulation of osteogenic gene expression, such as BMP-2 via the cyclic-AMP / protein kinase A pathway (Tada et al. 2011; Xiao et al. 2009). β-glycerophosphate also acts as a source of phosphates for mineralisation, although the concentration in the differentiation medium must be carefully optimised to avoid dystrophic mineralisation (Langenbach and Handschel 2013; Tada et al. 2011). Similar to the chondrogenic medium, AAP has a role in supporting collagen production, although during osteogenesis this is collagen I, since the presence of collagen I in the extra-cellular matrix is essential for osteoblast differentiation (Xiao et al. 2009).

Unlike chondrogenic differentiation, osteogenic differentiation is typically performed on monolayers of cells. In addition, normoxic conditions are considered optimal for osteogenic differentiation (Wagegg et al. 2012).

Adipogenic differentiation

Adipogenic differentiation stands apart from both chondrogenic and osteogenic differentiation. While the latter two pathways are related and there is some level of cross-talk between them, adipogenic differentiation is more distinct. This is fortunate in the context of osteochondral repair, since formation of adipocytes within the joint is highly undesirable. The adipogenic differentiation pathway leads to the formation of adipocytes, lipid-storing cells which are the primary cell type found in adipose tissue, as outlined in fig. 1.11.

The distinction of the adipogenic pathway extends to the medium used *in-vitro* for BMSC differentiation. Similar to osteogenic differentiation, adipogenic differentiation is performed in monolayer

cultures, but instead takes around 14 days. Due to the number of components required, their identities and functions are summarised in table 1.2.

Table 1.2 Medium supplements used during adipogenic differentiation

A summary of the supplements and functions thereof in adipogenic differentiation medium (Kuri-Harcuch et al. 1978; Obregon 2008; Styner et al. 2010; XingYun Wang et al. 2018; Xu et al. 2009).

Supplement	**Function**
Biotin	Co-enzyme for lipoprotein lipase and glycerophosphate dehydrogenase, the primary adipogenic enzyme
dexamethasone	Similar to in chondro- / osteogenic media, potentiates adipogenesis, increases cyclic-AMP and lipolysis
Indomethacin	Suppresses Cox-2, and increases PPAR-γ and C/EBPβ expression in a prostaglandin-independent manner
Insulin	Hormone influencing pro-adipogenic transcription factor expression, including PPARγ and FABP4
Isobutyl methylxanthine	Stimulates the cyclic-AMP-dependent protein kinase pathway, leading to upregulation of C/EBPβ
Pantothenic acid	B vitamin, similar to Biotin, which supports differentiation and increases lipid accumulation
Transferrin	As for pantothenic acid
Triiodothyronine	Increases expression of UCP-1 and PPAR-γ, enhancing differentiation and adipogenic metabolic activity

1.5.5 Use of hBMSC in cellular therapy

Due to their proposed regenerative properties and ability to home to sites of damage, BMSC have been used in therapies for conditions as disparate as cardiovascular disease, spinal lesions, diabetic nephropathy, acute respiratory distress syndrome, and sepsis (see fig. 1.12), and have shown moderate-to-good results in terms of outcomes in studies ranging from animal models through to Phase I and II clinical trials in humans (Espinoza et al. 2016; Khalilpourfarshbafi et al. 2017; Y.-C. Kim et al. 2016; Lalu et al. 2016; Quevedo et al. 2009). How BMSC (or similar cells from other tissues) contribute to repair and regeneration is not completely understood. Two key models of contribution have been suggested: cell replacement and cell empowerment, which can alternately be termed cell autonomous / direct and cell non-autonomous / indirect respectively (Ying Wang et al. 2014). In the cell replacement model, the progenitor cells differentiate into the cell types found within the damaged tissue and restore its structure and function. In the cell empowerment model, the same progenitors do not engraft into the tissue, but instead modulate the growth environment to enable and support intrinsic repair processes, for example through recruitment or immunomodulation.

In many studies, the influence of BMSC on repair does appear to be through cell empowerment or paracrine mechanisms. For example, a review of seven studies using BMSC to treat diabetic nephropathy showed the BMSC homed to the site of damage and resulted in improved repair outcomes (Khalilpourfarshbafi et al. 2017). However, examination of the mechanisms by which the BMSC

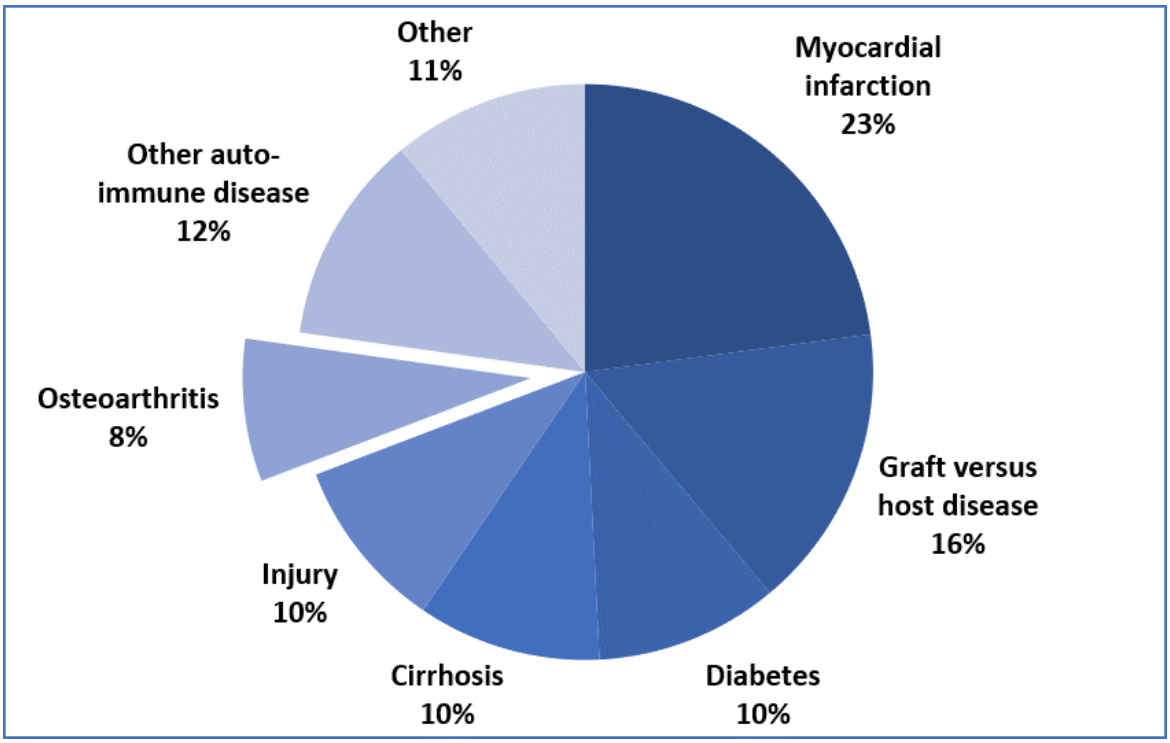

Fig. 1.12 Use of hBMSC in cellular therapies

Distribution of clinical trials using hBMSC as a treatment for various conditions. Based on data from Wei et al. 2013

contributed to repair showed that the majority of effects were mediated through paracrine mechanisms, such as through hepatocyte growth factor secretion, downregulation of Glucose Transporter 1 (GLUT1) membrane localisation, or upregulation of Vascular Endothelial Growth Factor (VEGF) and B-cell lymphoma 2 (Bcl-2) genes. A recent systematic review by Phinney and Pittenger examined 35 papers using cell free therapies based on BMSC exosomes, small extracellular vesicles released by BMSC which contain Ribonucleic Acid (RNA) and/or proteins that have paracrine effects on cells (Phinney and Pittenger 2018). The exosomes were used to treat a range of diseases including myocardial infarction, liver fibrosis, pulmonary hypertension and skin wounding: significant improvements in repair were seen in all of these models. While the study of exosomes is in its infancy, this provides strong evidence that BMSC are able to support repair through cell empowerment.

With regards to hBMSC contribution to repair through cell replacement, engraftment and differentiation of BMSC correlate to improved repair outcomes: studies into BMSC therapy in cardiomyopathy have found that BMSC engraftment is strongly correlated to improved repair outcomes, and that the BMSC contribute to the repair by differentiating into relevant cell types (Quevedo et al. 2009). This provides evidence that BMSC are involved with repair through cell replacement. Furthermore, a spinal lesion study showed that BMSC introduced into a spinal lesion with a scaffold showed higher engraftment and differentiation into neuronal cell types, indicating that BMSC are capable of

direct contribution to repair in multiple tissues (Y.-C. Kim et al. 2016). However, the BMSC were also secreting neurotropic factors and thereby supporting other cell types to effect the repair and regeneration. It is most likely that BMSC have a combinatorial influence on repair and regeneration, both contributing directly and supporting cell types. The relative contributions from the direct and indirect mechanisms are not currently known and may be heavily context dependent.

1.6 Cellular contributions to fracture repair

1.6.1 Bone Marrow Stromal Cells in fracture repair

The role of BMSC in fracture repair has been a long-term focus of study in the field of regenerative medicine. The success of therapuetic BMSC administration for example following myocardial infarction, has demonstrated their repair and regenerative potential (N. F. Huang et al. 2009; Lipinksi and Epstein 2016; Quevedo et al. 2009). Furthermore, the osteogenic properties of bone marrow have been known since the mid-19th century due to the work of Goujon (Goujon 1869) as described in (Bolontrade and García 2016) (see section 1.5.1). In addition, the work of Goujon's contemporary, Cohneim showed that fibroblastic cells, now known to be BMSC, migrate to sites of damage from the bone marrow (Rodríguez-Merchán and Liddle 2016). More recent studies have shown that BMSC have key roles in fracture repair, not only related to their differentiation potential, but also their secretory and immuno-modulatory roles as well as their ability to home to sites of damage for targeted drug-delivery purposes.

The importance of BMSC in fracture repair has been demonstrated in various ways. In a murine fracture model it was found that ovariectomy resulted in delayed and impaired bone repair (Pang et al. 2015). The study showed that the ovariectomy resulted in significantly lower BMSC numbers in both the peripheral blood and the bone marrow in the early stages of fracture (up to 72 hours post-injury), indicating both decreased BMSC numbers and mobilisation. The impaired repair was attributed in part to the decreased BMSC numbers, in addition to the hormonal perturbation resulting from the ovariectomy. In addition, exogenous administration of BMSC can lead to improved repair of large segmental bone defects in both animal models and human trials, compared to scaffolds alone, or segmental bone transplantation (Y. Chen et al. 2017; Dupont et al. 2010; Petri et al. 2013). Fluorescent tracking of administered BMSC labelled with fluorescent quantum nanocrystals (Q-dots) showed fluorescence could be detected at the defect site up to 12 weeks after administration, although the animals used in the tracking study did not show any bridging in the segmental defect and many Q-dots were found to be associated with macrophages.

Another piece of evidence for the importance of BMSC in fracture repair is the mobilisation and recruitment of the cells to the region of fractured bone. A fracture-repair study in mice using Green

Fluorescent Protein labelled Mesenchymal Stromal Cell (GFP-MSC) injected into the tail vein showed that GFP-MSC could be detected within the fracture site three days after injection (Granero-Moltó et al. 2009). Homing appeared to be mediated by the C-X-C motif chemokine Ligand 12 (CXCL12) (also Stromal Cell-Derived Factor 1 (SDF-1)) - C-X-C Motif Chemokine Receptor Type 4 (CXCR4) axis (CXCL12-CXCR4 axis), although only a subset of GFP-MSC homed to the damage site; most of the injected GFP-MSC were trapped in the lungs. The GFP-MSC which were recruited to the site of damage could then be detected in a quiescent state within a tissue-specific stem cell niche for six months after injection, although they were not detected within the callus itself, suggesting that the BMSC were providing trophic support to the repair (Granero-Moltó et al. 2009).

The osteogenic properties of bone marrow suggest that a key role of BMSC might be migrating to the site of damage and differentiating into osteoblasts which then produce mineralised matrix. However, the aforementioned tracing studies show that labelled BMSC are not found, or found at low numbers, within the callus long-term, indicating that cell replacement is unlikely to be the sole mechanism through which BMSC contribute to repair. This means that BMSC also contribute through cell empowerment, supporting other cell types to repair the damage. Further evidence for this can be found in a study characterising the exosomes released from hBMSC which showed evidence for both cell empowerment and replacement occurring simultaneously (Xiaoqin Wang et al. 2018). This study found that as the BMSC differentiated down the osteogenic lineage, they released exosomes which themselves stimulated osteogenic differentiation relative to the differentiation stage of the BMSC from which the exosomes were derived. In the early stages of osteogenic differentiation, the exosomes were able to induce osteogenic commitment, but only late-stage exosomes could induce mineralisation. This demonstrates how BMSC are able to contribute directly to repair, while also supporting repair by other cell types in a stage- and time-dependent trophic manner.

Evidence for this empowerment paradigm also comes from studies looking at cell-free therapies based on BMSC products to improve fracture repair. For example, an osteotomy model in hypothyroid rats showed that treatment of the defect site, with medium preconditioned by culture with BMSC, enhanced the bone repair at the osteotomy site by reducing healing time and improving the biomechanical properties of the repaired bone (Sefati et al. 2018). The CXCR4 recruitment study, which could not localise BMSC to the fracture repair site, found that instead the BMSC contributed to repair by secretion of BMP-2 (Granero-Moltó et al. 2009). In addition, another group examined how BMSC-derived exosomes influenced murine fracture repair in a Complement component C9 precursor knockout (C9-/-) mouse (Furuta et al. 2016). These mice have reduced exosome release and bone union rate following fracture is also significantly decreased compared to wild-type. However, treatment of fractures in the C9-/- mouse with exosomes isolated from wild-type BMSC conditioned medium rescued the phenotype, restored C9-/- mouse fracture repair to that seen in the wild-type. Although a brief snapshot, these studies demonstrate the multiple pathways through which BMSC provide trophic support to the regenerative process through paracrine signalling. In summary, BMSC interact with

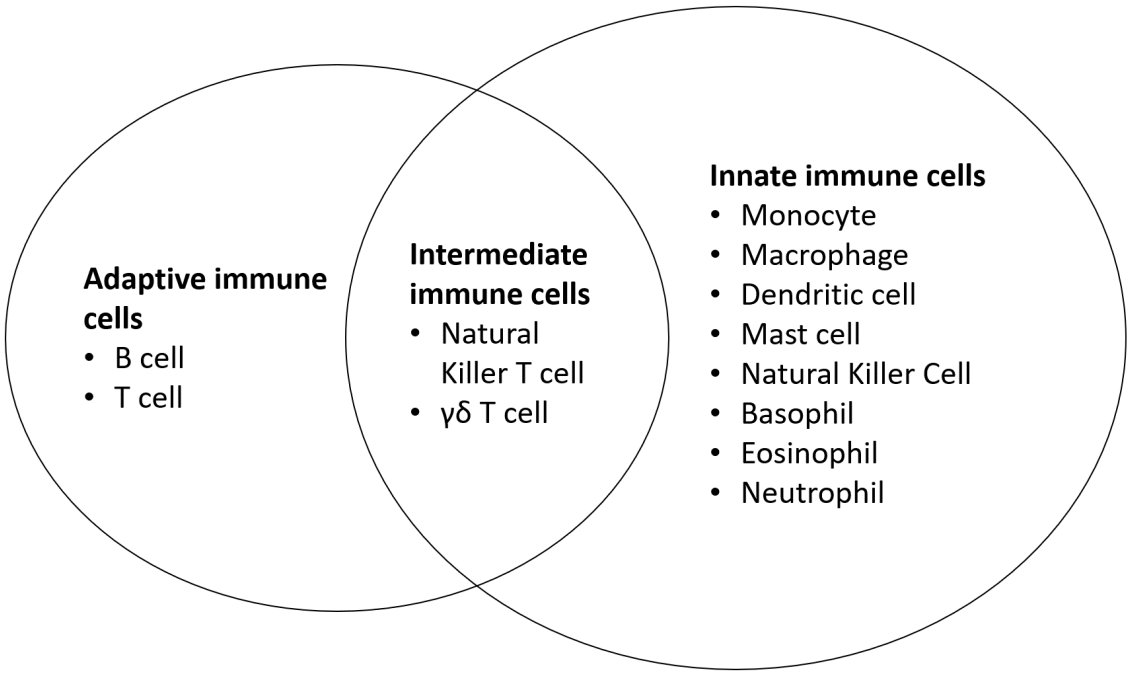

Fig. 1.13 Schematic showing division of immune cells into adaptive, intermediate, and innate cell types. Original work.

components of the immune system during repair and this results in altered contributions to the repair by both the immune cells and BMSC, and some of these specific interactions are explored in more detail in section 1.6.2.

1.6.2 Immune cell contributions to fracture repair

The immune system has a critical role in fracture repair. Severely immunocompromised mice show significantly impaired fracture repair, especially in the remodelling phase (Rapp et al. 2016). However, the individual immune cell subtypes have more nuanced roles in fracture repair. At first glance, the adaptive immune response appears to be detrimental to fracture repair. Recombination Activating Gene 1 knockout (RAG-1 -/-) mice, which lack an adaptive immune system, show more rapid fracture repair (Toben et al. 2011). However, this model removes all components of the adaptive immune system, obscuring the subtleties in how these cells contribute to fracture repair. The innate immune system has key roles in fracture repair, through a range of roles such as phagocytosis and cytokine release (Charles and Nakamura 2014). fig. 1.13.

Adaptive immune system: B-cells and T-cells

Following fracture, B and T cells infiltrate the injury in a two-wave process: there is an initial peak after 4 hours post-fracture, and then another peak after 21 days during re-vascularisation, with B-cells outnumbering T-cells at this point (Könnecke et al. 2014).

T-cells Studies in mice have shown that T-cells control the speed of endochondral ossification through manipulating the mineralisation of osteogenic cell types (Serra et al. 2012). CD4-positive T-helper cells, along with macrophages, are the dominant cell type in the haematoma 2 days post-fracture, despite CD8-positive cytotoxic T-cells being more prevalent in the bone marrow, indicating an enrichment for T-helper cells in the haematoma (Könnecke et al. 2014). In murine studies, CD8-positive cytotoxic T-cell enrichment in the haematoma which skews the CD8:CD4 ratio results in impaired regeneration, while depletion of CD8-positive cytotoxic T-cells enhanced repair in an osteotomy model (Reinke et al. 2013; Toben et al. 2011).

T-cells have bi-directional interactions with BMSC in fracture repair. Preconditioned medium from T-helper cells induces an osteogenic phenotype in BMSC by upregulating RUNX-2, osteocalcin and Bone Sialoprotein (BSP) production, possibly via TNFα secretion, while TGFβ1 from T-regulatory cells increase BMSC proliferation (El-Jawhari et al. 2016). Conversely, BMSC along with macrophages act to suppress the maturation of T-helper cells into Th1 / Th17 subtypes (Kovach et al. 2015). In a study looking at fibrosis following injury in mouse livers it was found that Bagg Albino inbred mouse strain c (BALBc) mice have a more severe fibrotic response than C57 black 6 inbred mouse strain (C57BL6) mice after trauma, attributed to the T Helper type 2 (Th2) skewed response in BALBc and T Helper type 1 (Th1) skewed in C57BL6 (Shi et al. 1997).

B-cells B-cells peak in numbers within the haematoma after around 4 hours post-fracture and are more numerous than T-cells in the haematoma during the remodelling phase (Könnecke et al. 2014). B-cells secrete both RANKL and OPG, being responsible for 64 % of total bone marrow OPG production in mice and are therefore key mediators of the OPG/Receptor Activator of Nuclear factor $\varkappa$ B (RANK)/RANKL axis (Y. Li et al. 2007). RANK/RANKL binding increases bone resorption by stimulating osteoclastogenesis, while OPG/RANKL binding blocks this and permits bone deposition (Boyce and Xing 2007). As a result, B-cells may have an important role in balancing bone deposition and resorption during the proliferative and remodelling phase of bone repair via their interaction with mature and precursor osteoclasts within the fracture callus (Schlundt, Hanna Schell, et al. 2013). Manipulation of fracture repair using B-cell therapy has not been performed although the manipulation of the OPG/RANK/RANKL pathway using monoclonal antibodies to reduce osteoporotic fractures and bone mineral density loss has improved health outcomes (Lacey et al. 2012). A study in skin lesions showed that application of naïve B-cells accelerated wound healing due to increased fibroblast

proliferation and anti-inflammatory effects, suggesting that B-cells may have other contributions to repair (Sîrbulescu et al. 2017).

Currently it is not known how B-cells might interact with BMSCs during fracture repair ((El-Jawhari et al. 2016). Studies have shown that BMSCs inhibit B-cell proliferation and activation, but functional consequences and bi-directional interactions have not been demonstrated (Kovach et al. 2015).

Intermediate immune system: T-cell subtypes

T-cell subtypes have been described which are considered intermediary between the innate and adaptive immune system: gamma-delta T-Cells ($\gamma\delta$ T-Cells) and Natural Killer T-cells (NKT-cells). Evidence regarding the role of $\gamma\delta$ T-Cells in fracture repair is mixed. On the one hand, murine studies have shown $\gamma\delta$ T-Cell deficient mice have improved fracture repair due to increased mineralised matrix production, although one study shows increased cartilage deposition while other work shows decreased tissue repair (Colburn et al. 2009). Conversely T-Cell Receptor δ Chain knockout (Tcrd-/-) mice which are also $\gamma\delta$ T-Cell deficient show delayed fracture repair due to decreased progenitor proliferation (Jameson et al. 2002; Ono and Takayanagi 2017). $\gamma\delta$ T-Cells may interact with hBMSC through their role as major producers of Interleukin 17a (IL-17a), a mediator of osteoclastogenesis: Interleukin 17a knockout (IL-17a-/-) mice show impaired fracture repair as a result of low osteoblast numbers, which suggests that IL-17a has an apparent role in BMSC differentiation and proliferation (Ono, Okamoto, et al. 2016).

The role of NKT-cells in fracture repair is relatively unexplored, although work has been done in other tissues. In the skin, NKT-cell depletion accelerated wound closure and increased collagen deposition, possibly via TGFβ1 regulation, without influencing immune cell, specifically neutrophil and monocyte / macrophage, infiltration(Schneider et al. 2011). In the liver, NKT-cells have opposing effects on fibrosis through production of pro-fibrotic factors, such as IL-4, Interleukin-13 (IL-13) and osteopontin, and anti-fibrotic factors, such as IFNγ (B. Gao and Radaeva 2013). BMSC appear to negatively regulate NKT-cell numbers in liver injury, reducing the number of NKT-cells and preventing NKT-cell mediated hepatotoxicity (Milosavljevic et al. 2017).

Innate immune system

Mast cells and basophils Following fracture, mast cell numbers increase within the callus and appear to concentrate in the convex side, indicating a possible role in bone resorption during callus remodelling (Taniguchi 1990). In early repair, mast cells appeared to have a pro-inflammatory role: mast cell deficient mice showed decreased pro-inflammatory cytokines and bone remodelling and increased stiffness of regenerated bone compared to wild type mice (Kroner, Kovtun, Messmann,

et al. 2016). In a c-Kit independent mouse fracture model, mast cells induced both local and systemic immune response following trauma as well as increasing osteoclastogenesis and activation via histamine, leading to bone absorption (Kroner, Kovtun, Kemmler, et al. 2017). Excessive numbers of mast cells, or mastocytosis, results in osteopenia and is a feature of osteoporosis; mast cell numbers inversely correlate to bone density (Cundy et al. 1987; Frame and Nixon 1968). There is some indication that mast cells may have an important role in regulating BMSC differentiation during fracture repair (Ramirez-GarciaLuna et al. 2017). By comparison, very little is known about basophil contribution to fracture repair: they have striking similarities to mast cells, and so the contributions may also be similar.

Monocytes and macrophages Monocyte and macrophage infiltration peaks 48 hours post-fracture, followed by peak lymphocyte infiltration at 72 hours (Pence and Woods 2014). Along with neutrophils, macrophages are very important in repair pathways, and together with T-helper cells, are one of the dominant cell types in the haematoma 2 days after formation (Könnecke et al. 2014). Monocytes and macrophages are primarily circulating phagocytic cells which migrate to sites of damage or infection where they are involved with cytokine release, immuno-modulation, and debris clearance, although some macrophages are tissue resident (Geissmann et al. 2010). In addition, monocytes are able to differentiate into effector cell types during repair, primarily macrophages but also dendritic cells. Macrophages are arguably the most important cell type derived from monocytes in terms of fracture repair. They are a highly heterogeneous population of cytokine-producing phagocytic cells with multiple polarisation subtypes. Aside from their ability to differentiate into macrophages, monocytes have important roles in fracture repair. During fracture repair, monocytes appear to have multiple bi-directional interactions with BMSC. In the first place, monocytes are able to recruit BMSC to fracture sites through Monocyte Chemoattractant Protein 1 (MCP-1) / C-C Motif Chemokine Receptor 2 (CCR2) signalling (Ishikawa et al. 2014). Following BMSC recruitment, monocytes appear to contribute to osteogenic differentiation of BMSC within the callus, regulating BMSC matrix mineralisation, and osteoblast differentiation through Signal Transducer and Activator of Transcription 3 (STAT3) signalling (Guihard et al. 2018; Nicolaidou et al. 2012). Evidence for bi-directional interactions in fracture repair comes from the observation that BMSC induce monocytes to differentiation into macrophages with a reparative and pro-angiogenic M2 phenotype (Guihard et al. 2018).

Macrophages Macrophage deficient mice show delayed cartilage resorption, poor revascularisation and lowered endochondral ossification during development (Schlundt, El Khassawna, et al. 2018). However, local macrophage depletion did not show an effect on early soft callus formation or repair but instead was more critical in the hard callus (Y. Y. Yu et al. 2012). In addition, the various macrophage subtypes appear to contribute in different ways to repair. Following fracture, circulating monocytes

infiltrate, differentiate and polarise into macrophages, which can be broadly grouped into two major subtypes, each of which can be further subdivided: proinflammatory M1 and immuno-modulatory M2 (Wu et al. 2013). The ratio of M1 : M2 macrophages appears to modulate fracture repair. Macrophages naturally skew towards the M2 phenotype in fracture repair: if this is enhanced, bone formation is increased, while M1 enrichment compromises the repair outcome (Schlundt, El Khassawna, et al. 2018).

Similar to monocytes, both M1 and M2 polarised macrophages have been implicated in BMSC osteoblast differentiation via secretion of BMP-2 and Oncostatin M, as well as recruitment of BMSC to the injury site through secretion of factors such as CCL2, CXCL8 and SDF-1 (Gu et al. 2017; Lu et al. 2017; Pajarinen et al. 2018). Both monocytes and macrophages appear to have important regulatory roles in fracture repair, including controlling BMSC contribution to repair through a variety of mechanisms.

Dendritic cells Dendritic Cell (DC) contribution to fracture repair appears to be through production of trophic factors, particularly Dendritic Cell Specific Transmembrane Protein (DC-STAMP) which is elevated in humans following fracture (Chiu and Ritchlin 2016; Chiu, Sheu, et al. 2015). DC-STAMP modulates interactions between osteoclasts and osteoblasts, as well as osteoclast differentiation thereby regulating bone resorption (Chiu, Schwarz, et al. 2017). In a murine fracture model, mice with a DC-STAMP knock out showed delayed bone repair (Chiu and Ritchlin 2016). Studies in mice have shown that DCs can differentiate into osteoclasts after interaction with CD4-positive T helper cells, suggesting a more active role in remodelling (Alnaeeli et al. 2006; Wakkach et al. 2008). DC-BMSC interactions are less described. DC are known to secrete Interleukin 2 (IL-2) leading to Th1 differentiation in T cells. This is prevented by IL-10 secretion from BMSC, indicating a potential regulatory interaction (Kovach et al. 2015).

Neutrophils Neutrophils are the most rapidly recruited cell type following fracture, arriving within 6 hours of fracture (Pence and Woods 2014). On arrival at the site of sterile trauma, they phagocytose debris and dying cells, and contribute to the initiation of the inflammatory phase (El-Jawhari et al. 2016). Treatment of fracture with TNFα recruits further neutrophils and macrophages, improving repair (Chan et al. 2015). Further, local depletion of neutrophils prior to fracture in mice resulted in increased cytokine production and macrophage recruitment leading to decreased bone deposition and callus strength after 21 days (Kovtun et al. 2016). However, chronic stimulation of trauma with damage associated molecular patterns resulted in increased scarring due to increased recruitment of neutrophils and persistent inflammation (Qian et al. 2016). This indicates a critical role for neutrophils in modulating the inflammatory environment in the early callus and the critical time-dependent nature of the repair process. Neutrophils also appear to have a physical contribution to fracture repair. A study in human patients indicated that fibronectin extracellular matrix was synthesised by neutrophils

in the 48 hours following initial trauma. (Bastian et al. 2016).There is little evidence for direct neutrophil-BMSC interaction during fracture repair. However, neutrophils may be important in the recruitment of BMSC; neutrophils secrete CCL2 and CXCL8 in response to fracture environments, which recruit monocytes and BMSC to the site of damage (Edderkaoui 2017).

Eosinophils Eosinophils are recruited to the fracture by the Th2 response and appear to be involved with the remodelling phase of bone repair (Chaplin 2010). Along with neutrophils and basophils, eosinophils express Complement 5a Receptor 1 (C5aR1), the complement 5 receptor. This is a key stimulator of bone resorption via osteoclastogenesis through the OPG/RANK/RANKL pathway; upregulation of this receptor impaired fracture healing in a murine model (Bergdolt et al. 2017). Further, Complement 5 knockout (C5-/-) mice have smaller callus formation and decreased mechanical strength compared to wild type (Ono and Takayanagi 2017). Eosinophils may contribute to fracture repair through this pathway. Other than generalised immunomodulatory functions, there is very little information on the interaction between BMSC and eosinophils during fracture repair.

Natural killer cells The exact contributions of Natural Killer (NK) cells to bone repair are still not clear; their contribution to fracture repair does not seem to be through their cytotoxic ability, although they do appear to have a trophic influence. NK cells do appear to have an involvement with osteoclastogenesis from monocytes through production of RANKL and Macrophage Colony Stimulating Factor (M-CSF) (Söderström et al. 2010). They are also potent producers of IFNγ and TNFα, already discussed as important in fracture repair (Chan et al. 2015; Toben et al. 2011). NK cells have roles in recruiting BMSC to sites of injury, and also prime the BMSC for repair through their IFNγ production (El-Jawhari et al. 2016). Studies on the direct interactions between BMSC and NK cells have shown mixed results. On the one hand, some studies have shown that NK cells have a cytotoxic effect on BMSC ((El-Jawhari et al. 2016), while others suggest that NK cells either do not lyse or display minimal cytotoxic behaviour towards BMSC (Almeida et al. 2012). Inversely, BMSC appear to suppress the proliferation, cytotoxic behaviour and cytokine production of NK cells (Sotiropoulou et al. 2006). This would indicate that BMSC-NK cell interactions are immunoregulatory and bidirectional, but their exact contributions to fracture are still incompletely understood.

1.6.3 Haematopoietic stem and progenitor cells in fracture repair

Haematopoietic stem and progenitor cells (HSPC) are known to have complex interactions with BMSC: within the bone marrow niche, interactions between the populations maintain quiescence and support haematopoiesis (Greenbaum et al. 2013; Méndez-Ferrer et al. 2010; Morrison and Scadden 2014; Walenda et al. 2010). A small pool of HSPC is present in the peripheral blood, with this number increasing following fracture, indicating a mobilisation response to trauma (Mehrotra et al. 2013)).

Fracture callus size and bone mineral density was improved in mice injected with AMD3100 (a CXCR4 antagonist), which mobilises stem and progenitor populations, including endothelial stem cells, BMSC and HSPC into the blood via the CXCR4 axis (Toupadakis et al. 2013). Once in the blood, these cell types migrate to sites of damage and may contribute to the improved fracture repair seen in the mice. At sites of injury, interactions between BMSC and HSPC appear to improve vasculogenesis: in a co-transplantation study, a gel containing a mix of HSPC and BMSC, or the cells alone, was implanted subcutaneously into a mouse (Moioli et al. 2008). Gels containing the mixture showed improved angiogenesis when compared to the single population gels. This would suggest that BMSC and HSPC have synergistic roles within fracture repair, although the mechanism is not fully known.

1.7 Summary

To summarise, OA is a large and growing health problem, which requires novel repair and regenerative strategies targeting the early stages of the disease. A group of possible candidate therapies are bone marrow stimulation techniques, which have been shown to have potential for treating early stage OA and cartilage defects, but result in repair tissue with suboptimal biomechanical properties and clinical performance. As a result, while the therapy has promise, greater understanding of the biology of the repair and regeneration occurring is needed to enable optimisation.

Bone marrow stimulation is based on the intrinsic regenerative properties of BMSC, which are introduced to the joint surface in a marrow clot during the therapy and assist in the repair and regeneration of the damaged region. Other therapies are already successfully using BMSC to treat a diverse range of conditions. BMSC are known to have key roles in fracture repair, although whether this is through indirect or direct contributions is currently not completely understood. At any rate, the BMSC within the marrow clot are certain to interact with populations of cells from the peripheral blood, primarily immune cells, which are trapped within or attracted to the region of damage. Drawing from research into immune involvement in fracture repair, it is clear that the interactions, both paracrine and cell-to-cell, between BMSC and peripheral blood / immune cells have consequences for the outcome of repair, although the knowledge in this area is by no means complete. Greater understanding of these interactions within the environment of the marrow clot could indicate targets which could be exploited by therapeutic intervention to improve repair outcomes. This body of work aimed to increase the understanding of BMSC-peripheral blood cell interactions within the environment of a marrow clot for osteochondral repair.

The aims of this work were:

1. To isolate robust, well-characterised populations of hBMSCs from human sources under normoxic and hypoxic culture conditions.

2. To identify a subpopulation of cells within the peripheral blood inducing significant migration in hBMSC in hypoxic and/or normoxic conditions

3. To characterise the interactions between NK cells and hBMSCs under normoxic and hypoxic conditions.

4. To characterise the interactions between monocytes and hBMSC under normoxic and hypoxic conditions.

Chapter 2

Methods

A list of equipment and reagents used may be found in Supplementary data (table A.2,table A.3).

2.1 Cell culture

2.1.1 Human Umbilical Vein Endothelial Cells

Human Umbilical Vein Endothelial Cells (HUVECs) were obtained from Lonza. For basic maintenance, cells were grown in complete HUVEC culture medium (Medium 199 4-(2-Hydroxyethyl)-piperazine-1-ethanesulfonic acid, N-(2-Hydroxyethyl)piperazine-N'-(2-ethanesulfonic acid) (HEPES) modification, 20 % volume per volume (v/v) Fetal Bovine Serum (FBS), 2 mmol L-Glutamax, 5 µg/ml Gentamicin, 1.5 µg/ml Amphotericin B, 50 ng/ml Endothelial Cell Growth Supplement (ECGS), 100 ng/ml Heparin) in T-75 flasks coated with 1% v/v Gelatine in Phosphate Buffered Saline (PBS), pH 7.4, under normoxic culture conditions (Normoxia / normoxic culture conditions: humidified tissue culture incubator at 37 degrees Celsius (°C), 5 % carbon dioxide (CO_2), 18.6 % oxygen (O_2) (ambient within normoxic incubator)). Initial seeding density was at 2500 cells per square centimetre (cm^2). Cells were passaged at between 80 to 90 % confluence as described in section 2.1.3, unless cells were at more than 50 % confluence prior to a 72 hour interval between feeds when cells were passaged at a lower confluence. During feeding or passaging, supernatants were centrifuged at 300 Relative Centrifugal Force (RCF), 5 minutes, room temperature to pellet suspension cells that were reintroduced to the culture. Excess cells were cryopreserved as described in section 2.1.3 using HUVEC culture medium with 5 % Dimethyl Sulfoxide (DMSO) instead of Cryopreservation Medium (FBS, 10 % v/v DMSO).

2.1.2 Isolation and culture of human primary adherent bone marrow cells

Bone marrow was obtained from total knee replacements from patients aged between 64 to 87 (Average 75.2 ± 9.7 years), both male and female, with consent. The marrow originated in the medullary cavity and was removed following femoral cuts during prosthetic sizing by the surgical team. Immediately after extraction, marrow was placed into a tube containing 5 ml of 400 µg/ml heparin sulphate solution.

Marrow was manually dissociated through 70 µm filters into 50 ml Falcons using a 5 ml syringe plunger, rinsing with Flow cytometry buffer (PBS with 3 % v/v FBS, and 5 mmol Ethylenediaminetetraacetic Acid (EDTA)) until no residual pink colouration could be seen. The cells were centrifuged at 300 RCF, 10 minutes, room temperature (spin-washed) and the fat and supernatants discarded. Pellets were pooled in a fresh 50 ml Falcon tube in Flow cytometry buffer and centrifuged at 300 RCF, 5 minutes, room temperature. This transfer and spin-wash was repeated twice more. Cells were then counted as described in section 2.1.3 at an appropriate dilution.

Cells were centrifuged at 300 RCF, 5 minutes, room temperature, resuspended in Complete Medium B (αMEM without nucleosides with 10 % v/v FBS, 2 mmol L-GlutaMAX, 5 µg/ml Gentamicin, and 1.5 µg/ml Amphotericin B, 10 ng/ml Fibroblast Growth Factor 2, and 14 µg/ml L-Ascorbic Acid Phosphate) and seeded into tissue culture flasks at 1×10^7 cells/cm^2. Flask size and number was determined by the cell yield. Flasks were maintained under either Normoxic or Hypoxic culture conditions for 72 hours. The flasks were washed with PBS and complete Medium B was added. Suspension cells were discarded. This wash step was repeated again after 96 hours. Cultures were maintained as in section 2.1.3.

2.1.3 Basic cell culture and maintenance

Cells were maintained as follows, unless specified within the relevant subsection.

Full medium changes were performed every 2 to 3 days into the appropriate culture medium. Cells were grown to between 70 to 80 % confluence before passaging. The flasks were rinsed with PBS and incubated with 5 ml 1x TrypLE Express for five minutes under either normoxic or hypoxic culture conditions. Flasks were gently agitated, and culture medium was added and triturated between 5 to 8 times, ensuring that the flask base was thoroughly rinsed. The cell suspension was transferred to a 50 ml Falcon tube and centrifuged at 300 RCF for 5 minutes at room temperature, resuspended in culture medium and quantified using a disposable haemocytometer, at an appropriate dilution. Three large squares were counted for each sample, and the average taken. This was accepted only if all counted values lay within 10 % of the mean, otherwise the count was repeated using a fresh sample. Calculations were performed as follows:

$$\text{cells/ml} = \text{cells}_{\text{average}} \times \text{dilution} \times 10^4$$

$$\text{cells}_{\text{total}} = \text{cells/ml} \times \text{volume}_{\text{total}}$$

The same procedure was followed to harvest cells for assays. Cells for assays were taken from all cultures between passage 2 to 4.

Following counting, an aliquot containing an appropriate number of cells, determined by the seeding density of the specific cell type as well as the required size of flask was resuspended in an appropriate volume of culture medium. 6 ml of medium was added to T-25 flasks, 15 ml to T-75 flasks, and 25 ml to T-175 flasks. Primary adherent bone marrow cells / bone marrow stromal cells were seeded at 2300 cells/cm^2 for human culture. Seeding density for other cells are recorded in the relevant section.

Expanded populations were cryopreserved after counting by centrifuging at 300 RCF, 5 minutes, room temperature and resuspending in Cryopreservation Medium (FBS with 10 % DMSO v/v). Aliquots were placed into labelled cryovials and frozen between −70 to −80 °C (departmental practices changed the temperature of the freezer from −80 to −70 °C during the study) in a CoolCell. After 24 to 48 hours, cells were transferred to long-term storage either within the −70 to −80 °C freezer, or within a liquid nitrogen storage system at −196 °C.

Cells were thawed by immersing the cryovial into a water bath at 37 °C until a small piece of ice remained. 1 ml of culture medium was added to the vial and the contents transferred to a 50 ml Falcon tube. 8 ml of culture medium was added to the cells over a period of 2 minutes, then 6 ml over a period of 1 minute. Cultures were centrifuged at 300 RCF, 5 minutes, room temperature and seeded as previously described within this section for culture.

2.2 Cell characterisation

Cells at 70 to 80 % were used between Passage 1 to 3. Cells were detached and counted as in section 2.1.3. Images were captured using a standard digital camera, or Leica light microscope at 100x magnification.

2.2.1 Osteogenic differentiation

Osteogenic differentiation *in vitro* drives bone marrow stromal cells down the osteogenic lineage, and may lead to osteocyte formation. Regions of mineralisation are commonly identified *in vitro*

by Alizarin Red staining; the stain reacts with calcium to form a crimson-red chelation complex. (Puchtler et al. 1969).

Cells were seeded into T-25 flasks or twelve well plates at 5×10^3 cells/cm^2 in culture medium and incubated for 2 hours under either normoxic or hypoxic culture conditions. The monolayers were rinsed with PBS, culture medium was added to control wells, and Osteogenic Medium (DMEM with high glucose and GlutaMAX with 10 % v/v FBS, 50 µg/ml L-Ascorbic Acid Phosphate Sesquimagnes, 10 mmol β-glycerol phosphate, 10 nmol dexamethasone) was added to test wells. Cultures were returned to the appropriate incubator and maintained for 21 days, with 50 % medium changes every 2 to 3 days.

After 21 days, cultures were rinsed with PBS and fixed with 10 % weight per volume (w/v) formalin for 30 minutes. Monolayers were rinsed twice with distilled water and stained with 2 % Alizarin Red (pH 4.2, w/v, pre-made) for 2 to 3 minutes. The monolayers were rinsed 3 times with distilled water and imaged.

2.2.2 Chondrogenic differentiation

Chondrogenic differentiation *in vitro* drives BMSC down the chondrogenic lineage, leading them to form chondrocytes that produce proteoglycan-rich matrix (Johnstone et al. 1998). Alcian blue staining binds to glycosaminoglycans resulting in a distinctive blue stain. The name 'Alcian blue' refers to a family of dyes, but generally refers to Alcian Blue 8G and is a polyvalent basic dye based on copper phthalocyanine (Hayat 1993)

Cells were centrifuged at 300 RCF, 5 minutes, room temperature and resuspended at 1×10^7 cells/ml. Five 10 µl droplets of the cell suspension (each containing 1×10^5 cells) were placed into the wells of a 12 well plate. Droplets were left for 2 hours under normoxic or hypoxic culture conditions. In-house Chondrogenesis Medium (DMEM, 100 µg/ml Sodium Pyruvate, 40 µg/ml Proline, 50 mg/ml ITS+ premix, 5 µg/ml Gentamicin, 1.5 µg/ml Amphotericin B, 10 ng/ml TGFβ1, 0.1 mmol AAP, 100 mmol dexamethasone) was added to test wells, and culture medium to control wells. Cultures were maintained for 14 days at under normoxic or hypoxic culture conditions, with 50 % medium changes every 2 to 3 days.

After 14 days, cultures were rinsed with PBS and fixed with 10 % w/v formalin for 30 minutes. Following fixation, wells were rinsed with PBS and stained overnight with 1 % w/v Alcian Blue in hydrochloric acid. The following day, wells were rinsed 3 times with 0.1 normality (N) hydrochloric acid, neutralised with distilled water, and imaged.

2.2.3 Adipogenic differentiation

Adipogenic differentiation assays push BMSC to differentiate into adipocytes containing lipid droplets (Scott et al. 2011). Differentiated cells are identified by Oil Red O staining. Oil Red O is a lysochromic dye related to the diazo Sudan family of dyes (*Histopathologic Techniques* 2006). The dye accumulates within lipid droplets in cells, allowing differentiated adipocytes to be visualised.

Cells were then centrifuged at 300 RCF for 5 minutes at room temperature and resuspended in culture medium. Cells were seeded at 1×10^5 cells/cm^2 (1×10^4 cells per well) into the wells of a 12 well plate. Cells were left to attach for 2 hours at 37 °C, 5 % CO_2 under either normoxic or hypoxic culture conditions. Stempro Adipogenesis Medium (StemPro Adipocyte Differentiation Basal Medium with 10 % v/v StemPro Adipocyte Differentiation Supplement, 5 µg/ml Gentamicin) was added to test wells, and culture medium to control wells. Cultures were maintained for 14 days under either normoxic or hypoxic culture conditions with 50 % medium changes every 2 to 3 days.

After 14 days cultures were rinsed with PBS and fixed with 10 % w/v formalin for 30 minutes. Wells were rinsed with PBS and incubated for 5 minutes with 60 % v/v Isopropanol in water. Wells were stained with Oil Red O for 5 minutes. Following staining, wells were rinsed 3 times with distilled water and imaged.

2.2.4 Colony forming unit fibroblast assay

The Colony Forming Unit (CFU) assay is a method of quantifying the proliferative potential of a cell population. The ratio of colonies formed per cell seeded is an indication of the proliferation potential of the cell population.

Cells were centrifuged at 300 RCF for 5 minutes at room temperature, resuspended in culture medium and seeded at 250 cells per well into six well plate in triplicate. Cells were cultured under normoxic conditions for 10 days. Following this incubation, cells were stained for histological analysis. Wells were rinsed twice with PBS and fixed for 20 minutes in 10 % w/v formalin, rinsed twice with PBS and stained for 30 minutes with 1 % w/v Crystal Violet. Wells were then washed three times with PBS and imaged. The number of colonies over 2 mm in diameter (approximately 50 cells) was quantified by visual assessment. CFUs were calculated per thousand cells.

2.2.5 Flow cytometry

Flow cytometry is a method for both counting and categorising cells. Cells were passed through a flow chamber one at a time, and lasers shone through the cells. The light signals produced were then

captured by photomultipliers and interpreted to give measurements. Cells were categorised by their forward and side scatter (that can be equivocated to their respective size and internal granularity) or by their marker expression that was identified using distinct fluorescently conjugated antibodies. Multiple fluorescently conjugated antibodies were used simultaneously to phenotype cell populations.

A list of markers used within this thesis and their supposed functions may be found the the Supplementary material (table A.1).

Controls used for flow cytometry were:

- Single stain controls: experimental cells stained with a single fluorophore. One made for each fluorophore in the panel (see tables 2.1 to 2.5). Used to set up initial experiment voltages the first time the experiment was run.
- Unstained or negative control: experimental cells with no antibody staining. One made for each sample. Used to check for auto-fluorescence in the cell population in all experiments.
- Isotype control: experimental cells stained with the isotype control for each fluorophore used in the experiment: may be individual for single colour, or full panel for multiparametric (see tables 2.1 to 2.5). One made for each sample and fluorophore (single colour), or sample (multiparametric). Used to check for non-specific binding within the cell population in all experiments.
- Compensation controls: beads stained with a single fluorophore. One made for each fluorophore within the panel (See tables 2.1 to 2.5). Used to correct for spectral overlap within the panel (see tables 2.1 to 2.5). Used only in multiparametric experiments.
- Fluorescence Minus One controls: experimental cells stained with the full panel of fluorophores (see tables 2.1 to 2.5) minus one fluorophore. One made for each fluorophore within the panel (See tables 2.1 to 2.5). Used for correct localisation of positive and negative gating. Used only in multiparametric experiments as described in tables 2.2 to 2.5.

Cells were detached and counted as outlined in section 2.1.3. A minimum of 5×10^4 cells were taken for each sample and centrifuged at 300 RCF for 5 minutes at room temperature. Cells were resuspended in Flow cytometry buffer. A sample of the cells was put aside for the unstained control. See tables 2.1 to 2.5 for details of the individual flow panel used. For Panels 3, 4, 5, and 6 (tables 2.2 to 2.5 respectively), excess cells were pooled for Fluorescence Minus One (FMO) controls. All subsequent steps were performed cold and in the dark to prevent non-specific staining or bleaching. Centrifugation occurred at room temperature due to equipment restrictions. Stainings and quantifications were performed in 5 ml polystyrene flow tubes.

FMO controls were also stained with 1 % Zombie Aqua, excepting the Zombie Aqua FMO. Cells were then centrifuged at 300 RCF for 5 minutes at room temperature in Flow cytometry buffer. As

Table 2.1 Human characterisation flow cytometry panel

Antibody / fluorochrome	**Channel / Filter λ (nm)**
HLA-DR FITC	Blue 530/30
CD73 PerCP EFluor710	Blue 695/40
CD317 PE	Yellow 585/15
CD19 Pe-Cy5	Yellow 670/14
CD271 PE-Cy7	Yellow 780/60
CD146 BV421	Violet 450/50
Zombie Aqua	Violet 525/50
CD34 BV605	Violet 610/20
CD105 BV650	Violet 660/20
CD45 BV785	Violet 780/60
CD14 APC	Red 660/20
CD90 AlexaFluor700	Red 730/45

much supernatant as possible was removed without disturbing the pellet. The pellet was resuspended in this minimal residual medium and 4 µl Forward Chain Receptor (FCR) block was added to all samples. Cells were incubated for 10 minutes at 2 to 8 °C and Flow cytometry buffer was added to give a final volume of 100 µl.

Master mixes for each panel were prepared as below using volumes of antibodies determined by titration. Antibody titration was performed by creating a dilution series based on the initial manufacturer's concentration suggestion. For example, a range of 0, 0.5, 1, 2.5, 5, 7.5 and 10 µl antibody per test was used if the initial suggestion was 5 µl per test. A standardised number of cells was stained for each concentration in the same method as described above and quantified on the flow cytometer. The concentration giving the best separation between positive and negative populations was selected. This was performed for each new batch of antibody, hence concentrations are not given in tables 2.1 to 2.5.

The antibody and isotype master mixes as specified in tables 2.1 to 2.5 were divided equally between polystyrene flow tubes and the cell samples split equally between them. Where FMO controls were prepared (tables 2.2 to 2.5), all the antibodies or isotypes were added individually at the volumes specified, excepting the one corresponding to the control.

Cells were stained for 40 minutes at 2 to 8 °C and all samples (including unstained) were centrifuged at 300 RCF for 5 minutes at room temperature, resuspended in Flow cytometry buffer and filtered using a CellTrix 70 µm filter. Compensation controls were prepared using Compensation Beads in PBS with each fluorophore at the volume determined by titration. Samples were transported in the dark, on ice to the National Institute for Health Research Biomedical Research Centre (NIHR BRC) Cambridge Phenotyping Hub where quantification was performed using a modified Becton Dickinson

Table 2.2 Subpopulation screening flow cytometry panel

Antibody / fluorochrome	Channel / Filter λ (nm)
CD68 FITC	Blue 530/30
CD73 PerCP EFluor710	Blue 695/40
CD133 PE	Yellow 585/15
CD16 Pe-Cy5	Yellow 670/14
CD309 PE-Cy7	Yellow 780/60
CD146 BV421	Violet 450/50
Zombie Aqua	Violet 525/50
CD34 BV605	Violet 610/20
CD105 BV650	Violet 660/20
CD45 BV785	Violet 780/60
CD14 APC	Red 660/20
CD31 AlexaFluor700	Red 730/45

Table 2.3 Monocyte characterisation flow cytometry panel

Antibody / fluorochrome	Channel / Filter λ (nm)
HLA-DR FITC	Blue 530/30
CD56 PE	Yellow 585/15
CD16 Pe-Cy5	Yellow 670/14
CD19 PE-Cy7	Yellow 780/60
CD3 Pacific Blue	Violet 450/50
Zombie Aqua	Violet 525/50
CD45 BV785	Violet 780/60
CD14 APC	Red 660/20
CD31 AlexaFluor700	Red 730/45

Table 2.4 hBMSC – NK cell co-culture phenotyping flow cytometry panel

Antibody / fluorochrome	Channel / Filter λ(nm)
HLA-DR FITC	Blue 530/30
CD73 PerCP EFluor710	Blue 695/40
CD56 PE	Yellow 585/15
CD16 Pe-Cy5	Yellow 670/14
CD19 PE-Cy7	Yellow 780/60
CD3 Pacific Blue	Violet 450/50
Zombie Aqua	Violet 525/50
CD34 BV605	Violet 610/20
CD105 BV650	Violet 660/20
CD45 BV785	Violet 780/60
CD14 APC	Red 660/20
CD90 AlexaFluor700	Red 730/45

Table 2.5 Monocyte differentiation phenotyping flow cytometry panel

Antibody / fluorochrome	Channel / Filter λ (nm)
CD200R FITC	Blue 530/30
CD163 PerCp Cy5.5	Blue 695/40
Tie2 PE	Yellow 585/15
CD16 Pe-Cy5	Yellow 670/14
CD64 PE-Cy7	Yellow 780/60
CD209 BV421	Violet 450/50
Zombie Aqua	Violet 525/50
CD11b BV605	Violet 610/20
CD80 BV650	Violet 660/20
CD45 BV785	Violet 780/60
CD14 APC	Red 660/20
CD31 AlexaFluor700	Red 730/45

(BD) Fortessa flow cytometer using the channels specified in the tables above on the FACSDiva software. Data were analysed using Kaluza v1.2. Graphs were plotted in GraphPad Prism.

A note on nomenclature regarding populations characterised by flow cytometry Throughout this body of work, populations characterised as positive will be labelled '+' while negative populations will be labelled '−'. Therefore, a population labelled 'CD56+' contains cells staining positive for CD56 and a population labelled 'CD14−' contains cells staining negative for CD14, as determined by gating. The same holds true for populations characterised by multiparametric analysis. A population labelled 'CD105+ CD90+ CD45− CD34−' is positive for both CD105 and CD90, and negative for CD45 and CD34. This will have been determined by sequential gating so every cell within that population has that exact marker phenotype. This nomenclature has been chosen to prevent confusion with cell populations isolated by magnetic activated cell sorting, that are labelled as described in section 2.3.2.

2.3 Peripheral blood mononuclear cell isolation from peripheral blood

2.3.1 Density gradient centrifugation

Density gradient centrifugation is a technique used to separate mononuclear cells and granulocytes / erythrocytes from blood and bone marrow. Fresh, whole blood has a specific gravity of between 1.0590 or 1.0650 g/ml (Trudnowski and Rico 1974). In order of increasing density, the components of whole blood are plasma, platelets, leukocytes, granulocytes and erythrocytes. By layering diluted

blood over a density gradient centrifugation medium, here Lymphoprep, and centrifuging the blood components were separated based on density.

Leukocyte Reduction System (LRS) cones were procured from NHS Blood and Transplant. The conditions of supply stipulate that LRS cones for research can only be received the day after isolation from the donor. The contents of the LRS cone were transferred into 150 ml bottles and diluted 10 -fold in Flow cytometry buffer. The suspension was layered over density gradient centrifugation medium with a specific gravity of 1.077 g/ml in 50 ml Falcon tubes and centrifuged at 800 RCF for 30 minutes at room temperature with low brake. Centrifugation took place at room temperature due to equipment restrictions. The buffy coat, which is buff-coloured and found at the phase interface between the density gradient centrifugation medium and the serum, was removed using a pastette and pooled in a fresh 50 ml Falcon. The pooled buffy coat was centrifuged twice in Flow cytometry buffer at 300 RCF for 10 minutes at room temperature. The washed buffy coat was then used in assays or further processed using Magnetic Activated Cell Sorting (MACS) as described in section 2.3.2.

2.3.2 Subpopulation isolation from buffy coat using magnetic beads

MACS was invented by Miltenyi Biotec. Magnetically labelled cells were run through a column containing iron particles that is placed inside a powerful magnet. Labelled cells were retained within the column, while unlabelled cells were washed through. The technique permits isolation of both labelled and untouched cell populations. Cells were labelled using antibodies against either specific, single cell surface markers or a cocktail of markers (to negatively label a population). Single marker antibodies were directly conjugated to superparamagnetic nanoparticles. Cocktail antibodies were biotinylated and a secondary anti-biotin antibody conjugated to the nanoparticles was used to magnetically label the cells. The nanoparticles were always conjugated and not free thus their uptake by phagocytic cell types, potentially resulting in undesirable cell activation, was avoided with this method.

Cells were isolated using magnetic bead isolation kits from Miltenyi Biotec as below. Throughout, enriched fractions are labelled ‘enr’ while depleted fractions are labelled ‘dep’. Therefore, a population designated ‘$CD45_{dep}CD31_{enr}$ PBMC’ has undergone a two-step isolation, the first step being a CD45 depletion and the second a CD31 enrichment. In the same way, the population ‘$CD45_{enr}$ PBMC’ has undergone a single step isolation and been enriched for CD45, and the population ‘$CD45_{dep}$ isolated PBMC’ has been depleted of CD45 positive in a single step. Where a cell marker is specified, the enriched fraction contains cells directly labelled with an antibody conjugated to a magnetic nanoparticle, and the depleted fraction contains unlabelled cells. This nomenclature has been chosen to prevent confusion with cell populations characterised by single-colour or multiparametric flow cytometry that are labelled as described in section 2.2.5.

2.3.3 Magnetic activated cell sorting

Magnetic activated cell sorting using kits containing conjugated bead and antibody

Buffy coat cells isolated from LRS cones as described in section 2.3.1 were quantified using a counting chamber as described in section 2.1.3 and samples were centrifuged at 300 RCF for 5 minutes at room temperature in a 15 ml Falcon tube. Cells were resuspended and incubated at 4 to 8 °C in MACS Buffer (autoMACS Rinsing buffer, 5 % v/v MACS Bovine Serum Albumin (BSA) Stock solution creates: PBS, pH 7.2, 0.5 % BSA, 2 mmol EDTA) and conjugated magnetic beads. Where required by the manufacturer's instructions, an FCR block was applied to cells and mixed thoroughly prior to magnetic bead addition. The volumes of MACS Buffer, FCR block (where used) and conjugated magnetic beads were calculated according to the manufacturer's instructions as shown in tables 2.6 to 2.8.

Table 2.6 Transwell Panel 1: Primary MACS of PBMC

Kit	**Addition per 1×10^7 cells (minimum isolation, scaled for larger)**		
	MACS Buffer (µl)	**FCR block (µl)**	**Antibody (µl)**
CD45 microbeads, human	80	None	20

Table 2.7 Transwell Panel 2: Secondary MACS of $CD45_{dep}$ PBMC with CD31 or CD146

Kit	**Addition per 1×10^7 cells (minimum isolation, scaled for larger)**		
	MACS Buffer (µl)	**FCR block (µl)**	**Antibody (µl)**
CD31 microbead kit, human	60	30	20
CD146 microbeads, human	60	20	20

Suspensions were mixed thoroughly and incubated at 2 to 8 °C for 15 minutes. Cells were washed in 1 ml MACS Buffer / 1×10^7 cells and resuspended in 500 µl MACS buffer / 1×10^8 cells. Labelled

Table 2.8 Transwell Panel 2: Secondary MACS of $CD45_{dep}$ PBMC with CD34

Kit	**Addition per 1×10^8 cells (minimum isolation, scaled for larger)**		
	MACS Buffer (µl)	FCR block (µl)	Antibody (µl)
CD34 microbeads, human	300	100	100

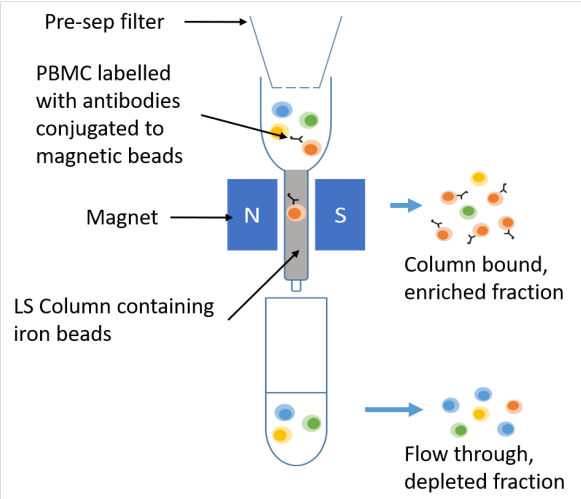

Fig. 2.1 Schematic showing outline of MACS separation

PBMC were labelled with antibodies conjugated to magnetic beads and passed through a pre-sep filter and LS column held within a magnet. The flow-through, containing the depleted fraction, and the column bound cells, containing the enriched fraction, were collected.

cells were passed through 30 µm Pre-Sep filters and LS columns pre-wetted with MACS Buffer in a QuadroMACS, and rinsed 3 times with 3 ml MACS Buffer as shown in fig. 2.1. The column was then removed from the QuadroMACS and eluted using 5 ml MACS Buffer. Both the flow-through and column-bound fractions were retained for further use. Where secondary isolations were performed, the flow-through fraction was used.

Magnetic activated cell sorting using kits containing biotinylated primary cocktail and anti-biotin bead conjugated secondary antibody

Isolations were performed in exactly the same way as the conjugated bead and antibody method described above, with the following exceptions:

- Incubation after addition of primary antibody was 5 minutes and not 15 minutes
- Secondary antibody was added after the first incubation (table 2.9) and incubated at 2 to 8 °C for a further 10 minutes (table 2.10)
- There was no wash step: the cell suspension was added directly to the pre-wetted filter / column

Table 2.9 Direct isolation of NK cells and monocytes from PBMC: first incubation (5 minutes, 2 to 8 °C)

Kit	Addition per 1×10^7 cells (minimum isolation, scaled for larger)		
	MACS Buffer (µl)	FCR block (µl)	Primary Antibody (µl)
NK Cell Isolation Kit, human	40	None	10
Pan Monocyte Isolation Kit, human	40	10	10

Table 2.10 Direct isolation of NK cells and monocytes from PBMC: second incubation (10 minutes, 2 to 8 °C)

Kit	Addition per 1×10^7 cells (minimum isolation, scaled for larger)	
	MACS Buffer (µl)	Secondary Antibody (µl)
NK Cell Isolation Kit, human	30	20
Pan Monocyte Isolation Kit, human	30	20

2.4 Molecular biology

2.4.1 Gene expression

Ribonucleic acid extraction from cells: Direct-zol

The Direct-zol method of Ribonucleic Acid (RNA) extraction is based on TRIzol / Tri-Reagent (brand names: scientific name guanidinium isothiocyanate-phenol-chloroform). The phenol and guanidinium isothiocyanate denatured proteins, leading to cell lysis, and solubilised organic material. The chloroform allowed isolation of proteins, Deoxyribonucleic Acid (DNA) and RNA by causing phase separation. Protein partitioned to the organic phase, DNA to the interface and RNA to the aqueous phase (Rio et al. 2010). The on-column method in the Direct-zol kit removed the need for manual fractioning, improving yields by binding RNA from the aqueous phase to a membrane.

The Zymo Research Direct-zol RNA MiniPrep Plus or Microprep Plus kit was used to extract RNA from cell cultures. Kit reagents were prepared as per manufacturer's instructions.

Medium was removed from the culture vessel, cells were rinsed with PBS, lysed using Trizol and frozen at −70 to −80 °C at least overnight in 1.5 ml Eppendorf tubes. Between 350 to 650 µl Trizol was used, depending on the cell number and as specified by the manufacturer. Cell lysates were thawed on ice and an equal volume of 100 % molecular-grade ethanol was added and thoroughly mixed by trituration. The lysate-ethanol mixture was applied onto a spin-column from the kit which contained a membrane and was housed within a collection tube. The spin-column could contain a maximum of 700 µl of liquid. Where a greater volume of liquid was present, the addition was done in separate stages. The spin-column was centrifuged at 14 000 RCF for 30 seconds at room temperature and the supernatant discarded. The spin-column was washed twice with RNA PreWash in the same way. The spin-column was then washed at 14 000 RCF for 2 minutes with RNA Wash Buffer. The spin-column was transferred to an Ribonuclease (RNAse) free tube and eluted with Deoxyribonuclease (DNAse)/RNAse free water. For the MiniPrep kit, 30 µl of water was used and 15 µl was used for the MicroPrep kit. The RNA was quantified with a Nanodrop5000 and either stored at −70 to −80 °C or used immediately.

Complementary deoxyribonucleic acid reverse transcription

The classical Polymerase Chain Reaction (PCR) cannot be performed using RNA. In order to measure the transcription levels of messenger Ribonucleic Acid (mRNA) within a sample, a reverse transcription reaction was performed. A reverse transcriptase enzyme synthesised the first strand DNA from the single-stranded mRNA using an RNA template and three-prime (3') complementary primer. The resulting single-stranded DNA is referred to as complementary Deoxyribonucleic Acid (cDNA) to identify that it was produced via reverse transcription from mRNA.

cDNA was prepared using the QuantiTect Reverse Transcription Kit according to the manufacturer's instructions from RNA isolated as described in section 2.4.1. The kit was thawed at room temperature, tubes were gently agitated to mix reagents and then a centrifuge was used to pulse-spin the tubes. Reagents were kept on ice. RNA was thawed on ice, gently agitated, spun down, and then placed on ice. An aliquot containing the desired quantity of RNA, determined by assay requirements, was taken for reverse transcription, with a sample also taken to prepare the reverse transcription control. Reverse transcription was performed as shown in table 2.11 and table 2.12 for up to 1000 ng RNA in 0.5 ml Eppendorf tubes using reagents supplied with the kit. Where more than 1000 ng RNA was used, volumes were scaled accordingly. Genomic DNA was removed by adding reagents as specified in table 2.11, then incubating for 2 minutes at 42 °C and placing on ice. Reverse transcription was performed by adding the reagents at volumes outlined in table 2.12, incubating for 30 minutes at 42 °C, then3 minutes at 95 °C.

Table 2.11 Reagent volumes for Genomic Deoxyribonucleic Acid (gDNA) removal from RNA

RNA / reagent	Volume µl / 1000 ng
RNA	As calculated above
RNAse/DNAse free water	12 µl – (Volume of RNA)
gDNA wipeout	2 µl

Table 2.12 cDNA master mix volumes

RNA / reagent	Volume µl / 1000 ng
Reverse Transcriptase	1 µl
Reverse Transcriptase Buffer	4 µl
Reverse Transcriptase Primer Mix	1 µl

Reverse transcriptase negative controls were produced in the same way, with the reverse transcriptase substituted for an equal volume of RNAse / DNAse free water. cDNA was either used immediately or stored at −20 °C. Full conversion of RNA to cDNA was assumed.

Reverse Transcription Quantitative Polymerase Chain Reaction

Reverse Transcription Quantitative Polymerase Chain Reaction (RT-qPCR) is used to quantify the transcription levels of mRNA within a sample. It can also be referred to as the Reverse Transcription Real Time Polymerase Chain Reaction, also given the acronym RT-qPCR. Since RT-qPCR requires DNA, the mRNA was first reverse transcribed as described in section 2.4.1 to form cDNA, a two-step method. RT-qPCR could also have been performed in a one-step method where the reverse transcription and RT-qPCR would have occurred within the same tube. This would have reduced pipetting steps, time and experimental variation but ultimately would have been less sensitive since conditions for the reverse transcription and RT-qPCR could not have been individually optimised. The cDNA produced in the reverse transcription reaction (section 2.4.1) was used as the template for the RT-qPCR reaction and was detected using specific primer sequences. The copy number of the cDNA was measured in real time after each amplification cycle (denaturation, annealing, elongation) using Sybr Green, a fluorescent double-stranded Deoxyribonucleic Acid (dsDNA) binding dye. The cycle number where the fluorescence generated by the Sybr Green binding to the amplified cDNA passed the background fluorescence threshold and gave a positive signal is the Cycle Threshold (Ct). The Ct is inversely proportional to the quantity of target nucleic acid present, allowing quantification of the transcript within the sample.

Table 2.13 Primer Sequences for RT-qPCR

Gene	Sense (5′–3′)	Antisense (3′–5′)	Source
CXCL10	TGGCATTCAAGGAGTACCTCTC	CGTGGACAAAATTGGCTTGC	1
HIF-1a	CCACAGGACAGTACAGGATG	TCAAGTCGTGCTGAATAATACC	2
IDO	CAAAGGTCATGGAGATGTCC	CCACCAATAGAGAGACCAGG	3
IL6	TTCAATGAGGAGACTTGCCTG	ACAACAACAATCTGAGGTGCC	4
SDF-1	TCAGCCTGAGCTACAGATGC	CTTTAGCTTCGGGTCAATGC	5
VEGFa	GAGCCTTGCCTTGCTGCTCTAC	CACCAGGGTCTCGATTGGATG	6
FGF-2	N/A	N/A	Quantitect
B2M	N/A	N/A	Quantitect

Primer sequences were obtained from 1: Marie Sicard (Division of Trauma and Orthopaedic Surgery), 2: Depoix et al. 2016, 3: Thomas et al. 2007, 4: Deng et al. 2016, 5: Laird et al. 2011, and 6: J. Zhang et al. 2012. Primers were produced by Integrated DNA Technologies and validated in-house. Primer kits were purchased through Quantitect.

Table 2.14 RT-qPCR master mix volumes using custom primers

Reagent	Volume per sample (µl)
Sybr Green	6
Forward primer (CONC)	0.77
Reverse primer (CONC)	0.77
RNAse / DNAse free water	2.46
Total volume	10

cDNA prepared as in section 2.4.1 was thawed on ice, along with primers and Sybr green, the flicked, centrifuged at 300 RCF for 5 minutes at room temperature briefly and kept cold. cDNA was diluted to 5 ng/µl in RNAse / DNAse free water. Master mixes were prepared as described in table 2.14, with volumes scaled according to number of samples plus 10 % excess. Primer sequences are outlined in table 2.13.

Custom primers were validated on a serial dilution of cDNA isolated from a cell or tissue source expressing the gene of interest. cDNA was serially diluted in triplicate at 1:5, 5 times from 100ng/µl to give six points ranging from 100ng/µl to 0.03ng/µl. Primers were prepared as intable 2.14 and added to the serially diluted cDNA. The cycling profile was performed as described below. Primers passed validation if they had a slope of -3.3 ± 0.2, an R^2 of > 0.95, an efficiency of (100 ± 10) %, and the melt curve showed a single, well-defined peak at the same temperature for all points on the serial dilution.

Following assessment, B2M was selected as the housekeeper for human samples. Reactions were dispensed into 96 well RT-qPCR plates, sealed and centrifuged at 300 RCF for 1 minute at room temperature before reading on a Thermo Fisher StepOne Plus Real-Time PCR System.

Table 2.15 RT-qPCR master mix volumes using pre-made commercial primer kits

Reagent	**Volume per sample (µl)**
Sybr Green	6
Primer mix (conc)	1.25
RNAse / DNAse free water	2.75
Total volume	10

The cycling profile for the RT-qPCR was as follows: 5 minutes at 95 °C followed by 40 cycles of denaturing at 95 °C for 10 seconds and combined annealing and extension at 60 °C for 30 seconds. A melt curve was then performed, starting with 15 seconds at 95 °C, followed by 1 minute at 65 °C and 15 seconds at each increment of 1 °C between 65 to 95 °C, recording data at each increment. Data were analysed in Excel and plotted in GraphPad Prism. Calculations were as follows:

$$\Delta Ct = Ct_G - Ct_H \tag{2.1a}$$

$$\Delta\Delta Ct = \Delta Ct_S - \Delta Ct_R \tag{2.1b}$$

$$Fold\ change\ in\ expression = 2^{-(\Delta\Delta Ct)} \tag{2.1c}$$

$$\sigma_{\Delta Ct} = \sqrt{\sigma^2_{\Delta Ct_G} + \sigma^2_{\Delta Ct_H}} \tag{2.2a}$$

$$\sigma_{\Delta\Delta Ct} = \sqrt{\sigma^2_{\Delta Ct_S} + \sigma^2_{\Delta Ct_R}} \tag{2.2b}$$

$$Low\ Range = 2^{-(\Delta\Delta Ct + \sigma_{\Delta\Delta Ct})} \tag{2.2c}$$

$$High\ Range = 2^{-(\Delta\Delta Ct - \sigma_{\Delta\Delta Ct})} \tag{2.2d}$$

$$Negative\ Error\ Bar = 2^{-(\Delta\Delta Ct)} - Low\ Range \tag{2.2e}$$

$$Positive\ Error\ Bar = High\ Range - 2^{-(\Delta\Delta Ct)} \tag{2.2f}$$

Where:

- Δ is difference or change
- Ct is the threshold cycle
- G is the gene of interest
- H is the housekeeper gene
- S is the sample of interest

- R is the reference sample
- σ is the standard deviation

2.4.2 Protein analysis

Preparation of preconditioned medium from PBMC subpopulations

PBMC subpopulations isolated as described in section 2.3.3 were seeded at 2×10^5 cells per well of a 12 well plate in Medium C (αMEM, 0.2 % v/v BSA, 2 mmol L-Glutamax, 5 µg/ml Gentamicin, 1.5 µg/ml Amphotericin B) and incubated under hypoxic culture conditions for 16 hours. Suspensions were passed through a 0.22 µm filter and stored at −20 °C for further work.

Chemokine array assay

The Proteome Profiler Human Chemokine Antibody Array (R & D Systems) is based on a dot blot assay. Capture antibodies were adsorbed on a nitrocellulose membrane in a dot matrix. Samples were labelled with a detection antibody cocktail and applied to the array. If a specific chemokine was present, the relevant protein-detection antibody complex formed and bound to its respective capture antibody. This binding was visualised by staining the membrane with Streptavidin-Horseradish Peroxidase and chemiluminescent dye and exposing X-ray film to the membranes.

The presence of a subset of chemokines within the supernatant was determined using the R&D systems Proteome Profiler Human Chemokine Antibody Array kit and following the manufacturer's instructions. The list of chemokines detected may be found in table 2.16. Chemokine array membranes were blocked twice in Array Buffer 6 for 1 hour while rocking at 60 RCF. Preconditioned medium isolated as described in section 2.4.2 was thawed, an aliquot places within a 1.5 ml Eppendorf tube, and Array Buffer 6, Array Buffer 4 and Detection Antibody Cocktail were added to each tube as per manufacturer's instructions. Tubes were incubated for 1 hour at room temperature.

All buffer was aspirated from the array films and the preconditioned medium-antibody cocktail mix was added to the membranes. The membranes were incubated on a shaker at 60 RCF overnight at 2 to 8 °C. After incubation, the membranes were transferred to a labelled dish containing 1 time concentration wash buffer prepared according to kit instructions and washed for 10 minutes, rocking at 60 RCF, three times. Membranes were stained with 1-in-2000 Streptavidin-horseradish peroxidase for 30 minutes at room temperature in the dark. Finally, membranes were washed 3 times in wash buffer as before, sealed into pouches and stained with Chemi Reagent Mix prepared as per kit instructions for 1 minute. Exposures were taken at 1, 3, 5, 8, 10 and 15 minutes onto GE Healthcare

Table 2.16 Subpopulation screening panel

		Chemokines detected
CCL1/I-309	CCL21/6Ckine	CXCL8/IL-8
CCL2/MCP-1	CCL22/MDC	CXCL9/MIG
CCL3/CCL4 (MIP-1 alpha/MIP-1 beta)	CCL26/Eotaxin-3	CXCL10/IP-10
CCL5/RANTES	CCL28	CXCL11/I-TAC
CCL7/MCP-3	Chemerin	CXCL12/SDF-1
CCL14/HCC-1/HCC-3	CX3CL1/Fractalkine	CXCL16
CCL15/MIP-1 delta/LKN-1	CXCL1/GRO alpha	CXCL17/VCC-1
CCL17/TARC	CXCL4/PF4	IL-16
CCL18/PARC	CXCL5/ENA-78	Midkine
CCL19/MIP-3 beta	CXCL7/NAP-2	XCL1/Lymphotactin
CCL20/MIP-3 alpha		

Amersham Hyperfilm ECL in a GE Healthcare Amersham Hypercassette Autoradiography Cassette and developed on a Protec Compact 2 NDT. A film digitiser was used to scan films and images were analysed using FIJI and Giles Carpentier Protein Array Analyzer for ImageJ.

2.5 Migration assays

2.5.1 Boyden chamber

The Boyden chamber assay (also called the transwell assay) was first described by Stephen Boyden in 1962 for assessing the migration of leukocytes (Boyden 1962). The cell population of interest was seeded onto a porous membrane held in a cell culture well insert. This insert was suspended in a cell culture well containing the chemotactic agent and incubated for a defined period of time. At the end of this time, the membranes were fixed and stained, and migrated cells were quantified.

Transwell inserts for 24 well plates with 8 µm pores were incubated for 30 minutes at room temperature in FBS and rinsed in PBS. Bone marrow stromal cells isolated and characterised as in section 2.1.2 were detached and counted as in section 2.1.3. 1×10^4 cells were seeded into each transwell and allowed to settle at room temperature for 30 minutes in 0.5 ml Medium C.

1×10^5 of the peripheral blood cells isolated in section 2.3 were added to the wells of 24 well plates. Negative control wells were prepared in using cell-free Medium C and positive control wells in with Medium A (DMEM with 10 % v/v FBS, 2 mmol L-GlutaMAX, 5 µg/ml Gentamicin, and 1.5 µg/ml Amphotericin B). All wells were prepared in triplicate. Transwells containing BMSC were suspended in the prepared 24 well plate using 2 mm Nitrile-70 O-rings to ensure separation between the transwell

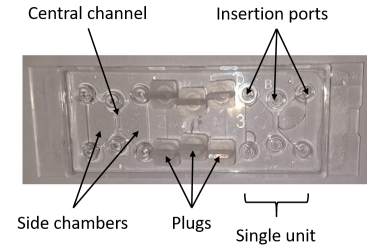

Fig. 2.2 Ibidi μ-slide 3D chemotaxis assay

The Ibidi μ-slide has three units, allowing three tests per slide. Each unit is composed of two side chambers, where chemoattractive agents are added, and a central observation channel, containing the migratory cells of interest. Samples are added through the insertion ports, which can be sealed using rubber plugs.

membrane and the well base. Plates were incubated for 16 hours under normoxic or hypoxic tissue culture conditions.

After 16 hours transwell inserts were removed from plates, fixed in 10 % v/v formalin, permeabilised with 0.1 % v/v Triton in PBS and stained for 1 hour in 14.3 mmol 4',6-diamidino-2-phenylindole (DAPI), in the dark at 2 to 8 °C. Non-migrated cells were physically removed from the interior surface of the membrane with a cotton bud and the membranes rinsed with PBS. Transwell membranes were placed into a fresh 24 well plate and kept hydrated in PBS. 3 images were taken of each transwell membrane on 40x magnification using a DAPI filter on a Nikon Eclipse TI microscope. Images were sited away from the rim of the transwell to prevent side-scatter influencing the assay. Images were processed using FIJI.

2.5.2 Real time Ibidi μ-slide 3D chemotaxis assay

The Ibidi μ-slide 3D chemotaxis assay is designed for measurement of chemotaxis. Migration of adherent cells, or cells within a gel matrix, can be viewed in real time. The bone marrow stromal cells were seeded into a central observation chamber, and a gradient of potential chemoattractant was applied over the central chamber by dosing the side chambers with the peripheral blood subpopulations. This allowed visualisation of the behaviour of individual bone marrow stromal cells in response to different peripheral blood subpopulations, permitting differentiation between chemotaxis, fugetaxis and chemokinesis as well as identification of subpopulation effects.

Ibidi μ-Slide Chemotaxis slides and plugs, pipette tips, Medium B and Medium C were equilibrated under normoxic or hypoxic culture conditions for 24 hours prior to the experiment. Human bone marrow stromal cells (hBMSC) were detached and resuspended in Medium B as described in section 2.1.3 at 3×10^6 cells/ml. 1.8×10^4 hBMSC were seeded into the central channel using the ports (fig. 2.2). The ports on the side chambers were kept sealed with plugs during hBMSC addition. To fill a chamber,

the medium or suspension was dropped onto the addition port. A pipette tip was then inserted into the removal chamber and an equivalent volume of air for first addition, or medium for subsequent additions, was aspirated. To avoid bubbles within the chambers, bevelled tips compatible with port design were used, ports were consistently used for addition of media to, or removal from, the slide, and the slide was tilted so the addition port was lower than the removal port, to encourage any extra bubbles to leave the slide. After incubation, the plugs were removed and the hBMSC were allowed to adhere for 2 hours under normoxic or hypoxic culture conditions in a petri dish kept hydrated with moistened tissue to minimise evaporation. Plugs were placed back into the side ports, the central chamber was then washed 3 times with Medium C and then filled with Medium C. Plugs were placed into the central chamber and removed from one side chamber which was then filled with Medium C as before. This was repeated with the other side chamber. All chambers were then re-sealed with plugs.

Blood subpopulations isolated as described in section 2.3 were centrifuged at 300 RCF for 5 minutes at room temperature and resuspended in Medium C at 8.33×10^5 cells/ml. 2.5×10^4 blood subpopulation cells were added to the left-hand chamber in the same way as before. The right-hand chamber was left containing Medium C only. A positive control was set up by adding Medium B to the left-hand chamber, while both chambers were left containing Medium C only for the negative control. All chambers were sealed with plugs.

Migration was imaged on 40 fold magnification, brightfield, every 5 minutes for 16 hours using a Nikon Eclipse TI microscope with automatic stage and shutter in a heated box kept at 37 °C. No gas control was available; the plugs used to seal the ports were assumed to minimise gas exchange. Advanced Biology Hamamatsu Legacy image capture software was used to record data. Time-lapse footage was analysed manually using the MTrackJ Plugin for FIJI (Erik Meijering). 30 individual cells were tracked every third frame (15 minutes) for the duration of the time-lapse, giving 65 time-points in total. Cells for tracking were randomly selected, and then checked that they conformed to the following criteria before tracking:

1. Cells were clearly individually distinguishable throughout the time-lapse
2. Cells did not divide throughout the time-lapse
3. Cells did not leave the observation chamber during the time-lapse
4. Cells did not die during the time-lapse
5. Cells were not within a clump or dense grouping of cells

Data were analysed using the Chemotaxis and Migration Tool from Ibidi and plotted in GraphPad Prism.

2.6 Human Bone Marrow Stromal Cell – Natural Killer cell co-cultures

2.6.1 7 day Human Bone Marrow Stromal Cell co-culture with Natural Killer Cells

NK cells were obtained from peripheral blood by magnetic-activated cell sorting as described section 2.3.3. Paired characterised normoxic and hypoxic cultured hBMSC isolated as in section 2.1.2 were used. hBMSC were detached and counted as described in section 2.1.3 and 4.5×10^4 seeded into the wells of a 48 well plate, then permitted to adhere for 1 hour under normoxic or hypoxic culture conditions in 50-50 Medium (half-and-half Medium B and Medium E (RPMI-1640, 2 mmol L-Glutamax, 5 µg/ml Gentamicin, 1.5 µg/ml Amphotericin B)). NK cells were added to the hBMSC at 0, 1, 5, 10 and 15 fold concentration (0, 4.5×10^4, 2.25×10^5, 4.5×10^5 and 6.75×10^5 cells per well respectively) in 50-50 Medium. An NK only condition containing 4.5×10^5 cells was also prepared in 50-50 Medium. Wells were prepared in quadruplets. 10 µg/ml IL-2 was added to 2 wells for each condition. Plates were incubated under normoxic or hypoxic conditions for 7 days. After 7 days wells were imaged using a Leica brightfield microscope, and cells were taken for assay work.

2.6.2 Real-Time Assessment of human bone marrow stromal cell – Natural Killer cell co-culture dynamics using XCelligence Real Time Cell Analyser

The ACEA Biosystems XCelligence Real Time Cell Analyser Dual Purpose (RTCA DP) E-plate 16 well allows real-time non-invasive monitoring of the dynamics of both cellular proliferation and death. Gold microelectrodes are fused to the glass internal base of the plates where the cells adhere (fig. 2.3a). When the plate, while containing culture medium, was placed into the RTCA DP, a 22 mV electrical potential was applied and current was conducted in a saltatory manner between the electrodes (fig. 2.3b). Following hBMSC addition and adhesion to the plate base, the flow of electrons between the electrodes was disrupted due to coverage of the electrode by the adhered cells, resulting in a change in measured current called impedence. The level of impedence was determined by cell size, number and strength of adhesion to the substrate; NK cells (both IL-2 stimulated and unstimulated) did not adhere and so did not alter the measured impedence. The output value was Cell Index, which is the change in impedence relative to the baseline impedence of the electrodes exposed to medium prior to cellular addition.

The XCelligence RTCA DP machine and Medium B and Medium E were placed into an incubator under normoxic or hypoxic culture conditions and permitted to equilibrate for 24 hours. Xcelligence E-plate 16 plates were coated with FBS for 2 hours, rinsed with PBS and allowed to dry overnight under normoxic or hypoxic culture conditions. 50 µl 50-50 Medium was added to all wells on the plates and the plates placed into the RTCA DP and blanked to provide a reference impedence value. hBMSC were detached and counted as described previously (section 2.1.3), and seeded into the wells

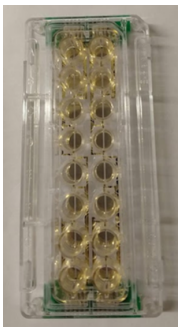

(a) Eplate View 16

(b) XCelligence RTCA DP containing Eplate 16

Fig. 2.3 Xcelligence RTCA DP and associated Eplate

The base of the Eplate 16 View is coated with gold micro-electrodes with a viewing strip to allow visual inspection of the adhered cell monolayer (fig. 2.3a). Once seeded, the plate is inserted into the XCelligence RTCA DP, pictured with a plate in the central cradle, which is placed in a tissue culture incubator for the duration of the experiment (fig. 2.3b).

at 5000 cells per well. For low concentration experiments, NK cells were added at 0, 0.1, 0.2, 1, 5, 10 and 15 fold concentration relative to hBMSC numbers (0, 500, 1000, 5000, 2.5×10^4, 5×10^4 and 7.5×10^4 cells per well respectively) in 50-50 Medium. Wells were prepared in quadruplet and 1 pair of each was treated with 10 µg/ml IL-2. The total volume in each well was 100 µl. Cells were permitted to settle for 1 hour at room temperature, then placed into the cradles on the XCelligence RTCA DP machine, ensuring that the plate placed in each cradle was the same plate previously used to provide a baseline in that cradle. Cell index was recorded at intervals of 5 to 15 minutes for 7 days under normoxic or hypoxic culture conditions. Each condition and set of concentrations was performed using matched hBMSC strains.

Calculation of area under the real time cell trace curve (AUC) and analysis was performed using eq. (2.3a), as described in Pan et al. 2013

$$AUC_{xj} = 100\frac{AUC_j}{AUC_c} \tag{2.3a}$$

Where:

- AUC_{xj} measured percentage quantification of toxic intensity.
- AUC_c represented the cumulative cell proliferation of control. AUC_c was calculated by GraphPad Prism for the hBMSC only culture in each condition using the mean Real Time Cell Trace (RTCT).

- AUC_j represented cumulative cell proliferation of sample. AUC_j was calculated by GraphPad Prism for each condition (oxygen level, NK cell dose, stimulation) using the RTCT.

GraphPad Prism was used to fit a sigmoidal model to the data with the Sigmoidal Dose-Response Curve (Variable Slope) to show the relationship between exposure and NK cell ratio using eq. (2.4a)

$$AUC_x = p_1 + \frac{p_2 - p_1}{(1 + \frac{\exp(-(log(x) - p_3)}{p_4})} \tag{2.4a}$$

Where:

- x represented the NK cell : hBMSC ratio
- p_1 represented the bottom of the curve fit, calculated by GraphPad Prism
- p_2 represented the top of the curve fit, calculated by GraphPad Prism
- p_3 represented the log(EC50), calculated by GraphPad Prism
- EC_{50} is the half maximal effective concentration
- p_4 represented the Hillslope, calculated by GraphPad Prism

The NK cell ratio required to cause a 50 % decrease in the AUC_c, the AUC_{50}, showing the cumulative cytotoxicity, was calculated using eq. (2.5a), with the same parameters as for eq. (2.4a).

$$AUC_{50} = exp(-ln(((\frac{p_2 - p_1}{50 - p_1}) - 1) * p_4) + p_3) \tag{2.5a}$$

2.6.3 CellTox Green

CellTox Green Cytotoxicity Assay is a fluorescent dye-based method of quantifying cell death. CellTox Green is a "proprietary asymmetric cyanine dye" which fluoresces green when bound to DNA (Promega 2018). The dye cannot pass through intact cellular and nuclear membranes of viable cells and therefore viable cells do not influence the fluorescence. However, when these membranes were disrupted during cell death, the dye was able to penetrate the cell and bind to the DNA, resulting in a bright punctate signal from the dying or dead cell. This signal could be detected using a fluorescent microscope to show the locations and numbers of dying cells.

NK cells and hBMSC were isolated as previously described (section 2.3.3, section 2.1.2). hBMSC were detached and counted as in section 2.1.3 and seeded at 5×10^4 cells per well in an 8 well EZslide in 50-50 Medium equilibrated under normoxic or hypoxic conditions. Cells were allowed to attach for 1 hour under normoxic or hypoxic culture conditions. NK cells were added at 0 or 10 fold concentration (0 or 5×10^5 cells per well). Wells were prepared in quadruplet and 10 µg/ml IL-2 was added to one pair of wells. 2 extra hBMSC control wells were also prepared: CellTox-free and Lysis Positive control.

For endpoint experiments, slides were incubated for 72 hours under normoxic or hypoxic culture conditions. After this point, CellTox Green and Lysis buffer were added. 0.5 µl of CellTox Green per well was diluted in 10 µl 50-50 Medium per well and 10 µl mixed into all wells except the CellTox-free control well to give a final dilution of 1-in-200 CellTox Green Dye. Lysis solution (from the CellTox Green kit) was added into the Lysis Positive control well at a 1-in-50 dilution. Slides were then imaged on a Nikon Eclipse TI microscope with automatic stage and shutter. Advanced Biology Hamamatsu Legacy image capture software was used to record data.

2.7 Human bone marrow stromal cell – monocyte co-cultures

2.7.1 Monocyte differentiation

Monocytes were obtained from peripheral blood by magnetic-activated cell sorting as described in section 2.3.3 and seeded into 6 well plates in Medium E. Wells were left unstimulated, or were treated for 5 days with 50 ng/ml Granulocyte-Macrophage Colony Stimulating Factor (GM-CSF) for classically activated macrophage (M1) priming, or 50 ng/ml M-CSF for alternatively activated macrophage (M2) priming. Primed cells were treated for 48 hours with cytokines for final differentiation under the same conditions. M1 primed cultures were stimulated with 10 ng/ml TNFα and 50 ng/ml IFNγ, and M2 primed cultures were treated with either 20 ng/ml IL-4 for alternatively activated macrophage type A (M2a) or 20 ng/ml IL-10 for alternatively activated macrophage type C (M2c) differentiation. After differentiation, wells were imaged using a Leica brightfield microscope, and differentiated monocytes used in assays.

2.7.2 hBMSC-monocyte co-cultures

Monocytes and hBMSC isolated as described previously were co-cultured for 7 days at a 1:1 ratio in 50-50 Medium under normoxic or hypoxic culture conditions. Controls of monocyte or hBMSC only wells were also made. Preconditioned medium was prepared and stored as in section 2.4.2

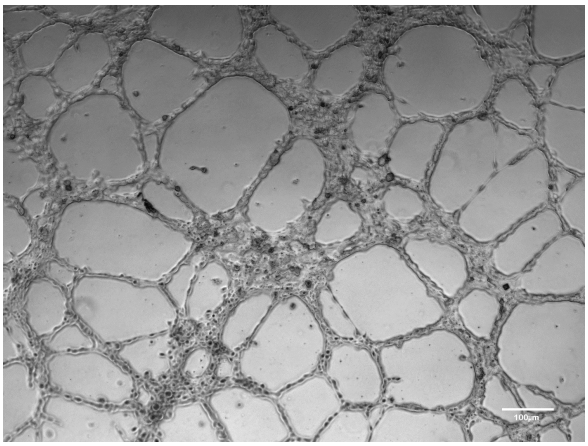

Fig. 2.4 Sample image of pseudo-tubule network observed during tube forming assay

Pseudo-tubule network formed by HUVEC seeded onto BME and treated with VEGF, Fibroblast Growth Factor 2 (FGF-2), Stromal Cell-Derived Factor (SDF) for 12 hours under normoxic conditions. Scale bar = 100 µm

2.7.3 Endothelial cell tube forming assay

The endothelial cell tube forming assay is used to assess the pro-angiogenic effect of a compound, cell mixture or supernatant. Endothelial cells with high angiogenic potential, here HUVECs, were seeded onto a gel matrix, here reduced growth factor Basement Membrane Extract (BME) and treated with supernatants from monocyte-hBMSC co-cultures. Pro-angiogenic effects could be observed through the formation of pseudo-tubule networks on the BME by HUVECs in response to stimulation (fig. 2.4). Characteristics of these networks, such as branching interval or total mesh area, gave an indication of the presence and relative potency of the pro-angiogenic factors within the supernatants.

BME was thawed slowly on ice. 8 well EZSlide slides were coated with BME and incubated for 30 minutes under normoxic conditions. HUVECs were detached and quantified as described in section 2.1.1. 2×10^5 HUVECs were added to each well containing BME in 20 µl 50-50 Medium. Supernatants isolated from hBMSC-monocyte cultures as in section 2.7.2 were thawed, mixed, and centrifuged at 14 000 RCF for 5 minutes and the pellet discarded. 200 µl supernatant was added to all test wells. Control wells contained either 50-50 Medium without cytokines (negative control) or 50-50 Medium with 200 µg/ml VEGF, 100 µg/ml FGF-2 and 100 µg/ml SDF (positive control).

Endpoint experiments were incubated for 12 hours under normoxic conditions, then imaged on a Nikon Eclipse TI microscope. Advanced Biology Hamamatsu Legacy image capture software was used to record data.

Gilles Carpentier's Angiogenesis Analyzer plugin for FIJI was used to analyse data. Graphs were plotted in GraphPad Prism.

Chapter 3

Isolation and characterisation of hBMSC under normoxic and hypoxic conditions

3.1 Abstract

Aim: To isolate robust, well-characterised populations of hBMSCs from human sources under normoxic and hypoxic culture conditions.

Methods: hBMSCs were isolated from human bone marrow taken from donors undergoing total knee replacement. Paired lines of hBMSCs were prepared from each donor by incubating under normoxic and hypoxic culture conditions. These lines were characterised using CFU assay, trilineage differentiation, and flow cytometry.

Results: hBMSCs showed features of hBMSC populations. The isolated hBMSCs had variable growth. Differentiation potential varied between donors and also oxygen levels. Hypoxic conditions ablated osteogenic differentiation, while enhancing chondrogenic and adipogenic differentiation. Characterisation by flow cytometry showed that at least 80 % of the isolated populations were (CD73+)(CD90+)(CD105+)(CD34−)(CD45−)(CD14−)(CD19−).

Conclusion: Robust populations containing a majority of hBMSCs were isolated in both normoxic and hypoxic conditions and characterised. The data suggests that current characterisation methods for BMSC do not encompass hypoxic isolation conditions.

3.2 Introduction

As an early intervention, surgical bone marrow stimulation techniques show promise as a therapy for cartilage defects and osteoarthritis. However, significant development is required to improve the biomechanical properties of the regenerated tissue. Studies have suggested that hBMSC are critical mediators of the repair and regeneration resulting from surgical bone marrow stimulation, with improved outcomes seen when the surgeries are combined with exogenous hBMSC administration (Broyles 2017b; Saw 2011, 2013). In addition, alteration of the repair's immune environment following surgical bone marrow stimulation, such as by addition of the anti-inflammatory agent hyaluronic acid, has been shown to improve the outcome of the therapy (K. Lee et al. 2007). Although the mechanism by which hBMSC contribute to repair is not fully understood, hBMSC are known to be potent immuno-modulatory cells: interactions between hBMSC and immune cells have been shown to have significant impact on the repair outcomes following fracture (El-Jawhari et al. 2016; Nicolaidou et al. 2012; Ramirez-GarciaLuna et al. 2017)

Understanding the significance of the interactions between hBMSC and immune cells could indicate possible interventions to improve the outcomes of surgical bone marrow stimulation. However, while the hBMSC niche and the environment of early repair are hypoxic, the majority of studies isolate, characterise, and study hBMSC under normoxic conditions, or use hypoxic pre-conditioning of hBMSC isolated under normoxic conditions as a proxy (Faulknor et al. 2017; Hung et al. 2012; Tian et al. 2013; Yang et al. 2011). At present, the influence of oxygen level during isolation and culture on hBMSC behaviour is poorly understood.

To allow the examination of hBMSC -immune cell interactions under both normoxic and hypoxic conditions, strains of hBMSC isolated and cultured under said conditions were required. Furthermore, the strains needed to be well-characterised to allow comparison between this work and work in the wider literature. In order to achieve this, paired strains were isolated under normoxic and hypoxic conditions from bone marrow obtained, following informed consent, from patients undergoing total knee arthroplasty. These strains were characterised using the ISCT guidelines for hBMSC characterisation: 1) the ability to differentiate into adipogenic, chondrogeneic, and osteogenic lineages; 2) plastic adhesion; 3) colony forming activity; and 4) cell surface marker expression of (CD73+)(CD90+)(CD105+)(CD34-)(CD45-)(CD14-)(CD19-) as determined by flow cytometry (Dominici et al. 2006).

3.3 Results

In order to permit investigation into the interactions between human BMSC and immune cell subpopulations, robust, well-characterised hBMSC populations were required. Bone marrow was obtained with consent from donors undergoing total knee replacement and strains of adherent bone marrow cells were isolated from the marrow of each donor under both normoxic and hypoxic conditions. The phenotypes of the paired isolates were morphologically similar: cells isolated under normoxic (fig. 3.1a) and hypoxic (fig. 3.1b) conditions both had a fusiform, fibroblastic appearance. Following isolation, cells subsequently grown under hypoxia appeared to proliferate faster than their counterparts in normoxia.

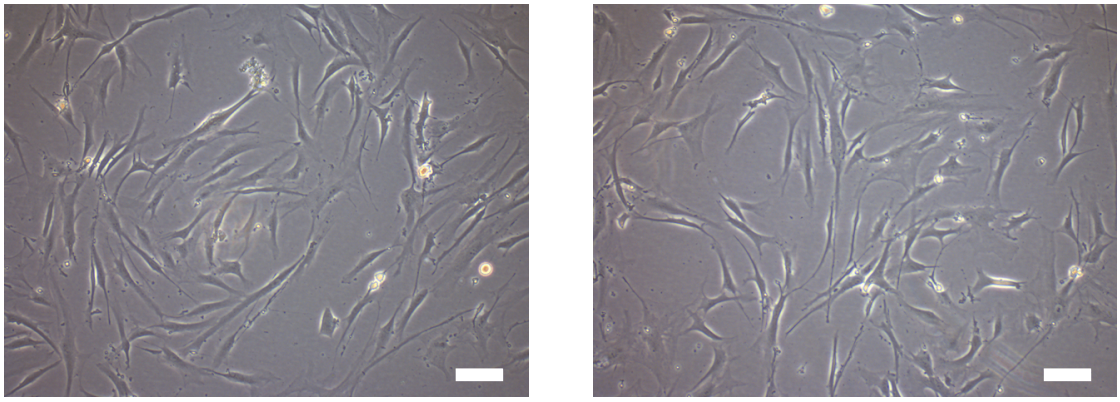

(a) Normoxic (b) Hypoxic

Fig. 3.1 Isolated adherent cells from human bone marrow under normoxic and hypoxic conditions

Human adherent bone marrow cells were isolated in Medium B under normoxic (fig. 3.1a) or hypoxic (fig. 3.1b) conditions from bone marrow extracted during total knee replacement. Cells were washed after 72 hours and cultured for 10 days. N = 15. Scale bar = 100 µm

In total, isolations were attempted from 16 donors, which were numbered sequentially (table 3.1). Paired isolations under normoxic and hypoxic condition were attempted from all donors received, aside from HUM-008 where only the hypoxic condition was attempted, due to the small size of the sample. Of the 16 donors, only 6 yielded paired strains in both normoxic and hypoxic conditions. Of the remaining 10 donors, 5 did not yield strains under either condition, 1 yielded a strain under normoxic conditions only, and the remaining 4 donors, including the aforementioned Donor 8, yielded a strain only under hypoxic conditions.

Eight strains, consisting of paired normoxic and hypoxic strains from the first 4 donors yielding strains under both conditions, were fully characterised by tripotential differentiation, colony forming unit assay and flow cytometry. Strains were all isolated at different points and frozen. Characterisation work was done simultaneously on all strains following thaw. There were clear differences between the strains isolated from different donors in all criteria.

Donor	Normoxic condition	Hypoxic condition
HUM-001	Y	Y
HUM-002	Y	N
HUM-003	N	N
HUM-004	Y	Y
HUM-005	Y	Y
HUM-006	N	N
HUM-007	N	Y
HUM-008	*	Y
HUM-009	Y	Y
HUM-010	N	Y
HUM-011	N	Y
HUM-012	N	N
HUM-013	Y	Y
HUM-014	Y	Y
HUM-015	N	N
HUM-016	N	N

Table 3.1 Isolated hBMSC strains from 16 donors

hBMSC were isolated under normoxic and hypoxic conditions from 16 donors. Strains which adhered and reached 70 to 80 percent confluence after isolation were considered successfully isolated. Y: successful isolation, N: unsuccessful isolation, *: no isolation attempted due to insufficient volume of bone marrow received.

Trilineage differentiation experiments using the 8 strains showed large variations. 3 out of 4 strains showed osteogenic differentiation under normoxic conditions (figs. 3.2a, 3.3a and 3.4a), while the fourth showed none (fig. 3.5a). In contrast, none of the hypoxic strains showed any osteogenic potential (figs. 3.2b, 3.3b, 3.4b and 3.5b). A preliminary crossover experiment suggested that normoxic strains differentiated in hypoxia had decreased osteogenic potential, but hypoxic strains differentiated in normoxia still showed no osteogenesis (Data not shown).

Chondrogenic potential was more consistent, with all strains forming micromasses which stained with Alcian Blue (figs. 3.2c, 3.2d, 3.3c, 3.3d, 3.4c, 3.4d, 3.5c and 3.5d). These micromasses were roughly spherical under both normoxia and hypoxia in 2 donors, Donors 1 and 2 (figs. 3.2c, 3.2d, 3.3c and 3.3d) however with Donors 3 and 4 the hypoxic micromasses (figs. 3.4d and 3.5d) were misshapen, but more spherical than their normoxic counterparts (figs. 3.4c and 3.5c). Donor 4, showed no adipogenesis under either normoxic or hypoxic conditions (Figure A13e,f). The remaining donors all had clear adipogenic differentiation, but this was weaker under normoxic (Figure A10e, A11e, A12e) compared to hypoxic (A10f, A11f, A12f) conditions.

The CFU assay showed further differences between the strains. Both the average CFU potential and the variability changed between donors (fig. 3.6). Donors 1 and 3 had the highest variability, while donors 2 and 4 had low variability in both normoxic and hypoxic conditions. A two-way

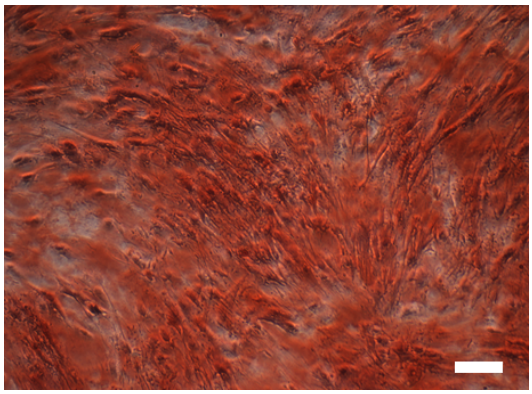

(a) Osteogenesis, normoxic

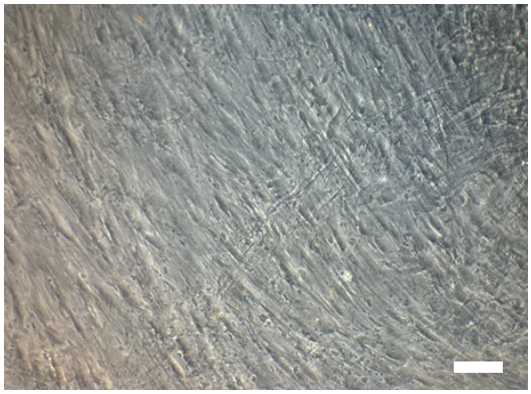

(b) Osteogenesis, hypoxic

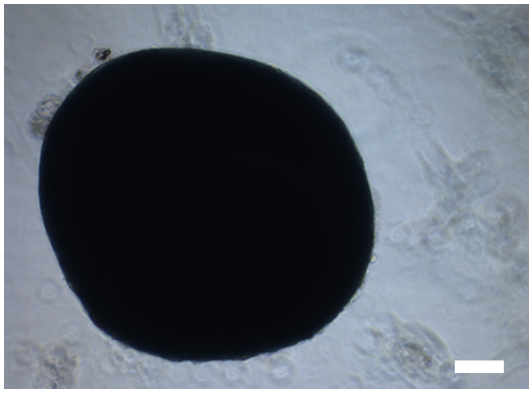

(c) Chondrogenesis, normoxic

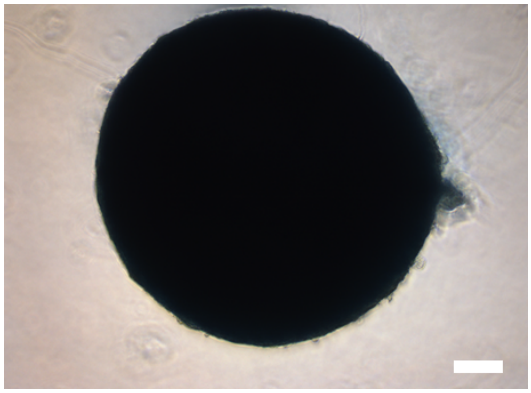

(d) Chondrogenesis, hypoxic

(e) Adipogenesis, normoxic

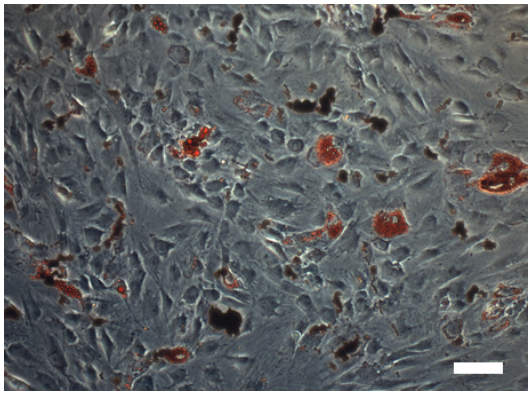

(f) Adipogenesis, hypoxic

Fig. 3.2 Tripotential differentiation of isolated adherent cells from human bone marrow under normoxic and hypoxic conditions from Donor 1

Adherent human bone marrow cells isolated from Donor 1 were differentiated under normoxic (figs. 3.2a, 3.2c and 3.2e) or hypoxic (figs. 3.2b, 3.2d and 3.2f) conditions corresponding to isolation conditions. Cell monolayers were driven down the osteogenic lineage for 21 days and stained with 2 % Alizarin Red (figs. 3.2a and 3.2b). Cell micromasses were driven down the chondrogenic lineage for 14 days and stained with 1 % Alcian Blue (figs. 3.2c and 3.2d). Cell monolayers were driven down the adipogenic lineage for 14 days and stained with Oil Red O (figs. 3.2e and 3.2f). N = 3. Scale bar = 100 µm.

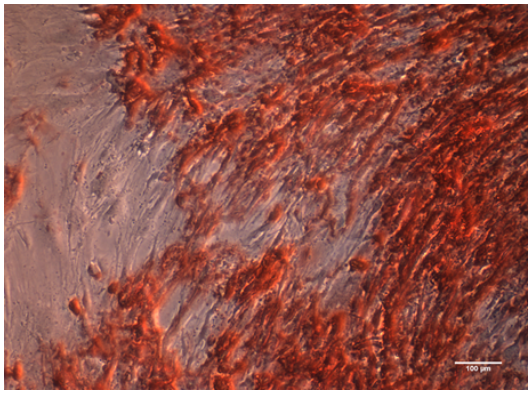

(a) Osteogenesis, normoxic

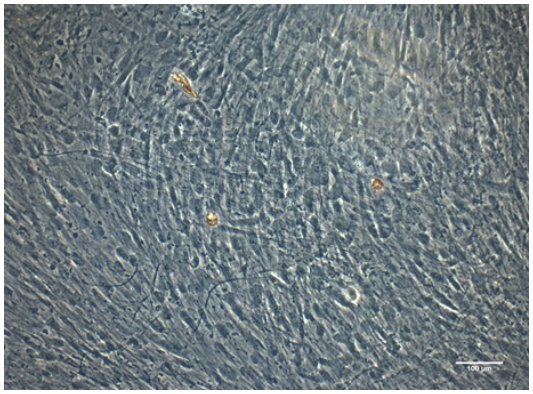

(b) Osteogenesis, hypoxic

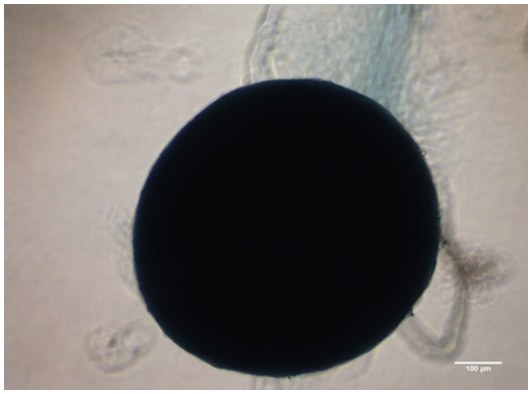

(c) Chondrogenesis, normoxic

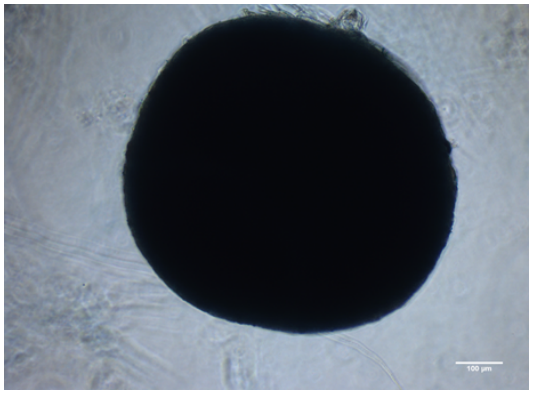

(d) Chondrogenesis, hypoxic

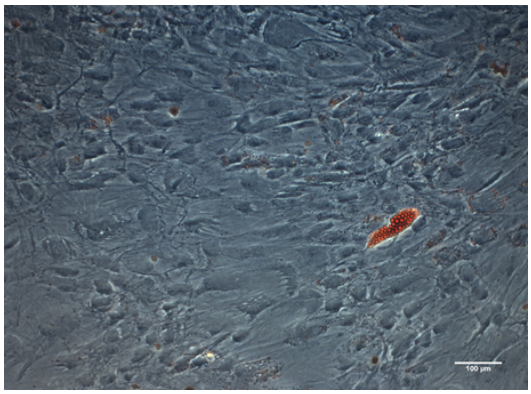

(e) Adipogenesis, normoxic

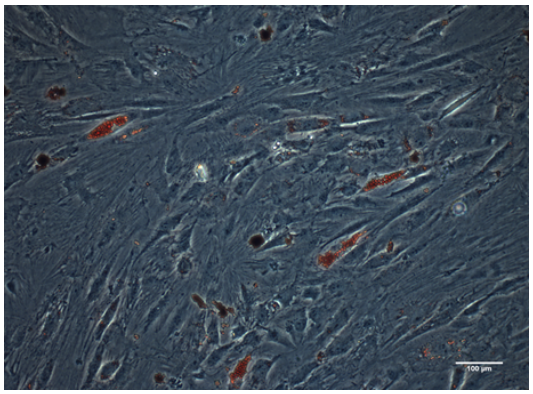

(f) Adipogenesis, hypoxic

Fig. 3.3 Tripotential differentiation of isolated adherent cells from human bone marrow under normoxic and hypoxic conditions from Donor 2

Adherent human bone marrow cells isolated from Donor 2 were differentiated under normoxic (figs. 3.3a, 3.3c and 3.3e) or hypoxic (figs. 3.3b, 3.3d and 3.3f) conditions corresponding to isolation conditions. Cell monolayers were driven down the osteogenic lineage for 21 days and stained with 2 % Alizarin Red (figs. 3.3a and 3.3b). Cell micromasses were driven down the chondrogenic lineage for 14 days and stained with 1 % Alcian Blue (figs. 3.3c and 3.3d). Cell monolayers were driven down the adipogenic lineage for 14 days and stained with Oil Red O (figs. 3.3e and 3.3f). N = 3. Scale bar = 100 µm.

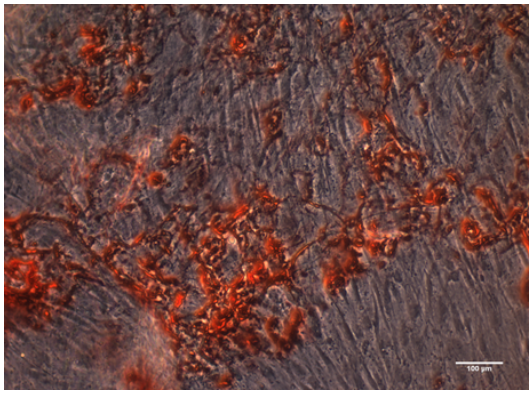

(a) Osteogenesis, normoxic

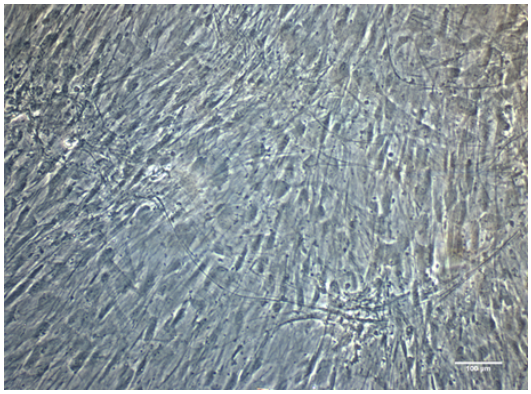

(b) Osteogenesis, hypoxic

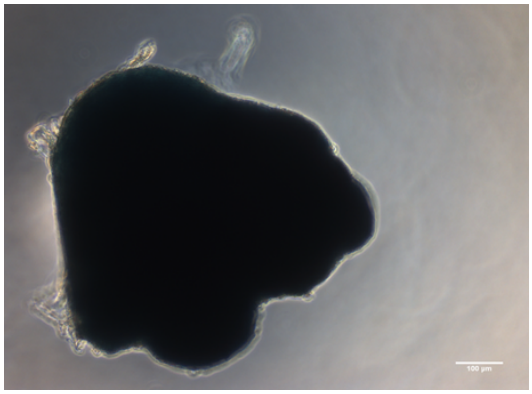

(c) Chondrogenesis, normoxic

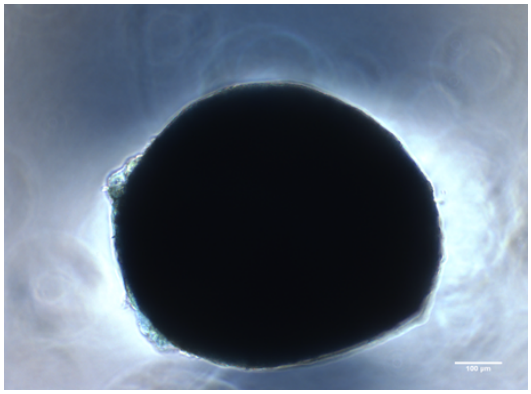

(d) Chondrogenesis, hypoxic

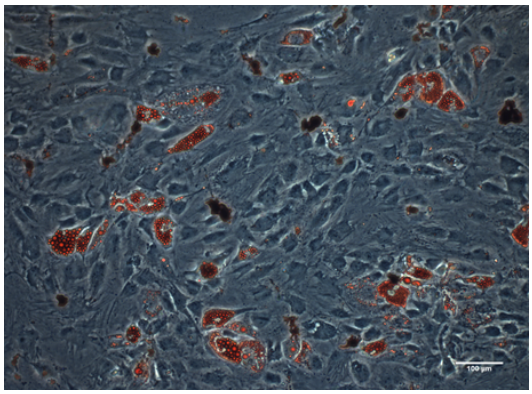

(e) Adipogenesis, normoxic

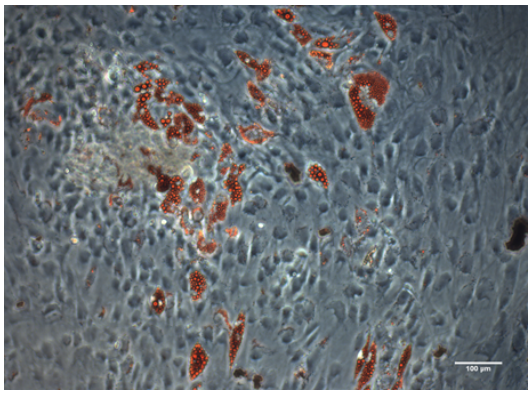

(f) Adipogenesis, hypoxic

Fig. 3.4 Tripotential differentiation of isolated adherent cells from human bone marrow under normoxic and hypoxic conditions from Donor 3

Adherent human bone marrow cells isolated from Donor 3 were differentiated under normoxic (figs. 3.4a, 3.4c and 3.4e) or hypoxic (figs. 3.4b, 3.4d and 3.4f) conditions corresponding to isolation conditions. Cell monolayers were driven down the osteogenic lineage for 21 days and stained with 2 % Alizarin Red (figs. 3.4a and 3.4b). Cell micromasses were driven down the chondrogenic lineage for 14 days and stained with 1 % Alcian Blue (figs. 3.4c and 3.4d). Cell monolayers were driven down the adipogenic lineage for 14 days and stained with Oil Red O (figs. 3.4e and 3.4f). N = 3. Scale bar = 100 µm.

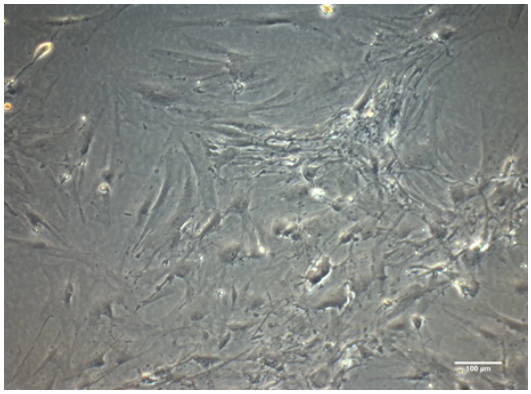

(a) Osteogenesis, normoxic

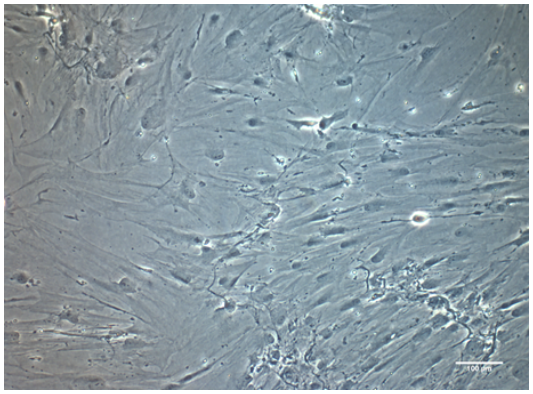

(b) Osteogenesis, hypoxic

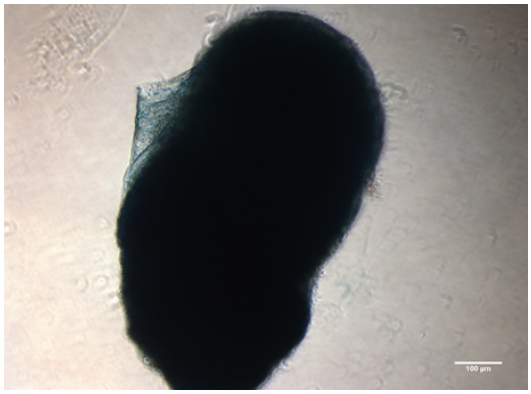

(c) Chondrogenesis, normoxic

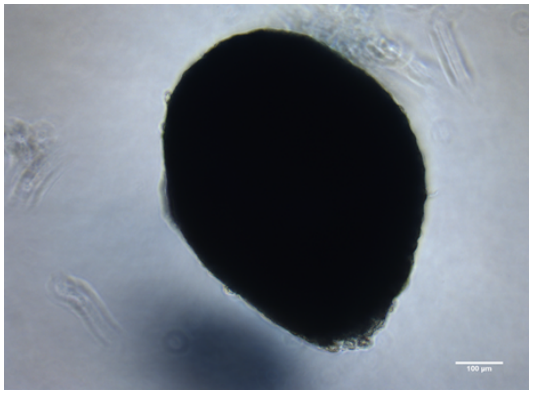

(d) Chondrogenesis, hypoxic

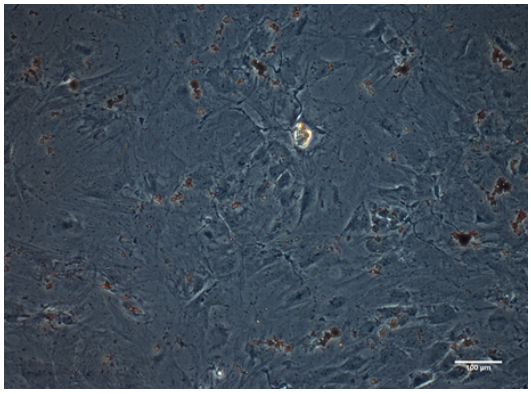

(e) Adipogenesis, normoxic

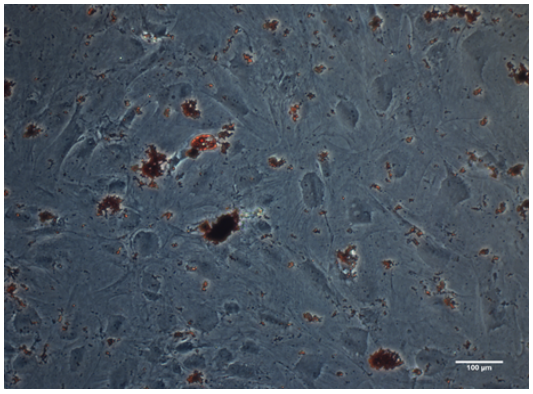

(f) Adipogenesis, hypoxic

Fig. 3.5 Tripotential differentiation of isolated adherent cells from human bone marrow under normoxic and hypoxic conditions from Donor 4

Adherent human bone marrow cells isolated from Donor 4 were differentiated under normoxic (figs. 3.5a, 3.5c and 3.5e) or hypoxic (figs. 3.5b, 3.5d and 3.5f) conditions corresponding to isolation conditions. Cell monolayers were driven down the osteogenic lineage for 21 days and stained with 2 % Alizarin Red (figs. 3.5a and 3.5b). Cell micromasses were driven down the chondrogenic lineage for 14 days and stained with 1 % Alcian Blue (figs. 3.5c and 3.5d). Cell monolayers were driven down the adipogenic lineage for 14 days and stained with Oil Red O (figs. 3.5e and 3.5f). N = 3. Scale bar = 100 µm.

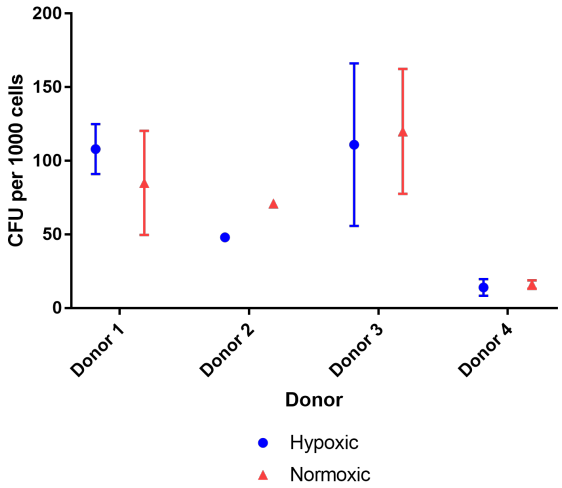

Fig. 3.6 Colony forming unit assay for adherent bone marrow cells from Donors 1, 2, 3 and 4

Adherent bone marrow cells isolated under normoxia and hypoxia from 4 Donors were used in a CFU assay. Error bars show standard deviation (smaller than symbol for Donor 2). 2-way ANOVA, no significant interactions. N = 4

Analysis Of Variance (ANOVA) was performed and found there were no statistically significant differences between CFU activity between normoxic and hypoxic conditions isolated from the same donor. The CFU activities of the donors can be grouped into 2: 2 donors with higher CFU activity, but higher variance, and 2 donors with lower CFU activity and less variance. Visual inspection of the data suggests that Donor 4 had the lower CFU, and that Donor 2 may have had a slightly lower CFU compared to Donors 1 and 4, but the differences between the variances preclude statistical comparisons.

The CFU results did not entirely reflect the observed *in vitro* growth rate of the BMSC, as indicated by the passage frequency and cell yield on passage. Firstly, the hypoxic cultured BMSC grew more rapidly than the normoxic culture BMSC and required more frequent splitting. Secondly, although the CFU for Donors 2 and 4 were similar, the observed passage frequency was not and the colonies within the CFU assay were larger in Donor 2, compared to Donor 4.

The isolated populations were characterised by multiparametric flow cytometry. Single colour analysis of the data shows that all strains meet the 95 % positivity threshold for CD73 expression (fig. 3.7a). 5 strains meet the threshold criteria for CD90 (fig. 3.7b), and 4 for (fig. 3.7c). However, with the exception of 1 donor, Donor 2, at 87 % CD90 positivity, all strains have over 90 % positivity for key BMSC markers. Aside from 1 donor, Donor 1, for CD14 with around 4 % expression, all strains had less than 2 % expression of each of 4 negative BMSC markers (fig. 3.8): CD34 (fig. 3.8a), CD45 (fig. 3.8b), CD14 (fig. 3.8c), and CD19 (fig. 3.8d). When multiparametric analysis was performed, the percentage

of 'true' BMSC, indicated by (CD73+)(CD90+)(CD105+)(CD45−)(CD34−)(CD14−)(CD19−) was between 83 to 94 % (fig. 3.9).

There was no consistent difference in expression between marker expression in hBMSC isolated under hypoxic or normoxic conditions for any donor. The normoxic condition isolated strains from Donors 3 and 4 were the closest to having 95 % of cells matching the phenotype (CD73+)(CD90+)-(CD105+)(CD45−)(CD34−)(CD14−)(CD19−), with the normoxic condition isolated strain from Donor 2 showing the least number of cells matching the stated phenotype.

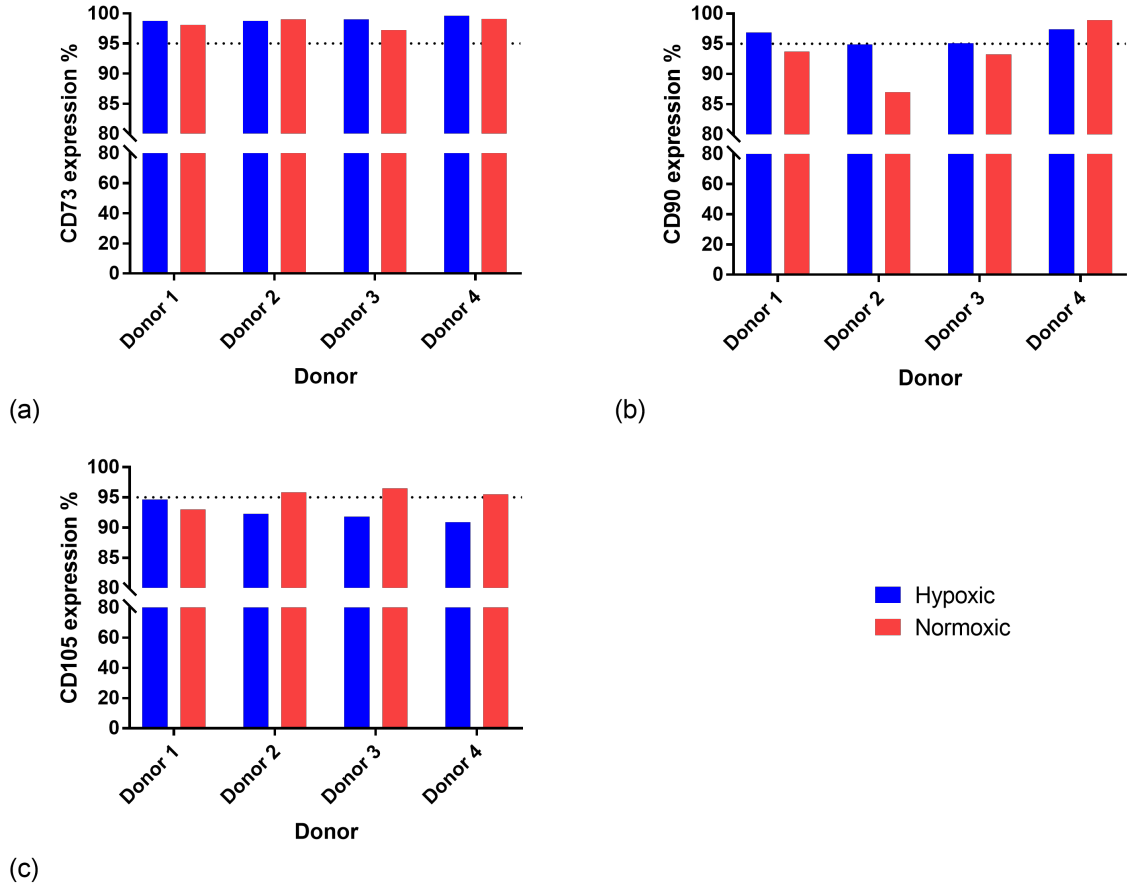

Fig. 3.7 Single colour positive marker analysis of adherent bone marrow cells from Donors 1, 2, 3 and 4 by flow cytometry.

Adherent human bone marrow cells from 4 Donors isolated under normoxia and hypoxia were characterised according to the ISCT criteria for human MSC using multiparametric flow cytometry. Cells were stained with fluorescently conjugated antibodies against CD73, CD90, CD105 and treated with a Zombie live-dead stain. Single-colour positive marker analysis of viable cells is shown using CD73 (fig. 3.7a), CD90 (fig. 3.7b) and CD105 (fig. 3.7c).

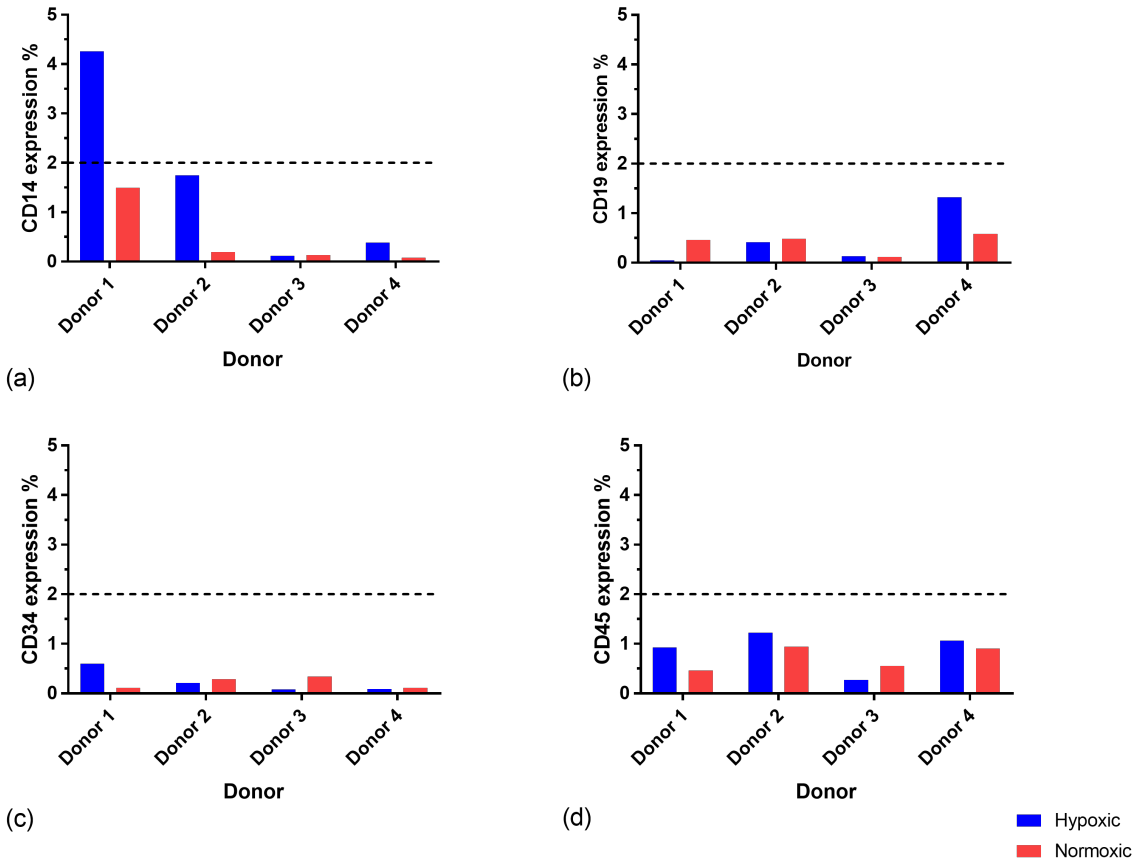

Fig. 3.8 Single colour negative marker analysis of adherent bone marrow cells from Donors 1, 2, 3 and 4 by flow cytometry.

Adherent human bone marrow cells from 4 Donors isolated under normoxia and hypoxia were characterised according to the ISCT criteria for human MSC using multiparametric flow cytometry. Cells were stained with fluorescently conjugated antibodies against CD34, CD45, CD14 and CD19 and treated with a Zombie live-dead stain. Single-colour negative marker analysis of viable cells is shown using CD34 (fig. 3.8a), CD45 (fig. 3.8b), CD14 (fig. 3.8c) and CD19 (fig. 3.8d).

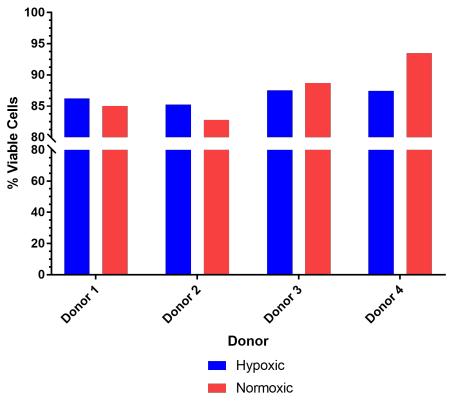

Fig. 3.9 Multiparametric analysis of adherent bone marrow cells from Donors 1, 2, 3 and 4 by flow cytometry.

Adherent human bone marrow cells from four Donors isolated under normoxia and hypoxia were characterised according to the ISCT criteria for human MSC using multiparametric flow cytometry. Cells were stained with fluorescently conjugated antibodies against CD73, CD90, CD105, CD34, CD45, CD14 and CD19 and treated with a Zombie live-dead stain. Multiparametric analysis was performed using all seven markers.

3.4 Discussion

In order to be able to compare the interactions between hBMSC and immune cell subpopulations under normoxic and hypoxic conditions, well-characterised, robust hBMSC populations were required. Current comparisons of hBMSC phenotype and their response to culture in varying oxygen levels have generally used hBMSC isolated under normoxic conditions and then exposed to hypoxic conditions, rather than continuous culture under a single condition (Fink et al. 2008; Hung et al. 2012; Wagegg et al. 2012; Yang et al. 2011). As a result, hBMSC isolated and cultured under hypoxic conditions may have experienced different selection pressures compared to those isolated under normoxic and then preconditioned in hypoxic conditions, with resulting changes in phenotype and behaviour. Furthermore, constant culture under hypoxic conditions has greater biological relevance to the conditions experienced in a haematoma or in the bone marrow due to the more comparable oxygen levels present in these tissue environments. The use of well-characterised, paired populations of hBMSC isolated from the same donor under normoxic and hypoxic conditions is a defining feature of this study.

hBMSC were isolated from human bone marrow by tissue adhesion under normoxic (18.6 % oxygen) and hypoxic (3 % oxygen). Oxygen levels were defined relative to ambient atmospheric levels within a normoxic incubator at sea level and not to physiological levels) conditions, then cells were continuously cultured and expanded under the same conditions. It should be noted that oxygen levels within a normoxic incubator are lower than the usually quoted 21 % due to the humidity within the incubator; saturation of air with water reduces the partial pressure of oxygen (Wenger et al. 2015). Once expanded, the populations were characterised through a combination of tri-potential differentiation, colony forming unit assay, and flow cytometry as per the ISCT guidelines (Dominici et al. 2006). This demonstrated that there were significant differences, not only between donors, but also between the lines of hBMSC isolated from the same patient under the normoxic or hypoxic condition. Surface marker expression and colony forming ability were similar between the paired lines, with colony forming ability showing greater differences between donors than surface marker expression. However, functional assessment of the hBMSC, as measured by their tripotential differentiation abilities, showed dramatic differences both between donors and between the lines isolated under normoxic and hypoxic conditions.

The greatest difference between the two conditions was the loss of osteogenic differentiation potential in hypoxic cultured lines. In 3 out of the 4 donors assessed, osteogenic differentiation potential was seen in the normoxic condition line, but not in the hypoxic. The fourth donor, Donor 4, was the weakest at differentiating and did not show osteogenic potential in either condition. Examination of the literature to date showed that no other study considered the influence of isolation and constant culture of hBMSC in hypoxic conditions on osteogenesis; other studies have only used hBMSC isolated in normoxic conditions and then preconditioned under hypoxic conditions. However, under

these conditions there is no consensus on the effect of hypoxic conditions on osteogenesis; some studies show hypoxic conditions enhance osteogenesis, while others show that osteogenesis is ablated under hypoxic conditions (Hung et al. 2012; Wagegg et al. 2012; Yang et al. 2011). However, the method and extent of the hypoxia created in these studies varied. Within *in vitro* biological research, the term 'hypoxia' does not denote a specific oxygen level, merely that the level within the humidified incubator is lower than ambient atmospheric at sea level (18.6 %), nor is there a single method for creating hypoxic conditions. In the studies from the literature mentioned above, hypoxic conditions of 1 to 2 % oxygen were either created by nitrogen injection, or induced via chemical methods through addition of desferrioxamine (DFO) or dimethyloxalylglycine (DMOG) to the culture, but only in cells which had been previously isolated under normoxic conditions. Chemically-induced hypoxia targets the Hypoxia Induced Factor 1 alpha (HIF-1α) pathway, while hypoxia via nitrogen injection more closely mirrors the pathway effects seen *in vivo* (Yang et al. 2011). Interestingly, DMOG and DFO appear to have differing effects on osteogenesis; a comparison of DFO and nitrogen injection induced hypoxia found downregulation of osteogenesis in both cases through inhibition of RUNX-2 by Twist (Formerly Dermo-1) (TWIST) / HIF-1α, while DMOG treatment appeared to enhance osteogenesis (L. Ding and Morrison 2013; Yang et al. 2011). This would firstly suggest that the method of developing hypoxia in the culture system has a strong effect on the outcome. Secondly, hypoxic conditions generated by nitrogen injection appear to influence osteogenic differentiation in hBMSC regardless of isolation condition. Performing a cross-over osteogenesis experiment, differentiating normoxic-isolated hBMSC under hypoxic conditions and vice versa, would indicate whether the observed effects presented here were a result of transient pathway alteration or due to selection of a functionally different hBMSC population.

In my study, while less dramatic than the influence seen in the osteogenic differentiation, alterations were seen in both the adipogenic and chondrogenic differentiation potential of the isolated strains. For both strains, differentiation was stronger in the hypoxic compared to the normoxic condition, although adipogenic differentiation was generally poor. While this is widely supported in the case of chondrogenic differentiation (Adesida et al. 2012; Bornes et al. 2015), there is conflicting evidence in the wider literature with regard to adipogenic differentiation with both enhancement and down-regulation of adipogenesis seen in hBMSC in hypoxic compared to normoxic conditions (Fink et al. 2008; Wagegg et al. 2012). Additionally, chondrogenesis was the only characteristic differentiation exhibited by all lines examined. Statements relating to the strength of the chondrogenic potential are based upon the sphericity of the micromasses formed by the different lines isolated; in all cases, the micromasses from hBMSC isolated and differentiated in hypoxic conditioned were more spherical than those in the paired normoxic treated lines. There was also donor-to-donor variation in sphericity; donors which showed greater osteogenic potential in the normoxic condition also had the most spherical micromasses, with the least variation between normoxic and hypoxic conditions. Differences in sphericity could result from variable chondrogenesis throughout the micromass, either due to a globally weak chondrogenic phenotype developing, or patchy differentiation due to hBMSC

subpopulation distribution resulting in uneven matrix deposition. This would result in unequal internal forces within the micromass, preventing condensation into a sphere and resulting in a misshapen mass. Despite the fact that adipogenic and chondrogenic differentiation appeared to be enhanced by the hypoxic isolation and culture conditions of the hBMSC, the two potentials appeared not to be linked; the donor with the most misshapen micromasses in both normoxic and hypoxic conditions, indicating weak chondrogenesis, in fact had the strongest adipogenic differentiation in both conditions. The use of sphericity as a measure of the homogeneity and stability of chondrogenically-differentiated hBMSC spheroids has been previously documented Bellotti et al. 2016. A more quantitative assessment of differentiation strength of the chondrogenic cultures, such as DNA or Glycosaminoglycan (GAG) content alongside immunohistochemistry could give a clearer indication of the source of the variation in sphericity of the micromasses.

Out of the 8 lines characterised, paired normoxic- and hypoxic-condition isolated hBMSC from 4 donors, only 3 met the ISCT hBMSC criteria for trilineage differentiation potential, all of which were lines isolated and differentiated under normoxic conditions, although strength of differentiation did vary between donors (Dominici et al. 2006). The paired hypoxic lines from the same donors all showed bi-lineage potential, being competent at differentiating down the adipogenic and chondrogenic lineages. The final donor characterised showed only chondrogenic differentiation potential in both conditions, being uni-lineage competent. The inhibition of osteogenic differentiation by hypoxic conditions may have functional significance in the healing cascade. The early trauma site is profoundly hypoxic due to vascular damage, with increasing oxygenation as a result of re-vascularisation and increased organisation (Epari et al. 2008; Hirao et al. 2006; Mountziaris and Mikos 2008). In a fracture, the haematoma is converted to soft callus, composed of unmineralised cartilage, which then becomes hard callus and ultimately remodelled bone (Einhorn and Gerstenfeld 2015). The increasing mineralisation progresses in synchronicity with increasing vascularisation, perhaps representing an intrinsic control mechanism to prevent heterotopic ossification. In this case, enhanced chondrogenesis and decreased osteogenesis in hypoxic conditions, and the reverse in normoxic conditions, may indicate a temporal and micro-environment dependent component to hBMSC differentiation ability.

The CFU assay demonstrated that all lines were capable of proliferation and colony forming activity, There was no significant difference between lines isolated under hypoxic or normoxic conditions from the same donor, but there were differences between the individual donors. Interestingly, the donor giving uni-lineage competent lines in normoxic and hypoxic conditions gave the lowest CFU of all the donors, although the CFU of the remaining 3 donors did not track with their differentiation potential or strength of observed differentiation. However, observations made during tissue culture indicated that cultures under hypoxic conditions required more frequent passaging, and that the colonies in the CFU assay were larger in hypoxic conditions compared to normoxic isolated and cultured lines. A study using similar hBMSC isolation and culture protocols, including a hypoxic condition of 3 % oxygen by nitrogen injection, found that lines isolated and cultured under hypoxic conditions had

measurably higher colony forming activity compared to those isolated and cultured under normoxic conditions (Adesida et al. 2012). The difference could be in part due to the variability in CFU seen in the lines in this study, demonstrating the heterogeneity of the population. The study also ran the CFU assay for 14 days, rather than the 10 days used in this study. Further, the contrasting study used marrow taken from the iliac crest of patients aged 34 to 62. In this study, marrow was obtained from the tibial and femoral reamings removed during prosthetic fitting as part of total knee replacement surgery, with patients being aged 64 to 87. Comparisons of CFU in tibial and iliac crest marrow have shown that tibial marrow derived hBMSC have lower CFU than those from the iliac crest (Suzuki et al. 2001). Further, CFU declines with age, particularly in females, although CFU does not appear to be decreased in marrow from patients with OA when compared to matched healthy individuals (Muschler et al. 2001; Stiehler et al. 2016). Taken together, this would indicate that the CFU observed in this study would be expected to have been lower than that in the iliac crest study, and that the effect of age and donation site may have concealed the variation between normoxic and hypoxic conditions.

Alongside this, the observed passage frequency and cell yield on passage did not necessarily track with the CFU value, again perhaps related to the donor age or population heterogeneity. Monitoring of the passage frequency showed that the paired isolates showing trilineage potential in normoxic, and bi-lineage in hypoxic conditions also had a passage frequency after initial adhesion to tissue culture plastic of around 5 to 7 days, being slightly lower in the hypoxic compared to the normoxic condition and varying between donors. To contrast, the paired isolates from the from the fourth donor, which were only uni-lineage competent, had a passage frequency of greater than 14 days. As a result, isolates with a passage frequency of more than 7 days were excluded from future experiments. The variation in differentiation potential and CFU activity might suggest that the populations could be easily distinguished by cell surface marker analysis using flow cytometry, but this was not the case. In fact, levels of expression for both positive and negative hBMSC markers as laid out by the ISCT flow cytometry criteria were fairly similar both between donors and between conditions. However, only 1 line completely met the criteria, with greater than 95 % expression of CD73, CD90, and CD105, and less than 2 % expression of CD34, CD45, CD14, and CD19 in single-staining analysis, and had the highest (CD73+)(CD90+)(CD105+)(CD34−)(CD45−)(CD14−)(CD19−) population using multiparametric analysis. This line was, in fact, the hypoxic line isolated from the uni-lineage competent donor. Furthermore, the donor with the lowest adherence to these flow criteria, both in single-staining and multiparametric analysis was the normoxic trilineage competent line from one of the donors with strong differentiation seen in each lineage. This might indicate that the marker expression could have relevance to the behaviour of the hBMSC. In one study, CD90 expression was found to be reduced on hBMSC in hypoxic conditions, with a correspondingly greater chondrogenic ability in the cell population (Adesida et al. 2012). However, my study showed that CD90 expression was slightly increased under hypoxic conditions. At the same time, marker expression has been seen to be strongly related to passage of hBMSC, with expression levels varying with increasing passage number (Karim Fekir, Unpublished data, University of Cambridge). Finally, and perhaps

most importantly, the ISCT criteria are based on hBMSC isolated from the iliac crest of healthy individuals; while there do not appear to be differences in surface marker expression between tibial and iliac crest hBMSC, a study has shown that CD90 expression is altered in hBMSC isolated from patients with OA relative to healthy patients, suggesting differences between diseased and healthy hBMSC (Narbona-Carceles et al. 2014; Stiehler et al. 2016).

3.4.1 Limitations of the study

This study had several limitations related to donor selection and generation of hypoxia. The conditions of supply and current ethics surrounding the bone marrow collection limited the information available about donors undergoing total knee replacement to age and sex. This precluded any possibility of stratifying or excluding patients, on the basis of information including co-morbidity or medication usage. As an example, bisphosphonate usage is a common reason for donor exclusion, due to its influence on hBMSC behaviour (Hu et al. 2016). During this study, all useable donor material was taken for hBMSC isolation. Due to the age of the donors, bone marrow was extremely fatty, being primarily comprised of yellow marrow as a result of reconversion in the appendicular skeleton, although islets of red marrow may have been present (Małkiewicz and Dziedzic 2012). Further, due to the isolated bone marrow essentially being a by-product of the surgical cuts performed during prosthetic fitting, the samples contained a mixture of marrow, blood, and some fluids used for washing the cavity. Sample volume was dependent on the discretion of the surgeon and, in some cases, was less than 5 ml including blood and other fluids. This means contaminating cell types may have been present and that the sample may not have contained truly representative populations of the bone marrow, perhaps with only a small subset being present at time of isolation; losses during adhesion to tissue culture plastic due to isolation and selection pressures may have resulted in skewed populations. It should be noted that other cell types in marrow or blood besides hBMSC also have the potential to adhere to plastic. Additionally, these populations were isolated from elderly patients with advanced OA. The use of tissue samples from elderly donors undergoing knee replacement is uncommon in this field, where most studies use tissue from younger donors taken from the iliac crest. Ageing has been shown to decrease chondrogenesis and adipogenesis, and CFU activity in adipose-derived MSC and alter hBMSC phenotypes and replicative ability under normoxic conditions, but the influence of hypoxia on hBMSC from elderly donors with OA has not been examined (Block et al. 2017; Ganguly et al. 2017; Marędziak et al. 2016). This represents a neglected area of research and therefore my study is a valuable contribution to the current knowledge.

A further limitation of this study related to the generation of the hypoxic culture condition, a well-acknowledged source of controversy. As already alluded to, there are a range of methods of generating hypoxic conditions *in vitro*. Modification of the oxygen level by nitrogen injection into a specific incubator was selected for this study due to the ability to select the oxygen level within the incubator,

and the less artificial, multi-pathway response on the part of the cells. However, oxygen level was determined by sampling the atmosphere within the incubator and not by peri-cellular measurement of the oxygen level. Since pericellular oxygen level is highly dependant on cell number and metabolism, the values given within this thesis refer only to the atmosphere within the incubator and not the oxygen level experienced by the cells. In addition, equilibration of media in hypoxic environments is slow – one estimate suggests that it takes 38 minutes for media at a depth of 1.78 mm to equilibrate to a 2 % oxygen level from external atmospheric levels (Wenger et al. 2015). To try and circumvent this, media were equilibrated within the incubator prior to use in culture. However, equilibration of bulk media within a warm environment is sub-optimal for removal of oxygen; a better solution would have been to bubble nitrogen gas through cold media, which was not possible in this instance due to lack of gas lines. Further, opening the door of a hypoxic incubator, or removal of the cells for processing rapidly disrupts the oxygen gradient within the medium, leading to multiple re-oxygenation insults. Due to the lack of hypoxic chambers for cell processing, this was mitigated where possible through rapid handling of the cells and use of equilibrated media. It is possible that cells will have been exposed to fluctuating oxygen levels, which may have had an impact on their biology. Finally, the selection of the oxygen level used, 3 % oxygen, was based upon a compromised value; ideally, a concentration of around 1 % would have been used to simulate bone marrow or haematoma conditions (Spencer et al. 2014). As a result, the hypoxic culture conditions throughout this study have flaws which were mitigated where possible, and are acknowledged here. Future work would ideally utilise a hypoxic incubator with the ability to monitor pericellular oxygen levels based on measurement of oxygen levels found *in vivo* within microfracture or haematoma environments. In addition, a hypoxic processing station with the ability to equilibrate media and prevent re-oxygenation insults would permit a more constant level of hypoxic conditions to be administered and prevent corresponding modification of the cellular behaviour due to fluctuations when handling cells. It should be remembered that this limitation was by no means unique to this study, and represents the significant challenges inherent in attempting to artificially create hypoxic environments.

On a related note, the temperature of the incubator used for hBMSC culture could also be considered a confounding factor. In line with standardised tissue culture techniques, and as described in all papers related to hBMSC culture, the incubators were set at 37 °C. As discussed in the introduction, this temperature may not represent the temperature experienced by hBMSC, particularly when isolated from the extremities, in this case the knee. Human knee intra-articular temperature ranges from 31 to 33 °C at rest, increasing during exercise (Becher et al. 2008; Harris and McCroskery 1974). Therefore, the incubator temperature is 4 to 6 °C higher than the potential resting temperature experienced by tibial or distal femoral hBMSC in-situ when at rest, although it may be close to the temperature within the knee during exercise. As a result, the culture conditions may mimic prolonged pyrexic conditions, resulting in increased stress on the hBMSC and therefore an increased risk of abnormal behaviour, such as early senescence or increased inflammatory response. While many studies do use iliac crest

isolated hBMSC, which may experience a temperature closer to 37 °C, there is a widespread lack of consideration given to the specific niche conditions of cells *in vitro*.

3.4.2 Future directions

This study considered the basic ISCT recommended phenotypic characteristics of hBMSC isolated from the proximal tibial and distal femoral region of a small group of unstratified donors. These donors were exclusively elderly and had advanced OA, in contrast to the primary group targeted in micro-fracture, which tends to be younger with focal cartilage defects. Recruitment of younger donors with less advanced disease would allow comparison between elderly and younger cohorts. Further, improved stratification of patients would permit identification and exclusion of donors with co-morbidities or medications which may confound the study, as well as enabling comparisons of the influence of different factors, such as sex, on hBMSC behaviour.

Additionally, a study making use of a greater range of phenotypic markers might allow greater identification of differences between the subpopulations. For example, use of additional flow markers such as CD44, CD146, CD271, and CD29 have been suggested to identify an hBMSC population (Adesida et al. 2012; W. Chen et al. 2018; James et al. 2015; Sotiropoulou et al. 2006). Use of a greater number of markers on a well-stratified patient population could assist identification of markers with functional significance, especially within the hypoxic condition isolated hBMSC. Running crossover tripotential differentiation experiments would further indicate whether the changes in behaviour seen in the hBMSC were a result of population selection, and therefore independent of oxygen level, or were a result of transient inhibition of specific pathways, and therefore reversible by culture in the opposite condition. Finally, a more comprehensive gene expression analysis could be undertaken, perhaps using Affymetrix or RNASeq, which would allow a more holistic picture of alterations to behaviour during hypoxic or normoxic isolation, culture, and differentiation to be elucidated. This would assist in updating the ISCT recommendations for characterising hBMSC, particularly with regard to those isolated and cultured under hypoxic conditions.

3.4.3 Summary

Paired hBMSC lines isolated under hypoxic and normoxic conditions from 4 donors were characterised and shown to have some features consistent with an MSC population as defined by the ISCT, although adherence to these criteria differed based on donor-to-donor variation and isolation / culture conditions (See table 3.2). As a result of differences between the ISCT MSC criteria and the findings of this study, the hBMSC denomination has been adopted. Based on the findings of this study, hBMSC populations isolated from further donors during this study were characterised solely by multiparametric flow cytometry and only populations with passage frequencies of less than 7 days were used in experiments.

Table 3.2 Summary of hBMSC phenotyping
A = adipogenic, C = chondrogenic, O = Osteogenic differentiation. Colony forming activity based on relative assessment of donors. Flow markers show multiparametric analysis with percentages relating to number of cells meeting the phenotype (CD73+)(CD90+)(CD105+)(CD45−)(CD34−)(CD14−)(CD19−)

Donor	ID	Oxygen level	Differentiation	Colony forming	Flow markers
1	HUM001	Normoxic	A, C, O	Good, but variable	86.3%
		Hypoxic	A, C	Good, but variable	85.0%
2	HUM004	Normoxic	A, C, O	Good	85.3%
		Hypoxic	A, C	Good	82.7%
3	HUM005	Normoxic	A, C, O	Good, but variable	87.8%
		Hypoxic	A, C	Good, but variable	88.7%
4	HUM009	Normoxic	C	Poor	87.9%
		Hypoxic	C	Poor	93.5%

This study has shown that the ISCT guidelines, which are still widely used, do not take into account cells isolated and cultured under hypoxic conditions, and therefore require updating. This study supports the finding that hypoxic differentiation conditions inhibit osteogenesis, and adds to the body of knowledge by suggesting that this is not due to a stress response from a normoxic condition isolated and cultured population entering a hypoxic condition, but rather an intrinsic inhibitory mechanism.

To conclude, hBMSC isolated from the bone marrow of elderly donors with OA were viable, although donor-to-donor variation was observable. Furthermore, isolation and culture of hBMSC under hypoxic conditions did not influence colony forming activity or cell surface markers, but did alter differentiation ability relative to normoxic conditions. As a result, well-defined strains of hBMSC were isolated for use in my studies.

Chapter 4

Characterisation of a peripheral blood subpopulation influencing hBMSC migration under normoxic and hypoxic conditions

4.1 Abstract

Aim: To identify a subpopulation of cells within the peripheral blood inducing significant migration in hBMSC in hypoxic and/or normoxic conditions

Methods: PBMC from leukocyte reduction system cones were fractionated using magnetic activated cell sorting. The resulting subpopulations were used in Boyden Chamber and real-time migration assays in normoxic and hypoxic conditions. The subpopulation causing the greatest migration compared to its partner was characterised through protein expression, cell surface marker expression, differentiation, and co-culture assays.

Results: The subpopulation inducing the greatest migration was the $CD45_{dep}CD31_{enr}$ population. This population secreted proteins which appeared monocytic but did not respond to monocyte differentiation stimuli. Flow cytometry demonstrated that the subpopulation had a (CD56+)(CD16+)-(CD3−)(CD19−) identity, indicating NK cells. Co-cultures of these cells with hBMSC and IL-2 resulted in an increased level of cell death in the hBMSC population.

Conclusion: The subpopulation inducing the greatest difference in migration compared to its paired opposite was characterised as being an NK cell subpopulation.

4.2 Introduction

The outcome of repair following trauma is heavily dependent on the cellular profile of the damaged region, a phenomenon seen in many studies. For example, ablation of the adaptive immune system is associated with improved fracture repair, while macrophage depletion leads to delayed and poor-quality bone repair and hBMSC administration can enhance healing of large bone defects (Y. Chen et al. 2017; Dupont et al. 2010; Petri et al. 2013; Schlundt, El Khassawna, et al. 2018; Toben et al. 2011). Furthermore, being strongly immuno-modulatory, hBMSC are known to have bi-directional interactions with many components of the immune system with consequences for the outcome of the repair. As an example, interactions with monocytes during fracture repair induce osteoblastic differentiation and matrix mineralisation by hBMSC, while interactions between HSPC and hBMSC promote vascularisation (Guihard et al. 2018; Moioli et al. 2008; Nicolaidou et al. 2012). In addition, hBMSC appear to have an anti-fibrotic effect through their regulation of the immune response: this is highly desirable in the case of surgical bone marrow stimulation, where reduction of fibrocartilage formation in favour of hyaline cartilage is critical to improving the outcome of the therapy (Phinney and Pittenger 2018). While paracrine signalling pathways play a role in these interactions, direct contact between cell types has been shown to mediate many of the responses. As a result, cell-to-cell interactions between hBMSC and components of the immune system are likely to have a powerful role in determining the outcome of a repair.

Both hBMSC and immune cells are highly migratory, and rapidly home to sites of damage, such as that caused by surgical bone marrow stimulation (Geissmann et al. 2010; Granero-Moltó et al. 2009). While this has been extensively studied, the partitioning of the cells within the damaged region, and the consequences thereof, are less well understood. In this work, the uni-directional recruitment of hBMSC from the bone marrow to the site of the surgically induced repair by immune cells was modelled. It was postulated that hBMSC would be recruited to the site of damage by the immune cells, resulting in co-localisation of the hBMSC and the recruiting cell type. In this case, the hBMSC would partition with the immune cell type producing the most powerful migratory response and, as a result, the hBMSC would therefore interact with said recruiting cells in a cell-to-cell manner, thereby indicating a common or significant interaction occurring in the repair site. This chapter aimed to identify a subpopulation of immune cells resulting in migration of hBMSC under normoxic and hypoxic conditions as a prelude to characterising the interaction between the hBMSC and the identified migration-inducing cell type.

In order to achieve the aim of this chapter, the hBMSC which had been isolated and characterised in the previous chapter were exposed in a paracrine system to peripheral blood populations fractionated using magnetic activated sorting. Sequential sorting was used to screen populations and identify the most active, which was then characterised through the use of protein secretion, flow cytometry and functional assays.

4.3 Results

Throughout this section, the subscript '$_{enr}$' refers to PBMC which have been enriched by MACS for a specific marker, and the subscript '$_{dep}$' likewise refers to populations depleted for a specific marker by the same method. Markers in brackets, such as (CD45+) or (CD16−) refer to cell surface marker expression as determined by flow cytometry.

4.3.1 Transwell part 1

PBMC were isolated from LRS cones by density gradient centrifugation and collection of the buffy coat. The PBMC were fractionated using magnetic bead activated cell sorting. Paired samples containing the enriched and depleted fractions were isolated from the same sample. The first transwell panel compared the migration of hBMSC in hypoxic and normoxic conditions when exposed to unfractionated PBMC, and $CD45_{enr}$ and $CD45_{dep}$ PBMC (fig. 4.1). Responses to PBMC were variable, although normoxic hBMSC seemed to have more consistently increased migration compared to hypoxic hBMSC, however this did not reach statistical significance (fig. 4.1a). The $CD45_{dep}$ PBMC appeared to induce greater hBMSC migration in both normoxic and hypoxic conditions, but statistical analysis using a paired T-test showed that this was only significant in the hypoxic condition ($p < 0.05$) (fig. 4.1b).

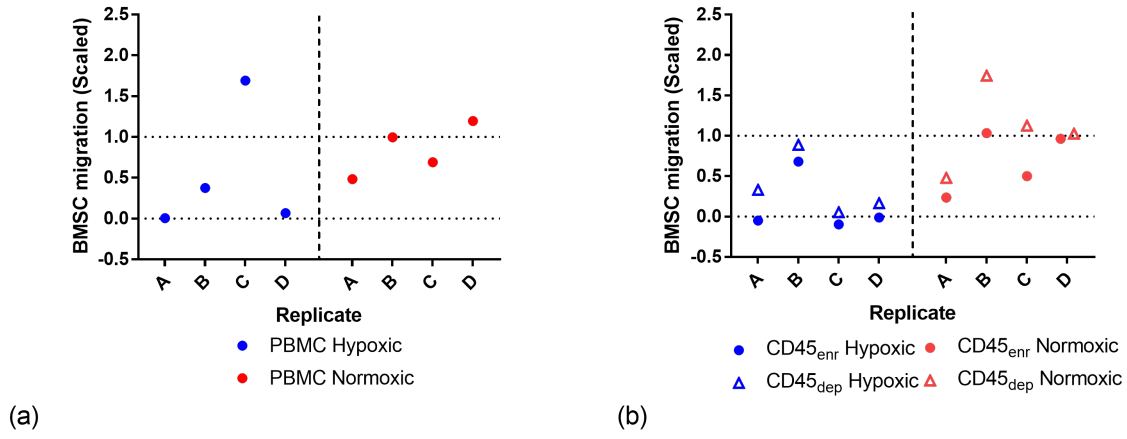

Fig. 4.1 Migration of BMSC across transwell membranes when in paracrine culture with peripheral blood subpopulations isolated using Panel 1

Results were scaled so negative control = 0 and positive control = 1 (dotted lines on graphs). Variance is not shown due to use of scaling. BMSC were co-cultured with PBMC (fig. 4.1a) or CD45 enriched and depleted PBMC subpopulation (fig. 4.1b). A, B, C, and D refer to biological replicates using different BMSC donors and separate isolations of PBMC (fig. 4.1a) or $CD45_{enr/dep}$ PBMC (fig. 4.1b). Statistical analysis showed that in hypoxic condition, $CD45_{dep}$ isolated subpopulation stimulated greater migration than $CD45_{enr}$ (Paired T-test, $p < 0.05$). No significance seen in normoxic condition. N = 4.

4.3.2 Transwell part 2

As the $CD45_{dep}$ PBMC were found to be of interest, this fraction was further divided by a second round of MACS isolation, using CD31 (fig. 4.2a), CD34 (fig. 4.2b) and CD146 (fig. 4.2c) enriched and depleted fractions as the most likely candidates. Due to the low yields from the double-step isolation, the transwell assay could only be repeated in the hypoxic condition. None of the differences between the conditions were statistically significant (paired T-test), although trends in the data indicated that the $CD45_{dep}CD31_{enr}$ and $CD45_{dep}CD146_{enr}$ PBMC may have caused greater migration in the hBMSC than their paired opposites.

Due to the limitations of Boyden chamber migration assays, these conditions were taken forward to a system capable of recording more aspects of migration: the Ibidi µ slide 3D. Since lower numbers of PBMC were required, both normoxic and hypoxic conditions could be used. Here, illustrative results from a single experiment will be discussed. The greatest differences were seen with the $CD45_{dep}CD31_{dep/enr}$ populations (fig. 4.3). In both hypoxia (figs. 4.3a and 4.3c) and normoxia (figs. 4.3b and 4.3d), hBMSC exposed to the $CD45_{dep}CD31_{enr}$ population moved further from their original starting point (figs. 4.3a and 4.3b) compared to those exposed to the $CD45_{dep}CD31_{dep}$ population (figs. 4.3c and 4.3d). While the $CD45_{dep}CD31_{dep}$ exposed hBMSC clustered around the origin, the $CD45_{dep}CD31_{enr}$ exposed hBMSC had much greater spread, with a possible increased distribution left of the origin, towards the chamber containing the $CD45_{dep}CD31_{enr}$ PBMC, with the gradient indicated by fig. 4.3e.

By contrast, there was much less difference between migration of the hBMSC exposed to the enriched and depleted fractions of the $CD45_{dep}CD146_{dep/enr}$ PBMC (fig. 4.4). All populations, whether hypoxic (figs. 4.4a and 4.4c) or normoxic (figs. 4.4b and 4.4d) were clustered around the origin. Distribution of the cells appeared to be roughly central, although there was greater spread and a possible left-wards shift towards the chamber containing the $CD45_{dep}CD146_{enr}$ PBMC (fig. 4.4e) for the hBMSC exposed to the $CD45_{dep}CD146_{enr}$ PBMC in normoxia (fig. 4.4b).

Analysis of the velocity of hBMSC in the real-time tracing experiment showed a difference between cell PBMC only in the hypoxic condition (fig. 4.5). The $CD45_{dep}CD31_{enr}$ PBMC induced a greater migration velocity in the hBMSC than the $CD45_{dep}CD31_{dep}$ PBMC, with no difference seen in the normoxic condition (two-way ANOVA with Tukey's post hoc test; fig. 4.5a). Further, the migration velocity stimulated by the $CD45_{dep}CD31_{enr}$ PBMC in the hBMSC was greater under hypoxic compared to normoxic conditions. The same analysis showed that the $CD45_{dep}CD146_{dep}$ PBMC induced a higher migration velocity in the hBMSC than the $CD45_{dep}CD146_{enr}$ PBMC in hypoxia, but again no difference was seen in the normoxic condition (fig. 4.5b). In both cases, differences in migration velocity were marginal, and velocity was similar between both the $CD45_{dep}CD31_{dep/enr}$ and $CD45_{dep}CD146_{dep/enr}$ PBMC.

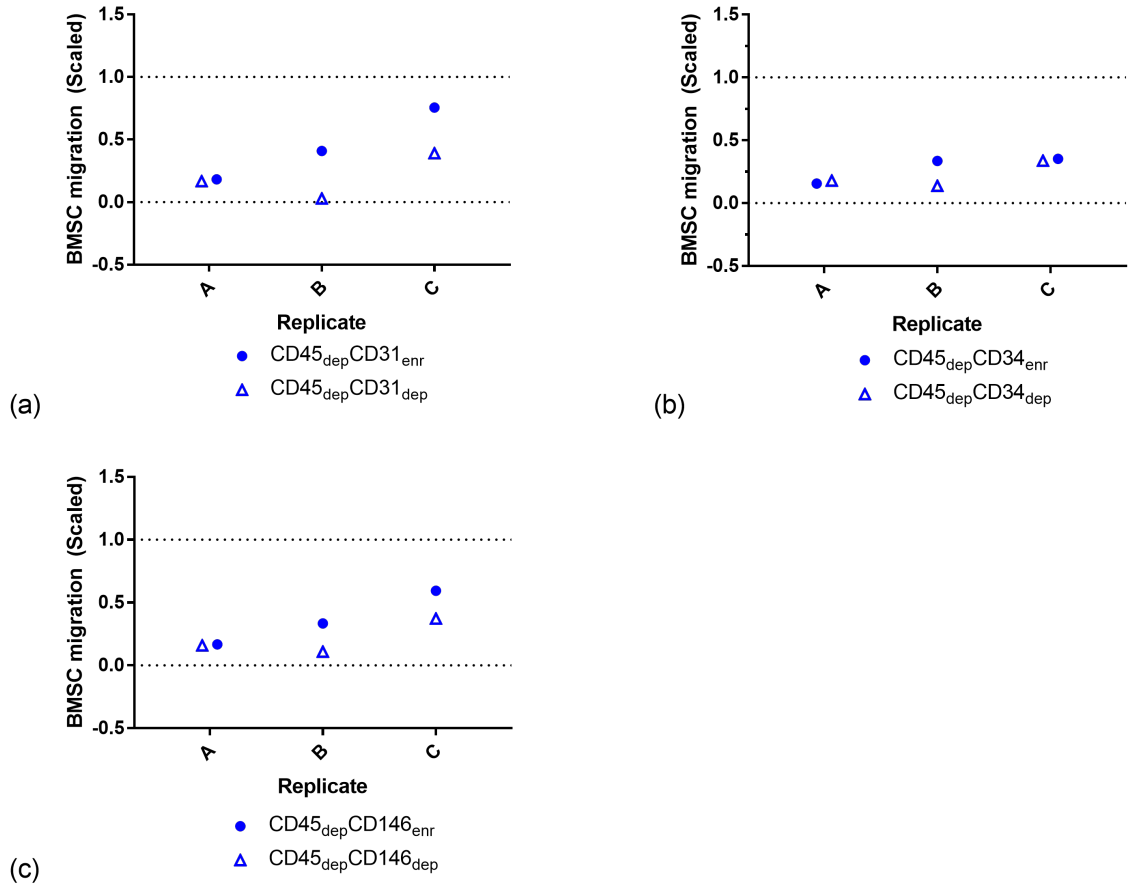

Fig. 4.2 Migration of BMSC across transwell membrane when in paracrine culture with peripheral blood subpopulations isolated using Panel 2

PBMCs were isolated from LRS cones by lymphoprep and run through a two-step magnetic-activated cell sorting protocol. BMSC were permitted to migrate across a transwell membrane for 16 hours under hypoxic conditions while in paracrine culture with blood subpopulations, then migrated cells were stained, imaged and quantified. Results were scaled so negative control = 0 and positive control = 1 (dotted lines on graphs). BMSC were co-cultured with $CD45_{dep}CD31_{enr/dep}$ (fig. 4.2a), $CD45_{dep}CD34_{enr/dep}$ (fig. 4.2b) and $CD45_{dep}CD146_{enr/dep}$ (fig. 4.2c) PBMC. Variance is not shown due to use of scaling. A, B, and C refer to biological replicates using different BMSC donors and separate isolations of PBMC (fig. 4.1a) or $CD45_{enr/dep}$ PBMC (fig. 4.1b). Statistical analysis (paired t-test, $p < 0.05$) did not show significant differences between any pairing. N = 3.

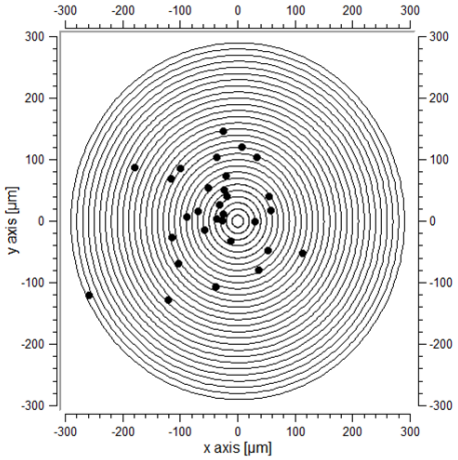

(a) Hypoxic $CD45_{dep}CD31_{enr}$ PBMC

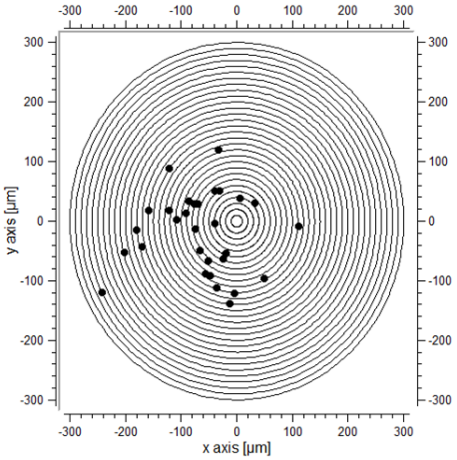

(b) Normoxic $CD45_{dep}CD31_{enr}$ PBMC

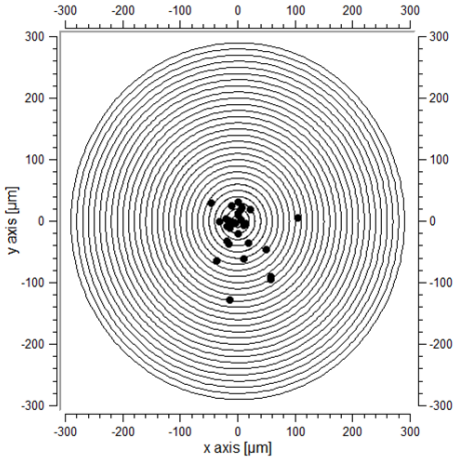

(c) Hypoxic $CD45_{dep}CD31_{dep}$ PBMC

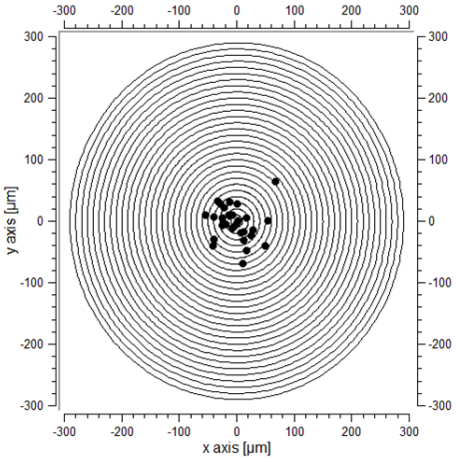

(d) Normoxic $CD45_{dep}CD31_{dep}$ PBMC

(e) Direction of gradient

Fig. 4.3 Raw traces for BMSC migrating in response to $CD45_{dep}CD31_{enr/dep}$ PBMC in normoxia and hypoxia

BMSC isolated under normoxic or hypoxic conditions were seeded into the central chamber of an Ibidi µ slide 3D. $CD45_{dep}CD31_{enr}$ and $CD45_{dep}CD31_{dep}$ PBMC were placed into a side chamber, creating a gradient of secreted factors across the BMSC. Migration of 30 BMSC was tracked for 16 hours and data analysed. Dots show relative end points of cell movements from a normalized start point (0,0). Location of maximum concentration: (0,−300), minimum: (0,300). Example data, N = 3

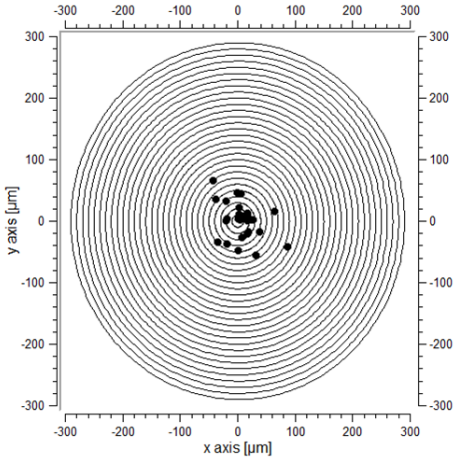

(a) Hypoxic $CD45_{dep}CD146_{enr}$ PBMC

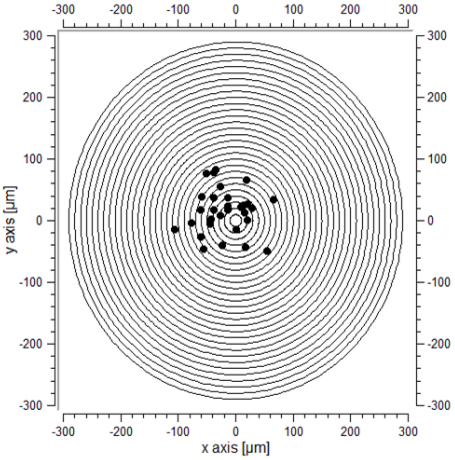

(b) Normoxic $CD45_{dep}CD146_{enr}$ PBMC

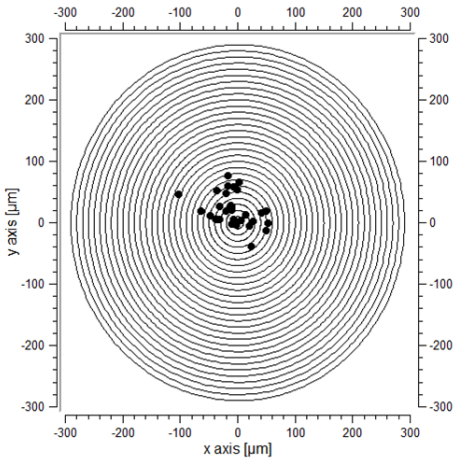

(c) Hypoxic $CD45_{dep}CD146_{dep}$ PBMC

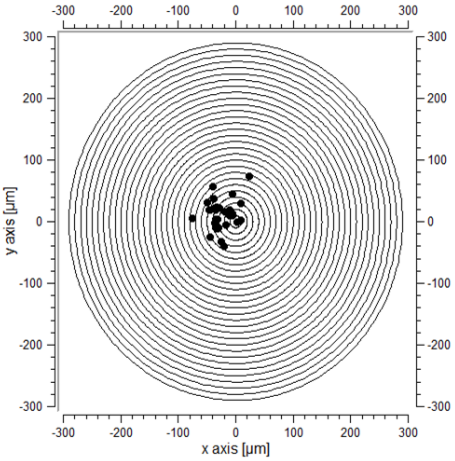

(d) Normoxic $CD45_{dep}CD146_{dep}$ PBMC

(e) Direction of gradient

Fig. 4.4 Raw traces for BMSC migrating in response to $CD45_{dep}CD146_{enr/dep}$ PBMC in normoxia and hypoxia

BMSC isolated under normoxic or hypoxic conditions were seeded into the central chamber of an Ibidi µ slide 3D. $CD45_{dep}CD146_{enr}$ and $CD45_{dep}CD146_{dep}$ PBMC were placed into a side chamber, creating a gradient of secreted factors across the BMSC. Migration of 30 BMSC was tracked for 16 hours and data analysed. Dots show relative end points of cell movements from a normalized start point (0,0). Location of maximum concentration: (0,−300), minimum: (0,300). Example data, N = 3

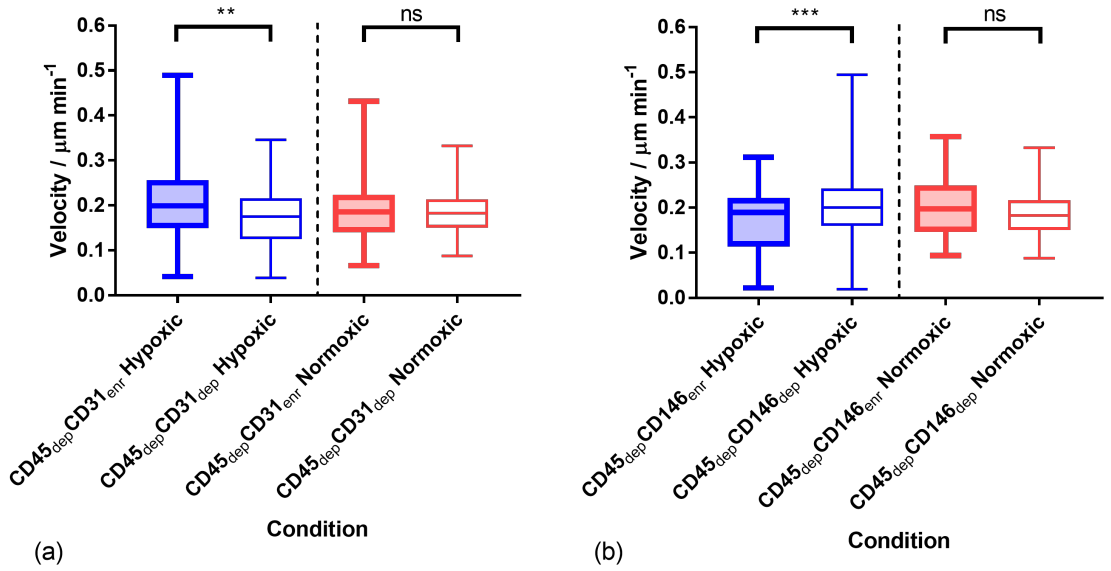

Fig. 4.5 Real-time tracing analysis of BMSC migration velocity in response to $CD45_{dep}CD31_{enr/dep}$ and $CD45_{dep}CD146_{enr/dep}$ PBMC

Analysis of real time tracing showing BMSC migration velocity in response to $CD45_{dep}CD31_{enr/dep}$ (fig. 4.5a) or $CD45_{dep}CD146_{enr/dep}$ (fig. 4.5b) PBMC in normoxic and hypoxic conditions. Two-way ANOVA with Tukey's post hoc test, $p < 0.05$. N = 3, 30 tracks per replicate

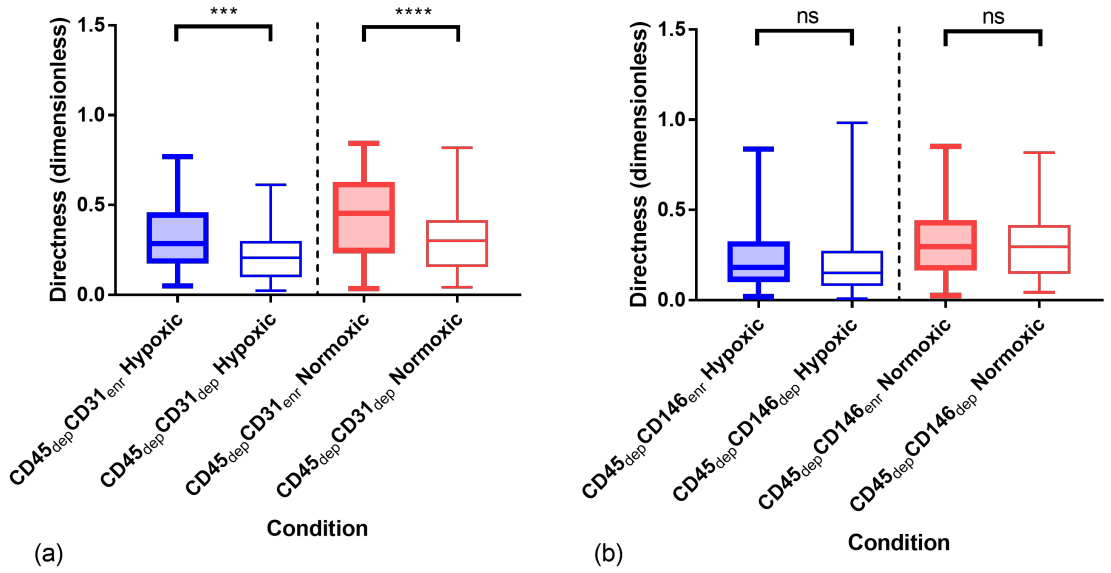

Fig. 4.6 Real-time tracing analysis of BMSC migration directness in response to $CD45_{dep}CD31_{enr/dep}$ and $CD45_{dep}CD146_{enr/dep}$ PBMC

Analysis of real time tracing showing BMSC migration directness in response to $CD45_{dep}CD31_{enr/dep}$ (fig. 4.6a) or $CD45_{dep}CD146_{enr/dep}$ (fig. 4.6b) PBMC in normoxic and hypoxic conditions. Two-way ANOVA with Tukey's post hoc test, $p < 0.05$. N = 3, 30 tracks per replicate

There were clear differences between the directness of migration, i.e. the ratio between total distance travelled and linear distance from the origin, stimulated by the $CD45_{dep}CD31_{dep/enr}$ and the $CD45_{dep}CD146_{dep/enr}$ populations (fig. 4.6). The $CD45_{dep}CD31_{enr}$ PBMC stimulated migration of the hBMSC with significantly greater directness under both normoxic and hypoxic conditions compared to the $CD45_{dep}CD31_{dep}$ PBMC (fig. 4.6a). The directness of hBMSC migration was higher in the normoxic condition, as opposed to the hypoxic condition, with the $CD45_{dep}CD31_{enr}$ PBMC. To contrast, there were no significant differences between the directness of migration of the hBMSC under either normoxic or hypoxic condition with the $CD45_{dep}CD146_{enr}$ and $CD45_{dep}CD146_{dep}$ PBMC (fig. 4.6b). The directness of migration stimulated by the $CD45_{dep}CD31_{enr}$ PBMC was greater than that stimulated by either the $CD45_{dep}CD146_{enr}$ or $CD45_{dep}CD146_{dep}$ PBMC. As a result, it was concluded that the $CD45_{dep}CD31_{enr}$ PBMC identified as having a greater role in stimulating hBMSC migration than its paired negative, or the $CD45_{dep}CD146_{dep/enr}$ isolated PBMC and was taken forward for characterisation.

4.3.3 Characterisation of $CD45_{dep}CD31_{enr}$ PBMC

Identification of secreted chemokines can indicate cell identity. Supernatants were taken from the $CD45_{dep}CD31_{enr}$ PBMC and used in a Proteome Profile Human Chemokine array (fig. 4.7). The strongest signals from the $CD45_{dep}CD31_{enr}$ double-step population were SDF-1, Macrophage Derived Cytokine (MDC) and IFNγ-inducible protein 10 (IP-10), also known as C-X-C motif chemokine Ligand 10 (CXCL10) expression with lower Chemerin and Macrophage Inflammatory Protein 3 beta (MIP-3b) levels, indicative of a monocyte population.

A screening panel based on the protein secretion data and expected cell phenotypes due to the double-step isolation method was used to characterise the cell populations (fig. 4.8). Single colour analysis demonstrated that the $CD45_{dep}CD31_{enr}$ PBMC was in fact over 50 % positive for CD45, and over 40 % positive for CD16 with less than 10 % expression of CD31 (fig. 4.8a). Expression of other markers was less than 3 %. Considering the CD16 and CD45 positive cells further, 21.5 % were (CD45+)(CD16+), 20.1 % were (CD45+)(CD16−), but the majority (58.4 %) were (CD45+)(CD16+) (fig. 4.8b). Of the (CD45+)(CD16+) population, over 97.5 % were negative for CD31 (fig. 4.8c). The greatest concentration of CD31 positive cells was found within the dead cell fraction (data not shown).

Characterisation by flow cytometry indicated a myeloid origin for the $CD45_{dep}CD31_{enr}$ PBMC. To confirm this, a macrophage differentiation assay was run using monocytes isolated using MACS Pan Monocyte isolation kit (figs. 4.9a and 4.9c), and the $CD45_{dep}CD31_{enr}$ PBMC (figs. 4.9b and 4.9d). Cells were exposed to GM-CSF to stimulate M1 macrophage differentiation (figs. 4.9a and 4.9b) and M-CSF to stimulate M2 macrophage differentiation (figs. 4.9c and 4.9d) for 5 days under hypoxic conditions. Monocytes exposed to GM-CSF became adherent with a rounded, M1-like morphology (fig. 4.9a), while those exposed to M-CSF had a fusiform, adherent phenotype consistent with an

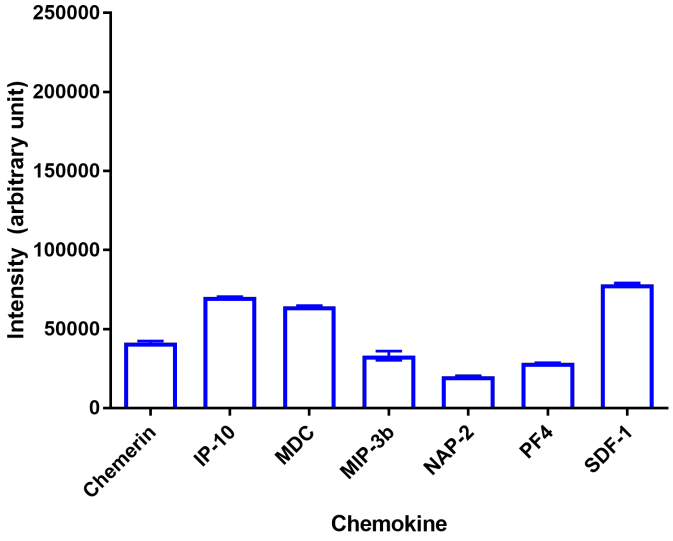

Fig. 4.7 Proteome profiler Human Chemokine array blot using $CD45_{dep}CD31_{enr}$ PBMC

16 hour hypoxic supernatants from $CD45_{dep}CD31_{enr}$ PBMC were applied to the Proteome Profiler Human Chemokine Array. Hits with an intensity of greater then 30 000 were taken. N = 2.

M2-like morphology (fig. 4.9c). The $CD45_{dep}CD31_{enr}$ PBMC did not respond to either GM-CSF (fig. 4.9b) or M-CSF (fig. 4.9d) and instead all cells within these cultures died.

Further multiparametric flow characterisation using a monocyte-specific panel demonstrated that cells isolated from the LRS cone using the Pan Monocyte kit had a typical monocyte distribution of (HLA-DR+)(CD56−)(CD3−)(CD19−) cells with CD14/CD16 markers giving the expected 80:5:15 ratio of Classical : Intermediate : Non-classical monocytes (fig. 4.10a). However, the same panel run on the $CD45_{dep}CD31_{enr}$ cells showed that there were fewer than 1 % monocytes within the population (fig. 4.10b). Further analysis showed that the double-step population had strong staining for CD56 and CD16 (fig. 4.11a). Of cells expressing CD56 and CD16, over 83 % were double positive (CD56+)(CD16+) cells. This double positive population was negative for both CD3 (fig. 4.11b) and CD31 (fig. 4.11c). Again, CD31 positive staining was found only within the dead cell fraction (data not shown). This (CD56+)(CD16+)(CD3−)(CD19−) phenotype suggested the possibility of a NK cell identity. Deeper examination of the flow cytometric characterisation allowed subdivision of the NK cell population into the five classical NK cell subpopulations based on CD56 and CD16 expression (fig. 4.12). The majority of NK cells were $(CD56_{dim})(CD16_{bright})$ at over 87 % expression (table 4.1). $(CD56_{bright})$(CD16−) NK cells made over 6 % of the population, with the remaining NK cells being split between $(CD56_{bright})(CD16_{dim})$, $(CD56_{dim})$(CD16−), and (CD56−)$(CD16_{bright})$ resulting in 8.46 % of cells being $(CD56_{bright})$.

To further examine the NK phenotype, co-cultures of $CD45_{dep}CD31_{enr}$ PBMC and hBMSC were cultured with and without IL-2 stimulation under hypoxic (Figure B13) and normoxic (Figure B14)

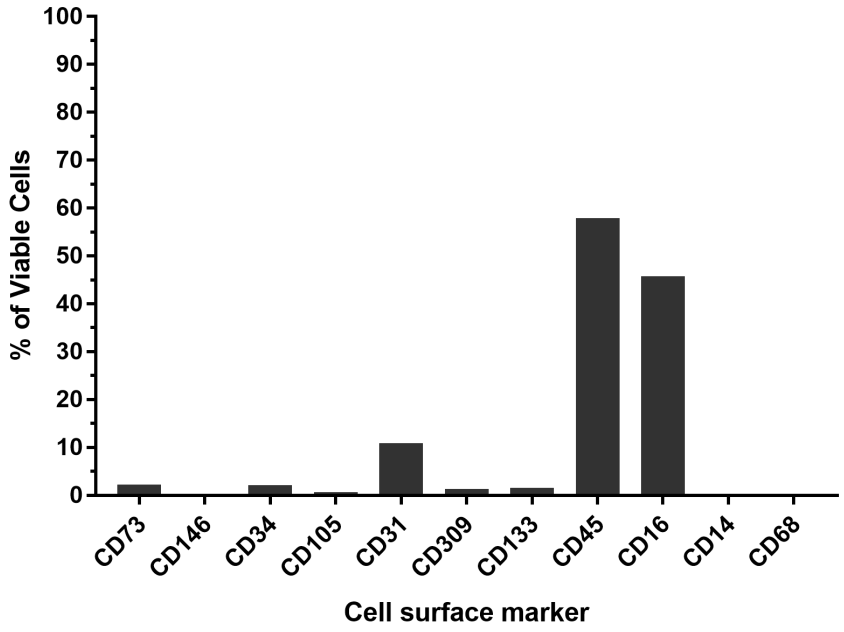

(a)

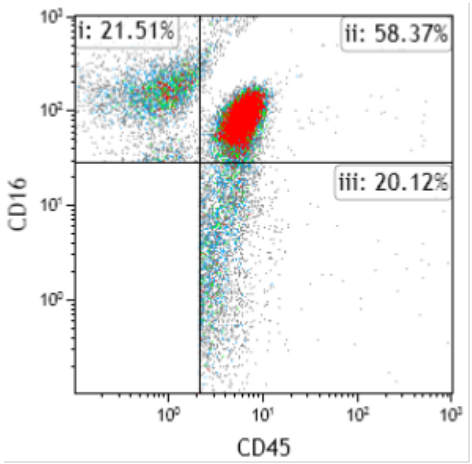

(b)

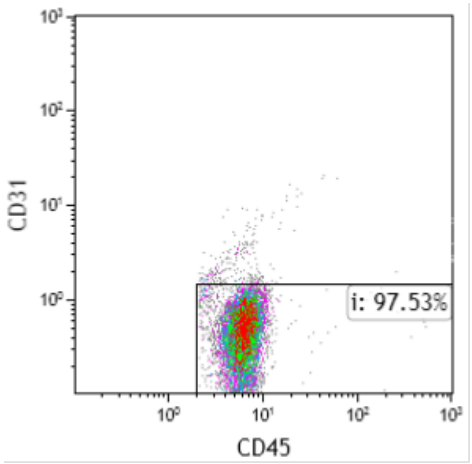

(c)

Fig. 4.8 Flow screening panel for $CD45_{dep}CD31_{enr}$ PBMC

$CD45_{dep}CD31_{enr}$ double-step isolated PBMC were characterised using a 10 colour plus viability multiparametric flow cytometry panel immediately after isolation. Results were assessed by single colour (fig. 4.8a) and multiparametric (figs. 4.8b and 4.8c) analysis, showing that 58.37 % of cells were (CD45+)(CD16+) and of those, 97.53 % were (CD31−), resulting in a majority population (CD45+)(CD16+)(CD31−).

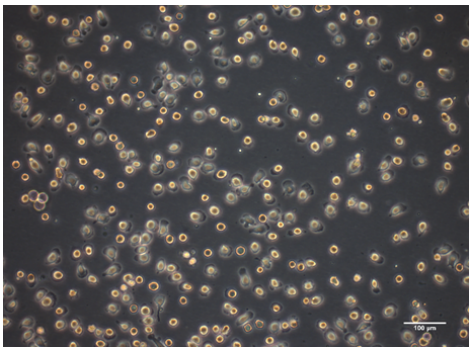

(a) Monocytes with GM-CSF

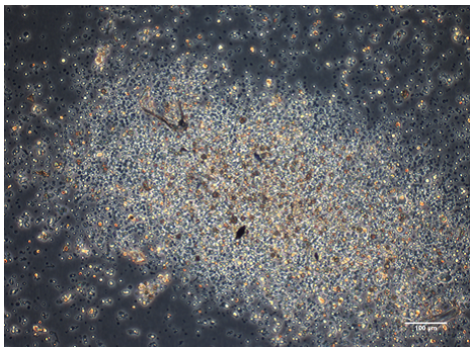

(b) $CD45_{dep}CD31_{enr}$ PBMC with GM-CSF

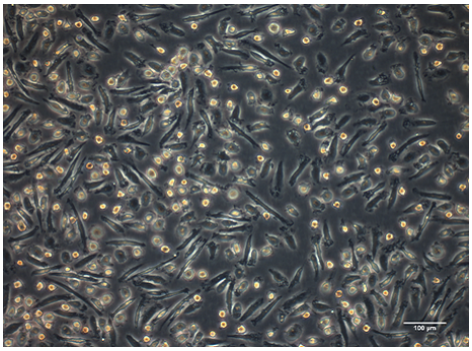

(c) Monocytes with M-CSF

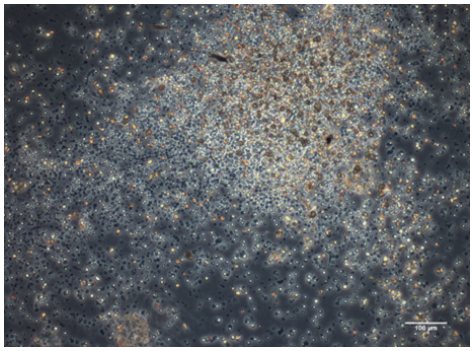

(d) $CD45_{dep}CD31_{enr}$ PBMC with M-CSF

Fig. 4.9 Stimulation of magnetically separated peripheral blood fractions with GM-CSF and M-CSF

Peripheral blood fractions were stimulated for 5 days with either GM-CSF (figs. 4.9a and 4.9b) or M-CSF (figs. 4.9c and 4.9d) under hypoxic conditions. Fractions used were Monocytes (figs. 4.9a and 4.9c) using the Pan Monocyte MACS kit, and $CD45_{dep}CD31_{enr}$ PBMC (figs. 4.9b and 4.9d) using the CD45 and CD31 MACS kits. N = 3. Scale bar = 100 µm

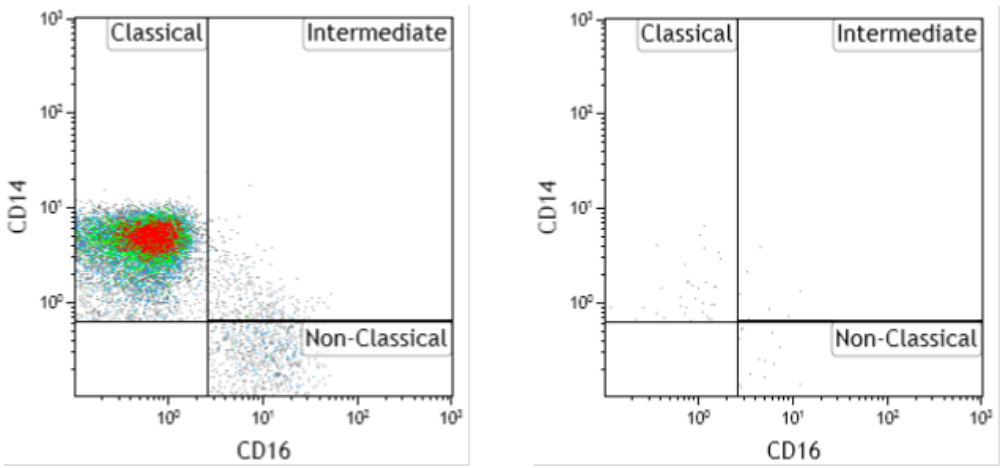

(a) (b)

Fig. 4.10 Comparison of monocytes and $CD45_{dep}CD31_{enr}$ PBMC using monocyte characterisation panel

Monocytes were isolated using the Miltenyi MACS Pan Monocyte isolation kit, and $CD45_{dep}CD31_{enr}$ PBMC using the Miltenyi MACS CD45 and CD31 kits. Cells were characterised immediately using a flow panel designed for monocyte characterisation containing fluorescently conjugated antibodies against HLA-DR, CD19, CD56, CD3, CD14 and CD16 (Mukherjee et al. 2015). Cells were characterised as using Boolean gating and then assessed to characterise monocyte subpopulation distribution. Both monocytes (fig. 4.10a) and $CD45_{dep}CD31_{enr}$ PBMC (fig. 4.10b) were characterised.

culture conditions. Solo cultures of $CD45_{dep}CD31_{enr}$ PBMC contained more phase bright cells when treated with IL-2 in both hypoxic (fig. 4.13a) and normoxic (fig. 4.14a) conditions compared to untreated (fig. 4.13b and fig. 4.14b respectively), suggesting increased viability of cells. Co-cultures of hBMSC and $CD45_{dep}CD31_{enr}$ PBMC with IL-2 under both hypoxic (fig. 4.13c) and normoxic (fig. 4.14c) conditions contained clumps of floating debris, which were not visible in co-cultures without IL-2 (fig. 4.13d and fig. 4.14d respectively). Significantly more debris can be seen in both normoxic co-cultures (figs. 4.14c and 4.14d) than in the hypoxic co-cultures (figs. 4.13c and 4.13d). Cellular morphology in normoxic co-cultures treated with IL-2 is poorer than those without, with cells having a more senescent appearance and lower confluence. There was no apparent difference between hBMSC cultured with IL-2 under hypoxic (fig. 4.13e) or normoxic conditions (fig. 4.14e), and those cultured without IL-2 (fig. 4.13f and fig. 4.14f respectively). Thus, IL-2 activated the $CD45_{dep}CD31_{enr}$ PBMC to induce cell death in hBMSC.

There were no visible differences between phase bright cells in $CD45_{dep}CD31_{enr}$ PBMC cultures with (fig. 4.14a) or without IL-2 (fig. 4.14b). BMSC morphology appeared poorer in co-cultures with $CD45_{dep}CD31_{enr}$ PBMC , although more clumps of debris were visible in cultures with IL-2 (fig. 4.14c) than those without (fig. 4.14d). No difference was visible between BMSC grown with (fig. 4.14e) and without (fig. 4.14f) IL-2. N = 3.

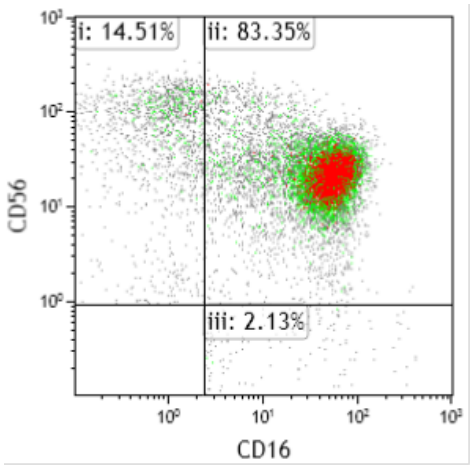

(a)

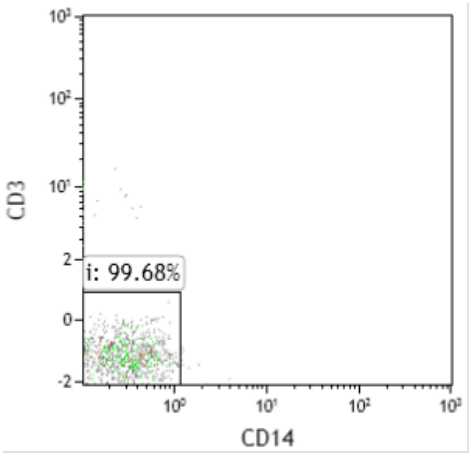

(b)

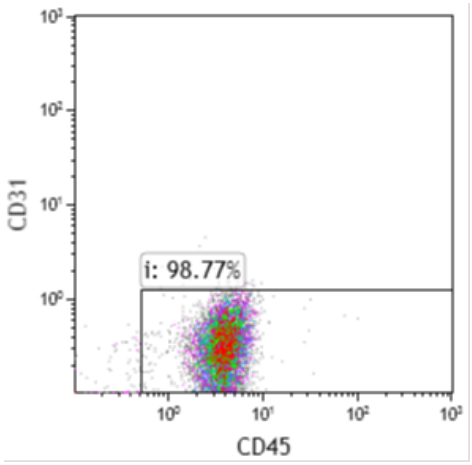

(c)

Fig. 4.11 $CD45_{dep}CD31_{enr}$ PBMC characterised using alternative gating on monocyte characterisation panel

$CD45_{dep}CD31_{enr}$ PBMC were analysed using a novel gating strategy. CD56 and CD16 positive cells were examined for double-positive staining (fig. 4.11a). The double positive cells were then tested for CD3 and CD14 staining (fig. 4.11b), and then finally for CD31 positive staining (fig. 4.11c).

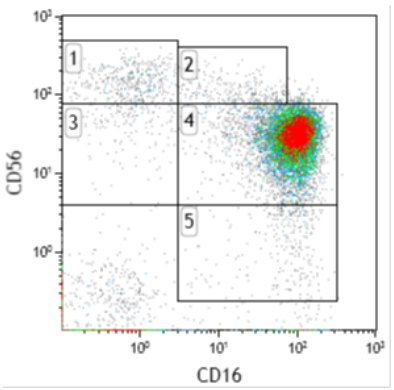

Fig. 4.12 NK cell subtype analysis of $CD45_{dep}CD31_{enr}$ PBMC

$(CD3-)(CD19-)$ $CD45_{dep}CD31_{enr}$ PBMC were gated as:

1. $(CD56_{bright})(CD16-)$
2. $(CD56_{bright})(CD16_{dim})$
3. $(CD56_{dim})(CD16-)$
4. $(CD56_{dim})(CD16_{bright})$
5. $(CD56-)(CD16_{bright})$

Percentages can be found in table 4.1.

Table 4.1 NK cell subtype abundance of $CD45_{dep}CD31_{enr}$ PBMC, NK cell subtypes as gated in fig. 4.12 expressed as a percentage of total NK cell present based on five major subtypes.

Subset	**Percentage of NK cells**	**Percentage of $CD56_{bright}$**
$(CD56_{bright})(CD16-)$	6.09 %	72.20 %
$(CD56_{bright})(cd16_{dim})$	2.35 %	27.80 %
$(CD56_{dim})(CD16-)$	2.01 %	n/a
$(CD56_{dim})(cd16_{bright})$	87.01 %	n/a
$(CD56-)(CD16_{bright})$	2.54 %	n/a

The average cell yield for the $CD45_{dep}CD31_{enr}$ PBMC from buffy coat was <0.1 % (N=3, range: 0.04 to 0.1 %), equating to 1×10^5 to 2×10^5 cells per processed LRS cone. Since characterisation experiments suggest at an NK identity for the $CD45_{dep}CD31_{enr}$ PBMC, it was decided to use the Miltenyi MACS NK Cell kit to isolate untouched NK cells directly from the buffy coat, rather than use a two-step process. Cell yield was improved by using the NK cell isolation kit: a sample of 8 isolations gave an average yield of 4.8 % (range: 2.0 to 7.1 %) from the buffy coat. Between 1×10^7 and 3×10^7 NK cells could be obtained per isolation.

A comparison of the cell markers on cell isolated from the NK cell kit and through the $CD45_{dep}CD31_{enr}$ double-step process was performed by flow cytometry (fig. 4.15). Populations were extracted from buffy coat using the NK kit and the CD45/CD31 kit, then characterised using the panel and gating

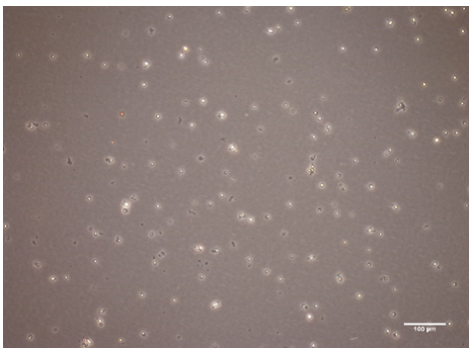

(a) $CD45_{dep}CD31_{enr}$ PBMC alone, with IL-2 stimulation

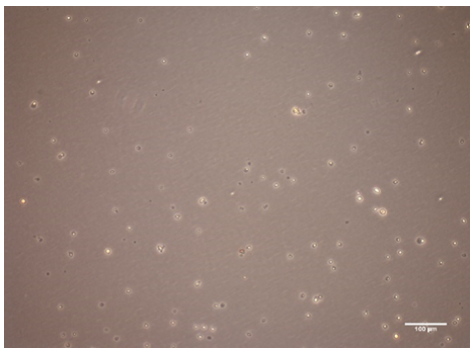

(b) $CD45_{dep}CD31_{enr}$ PBMC alone, with no cytokine stimulation

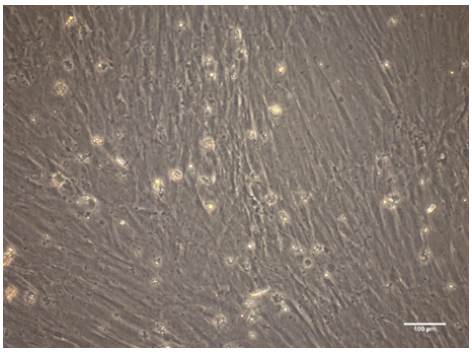

(c) $CD45_{dep}CD31_{enr}$ PBMC co-cultured with hBMSC, with IL-2 stimulation

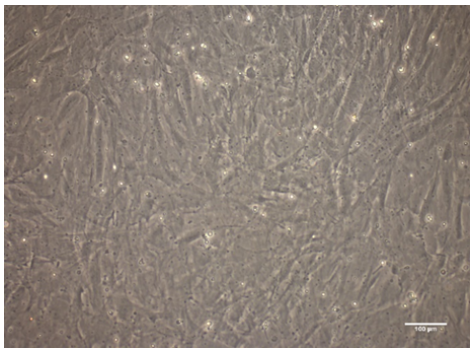

(d) $CD45_{dep}CD31_{enr}$ PBMC co-cultured with hBMSC, with no cytokine stimulation

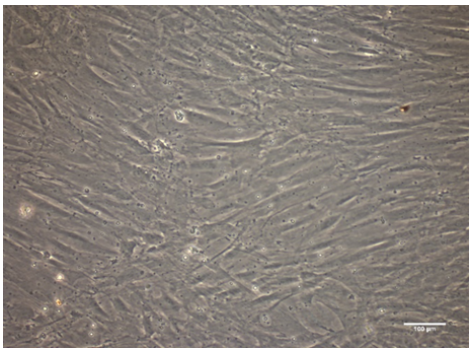

(e) hBMSC alone, with IL-2 stimulation

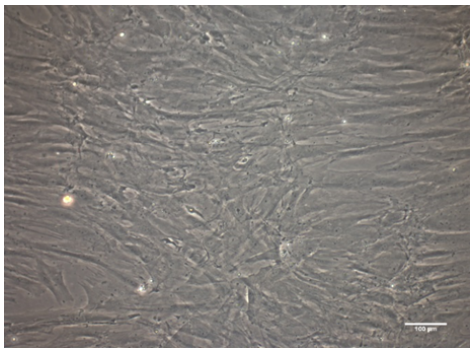

(f) hBMSC alone, with no cytokine stimulation

Fig. 4.13 Co-cultures $CD45_{dep}CD31_{enr}$ PBMC and BMSCs with or without IL-2 stimulation in hypoxia

$CD45_{dep}CD31_{enr}$ PBMC were obtained using magnetic selection with Miltenyi MACS CD45 and CD31 kits. Cultures were set up containing $CD45_{dep}CD31_{enr}$ PBMC cells alone (figs. 4.13a and 4.13b), $CD45_{dep}CD31_{enr}$ PBMC with BMSC (figs. 4.13c and 4.13d) or BMSC alone (figs. 4.13e and 4.13f) under hypoxic culture conditions for 7 days. Half of the cultures were treated with IL-2 (figs. 4.13a, 4.13c and 4.13e) and half were left unstimulated (figs. 4.13b, 4.13d and 4.13f). N = 3. Scale bar = 100 µm

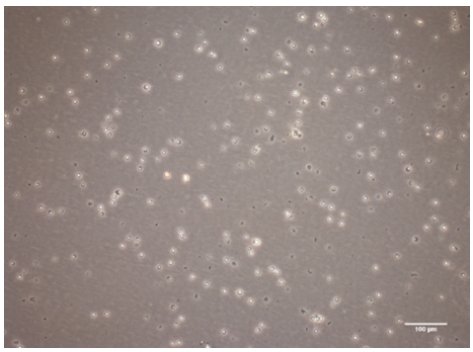

(a) $CD45_{dep}CD31_{enr}$ PBMC alone, with IL-2 stimulation

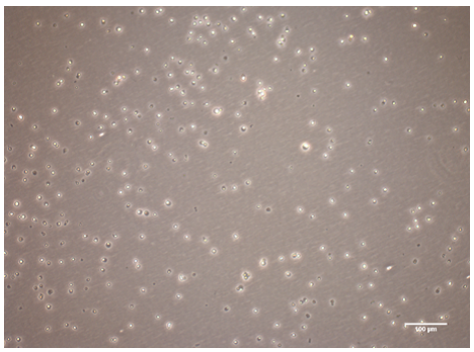

(b) $CD45_{dep}CD31_{enr}$ PBMC alone, with no cytokine stimulation

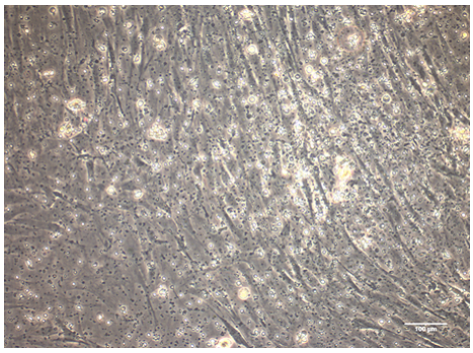

(c) $CD45_{dep}CD31_{enr}$ PBMC co-cultured with hBMSC, with IL-2 stimulation

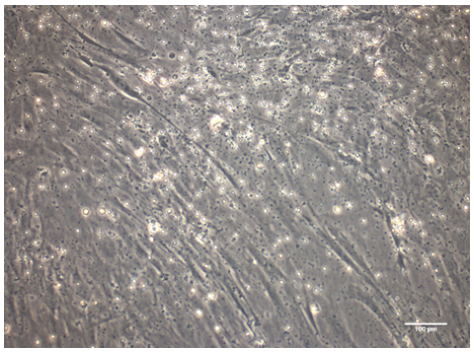

(d) $CD45_{dep}CD31_{enr}$ PBMC co-cultured with hBMSC, with no cytokine stimulation

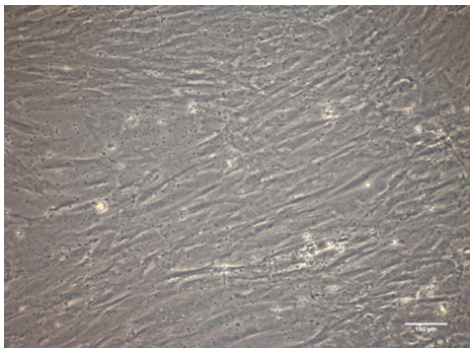

(e) hBMSC alone, with IL-2 stimulation

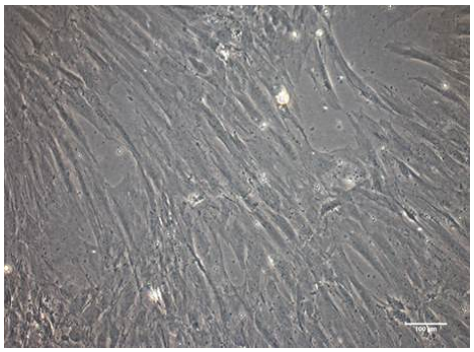

(f) hBMSC alone, with no cytokine stimulation

Fig. 4.14 Co-cultures of $CD45_{dep}CD31_{enr}$ PBMC and BMSCs with or without IL-2 stimulation in normoxia

$CD45_{dep}CD31_{enr}$ PBMC were isolated by double-step MACS. Cultures containing $CD45_{dep}CD31_{enr}$ PBMC only (figs. 4.14a and 4.14b), $CD45_{dep}CD31_{enr}$ PBMC and BMSC (figs. 4.14c and 4.14d) and BMSC only (figs. 4.14e and 4.14f) were grown for 7 days under normoxic conditions. Half the cultures were stimulated with IL-2 (figs. 4.14a, 4.14c and 4.14e) and the other half were left untreated (figs. 4.14b, 4.14d and 4.14f). Scale bar = 100 µm

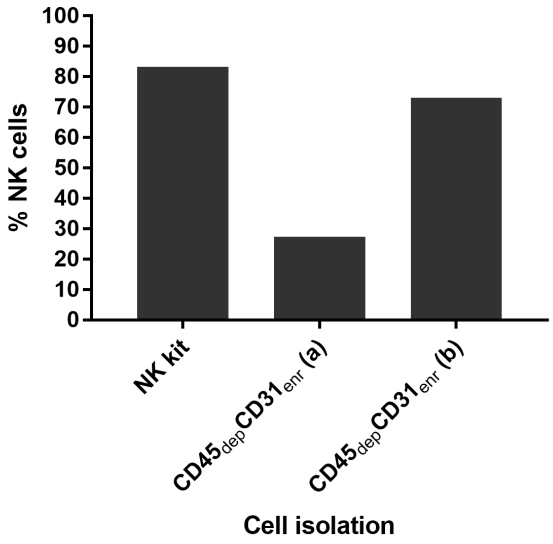

Fig. 4.15 Flow comparison of NK kit and $CD45_{dep}CD31_{enr}$ PBMC containing (CD45+)(CD56+)(CD16+)(CD3−)(CD19−) cells

Cells were freshly isolated from the buffy coat of LRS cones and either enriched for NK cells using the Miltenyi MACS NK cell kit or $CD45_{dep}CD31_{enr}$ PBMC . Viable cells were gated for (CD56+)(CD16+)(CD45+)(CD31−)(CD3−)(CD14−) and percentage of viable cells with said marker profile calculated. N = 2

strategy described in fig. 4.13. Cells from a single donor were characterised for the NK cell kit, and 2 donors for the $CD45_{dep}CD31_{enr}$ PBMC. The NK cell kit gave over 80 % purity of NK cells in the viable cell fraction, determined by the marker profile (CD45+)(CD56+)(CD16+)(CD3−)(CD19−). The proportion of cells with these markers isolated by the double-step method was variable. 1 donor gave less than 30 % purity, while the other yielded a population containing more than 70 % cells with the aforementioned marker profile. Cell viability was lower in the double-step isolations compared to the direct method; the viability of cells isolated using the NK kit in fig. 4.15 was 88 %, compared to 49 % and 64 % respectively for the double-step isolations.

4.4 Discussion

Recruitment of hBMSC to the site of trauma-induced repair following micro-drilling is thought to be important to the eventual resolution of injury, based on their contributions to repair in fracture as as well as other tissues such as the kidney (Dupont et al. 2010; Granero-Moltó et al. 2009; Khalilpourfarshbafi et al. 2017). This recruitment occurs through a combination of direct signalling from damaged tissues, and factors released by rapid-infiltrating immune cells. The migration of hBMSC towards these subpopulations may lead to specific partitioning of cells within the haematoma, as well as cell-cell contact between the recruiting cell type and the migrating hBMSC. Understanding which immune subpopulations have the strongest influence on hBMSC recruitment would indicate the PBMC subpopulations that hBMSC are most likely to co-localise, and potentially interact, with.

The aim of this chapter was to isolate and characterise an immune subpopulation which stimulated hBMSC migration under normoxic and hypoxic conditions. To understand how this may be significant in repair, I used hBMSC isolated and characterised under normoxic and hypoxic conditions as described in chapter 3. Immune cell subpopulations were isolated from LRS cones obtained as a by-product of platelet donation from healthy, consenting donors using MACS. The migratory influence of these subpopulations on the hBMSC was established through the use of Boyden chambers and real time migration assays. Protein secretion, cell surface markers, and functional assays were used to establish the identity of the active immune subpopulation. The use of paired normoxic and hypoxic conditions indicated not only how migratory behaviour may be modified by the changing oxygen levels within the early haematoma, but also the importance of culture conditions when developing *in vitro* models of cell behaviour. The unique feature of this study was the comparison between the chemoattractant properties of paired enriched and depleted fractions of the peripheral blood in both normoxia and hypoxia, rather than comparison of specifically selected cell subtypes. Using these techniques, I have shown that a population obtained through a CD45− depleted CD31− enriched ($CD45_{dep}CD31_{enr}$) double-step MACS isolation had a stronger migration-inducing influence on the hBMSC than its counterpart under both normoxic and hypoxic conditions. This population was subsequently identified to primarily contain a complete NK cell population. NK cells as a whole are among the earliest infiltrators to the sites of damage, accumulating in sites of inflammation through multiple signalling pathways including the CXCR1 / CXCL8 axis (Agaiby and Dyson 1999). In addition, a biomaterial study has shown that NK cells can recruit hBMSC into artificial scaffolds therefore, this timeline supports the putative role of NK cells in recruiting hBMSC to the site of damage (Almeida et al. 2012) .

The initial Boyden chamber experiments showed that the $CD45_{dep}$ subpopulation resulted in greater hBMSC migration than the paired $CD45_{enr}$ subpopulation in the hypoxic condition, with an apparently similar trend in the normoxic condition. Granulocytes such as basophils may express low levels of CD45 ($CD45_{dim}$) and hence not be selected by the MACS method, but these populations had

already been removed using the density gradient centrifugation (Gane et al. 2018). The CD45 negative fraction of blood contains haematopoietic, "mesenchymal" (see section 1.5), endothelial, skeletal and osteogenic stem and progenitor cells (Golledge et al. 2007). Other CD45 negative populations found in the peripheral blood include circulating endothelial cells, subsets of mature, terminally-differentiated haematopoietic populations, such as T cells, and cells of the erythroid or megakaryocyte lineage (Golledge et al. 2007; Noulin et al. 2013; Starlinger et al. 2011; Tomer 2004). A common combination of markers used to characterise these subpopulations is CD31, CD34 and CD146, and so these markers were selected for further subdivision of the $CD45_{dep}$ subpopulation in order to identify the key subpopulations which induced hBMSC migration.

Boyden chamber experiments comparing the double-step isolated $CD45_{dep}CD31_{enr/dep}$, $CD45_{dep}$-$CD34_{enr/dep}$, and $CD45_{dep}CD146_{enr/dep}$ showed that there were no differences between the $CD45_{dep}$-$CD34_{enr}$ and $CD45_{dep}CD34_{dep}$ fractions, with a non-significant difference in favour of $CD45_{dep}$-$CD146_{enr}$ subpopulation, and a significant difference in favour of $CD45_{dep}CD31_{enr}$ being seen over their respective negative partners. The lack of directional data in the Boyden chamber meant that chemotaxis could not be distinguished from chemokinesis or fugetaxis, and so a real-time chemotaxis assay based on the Ibidi µ slide system was used. Since the $CD45_{dep}CD146_{enr}$ and $CD45_{dep}CD31_{enr}$ subpopulations had shown a level of altered hBMSC migration, both were taken forward, but the $CD45_{dep}CD34_{enr}$ and $CD45_{dep}CD34_{dep}$ subpopulations were not due to lack of any observed difference.

The $CD45_{dep}CD146_{enr}$ and $CD45_{dep}CD146_{dep}$ populations showed minimal differences in the real-time migration assay, with the only difference being marginally increased migration velocity in hBMSC stimulated with $CD45_{dep}CD146_{dep}$ cells in the hypoxic condition. The hBMSC directness appeared to be higher in the normoxic compared to the hypoxic condition, but was not different between the $CD45_{dep}CD146_{enr}$ and $CD45_{dep}CD146_{dep}$ subpopulations, suggesting that the hBMSC isolated and cultured under normoxic conditions had a greater underlying directness of migration independent of treatment. As a result, the $CD45_{dep}CD146_{enr/dep}$ populations were not taken forward.

The $CD45_{dep}CD31_{enr}$ cell population isolated using double-step MACS stimulated hBMSC migration with increased directionality in both the normoxic and hypoxic conditions, although the directness was higher under normoxic conditions when studied in the real-time migration assay, as seen in the $CD45_{dep}CD146_{enr/dep}$ subpopulations. Further, in the hypoxic condition, the hBMSC migration had marginally higher velocity than when stimulated with either the $CD45_{dep}CD31_{dep}$ subpopulation under any condition, or the NK population in normoxic conditions. hBMSC isolated and cultured under hypoxic conditions have been previously found to have greater baseline migration compared to equivalent cells isolated and cultured under normoxic conditions, but this was not seen here (Vertelov et al. 2013). This could be due to the source of bone marrow in the aforementioned study which was obtained commercially from the iliac crest of a healthy donor aged 18 to 45 years (Lonza 2018). As discussed in chapter 3, age has a significant effect on hBMSC behaviour, meaning that the observed

migration in the hBMSC derived from aged, OA patients could be very different to that from the commercial donors. Furthermore, the oxygen level within the quoted study was 5 % as opposed to the 3 % used in my study. It is possible that the directness of the hBMSC was lower in the hypoxic condition due to a weak chemokine gradient, resulting from the low cell number used, which was insufficient to overcome the baseline non-directed migration of the hBMSC and induce directed migration.

As a result, the $CD45_{dep}CD31_{enr}$ subpopulation was identified as the population of interest, and later characterised as a whole NK cell subpopulation. This might seem unexpected, since NK cells do express CD45 and therefore might not be thought to be found within the CD45 depleted fraction. However, the MACS technique, unlike flow sorting, does not produce a pure population. Prior work has shown that, in the case of rare markers with less than 2 % expression in the original population, positive selection using MACS results in a ten-fold enrichment of said marker within the resulting population, with the depleted fraction still containing a reduced number of cells expressing the marker of interest (Sophie Frankham-Wells, unpublished work, Kymab Ltd). Accordingly, since the cells isolated from the LRS cone are predominately CD45 positive, with one study suggesting up to 98 % positivity, it follows that negative selection would result in a depletion, rather than complete removal of CD45 positive cells (Néron et al. 2007). The same study found that NK cell abundance within an LRS cone may be up to 17 %, accounting for their abundance within the $CD45_{dep}$ subpopulation. Further, NK cells express CD31, also known as PECAM-1, and so these cells would have been captured in the second round of MACS using the CD31 beads (Berman et al. 1996). However, CD31 is also expressed on many other immune populations, including monocytes (Geissmann et al. 2010). Differentiation of cells isolated from the LRS cone and enriched for CD31 by single-step MACS into macrophages showed that the CD31 beads were able to capture functional monocytes in a single-step method (data not shown). With that being said, the $CD45_{dep}$ subpopulation lacked CD14 expression, indicating that any monocytes present had likely been partitioned into the $CD45_{enr}$ subpopulation (data not shown). As a result, the presence of the enriched NK cell subpopulation within the $CD45_{dep}CD31_{enr}$ subpopulation was likely a combination of overflow from the CD45 depletion step and then selection in the CD31 enrichment step. This lack of purity in the MACS isolated fractions made characterisation more challenging, but the speed and minimal handling required for manual MACS as opposed to flow sorting, as well as the possibility of serendipitous findings as in the case of this thesis, made MACS an attractive option.

NK cells can be subdivided into 5 subpopulations based on their relative expression of CD56 and CD16, with the relative expression patterns of these markers indicating the function of the NK cell subpopulation (Poli et al. 2009). In fresh whole blood, the ($CD56_{dim}$) NK cells form over 90 % of all NK cells, and 95 % of those are ($CD56_{dim}$)($CD16_{bright}$) (Cooper et al. 2001). In the population isolated from the LRS cone using the double-step method, 85 % of NK cells were ($CD56_{dim}$) and of

those, nearly 98 % were ($CD56_{dim}$)($CD16_{bright}$). This agreed with the proportions seen in whole blood and indicated that the population isolated was functionally relevant.

Although the majority of NK cells present within the population of interest were $CD56_{dim}$, the $CD56_{bright}$ subset are the major producers of IFNγ in the haematopoietic system, as well as producing many other cytokines including TNFα, GM-CSF, IL-10, IL-13, and IP-10 (Fauriat et al. 2010; Poli et al. 2009). IP-10 was among the strongest signals in the protein array analysis of the $CD45_{dep}CD31_{enr}$ subpopulation, and is a known hBMSC chemoattractant, albeit more typically in the context of macrophage-driven hBMSC migration (Anton et al. 2012). Indeed, the positive hits on the panel suggested a monocytic identity for the, at the time, unidentified $CD45_{dep}CD31_{enr}$ subpopulation. As already discussed, the presence of contaminating cell types was anticipated due to the MACS method for isolating the subpopulations. Moreover, the cell number in the isolated subpopulation was very low, and therefore the supernatants isolated for this work would have been very dilute due to the volumes required for said assay. The basal medium used only contained 0.2 % BSA, reducing the risk of contaminating cytokines from the serum, although use of a charcoal stripped or xeno-free serum substitute would have been preferable to ensure a complete lack of contamination from serum was present. Future work would use a cell-free control to provide an accurate baseline for cytokine presence within the supernatants. As a result of this, the protein array data was used to help inform the design of the later flow panels, in particular the inclusion of CD16 and CD14.

Crucially, NK cell recruitment of hBMSC is known to be dose-dependent, which may explain the weaker migration induced in the hBMSC population during this experiment, resulting from the low cell number used as the chemoattractive agent within the assay (Almeida et al. 2012). Using the live cells as a chemoattractive agent was intended to allow for bi-directional paracrine interactions occurring between the population of interest and the hBMSC. However, due to the extremely low yields of cells isolated using the double-step MACS procedure, an improved method might have been to use pre-conditioned medium formed from the supernatants of the PBMC subpopulations. This would have prevented bi-directional paracrine interactions from occurring but would have created a greater concentration of NK cell secreted factors which may have enhanced the observed migration. Further, the cells used in the migration assays were non-activated, and hence secreted lower levels of cytokines compared to activated NK cells.

4.4.1 Limitations of the study

LRS cones are a waste product generated during platelet donation and contain leukocytes, which are retained in the cone and not returned to the donor following the procedure. While the PBMC isolated from LRS cones were from allogenic sources, the use of LRS cones has several advantages, and is a common source of leukocyte for research purposes. The cones are easily accessible and permit a consistent method for obtaining large numbers of leukocytes without the specific ethical or

safety concerns and logistical complexities of direct donations for research. Further, the donors from which the LRS cones originate are healthy and regularly screened. This improves both the quality of cells obtained, and the safety of the blood product. While LRS cone cell numbers are lower than in whole blood, the ratios of different cell types within the cone are the same as whole blood and cell activities are also not affected (Néron et al. 2007). The drawbacks include lower leukocyte numbers than in whole blood, so rare populations present in whole blood are correspondingly scarce within the cones. Further, cones are received the day after they are isolated from the donor and so there could be changes in the cell activation states, or loss of short-lived cell types in the time between donation and processing. However, the use of LRS cones to isolate active leukocytes, such as NK cells, B cells or T cells, for research is well-documented, and isolated cells have characteristics and behaviour consistent with cells isolated from fresh, whole blood (Dietz et al. 2006; Hwang et al. 2012; Néron et al. 2007; Wiencke et al. 2016). The drawbacks of using allogenic PBMC will be considered in chapter 5.

On a related note, the yields of cells obtained through the $CD45_{dep}CD31_{enr}$ double-step isolation method were extremely low, of the order of 1×10^5 cells per cone, severely limiting the potential assay work. Each cone could often only be used for a single replicate of a single condition, increasing the risk of donor-to-donor or sample-to-sample variation. As a result, when the population was characterised as containing a majority of NK cells, the isolation method was altered to use the Miltenyi MACS NK cell isolation kit rather than the double-step isolation method in order to permit a greater number of assays. As seen in the protein array data and indeed within the flow cytometry, the population was not pure NK cells, with other cell types present that may also have influenced the observed hBMSC migration. A future study should directly compare the hBMSC migration stimulated and the proteins secreted by the double-step population with that observed from the NK cells isolated with the kit to confirm that the NK cells present within the double-step population were in fact the driving force behind the observed migration.

The flow characterisation of the $CD45_{dep}CD31_{enr}$ subpopulation did not show CD31 positive staining in the characterisation panel. CD31, also known as Platelet and Endothelial Cell Adhesion Molecule 1 (PECAM-1), has multiple splice variants, which may be expressed on different cell subsets and therefore the epitope recognised by specific antibody clones may vary in abundance on the subsets (Yongji Wang and Sheibani 2002). The anti-CD31 antibody clone used in the flow cytometric phenotyping was WM-59 and, while this clone is routinely used in flow cytometry to examine human CD31 expression, it might have been more appropriate to use L133.1, which was generated specifically using human NK Cells (Biosciences 2018).

4.4.2 Future directions

Future work could attempt to unpick the interactions between the isolated NK cell population and the hBMSC resulting in hBMSC migration. Greater understanding of the secretome of the NK cells, and

how it is altered under normoxic and hypoxic conditions could explain the differences observed in hBMSC migration. Crossing over the conditions, with normoxic hBMSC migration studied in hypoxic conditions and vice versa could indicate whether the behaviours again were transiently influenced or a result of subpopulation selection resulting from the oxygen level. Further, the influence of the hBMSC on the migration of NK cells could be explored, to establish whether any potential co-localisation was bi-directional. Additionally, examination of the hBMSC genome, with particular attention paid to genes related to migration, could indicate whether the migration under normoxic or hypoxic conditions occurs through stimulation of the same, or different pathways. Another layer which could be added is the consideration of a pro-inflammatory environment. The isolated NK population was not activated, which would not be the case in NK cells found within a haematoma following micro-drilling. NK cell activation results in vastly heightened secretion of a range of cytokines, including those such as IP-10 which have a strong chemotactic effect on hBMSC (Anton et al. 2012). Examining how an inflammatory microenvironment, modelled using cytokine mixtures, would impact on the hBMSC migration could have more functional relevance to the model in question. Further, the NK cells themselves could be fractionated to observe which fraction had the greatest chemoattractive influence on the hBMSC. *in vivo* validation of this finding, by looking for markers of NK cell and stromal populations in osteochondral defects using immunohistochemistry, or fluorescent reporter mice, could indicate whether the observed *in vitro* migration results in *in vivo* co-localisation. This would be challenging, due to the cytotoxic behaviours observed in NK cells, which will be covered in chapter 5.

4.4.3 Summary

This work has identified that a whole NK cell population isolated by double-step MACS isolation resulted in increased hBMSC migration in both normoxic and hypoxic conditions. hBMSC migration in the normoxic condition was more direct, regardless of the stimulating PBMC subpopulation, than that seen in the hypoxic condition. NK cell mediated migration of hBMSC has been previously observed, although the approach taken in this study of comparing the paired enriched and depleted PBMC populations is a novel approach.

NK cells play a key role in the recruitment of hBMSC to sites of trauma. The more direct migration in the normoxic condition may indicate a stress response stimulated *in vivo* by the oxygen burst following trauma.

Chapter 5

Functional consequences of hBMSC - NK cell co-cultures under hypoxic and normoxic conditions

5.1 Abstract

Aim: To characterise the interactions between NK cells and hBMSCs under normoxic and hypoxic conditions.

Methods: hBMSCs were co-cultured with varying ratios of NK cells, with or without IL-2 stimulation, and under either normoxic or hypoxic conditions. Co-cultures were assessed by visual inspection, CellTox Green, real-time impedence assay, and flow cytometry. Paracrine cultures were set up in a Boyden chamber and compared to cell-to-cell contact assays. Gene expression of CXCL10, Indoleamine-2 3-dioxygenase (IDO), and HIF-1α were examined using RT-qPCR.

Results: Non-activated NK cells had greater effects on hBMSC proliferation in normoxic compared to hypoxic conditions. IL-2 activated NK cells caused hBMSC lysis in both normoxic and hypoxic conditions. The ratio of NK cells influenced the effects seen. NK cell mediated effects were reliant on cell-to-cell contact. Co-cultures of NK cells and hBMSC did not alter hBMSC marker expression as measured by flow cytometry, but did result in oxygen-dependent changes in all genes examined.

Conclusion: NK cell interactions with hBMSC vary with oxygen level, activation status, and ratio of NK : hBMSC numbers. Interactions in hypoxic conditions increase immunomodulatory gene expression, while normoxic conditions increase inflammatory gene expression.

5.2 Introduction

Natural Killer cells are a component of the innate immune system, and make up 5 to 20 percent of lymphocytes within the peripheral blood (Néron et al. 2007). They are an effector cell type, and are recruited and activated through a variety of pathways, including cytokines such as IL-2, Interleukin 15 (IL-15), and Interleukin 18 (IL-18), other immune cells such as macrophages or dendritic cells, and cell-surface receptor interactions, particularly Natural Killer Group 2 Member D (NKG2D) and toll-like receptors (Vivier et al. 2008). NK cells are typically considered to be primarily involved with control of microbial infection and tumour suppression through their cytotoxic abilities. However, there is increasing evidence that subpopulations of NK cells also have regulatory roles, such as in maternal-fetal tolerance and suppression of auto-immunity, suggesting that NK cells are involved with immune surveillance and tolerance (Fu et al. 2014; Gross et al. 2016). Indeed, the role of NK cells in repair also encompasses immuno-modulatory functions, such as regulation of pro- and anti-inflammatory macrophages during inflammation, or secretion of TNFα, which increases recruitment and differentiation of progenitor cells in fracture repair as well as cytotoxic behaviour (Glass et al. 2011; El-Jawhari et al. 2016; Tosello-Trampont et al. 2017). The previous chapter demonstrated that NK cells appeared to be the most potent recruiting cell type for hBMSC in both normoxic and hypoxic conditions, based on the system used. The premise of this chapter is that the recruited hBMSC will partition with the NK cells within the repair site, leading to direct cell-to-cell interactions between hBMSC and NK cells. While studies have examined the interactions between NK cells and hBMSC, the results have been mixed. Some studies have shown that NK cells are important in priming hBMSC for repair and that NK cells do not kill hBMSC, while others have shown that any interaction between NK cells and hBMSC leads to the death of the hBMSC through NK cell mediated cytotoxicity (Almeida et al. 2012; El-Jawhari et al. 2016). The majority of current studies examining the interactions between NK cells and hBMSC have done so under normoxic conditions, or through the use of hypoxic pre-conditioning, despite work showing that both hBMSC and NK cell biology is influenced by oxygen level (W.-H. Huang et al. 2014; Hung et al. 2012; Loeffler et al. 1991; Wagegg et al. 2012; Yang et al. 2011). As a result, there is a lack of understanding of the functional consequences of interactions between hBMSC and NK cells under hypoxic conditions. This chapter aims to explore the consequences of direct cell-to-cell interactions between hBMSC and NK cells under normoxic and hypoxic conditions through co-cultures and functional assays. Interactions modelled in hypoxic conditions may be more biologically relevant to the early, pre-revascularisation phase of repair, while normoxic interactions may have more relevance to later stages of repair, as well as allowing a comparison between the models used in the wider literature and those used in this study.

5.3 Results

NK cells cultured with IL-2 for seven days under hypoxic (fig. 5.1a) or normoxic (fig. 5.1c) conditions became semi-adherent and formed colonies of replicating cells. These colonies were noticeably larger in hypoxic conditions (fig. 5.1a). NK cells cultured without IL-2 did not adhere or proliferate under either hypoxic (fig. 5.1b) or normoxic (fig. 5.1d) conditions, and when observed appeared to be dead; the cells were not phase-bright, but instead were dull with an irregular, shrivelled appearance.

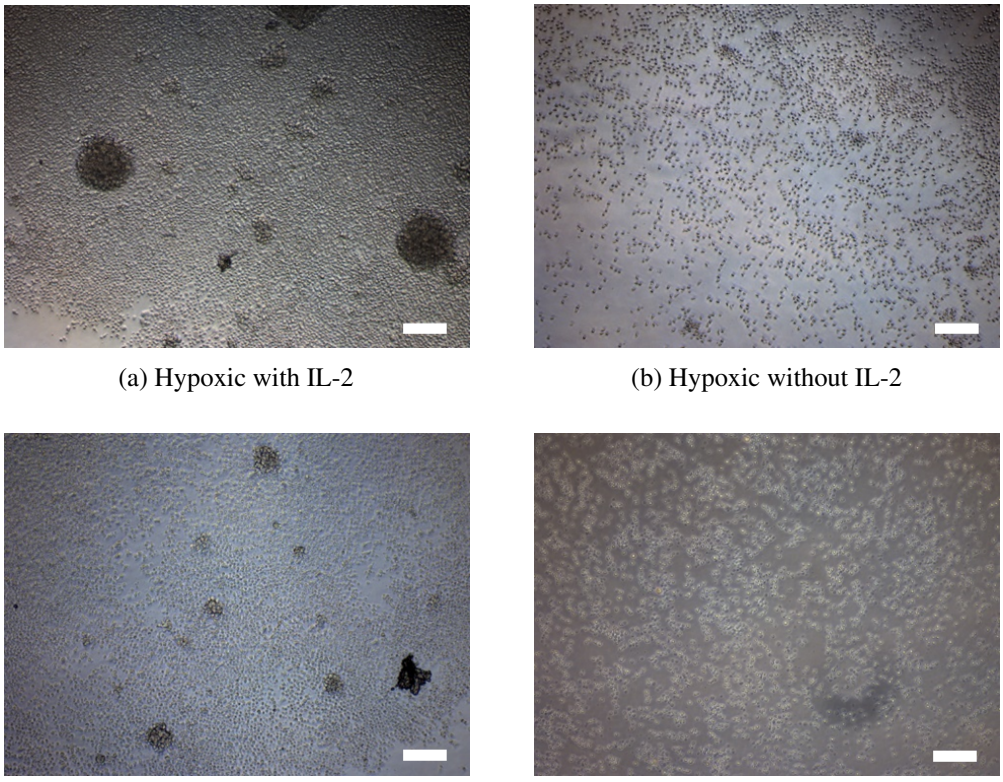

(a) Hypoxic with IL-2

(b) Hypoxic without IL-2

(c) Normoxic with IL-2

(d) Normoxic without IL-2

Fig. 5.1 Culture of NK cells with or without IL2 stimulation under normoxic and hypoxic conditions

NK cells isolated using Miltenyi MACS NK cell kit were cultured under hypoxic or normoxic conditions for one week with or without IL-2 stimulation. Scale Bar = 100 µm, N = 3

Co-cultures of hBMSCs and NK cells, with or without IL-2 stimulation, were set up and incubated for 7 days under hypoxic (figs. 5.2 and 5.3) or normoxic (figs. 5.4 and 5.5) conditions using the corresponding hBMSC isolates. Ratios of NK cells ranged from 1 NK cell (figs. 5.2b, 5.3b, 5.4b and 5.5b), 5 NK cells (figs. 5.2c, 5.3c, 5.4c and 5.5c), 10 NK cells (figs. 5.2d, 5.3d, 5.4d and 5.5d) through to 15 NK cells (figs. 5.2e, 5.3e, 5.4e and 5.5e) per 1 hBMSC, with an hBMSC-alone (figs. 5.2a, 5.3a, 5.4a and 5.5a) condition as a control for IL-2 stimulation. Visual inspection of cultures showed that, regardless of oxygen level, there was no visible difference in hBMSC morphology or number between hBMSC cultured alone with (figs. 5.2a and 5.4a) or without (figs. 5.3a and 5.5a) IL-2. Further,

unstimulated NK cells did not appear to influence hBMSC morphology or number, regardless of cell ratio (figs. 5.3 and 5.5). In the unstimulated cultures, NK cell numbers appeared low compared to the IL-2 stimulated cultures in both hypoxic (fig. 5.2) and normoxic (fig. 5.4) conditions. The non-stimulated NK cells did not adhere or proliferate.

IL-2 stimulated co-cultures contained semi-adherent NK cells, with numbers increasing with increasing NK cell : hBMSC ratio. Loss of the hBMSC, interpreted as hBMSC death, was seen at ratios above 5:1 NK cells : hBMSC in both hypoxic and normoxic (figs. 5.4c to 5.4e) conditions. The perceived hBMSC death scaled with increasing ratios, with the highest ratio of NK cells (15:1 NK cells : hBMSC) showing the greatest loss from the hBMSC monolayer. Further, clumping in the NK cell populations was seen at higher NK cell : hBMSC ratios, although definitive NK cell colony formation was not seen.

The co-cultures gave observational results at an individual time-point. To quantify the effect of the NK cells on the hBMSC in more detail, the XCelligence RTCA E-plate system was used to give a real-time indication of cytotoxicity. NK cell to hBMSC ratios of 0, 0.1, 0.2, 1, 5, 10 and 15 to 1 were used to give a range for dose-response analysis. The co-cultures were set up and run for 7 days in hypoxic (fig. 5.6) and normoxic (fig. 5.7) conditions without IL-2 (figs. 5.6a and 5.7a) and with IL-2 (figs. 5.6b and 5.7b). Optimisation experiments showed that NK cells, both unstimulated and stimulated with IL-2 did not influence the impedance measured, demonstrating that only hBMSC were quantified (data not shown). A Cell Index value of zero or lower on the Real Time Cell Trace (RTCT) was interpreted as complete cell death.

In hypoxic conditions, the RTCT for the unstimulated NK cell – hBMSC co-cultures clustered together following a similar initial trend (fig. 5.6a). A trough during the adhesion period was observed after approximately 10 hours (fig. 5.6a, black arrow), followed by an inflexion point at approximately 50 hours (fig. 5.6a, blue arrow) in the RTCT for hBMSC with unstimulated NK cells. Following the inflexion, all RTCT except the 15:1 NK cell : hBMSC condition, which plateaued, appeared to have an increasing cell index. In co-cultures with IL-2 stimulation, the same adhesion trough was seen at around 10 hours on the RTCT (fig. 5.6b, black arrow). However, while the inflexion point was around 50 hours again for the hBMSC with lower NK cell ratios (fig. 5.6b, blue arrow), the hBMSC with higher NK cell ratios showed a peak at around 23 hours followed by a decline in the RTCT (fig. 5.6b, red arrow). The lower NK cell numbers (0.1 to 1 NK cell per hBMSC) showed the same trend as seen in the unstimulated co-cultures, with an apparent increase in cell number. To contrast, the RTCT of hBMSC with higher NK cell numbers (5 to 15 NK cell per hBMSC) showed a decrease in cell index. The trace for hBMSC with 5 NK cells per hBMSC did not reach zero, and had a less steep slope than those for both the 10 and 15 NK per hBMSC RTCT, which both reached zero. This indicated that the hBMSC were dying at a slower rate in the 5 NK per hBMSC compared to the 10 and 15 NK per hBMSC co-cultures.

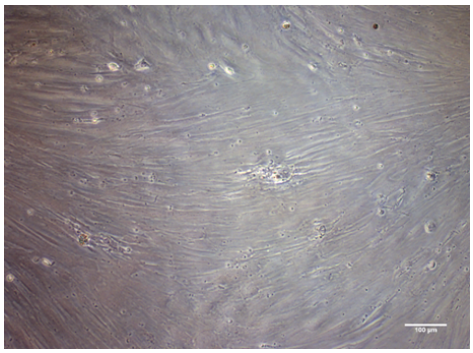

(a) hBMSC only

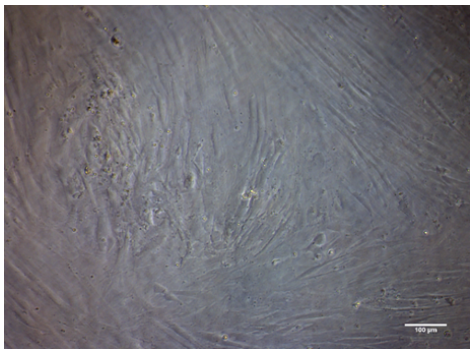

(b) 1:1 NK cells to hBMSCs

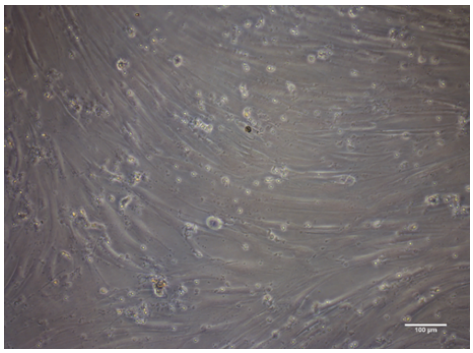

(c) 5:1 NK cells to hBMSCs

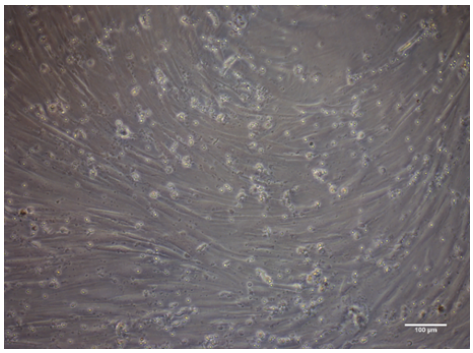

(d) 10:1 NK cells to hBMSCs

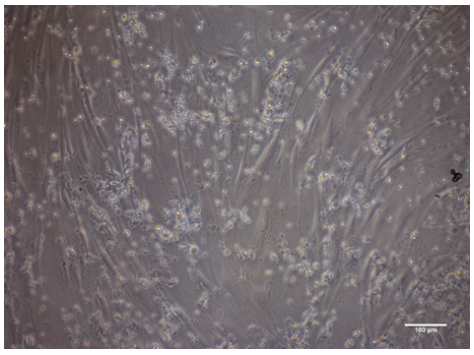

(e) 15:1 NK cells to hBMSCs

Fig. 5.2 Hypoxic co-culture of BMSC and varying NK cell ratios with IL-2 stimulation

NK cells isolated using Miltenyi MACS NK cell kit were co-cultured for 1week with hypoxic-isolated hBMSC at ratios of 0, 1, 5, 10, and 15 NK cells per hBMSC under hypoxic conditions with IL-2 stimulation. Scale Bar = 100 µm, N = 3

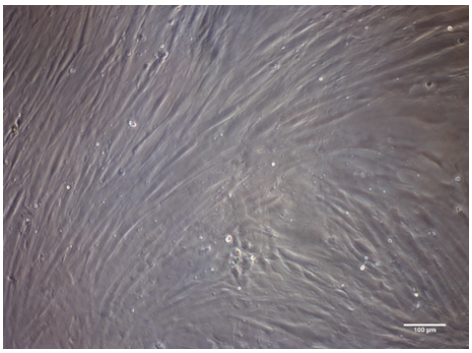

(a) hBMSC only

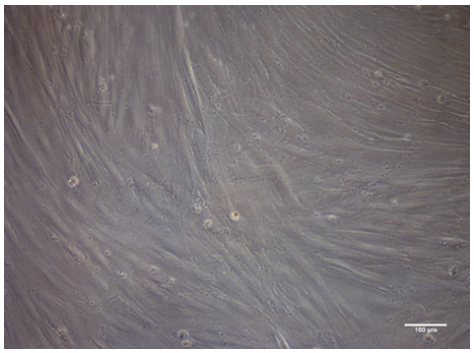

(b) 1:1 NK cells to hBMSCs

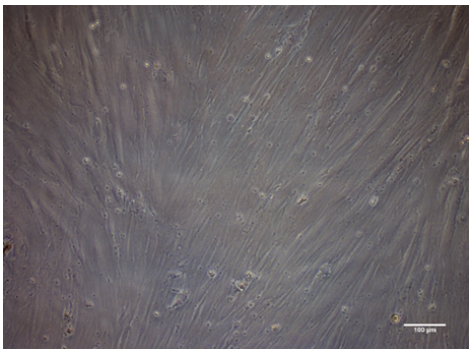

(c) 5:1 NK cells to hBMSCs

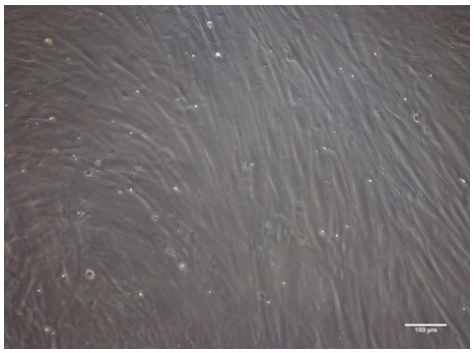

(d) 10:1 NK cells to hBMSCs

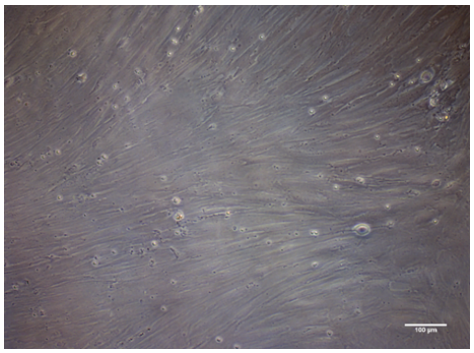

(e) 15:1 NK cells to hBMSCs

Fig. 5.3 Hypoxic co-culture of BMSC and varying NK cell ratios without IL-2 stimulation

NK cells isolated using Miltenyi MACS NK cell kit were co-cultured for 1week with hypoxic-isolated hBMSC at ratios of 0, 1, 5, 10, and 15 NK cells per hBMSC under hypoxic conditions with no cytokine stimulation. Scale Bar = 100 µm, N = 3

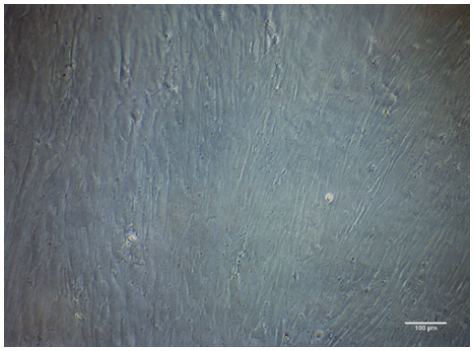

(a) hBMSC only

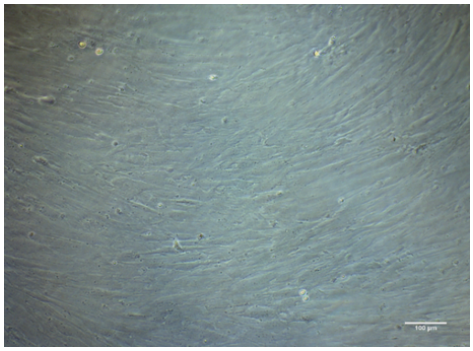

(b) 1:1 NK cells to hBMSCs

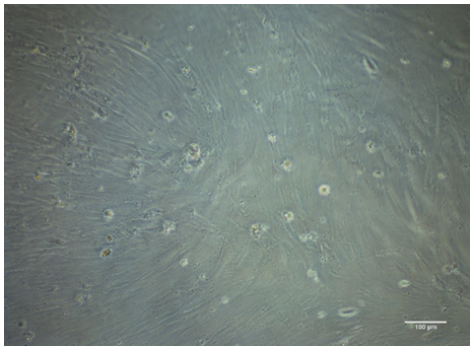

(c) 5:1 NK cells to hBMSCs

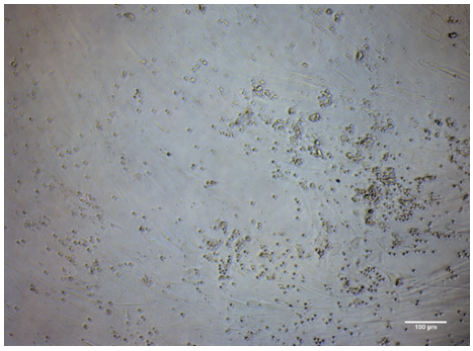

(d) 10:1 NK cells to hBMSCs

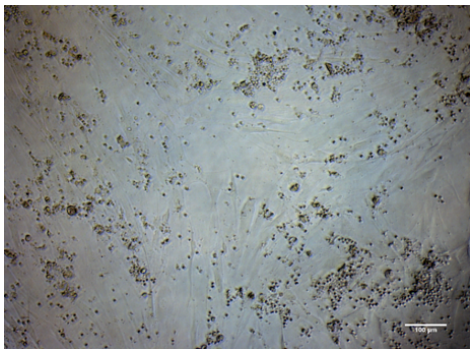

(e) 15:1 NK cells to hBMSCs

Fig. 5.4 Normoxic co-culture of BMSC and varying NK cell ratios with IL-2 stimulation

NK cells isolated using Miltenyi MACS NK cell kit were co-cultured for 1week with normoxic-isolated hBMSC at ratios of 0, 1, 5, 10, and 15 NK cells per hBMSC under normoxic conditions with IL-2 stimulation. Scale Bar = 100 µm, N = 3

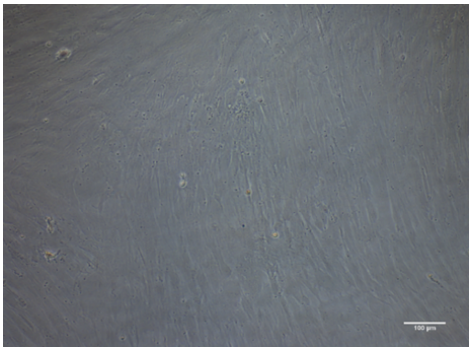

(a) hBMSC only

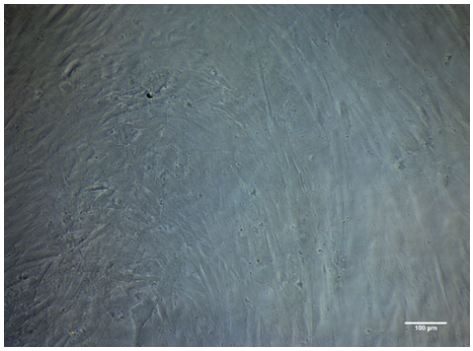

(b) 1:1 NK cells to hBMSCs

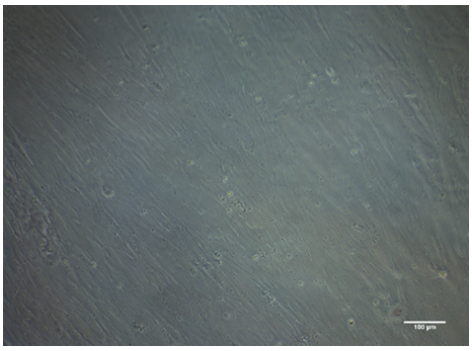

(c) 5:1 NK cells to hBMSCs

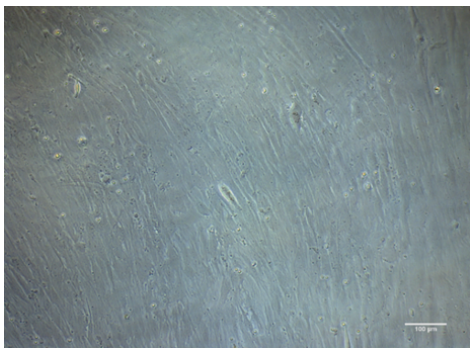

(d) 10:1 NK cells to hBMSCs

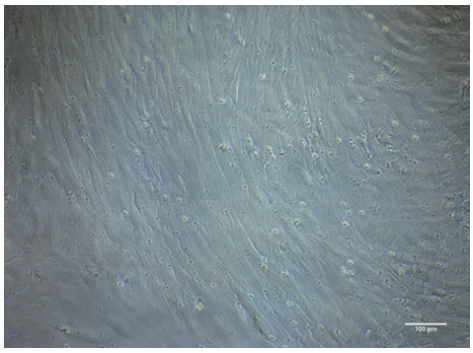

(e) 15:1 NK cells to hBMSCs

Fig. 5.5 Normoxic co-culture of BMSC and varying NK cell ratios without IL-2 stimulation

NK cells isolated using Miltenyi MACS NK cell kit were co-cultured for 1week with normoxic-isolated hBMSC at ratios of 0, 1, 5, 10, and 15 NK cells per hBMSC under normoxic conditions with no cytokine stimulation. Scale Bar = 100 µm, N = 3

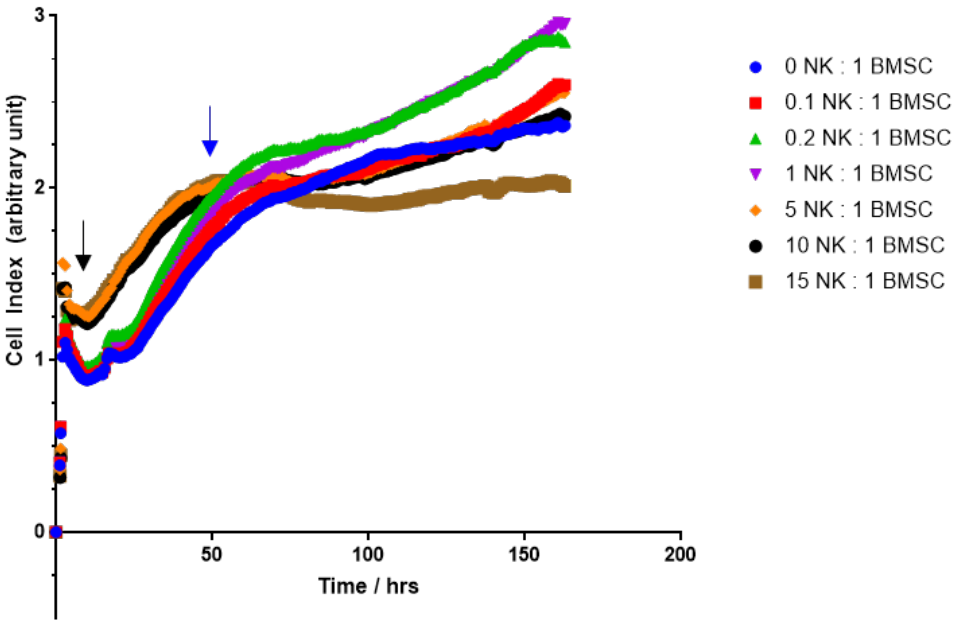

(a)

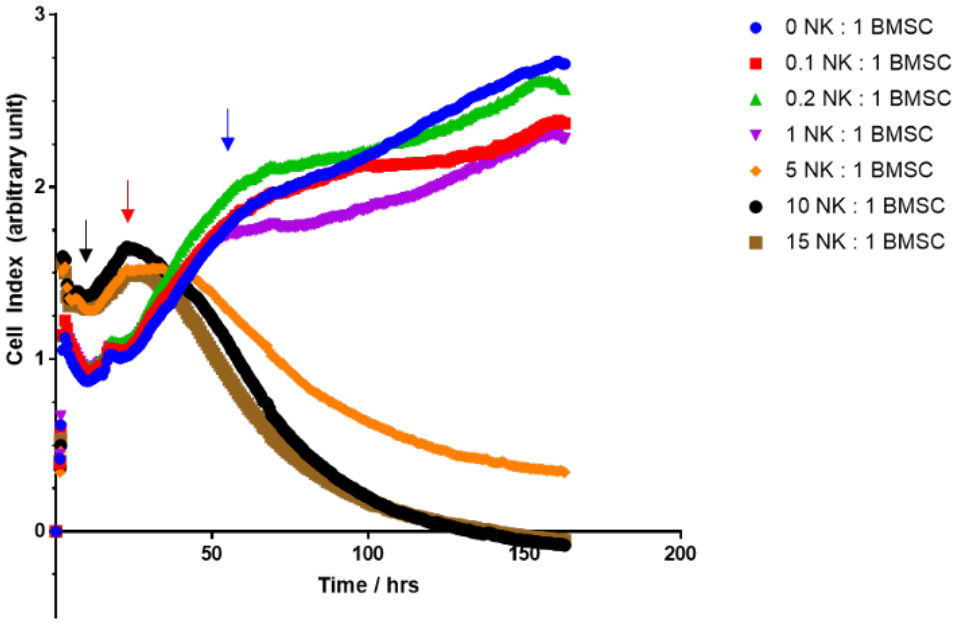

(b)

Fig. 5.6 Real-time cell killing assay using hBMSC with varying NK ratio and IL-2 stimulation in hypoxia

hBMSC were co-cultured with varying ratios of NK cells without (fig. 5.6a) or with (fig. 5.6b) IL-2 stimulation under hypoxic conditions in Xcelligence RTCA E-plate 16 for 7 days. Measurements were taken every 10 minutes. Black arrow: adhesion trough. Blue arrow: inflexion point 1. Red arrow: inflexion point 2. N = 6.

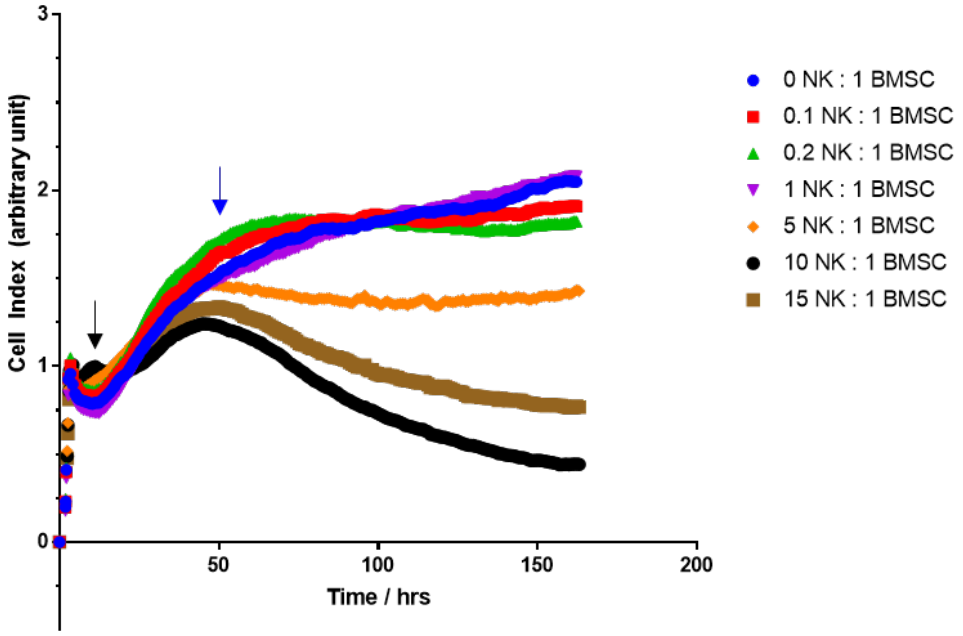

(a)

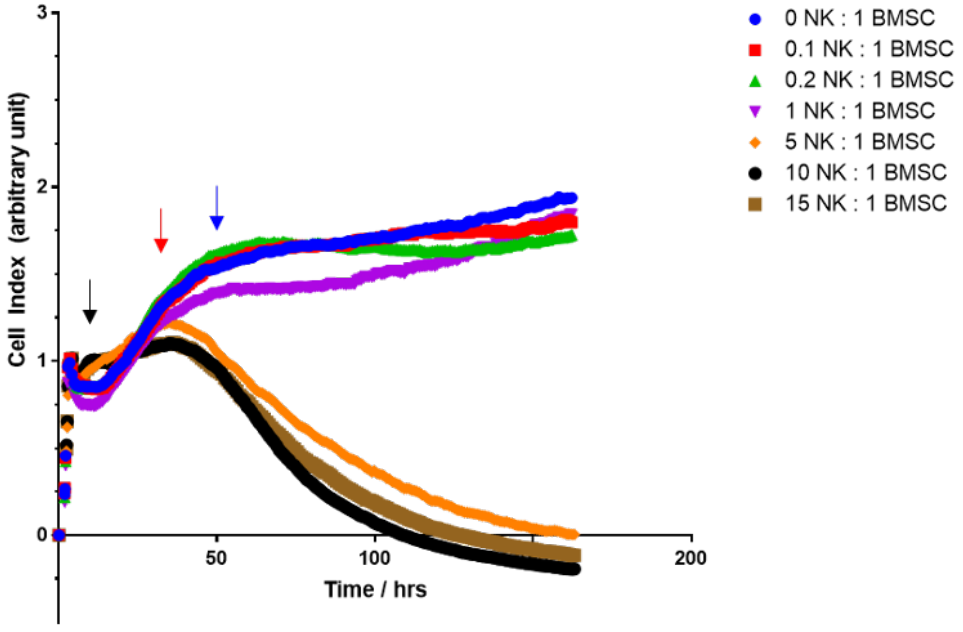

(b)

Fig. 5.7 Real-time cell killing assay using hBMSC with varying NK ratio and IL-2 stimulation in normoxia

hBMSC were co-cultured with varying ratios of NK cells without (fig. 5.7a) or with (fig. 5.7b) IL-2 stimulation under normoxic conditions in Xcelligence RTCA E-plate 16 for 7 days. Measurements were taken every 10 minutes. Black arrow: adhesion trough. Blue arrow: inflexion point 1. Red arrow: inflexion point 2. N = 6.

In normoxic conditions, the RTCT for hBMSC co-cultured with the different ratios unstimulated NK cells did not show the same trends (fig. 5.7a), unlike the equivalent experiment in hypoxic conditions (fig. 5.6a). The adhesion trough at 10 hours and inflexion at 50 hours were still present (fig. 5.7a black and blue arrows, respectively), however after the inflexion the RTCT diverged. The lowest NK cell ratios (0.1 to 1 NK cell per hBMSC) clustered with the hBMSC alone and appeared to plateau, rather than increase as seen in the hypoxic condition. However, a clear separation was seen between these RTCT and the RTCT for the hBMSC with 5 NK cells per hBMSC, which still plateaued but at a lower value, and again for the 10 to 15 NK cell per hBMSC, which showed decreases in cell index. The co-cultures with IL-2 stimulated NK cells behaved similarly to those in the hypoxic condition, although the lower ratios had a lower final cell index, and the 5 NK per hBMSC RTCT reached zero (fig. 5.7b). Further, the inflexion point for the higher ratios occurred later, at around 34 hours (fig. 5.7b, red arrow).

Analysis of the endpoint values (7 days) showed that for the 0.1, 0.2 and 1 NK cell per hBMSC condition, and hBMSC alone, there was no difference in RTCT end-point between the unstimulated and IL-2 stimulated cultures in both the hypoxic (fig. 5.8a) and normoxic (fig. 5.8b) conditions. In hypoxic conditions, the endpoint values for the unstimulated 5, 10 and 15 NK cell per hBMSC condition were not different from those for the lower ratios (fig. 5.6a). However, the values for the IL-2 stimulated conditions were significantly lower than their unstimulated counterparts at the higher ratios.

The normoxic condition showed a similar trend: there were no differences between the traces for hBMSC alone or co-cultured with the lower NK cell ratios (between 0.1 to 1 NK per hBMSC). In addition, at these lower ratios there were no differences between co-cultures with or without IL-2 stimulation (fig. 5.8b). Addition of IL-2 resulted in the same decrease in RTCT endpoint for the higher ratios (5 to 15 NK cells per hBMSC). However, while the RTCT for the unstimulated 5 NK per hBMSC was not different to the lower ratios, the unstimulated 10 or 15 NK per hBMSC were lower. Directly comparing the unstimulated co-cultures in normoxic and hypoxic showed that the RTCT endpoint at higher ratios were significantly lower in normoxic conditions compared to hypoxic conditions (fig. 5.9a). However, there were no differences between the RTCT end-points in normoxic and hypoxic conditions when co-cultures were stimulated with IL-2 (fig. 5.9b).

Further analysis was performed considering when the RTCT reached zero Cell Index for the IL-2 stimulated co-cultures (fig. 5.10). Only the ratios of between 5 and 15 NK cells per hBMSC with IL-2 stimulation were used, since no other traces reached zero. As indicated on the chart, in the 5 NK per hBMSC condition, 5 out of 6 RTCT in the hypoxic, and 3 out of 6 in the normoxic condition never reached zero. In fact, even in the higher ratios, 1 of the hypoxic condition RTCT still never reached zero, although consideration of the data shows that the RTCT was close to the cut-off. An apparent trend was seen in the data, particularly in the hypoxic condition, with the time to reach zero decreasing with increasing NK cell numbers. However, this was not significant, nor was there any

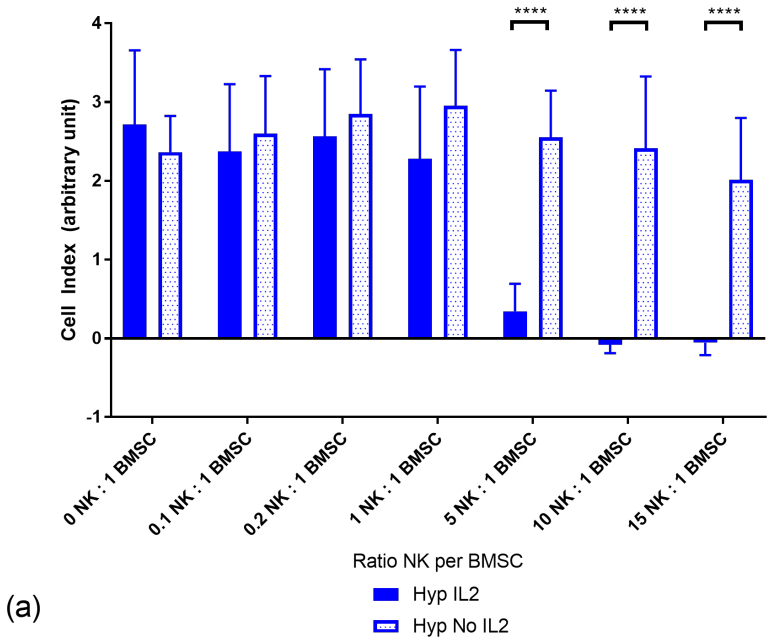

(a)

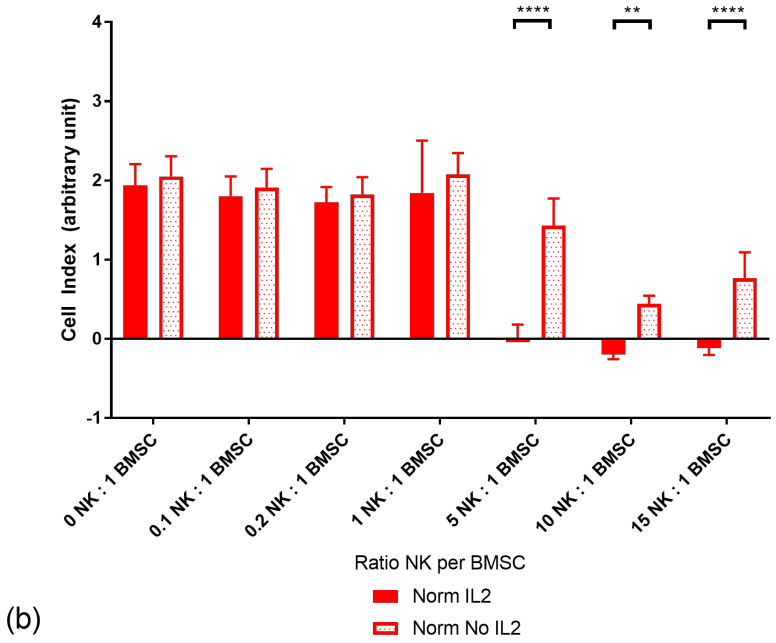

(b)

Fig. 5.8 Endpoint analysis of real-time cell killing comparing condition with or without IL-2 stimulation

Endpoint analysis of Xcelligence RTCA traces at 7 days showing comparison between hBMSC and varying NK cell ratios co-cultured with and without IL-2 stimulation under hypoxic (fig. 5.8a) or normoxic (fig. 5.8b) culture conditions. Significances shown on charts, Two-way ANOVA with Tukey's post hoc test, p values: $** < 0.005$, $**** < 0.0001$. Error bars show standard deviation. $N = 6$.

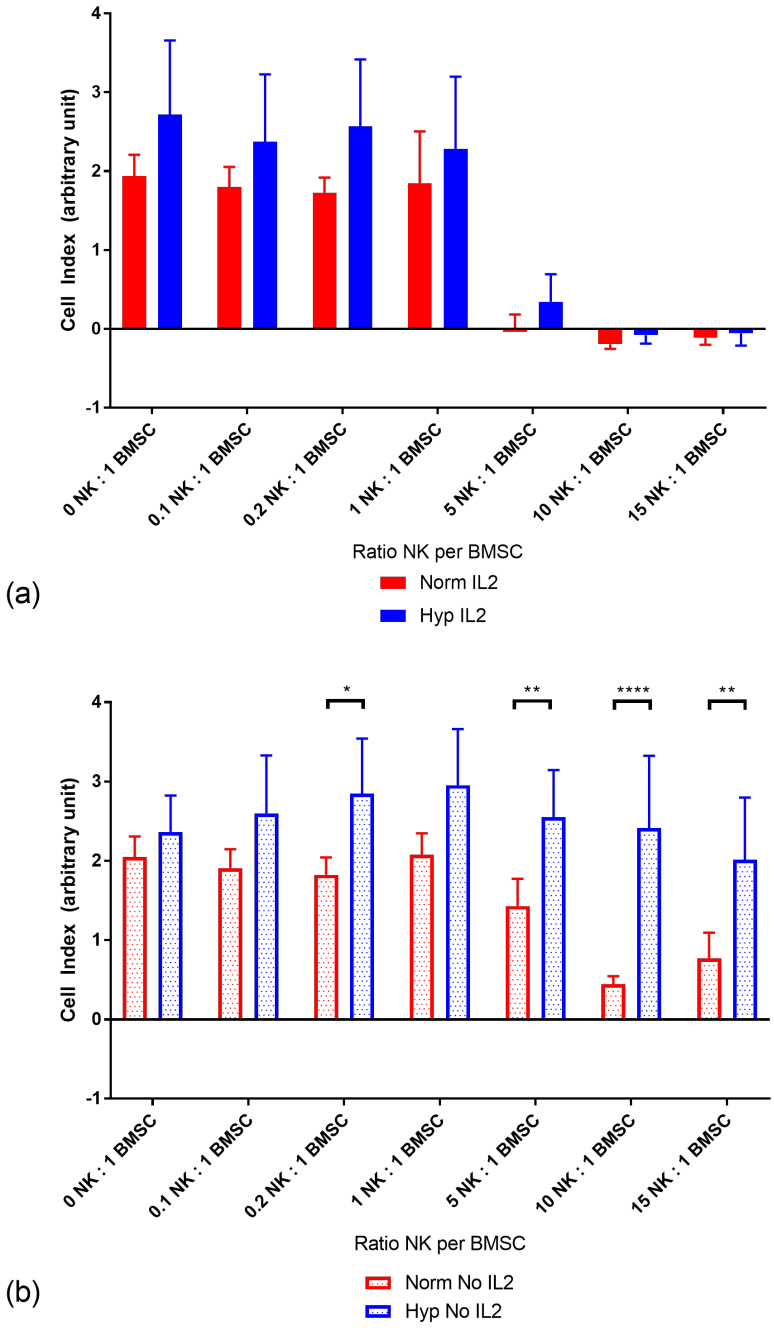

Fig. 5.9 Endpoint analysis of real-time cell killing comparing hypoxic and normoxic condition

Endpoint analysis of Xcelligence RTCA traces at 7 days showing comparison between hBMSC and varying NK cell ratios co-cultured hypoxic or normoxic culture conditions without (fig. 5.9a) and with (fig. 5.9b) IL-2 stimulation. Significances shown on charts, Two-way ANOVA with Tukey's post hoc test, p values: $* < 0.05$, $** < 0.005$, $**** < 0.0001$. Error bars show standard deviation. $N = 6$.

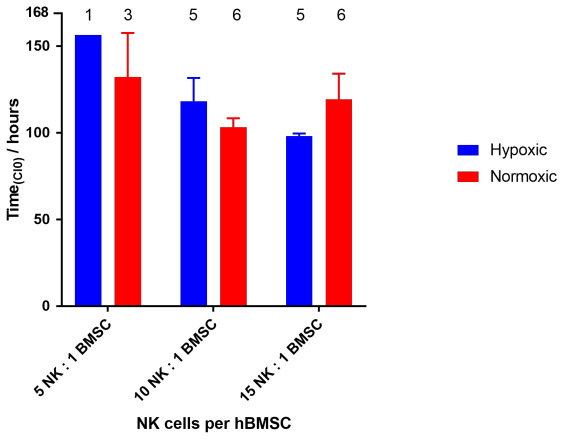

Fig. 5.10 Time when cell index of IL-2 stimulated NK cell – hBMSC co-cultures reached zero

Analysis of Xcelligence RTCA traces showing the time RTCT reached zero for hBMSC cultured with various NK ratios and stimulated with IL-2. Line at 168 shows end-point time for experiment (7 days). Ratios 0, 0.1, 0.2 and 1 NK : 1 hBMSC are not shown since these traces never reached zero. The number above the bar indicates the number of traces reaching the cut-off within the period of measurement. No significant differences found, Two-way ANOVA with Tukey's post hoc test, $P < 0.05$. Error bars show standard deviation. $N = 6$ (except where shown; the numbers above the bars indicate the number of traces which reached zero within the measure time-frame)

difference between the time to reach zero under hypoxic or normoxic conditions for each NK cell dose.

Assessment of NK cell cytotoxicity showed clear differences between co-cultures with and without IL-2 stimulation, and between the hypoxic and normoxic condition. The dose-response curves for the hypoxic condition show that as the ratio of IL-2 stimulated NK cells to hBMSC increases, the $AUC_{(xj)}$ decreases in a dose-dependent fashion (fig. 5.11). The AUC_{50} for hBMSC co-cultured with IL-2 stimulated NK cells was 4.98 NK cells per hBMSC. To contrast, co-cultures of hBMSC with non-stimulated NK cells showed either no difference between the AUC_j and the AUC_c, or a higher AUC_j relative to the AUC_c at all concentrations studied. In the normoxic condition, the same trend could be seen in the co-cultures stimulated with IL-2 as in the hypoxic IL-2 stimulated condition, although the AUC_{50} was slightly lower at 4.51 NK cells per hBMSC (fig. 5.12). However, the result for the non-stimulated co-cultures was starkly different to that seen in the hypoxic condition. At lower NK cell concentration (0.1 to 1 NK cell per hBMSC), the AUC_j and the AUC_c were the same, but at higher concentrations, the $AUC_{(xj)}$ increased, showing that the AUC_j had decreased relative to the AUC_c. An AUC_{50} could not be calculated for the non-stimulated co-cultures in normoxic conditions, since the $AUC_{(xj)}$ did not reach 50 % in the range of NK cell ratios studied.

To identify whether NK cell killing of hBMSC was specific, i.e. individual hBMSC were actively targeted and killed by NK cells, as opposed to hBMSC dying en-masseco-cultures of 10 NK cells per hBMSC with IL-2 stimulated were set up under normoxic and hypoxic conditions for 72 hours, then

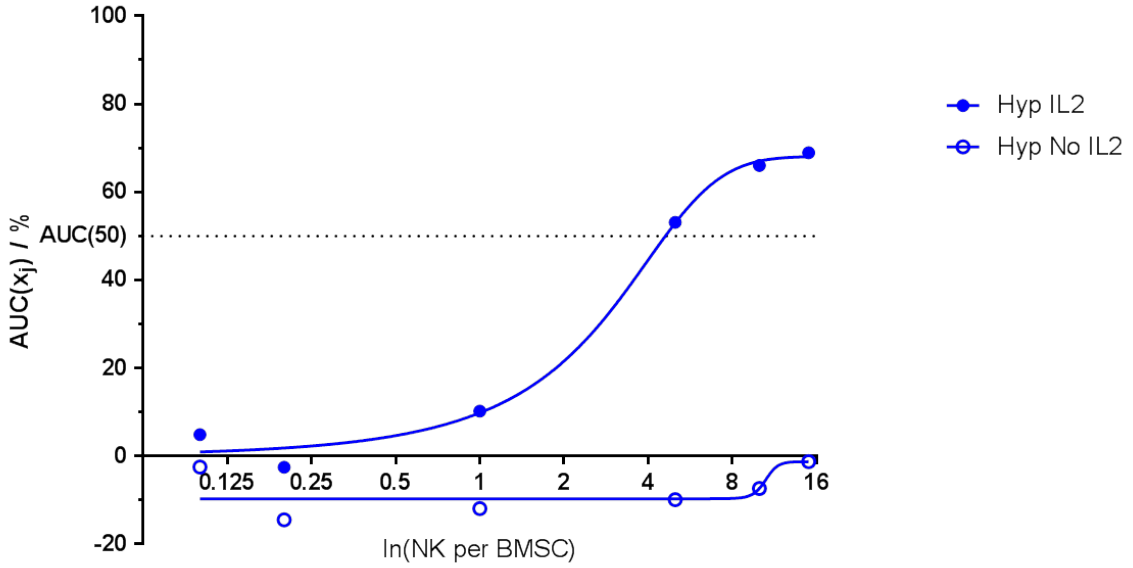

Fig. 5.11 Assessment of NK cell cytotoxicity in hypoxic conditions using glsAUC$_{50}$

The AUC was calculated based on the real time cell traces from NK cell co-cultures with hBMSC, with or without IL-2 stimulation under hypoxic conditions using the hBMSC-alone cultures as a reference. A sigmoidal dose-response curve with variable slope was fitted using GraphPad Prism. With IL-2, AUC$_{50}$ = 4.98. Without IL-2, no cytotoxicity was seen in range examined. $N = 6$.

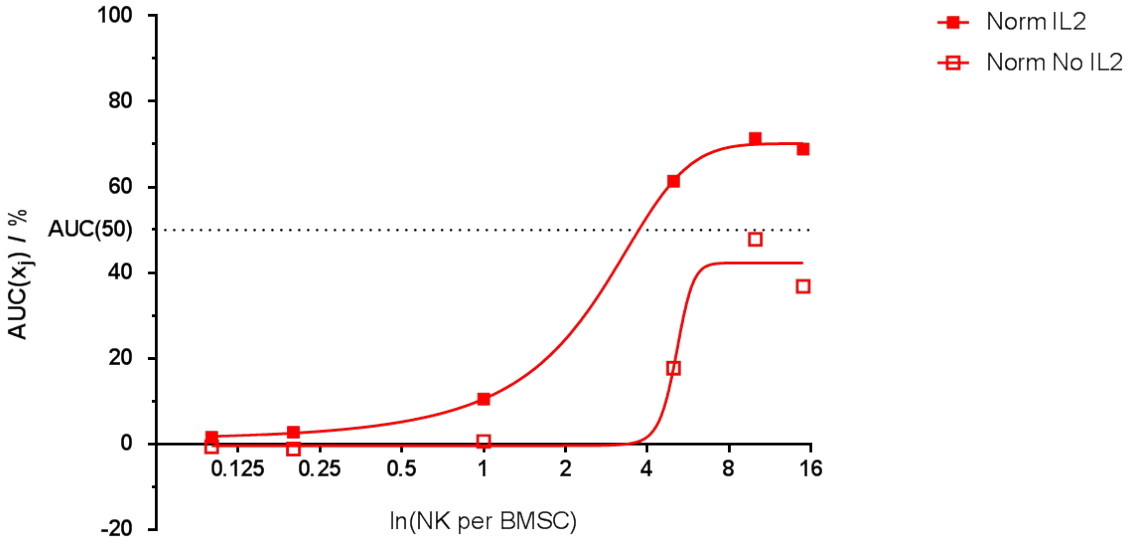

Fig. 5.12 Assessment of NK cell cytotoxicity in hypoxic conditions using AUC$_{50}$

The AUC was calculated based on the real time cell traces from NK cell co-cultures with hBMSC, with or without IL-2 stimulation under normoxic conditions using the hBMSC-alone cultures as a reference. A sigmoidal dose-response curve with variable slope was fitted using GraphPad Prism. With IL-2, AUC$_{50}$ = 4.51. Without IL-2, cytotoxicity was too low to calculate AUC$_{50}$ within range examined. $N = 6$.

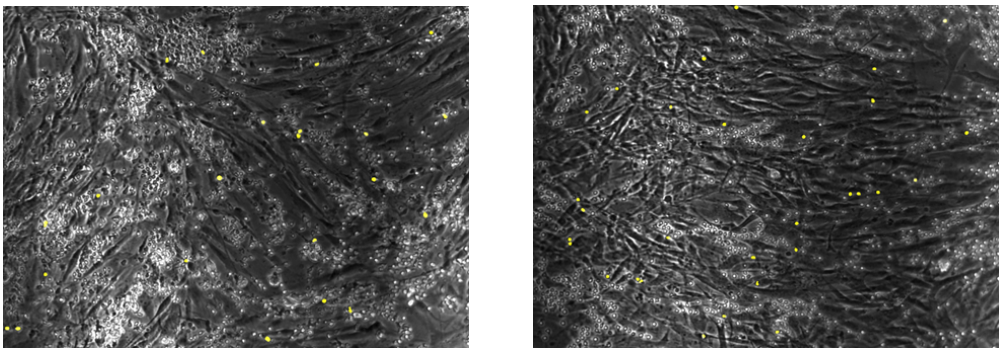

(a) Hypoxic (b) Normoxic

Fig. 5.13 72 hour CellTox Green of hBMSC - NK cell cultures stimulated with IL-2

hBMSC were co-cultured with IL-2 stimulated NK cells at 1:10 hBMSC : NK cells under normoxic (fig. 5.13b) and hypoxic (fig. 5.13a) culture conditions for 72 hours. Nuclei of dying hBMSC highlighted in yellow, Scale bar = 100 µm. $N = 3$.

treated with CellTox Green to visualise hBMSC death (fig. 5.13). Under both hypoxic (fig. 5.13a) and normoxic (fig. 5.13b) conditions, hBMSC death was punctate and discrete, with the death isolated to single hBMSC and not being transmitted to the neighbouring hBMSC surrounding the dying hBMSC. To investigate whether the hBMSC death was a result of cell-to-cell interaction, co-cultures were set up in hypoxic conditions with NK cells either in direct co-culture, or in a Boyden chamber, incubated for 7 days, and the hBMSC death quantified (fig. 5.14). The data showed that cell death in cultures of hBMSC alone, and hBMSC with IL-2 stimulation were similar, supporting the observations made using the Xcelligence. While hBMSC death appeared slightly higher in direct co-cultures of hBMSC and NK cells without IL-2, this interaction was not significant, but stimulation with IL-2 resulted in significantly higher levels of hBMSC death. To contrast, paracrine (transwell) co-cultures of hBMSC and NK cells, whether or not they were stimulated by IL-2, showed little hBMSC death, comparable to the hBMSC alone condition and significantly lower than the direct co-culture with IL-2 stimulation and NK cells.

To determine whether the NK cell – hBMSC interactions had consequences beyond the death of the hBMSC, gene expression analysis was performed by RT-qPCR on co-cultures of hBMSC and NK cells incubated under normoxic and hypoxic conditions for 7 days (fig. 5.15). 3 genes were examined: HIF-1α, an important moderator in cellular responses to hypoxic conditions, and IDO and CXCL10, both important immunoregulatory genes involved with various reparative pathways. Under hypoxic conditions, CXCL10 expression was increased in the co-cultures, while under normoxic conditions expression levels did not change (fig. 5.15a). The opposite was true of IDO expression, where an increase was seen in the normoxic condition with an apparent decrease under hypoxic conditions (fig. 5.13b). HIF-1α expression was not affected by the IL-2 stimulated co-culture under either hypoxic or normoxic conditions (fig. 5.15c).

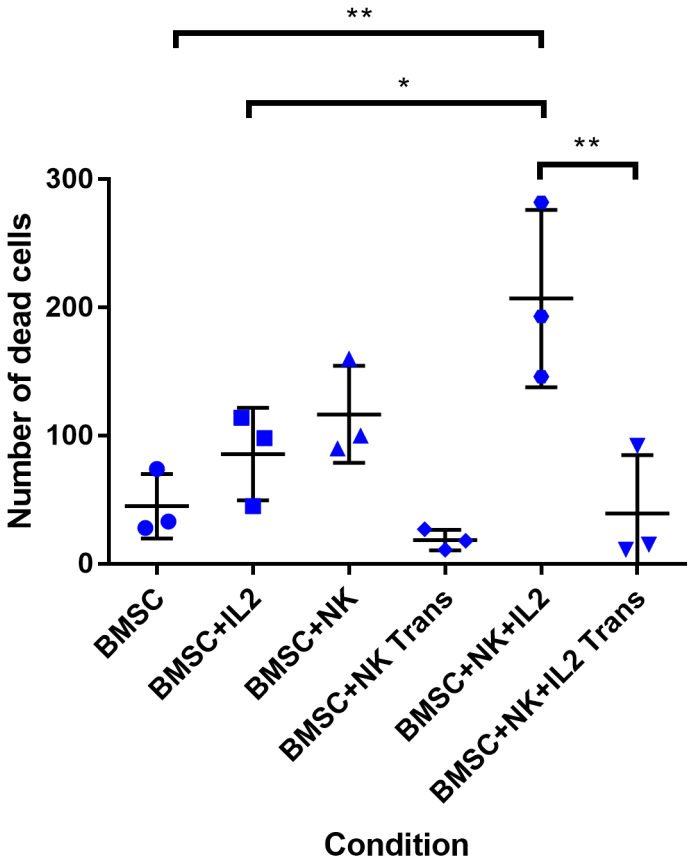

Fig. 5.14 NK cells kill hBMSC in a cell contact dependant manner

hBMSC were co-cultured with NK cells, with or without IL-2 stimulation. Co-cultures were at 1:5 hBMSC : NK cell and were either direct cell-cell (juxtacrine) or with NK cells seeded into a Boyden chamber with 0.4 µm pore size above hBMSC (paracrine). BMSC: BMSC alone, no cytokines or NK cells, BMSC + IL-2: BMSC alone with IL-2, no NK cells, BMSC + NK: BMSC with no cytokines in juxtacrine culture with NK cells, glsBMSC + NK Trans: BMSC with no cytokines in paracrine culture with NK cells, BMSC + NK + IL-2: BMSC with IL-2 in juxtacrine culture with NK cells, BMSC + NK + IL-2 Trans: BMSC with IL-2 in paracrine culture with NK cells. Cultures were maintained for 7 days under hypoxic culture conditions. At the end of incubation, wells were treated with CellTox Green and the number of dying hBMSC nuclei quantified using ImageJ. Significance shown on chart, Two-way ANOVA with Tukey's post hoc test, $p < 0.01$. Error bars show standard deviation. $N = 3$.

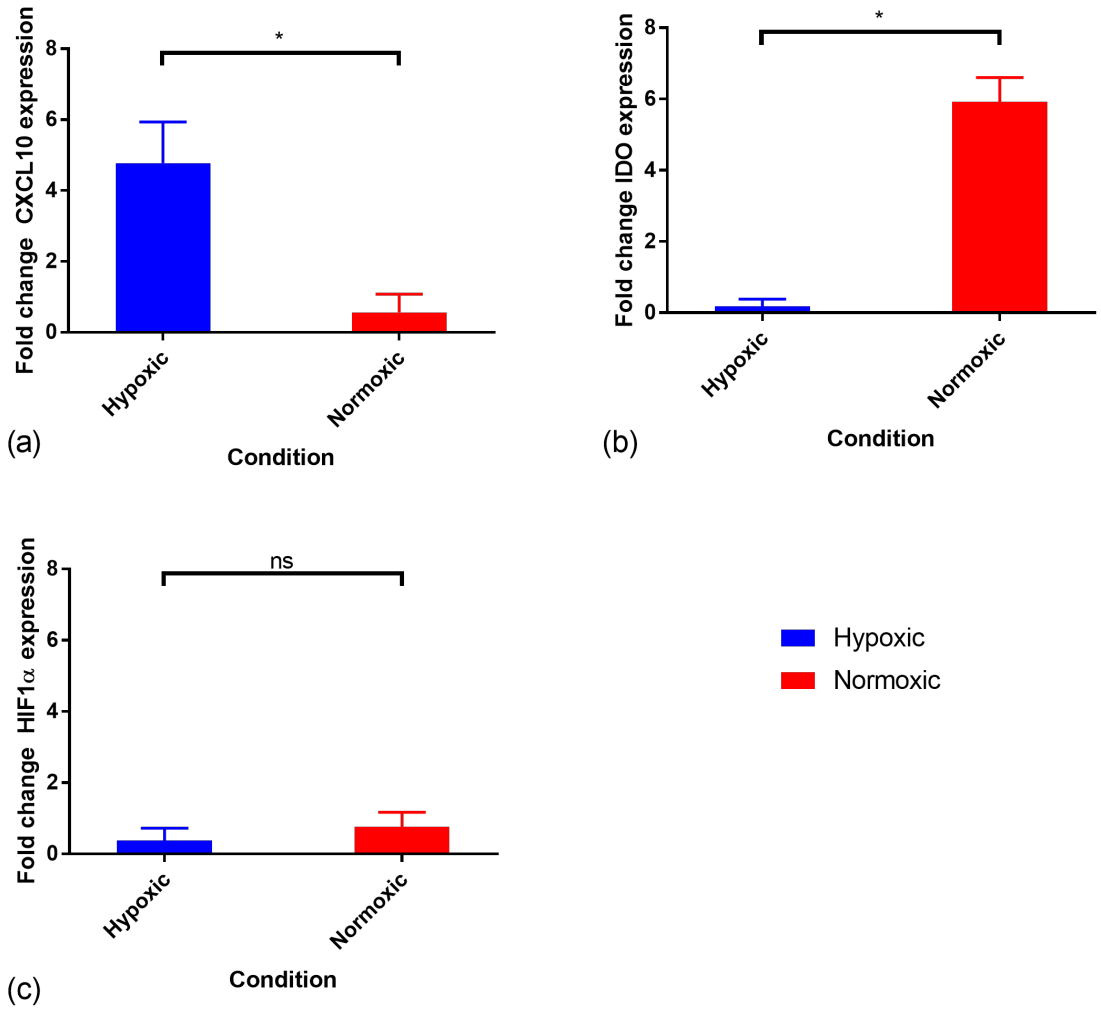

Fig. 5.15 Gene expression data for hBMSC – NK cell co-cultures stimulated with IL-2 in normoxic and hypoxic conditions

hBMSC were co-cultured with NK cells and IL-2 stimulation for 7 days in normoxic and hypoxic conditions. cDNA was prepared from the samples and RT-qPCR performed to investigate the expression of CXCL10 (fig. 5.15a), IDO (fig. 5.15b), and HIF1a (fig. 5.15c) in the co-cultures. Fold change relative to unstimulated cultures. Student's T-test, p values: $* < 0.05$. Error bars show compound standard deviation, as described in section 2.4.1 N = 3.

5.4 Discussion

NK cells are among the earliest infiltrating cell types into regions of trauma, and were shown to influence hBMSC migration under both normoxic and hypoxic conditions (chapter 4). It therefore follows that co-localisation of NK cells and hBMSC within the marrow clot is likely to occur early on in the repair process. At present, the implications of NK - hBMSC interactions following bone marrow stimulation are not fully explored. However, a study found that hBMSC were lost to tracing after 48 hours within the haematoma, indicating either migration away from the site of damage, or death of the hBMSC: it is possible that the hBMSC were lost as a result of NK cell activity (Bastian et al. 2016). Understanding the consequences of these interactions, and how they are influenced by NK cell number and oxygen level could indicate fundamental mechanisms governing the outcome of repair, as well as indicating potential therapeutic interventions.

The aim of this chapter was to understand how oxygen level and dose of NK cells influenced the behaviour and survival of hBMSC. Co-cultures of hBMSC and NK cells were set up, under normoxic (18.9 % oxygen) and hypoxic conditions (3 % oxygen), with varying IL-2 stimulation and NK cell ratios. These co-cultures were interrogated through visual inspection, CellTox Green (a fluorescent marker of cell death), real-time cell growth monitoring using the Xcelligence RTCA system, and gene expression by RT-qPCR. Paracrine (transwell / Boyden chamber) co-cultures were used to demonstrate the importance of direct cell-to-cell contact on NK cell mediated hBMSC cytotoxicity. As in described in earlier data presented in chapter 3, the hBMSC used in the co-cultures had been isolated and cultured under the corresponding experimental oxygen level, with allogeneic NK cells isolated from LRS cone buffy coats using NK specific negative MACS. This work demonstrated that NK cells had dose-dependent, saturable effects on hBMSC which were modified by IL-2 stimulation and oxygen level as summarised in tables 5.1 and 5.2.

Co-cultures of non-stimulated NK cells and hBMSC with low ratios (0.1 to 1 NK per hBMSC) showed similar behaviour in both normoxic and hypoxic conditions when studied using real time cell tracing, with the hBMSC continuing to proliferate following the inflexion point, albeit to a greater

Table 5.1 Summary of the effects of NK cells on hBMSC *in vitro* without IL-2.

		Oxygen Level	
		Hypoxic (3 %)	**Normoxic (18.9 %)**
Ratio of NK : hBMSC	Low[1]	Proliferate	Proliferate
	High[2]	No change	No change / Death

[1] 0.1 to 1 NK cell per hBMSC.
[2] 5 to 15 NK per hBMSC.

Table 5.2 Summary of the effects of NK cells on hBMSC *in vitro* with IL-2.

		Oxygen Level	
		Hypoxic (3 %)	**Normoxic (18.9 %)**
Ratio of NK : hBMSC	Low[1]	Proliferate	No change
	High[2]	Death	Death

[1] 0.1 to 1 NK cell per hBMSC.
[2] 5 to 15 NK per hBMSC.

extent in the hypoxic condition. This would agree with the previous observation (chapter 3) that hBMSC isolated and cultured under hypoxic conditions have a greater proliferation rate than those in normoxic conditions. Other studies have shown that hBMSC are able to suppress the proliferation of resting NK cells and hBMSC lysis when co-cultured at up to 20 resting NK cells per hBMSC under normoxic conditions, contradicting the results of my work in the real time system at high ratios (Rasmusson et al. 2003; Sotiropoulou et al. 2006; Spaggiari et al. 2006). However, these studies all used hBMSC isolated from healthy young adult iliac crest, or healthy paediatric spinal marrow and, as discussed earlier (chapter 3), ageing has significant effects on the qualities of hBMSC. That being said, the co-cultures assessed visually do appear to agree with the work in the aforementioned studies, with minimal apparent effects being seen in either the non-stimulated normoxic co-cultures, or the non-stimulated hypoxic co-cultures, even at the higher ratios. However, visual assessment did not quantify the cell numbers, and it was noted that NK cell distribution across the wells was not even: NK cells were concentrated at the well edges, likely due to vortex effects on the non-adherent cells in the unstimulated co-cultures. As a result, hBMSC distribution may also have had variable distribution across the well base, which was not shown in the images. Due to this lack of quantification, the visual assessment was chiefly used to assess feasibility, the appropriate NK cell ratios, and identify possible outcomes prior to translation into the Xcelligence RTCA system.

While the effect of altering NK cell to hBMSC ratio on hBMSC behaviour has been studied under normoxic conditions, comparable work has not been done under hypoxic conditions. While not apparent in the non-stimulated co-cultures assessed visually, this was very clearly indicated in the real time cell tracing. Unstimulated co-cultures in hypoxic conditions showed cell growth following the inflexion point, regardless of the NK cell ratio used. However, in the normoxic conditions, the low ratios showed no growth and the highest ratios (10 or 15 NK per hBMSC) showed hBMSC death. Allogeneic co-cultures of hBMSC and NK cells in normoxic conditions in a study actually showed very low levels of lysis of hBMSC by resting NK cells, with around 5 % lysis being seen at ratios of 40 NK per hBMSC, significantly lower than values seen in my study, and possibly due again to the use of hBMSC from younger donors (Poggi et al. 2005). In both the normoxic and hypoxic condition, the traces from the low ratio co-cultures tracked with the solo hBMSC cultures, indicating

that the presence or lack or growth was due to the inherent properties of the hBMSC used and was not influenced by the NK cells. However, while the high ratios also did not influence hBMSC growth in the hypoxic conditions, clear differences could be seen between the high and low ratios in the normoxic condition. The 5 NK per hBMSC condition showed a growth plateau at a lower value, while the highest ratios showed decreases indicating hBMSC death. Further, the NK cells were found to be unable to result in a 50 % decrease in the area under the real time cell trace curve (AUC_{50}) in either normoxic or hypoxic conditions.

However, while the unstimulated hypoxic NK cell co-cultures showed no influence on the area under the real time cell trace curve at any ratio, the same system in the normoxic condition showed a definite change with ratios of 5 NK per hBMSC or higher. Although the high NK cell ratios never achieved an AUC_{50}, the 10 and 15 NK per hBMSC conditions approached this value. This showed that the unstimulated NK – hBMSC co-cultures in the normoxic condition had a dose-dependent effect, and may have had a quantifiable AUC_{50} if higher ratios than 15 NK per hBMSC had been used, but that hypoxic NK – hBMSC co-cultures were not dose dependent within this range. It is not possible to say whether higher NK cell ratios could have resulted in hBMSC lysis in the hypoxic co-culture based on this data.

There are three possible explanations for these results:

1. That NK cells are less cytotoxic under hypoxic conditions than normoxic conditions.
2. That hBMSC isolated under hypoxic conditions are more immunomodulatory than those isolated under normoxic conditions.
3. A combination of both factors.

Addressing the first point, one study has shown that resting NK cell cytotoxicity against multiple myeloma is decreased under anoxic (here pre-conditioning with 0 % oxygen) relative to normoxic conditions (Sarkar et al. 2013). When comparing co-culture of hypoxic pre-conditioned or normoxic hBMSC with unstimulated NK cells, no lysis was seen in the former, while normoxic hBMSC were lysed (W.-H. Huang et al. 2014). More generally, hypoxic conditions have been shown to influence NK cell cytotoxicity by downregulating receptors which result in activation of NK cell killing behaviour (W.-H. Huang et al. 2014; Loeffler et al. 1991). With regard to the second point, a study in mice has shown that implanted hypoxic murine hBMSC resulted in decreased NK cell accumulation in regions of damage compared to normoxic murine hBMSC (W.-H. Huang et al. 2014). Furthermore, the hypoxic murine hBMSC engraftment was improved compared to the normoxic hBMSC due to decreased NK cell mediated lysis. A similar study examining xenogenic hBMSC administration in a murine myocardial infarct model showed that hypoxic hBMSC not only decreased infiltrating NK cells in the region of the infarct, but also the number of NK cells in the spleen when compared to the results with normoxic hBMSC (Lipinksi and Epstein 2016). This would suggest that hypoxic

isolated and cultured hBMSC have potent immuno-modulatory capacity against NK cells even when implanted in a xenogenic in-vivo model, and support the greater immuno-modulatory potential seen in my allogeneic, in-vitro model. As a result, the third explanation is likely to be correct: a combination of reduced NK cell cytotoxicity and increased hBMSC immuno-modulatory ability when isolated and cultured under hypoxic conditions resulted in the decreased effects of unstimulated NK cells on the hBMSC.

The results for the IL-2 stimulated NK cells were very different. This was immediately apparent in the visually assessed co-cultures, where the NK cells had apparently become semi-adherent and therefore were more evenly distributed across the well base, and clear hBMSC death could be seen through the loss of the monolayer in both normoxic and hypoxic conditions, albeit on a dose-dependent basis. In both conditions, alterations in the hBMSC monolayer could be seen above 5 NK per hBMSC. The IL-2 stimulated co-cultures traced on the Xcelligence RTCA further supported this observation. Under both normoxic and hypoxic conditions, the low ratios of NK to hBMSC showed the same growth as the hBMSC cultured alone. Furthermore, the endpoints of these co-cultures were not different to the corresponding endpoints without IL-2 stimulation, indicating that neither the IL-2, nor the activated NK cells were influencing the hBMSC. The lack of IL-2 influence on the hBMSC contrasts with a previous study using human Adipose-Derived Stromal Cell (hADSC), supposedly functionally equivalent cells to hBMSC but derived from adipose tissue. This study showed that a lower level of IL-2 exposure for a shorter period of time than in my study triggered replicative senescence and decreased immuno-modulatory properties in the hADSC (Niu et al. 2015). However, while hADSC have similar functional properties to hBMSC, they are derived from a different tissue source, with a very different microenvironment particularly related to inflammatory status and as such may not be directly comparable.

Interestingly, IL-2 stimulation in the highest (10 and 15 NK per hBMSC) ratio co-cultures completely restored NK cell cytotoxicity in hypoxic conditions, with the end point and general trend of the real time trace being very similar to the normoxic condition. At 5 NK per hBMSC, the killing was complete in the normoxic condition, but incomplete in the hypoxic condition, which indicates that although NK cell cytotoxicity was induced in high ratios stimulated with IL-2, the hypoxic conditions still exerted an immuno-modulatory effect, either directly on the NK cells or via the hypoxic culture hBMSC. The restoration of hypoxic NK cell cytotoxicity with IL-2 treatment to similar levels to normoxic IL-2 stimulated NK cells has been seen before in studies on NK – multiple myeloma co-cultures (Sarkar et al. 2013). This study did not consider variable doses of NK cells, instead only using 20 NK cells per myeloma cell, nor did it consider hBMSC. However, the restoration of NK cell cytotoxicity upon IL-2 stimulation does support the results seen here in the highest ratio used in my study, 15 NK cells per hBMSC.

In work presented here, IL-2 stimulated NK cells exhibited an AUC_{50} when at a ratio of 4.98 NK cells per hBMSC in hypoxic conditions and 4.51 NK cells per hBMSC in normoxic conditions.

The slight difference in AUC_{50} could result from the immuno-modulatory effects of the hypoxic system. Previous studies have shown that IL-2 stimulation restores hypoxic NK cell cytotoxicity to near the level seen in normoxic cultures, which agrees with the results shown here (Sarkar et al. 2013). Interestingly, other studies have given different values for the ratio, albeit only in the normoxic condition. One study suggests the ratio is around 6 NK cells per hBMSC to cause 50 % lysis, while another, which used IL-15 stimulation, claimed that hBMSC inhibited NK cell lysis up to 10 NK cells per hBMSC, with the number causing 50 % lysis presumably somewhat higher (Sotiropoulou et al. 2006; Spaggiari et al. 2006). Once again, both studies used hBMSC from healthy paediatric spinal or healthy young adult iliac crest sources, indicating that hBMSC immunomodulation of NK cell cytotoxicity decreases with age, although the 10 NK per hBMSC value was from the adult patients. That particular study did use IL-15 to stimulate the NK cells, but was able to replicate the same result using IL-2, combined Interleukin 12 (IL-12) and IL-15, or combined IL-12 and IL-18 stimulation, showing that the cytokine(s) used to activate the NK cells did not appear to influence the result in that system (Sotiropoulou et al. 2006).

It is important to note that when NK cells were cultured alone, NK cells stimulated with IL-2 formed more and larger colonies in the hypoxic condition when compared to the normoxic condition. This would suggest that hypoxic conditions enhance NK cell proliferation independently of the influence on the NK cell cytotoxic effect. There is very little research on the in-vitro growth of NK cells under hypoxic conditions as the research has focussed instead on NK cell cytotoxicity, but one study claimed that NK cell proliferation was decreased 1000 times after 28 days at 1 % oxygen, compared to normoxic conditions (Ang et al. 2010). However, these NK cells were grown under more extreme hypoxia, 1 % compared to 3 % oxygen used in work presented here, for a longer period, 28 days compared to 7 days which may explain the difference. As previously noted, hypoxic culture of NK cells did not appear to influence their viability (Sarkar et al. 2013). The anti-proliferative effects of hypoxic hBMSC and hypoxic co-culture on NK cell proliferation have not been established, but normoxic co-cultures of up to 16 NK cells per hBMSC with IL-2 stimulation showed reduced NK cell proliferation (Spaggiari et al. 2006). This indicates that the observed cytotoxic effects are due to alterations in the activation state and degranulation of the NK cells present within the well, and not due to increasing numbers of NK cells resulting in greater levels of hBMSC lysis.

The killing of the hBMSC by the NK cells was cell-contact dependent and isolated to interacting cells, as demonstrated by Boyden chamber experiments. The cell death was therefore targeted and not a generalised response by the hBMSC to NK cell cytotoxic effects. This is in line with the literature which suggests that hBMSC - NK cell interactions require cell-to-cell contact (Smyth et al. 2005). Critically there was a significant difference between direct co-culture of hBMSC with IL-2 activated NK cells and indirect, paracrine co-culture of hBMSC with IL-2 activated NK cells in a Boyden chamber. The cultures of hBMSC alone treated with IL-2 did not show increased death compared to the untreated solo hBMSC cultures during the assay indicating that the cell death seen was a direct

result of activated NK cells killing hBMSC. This demonstrates that the IL-2-activated NK cells must have cell-cell contact with the hBMSC in order for killing to occur, and that paracrine signalling is not influencing hBMSC death. Further, this indicates that the cytotoxic effect on the hBMSC is a result of NK cell directed killing, rather than hBMSC death in response to NK cell death. The cell-contact dependant, target-specific cytotoxicity of NK cells is widely known, therefore the combination of results showing that the killing was specific and relied on cell-cell contact validated both the model and approach used in this study (Smyth et al. 2005).

NK cell mediated lysis of hBMSC became visible after between 23 to 50 hours, following the inflexion point on the real time cell traces from the Xcelligence. At this point, the traces began to decline, indicating that cell death was occurring. This timeframe aligns with the described timings after which transplanted hBMSC cease to be traceable when administered *in vivo* in some studies (S.-H. Li et al. 2009). As a result, it is possible that the loss of hBMSC following administration *in vivo* results at least in part from the action of NK cells within the region of trauma. This is supported by murine in-vivo studies which have found NK cell accumulation and activation in the damaged region following trauma is correlated with death of the grafted hBMSC (W.-H. Huang et al. 2014).

A further observation is the alteration of gene expression in the co-cultures under hypoxic and normoxic conditions when stimulated with IL-2. Opposite influences were seen in terms of CXCL10 and IDO transcript levels, with CXCL10 increasing in hypoxic co-cultures, and remaining unchanged in normoxic and the reverse being seen with IDO. On the other hand, no change in HIF-1α expression was seen in either condition. HIF-1α was chosen as it is the quintessential marker of cellular response to hypoxic conditions, being widely used as a marker of low-oxygen conditions, and was used here to examine responses to the hypoxic co-cultures (Komatsu and Hadjiargyrou 2004; Mills et al. 2009; Raheja et al. 2011).CXCL10 and IDO were selected for examination as together they act as a barometer of early inflammatory changes associated with responses to disease or injury, providing rapid, clear responses. Broadly speaking, CXCL10 is associated with pro-inflammatory and IDO with immuno-modulatory responses. Although changes in gene expression do not necessarily translate to changes in protein secretion, alterations in these genes could indicate a global shift towards a pro-inflammatory or immuno-modulatory phenotype. To extend this work, other inflammatory markers such as IFNγ, TNFα, IL-10, or IL-6 could be examined.

CXCL10, also called IP-10, has diverse roles in the pro-inflammatory response, including the recruitment of hBMSC (Anton et al. 2012). As the name suggests, it is a cytokine upregulated by release of IFNγ by cells in the region of damage, and is used as a key marker for disease severity and inflammatory status in infection, auto-immune disorders and wound repair (J. Li et al. 2017; Liu et al. 2011; Rees et al. 2015; Ridiandries et al. 2018). CXCL10 acts as a regulator of diverse pathways, including PI3K, cAMP kinase, and MAPK, mediating inflammation through recruitment, adhesion, and proliferation of cells. More to the point, the release of CXCL10/IP-10 by the was observed in the preceding chapter by the $CD45_{dep}CD31_{enr}$ (later characterised to be NK cells), indi-

cating that it is present in the system and therefore expression may be influenced by the co-culture (chapter 4).CXCL10 can be expressed by NK cells, but is more likely to be produced by hBMSC as a result of IFNγ secretion by activated NK cells (Croitoru-Lamoury et al. 2007; Fauriat et al. 2010; Keppel et al. 2015). CXCL10 is a potent cytokine, acting on multiple cell types including NK cells (Saudemont et al. 2005). In addition, hBMSC CXCL10 expression is regulated by interaction with immune cells, including macrophages and NK cells, leading to an hBMSC phenotype with increased migration, pro-angiogenic and pro-inflammatory properties (Anton et al. 2012; Y. Yu et al. 2016). However, studies in hADSC have shown that hypoxic conditions do not alter CXCL10 expression under cytokine stimulation, which does not explain the upregulation seen only in the hypoxic IL-2 stimulated co-cultures (Roemeling-Van Rhijn et al. 2013). A possible explanation is related to the role of NK cells and CXCL10 in tumour suppression. In-vivo models of tumour suppression have shown that CXCL10 secretion by transfected tumour cells, or engrafted hBMSC, can result in tumour regression through the recruitment of NK cells, due to their anti-tumour activity (Saudemont et al. 2005; Y. Yu et al. 2016). Early tumour development has many features in common with wound healing: formation of a fibrin clot, presence of stromal cells, inflammation, hypoxia, initiation of neo-angiogenesis and similarities in gene expression changes (Schäfer and Werner 2008).

The microenvironment within a tumour tends to be hypoxic, even compared to 'physoxia', the normal physiological oxygen level for a tissue. In normal tissues, aside from bone marrow, which, as discussed in the introduction, is profoundly hypoxic, oxygen levels tend to range from 3 to 7.4 %, while median tumour oxygen levels range from 0.3 to 4.2 % with most having below 2 % oxygen (McKeown 2014). Furthermore, NK cells themselves are known to selectively target undifferentiated, de-differentiated, or poorly differentiated stem and progenitor cells (Tseng et al. 2010). It is therefore possible that the different response to the IL-2 stimulation in the normoxic and hypoxic co-cultures was a result of an anti-tumour-like response caused by the hypoxic conditions. Due to the lack of alteration in HIF-1α expression in the hypoxic IL-2 stimulated co-cultures, it is reasonable to suggest the involvement of other pathways or down-stream post-transcriptional regulation of HIF-1α activity, which could perhaps be identified through RNA Sequencing (RNA-Seq) or Western blotting. In addition, other hypoxia-related genes with more direct responses could be interrogated, such as TNFα, VEGF, or MMP9 (Ohnishi et al. 2007). On the other hand, the CXCL10 upregulation could represent the induction of a pro-reparative phenotype in the hBMSC, potentially heralding the initiation of the pro-angiogenic response.

To contrast, co-cultures of NK cells and hBMSC with IL-2 stimulation in normoxic conditions showed an increase in IDO expression, which was unchanged in the hypoxic co-cultures. Similar to CXCL10, IDO is also upregulated by the release of IFNγ, although IDO itself is an enzyme. However, IDO has a marked immunosuppressive effect through its local degradation of tryptophan (Soliman et al. 2010; Thomas et al. 2007). This degradation of tryptophan in the region of inflammation results in decreased immune cell activation, either as a result of the decreased supply of a critical amino acid

for activation, or due to possible pro-apoptotic effects of the resulting break-down products (Moffett and Namboodiri 2003). Interestingly, IDO plays a key role in immune evasion during tumourigenesis to allow cancerous cells to 'hide' from the immune system (Soliman et al. 2010). It is possible that the hBMSC were producing IDO in response to the NK cell cytotoxic effects as a regulatory response to the cell lysis. IDO production by hBMSC is stimulated by IFNγ, among other cytokines (Roemeling-Van Rhijn et al. 2013). IFNγ can be secreted by NK cells, and is significantly upregulated by binding with hBMSC, in normoxic co-cultures (Poggi et al. 2005). It is possible that no IDO upregulation was seen in the hypoxic condition since expression was already maximal. The other possibility is that IFNγ secretion by NK cells is downregulated by hypoxic conditions. There is very little work on this, but one study using oligomycin treatment of NK cells, which approximates chemical hypoxia by inhibiting oxidative phosphorylation, showed that IFNγ synthesis following NK cell receptor activation was decreased in treated NK cells (Keppel et al. 2015). However, CXCL10 expression is dependent on IFNγ and so this is unlikely to be the sole mechanism. Further work on the cytokine profiles of NK cells in hypoxic conditions with or without stimulation with IL-2, or other cytokines, might demonstrate whether IFNγ secretion is altered by oxygen level. The lack of alteration in the HIF-1α expression following IL-2 stimulation again may not indicate no response to hypoxic conditions, but rather that the expression in the unstimulated co-cultures was already maximal and therefore no further increase was possible. It must be noted that this work solely examined the gene expression and not the transcription or secretion of these proteins. To truly understand the functional consequences of these changes, protein analysis is required.

A final finding from this work is a potential new characterisation marker for hBMSC. During the adhesion phase of the hBMSC on the Xcelligence, an adhesion trough was observed on the traces. This trough appears to be unique to hBMSC, and was remarkably consistent between all donors, as well as hypoxic and normoxic strains. The feature has been previously observed on normoxically cultured hBMSC, but not on those isolated under hypoxic conditions (Moniri et al. 2014). The initial peak in the Xcelligence traces and the trough appeared at approximately the same times on all hBMSC traces, regardless of donor, oxygen level, or indeed treatment with NK cells or IL-2. The initial peak value, minimal value and magnitude of the trough was also consistent. This feature has not been observed on Xcelligence traces of any other cell type, including astrocytes, lung carcinoma, HeLa, peripheral blood lymphoma, pancreatic cancer, embryonic stem cells, or embryonic stem cell / induced pluripotent stem cell-derived cardiomyocytes, suggesting that it could be used as a novel characterisation technique for hBMSC (Bio 2018; Moodley et al. 2011; Papke et al. 2016; Zhao et al. 2017).

5.4.1 Limitations of the study

Use of the Xcelligence further permitted real-time monitoring of hBMSC lysis by NK cells. The Xcelligence system records impedance of signal across the well base, and uses a function of the impedance ('Cell Index') to indicate changing coverage of the well base with cellular material. An increased Cell Index can therefore indicate increasing numbers of cells, increased cell size, or a combination of the two, with the inverse also being true. The concern was that a decreased cell index in the experiment might have been due to cells decreasing in size, or entering suspension rather than dying. However, other experiments performed in this chapter demonstrated that lysis was occurring in the hBMSC population. Decreased adhesion and hBMSC rounding may have been occurring during the lysis process, but this cannot be separated from the cell index change due to cell death. The output is qualitative only, and therefore only relative statements regarding numbers of cells remaining can be made. Further experiments could quantify this with complementary assays such as lactate dehydrogenase or Pico Green to give an absolute number of hBMSC in the well at specific time-points. A potential confounding factor was that IL-2-activated NK cells did show semi-adherence which could have altered the impedance. However, neither in this experiment, nor in a similar experiment using astrocytes and activated NK cells, was interference from the NK cells seen (Moodley et al. 2011). This particular study also supports the conclusions made here that the decreased cell index was due to NK cell mediated lysis.

A final consideration with the system was the presence of gold on the well base which was in contact with the adhered hBMSC. The gold was fixed to the well base, and hence transfer of material was expected to be negligible. While gold is considered biologically inert, gold nanoparticles have been observed to alter cell morphology in culture (Söderstjerna et al. 2013). However, gold films used as substrates appear to promote normal cell growth, viability, and morphology and so any influence from the basal gold electrodes was considered to have no influence on the results (Menti et al. 2016).

Co-cultures were not fed during the assay, in line with similar experiments performed using the Xcelligence, so the wells containing higher numbers of NK cells could have been influenced due to culture medium exhaustion. The decreased energetic requirements of cells in hypoxic culture conditions could explain the difference in the traces of different oxygen levels. However, there are several points against this. First is that visual inspection of the plates after the 7 day period did not show large variation in the colouration of medium, which retained a pink tint, across the different NK to hBMSC ratios indicating that the medium was not fully depleted. Secondly, increasing ratios of NK cells are known to have greater growth suppressive effects (Moodley et al. 2011). Further, the stratification of cell index relative to NK cell ratio was evident from approximately 50 to 60 hours and was relatively consistent thereafter with the trends established at this point being maintained. This early indication and trend stability argues against medium depletion being a factor, as this would be expected to be visible at a later timepoint.

A further limitation of this work, and many similar studies, could be that observed phenomena were due to the use of allogenic NK cells, rather than autologous. NK cells display self-tolerance in healthy individuals, preventing auto-aggression through interaction with Major Histocompatibility Complex (MHC) Class I and various other inhibitory receptors (Orr and Lanier 2010). It might be expected, therefore, that co-cultures of NK cells with autologous hBMSC would not show lysis due to the suppression of NK cell cytotoxicity by the regulatory receptors. However, this is not the case. In-vitro experiments using autologous and allogenic NK cell – hBMSC co-cultures showed that, when activated, NK cells had equal lytic ability against both autologous and allogenic hBMSC in normoxic conditions (Sotiropoulou et al. 2006; Spaggiari et al. 2006). A study examining NK responses to engraftment of murine hBMSC isolated from an inbred mouse strain and implanted into the same strain showed that the NK cells lysed the hBMSC (W.-H. Huang et al. 2014). Although not truly autologous, the use of inbred mouse strains where individuals are considered genetically identical suggests that NK cells lyse autologous hBMSC in-vivo.

Although the use of allogenic hBMSC and NK cells has been reported in previous studies, my study differs in the use of NK cells isolated from presumably younger, healthy donors, and hBMSC from aged donors with advanced OA. This difference in donor age and health status may have resulted in some of the observed differences seen between my results and other studies. As previously discussed (section 3.4), ageing influences hBMSC, reducing their proliferative and immuno-modulatory potential, among other features (Muschler et al. 2001; Stiehler et al. 2016). However, ageing also influences NK cells, resulting in decreased activity in addition the generalised dysregulation of innate immunity, leading to alterations in relative subpopulation prevalence and activation status, seen as ageing progresses (Hazeldine and Lord 2013; Shaw et al. 2013). As a result, the observed interactions between ‘elderly’ hBMSC and ‘young’ NK cells may differ from those seen where donors are age matched: it is possible that the ‘young’ NK cells have higher activity due to the age of the donor and the fact that the ‘elderly’ hBMSC have lost immuno-modulatory potential, leading to a more potent observed NK cell cytotoxic effect. The use of aged donors is uncommon, making comparable research scarce.

The IL-2 concentration used in this study was widely supported by other studies and selected due to its ability to activate NK cells in-vitro. However, the concentration may not be representative of the in-vivo concentration in a haematoma. Furthermore, a haematoma contains a complex mixture of cytokines as well as other NK cell activating factors, with both temporal and spatial variations in the composition. As previously discussed, IL-2 stimulation was found to have similar effects on NK cell activation as other single or combination cytokine treatments, such as combine IL-12 / IL-15 administration (Sotiropoulou et al. 2006) This drawback is not unique to this study.

5.4.2 Future Directions

While both autologous or allogenic NK cells have been shown to have similar effects on the hBMSC, the donor age and health status mismatch may alter the observed interactions. The wider research has used samples taken solely from young donors. Use of autologous samples from elderly donors would be ideal, but would have ethical and practical constraints: NK cells would need to be isolated between 14 to 28 days after hBMSC isolation to allow hBMSC adhesion and expansion. Donors would have therefore recently undergone a significant surgery, which may alter their immune status. Therefore, allogenic cultures could be used, although donor inclusion criteria would be challenging due to the prevalence of co-morbidities in elderly cohorts. In this instance, use of non-human tissue sources, such as inbred mice, would be preferable. Additionally, the replication of this work on hBMSC and NK cells isolated from young, healthy, human donors, where the hypoxic / normoxic comparison has not been done, would allow for autologous cell usage, as well as being in a more relevant population due to the suggested age at which bone marrow stimulation treatments might be employed.

The ratios of NK cells and the stimulation technique, IL-2, were derived from optimisation work and previous studies. However, the biological significance of these conditions is unknown. Use of an in-vivo model of bone marrow stimulation, or of early fracture haematoma samples from human donors would provide evidence of the prevalence of relevant cell types. This could be examined through techniques including immunohistochemistry or flow cytometry. Further, the cytokine profile of the haematoma could be identified. This could provide more biologically relevant stimulation methods, either through artificial addition of supplements to medium, or through addition of haematoma supernatants to co-cultures. Understanding how the hBMSC, NK cells, and their combination interact and react to these conditions could provide greater understanding of the functional consequences of the early haematoma microenvironment on repair outcome. Future work could focus more closely on the functional changes occurring within the hBMSC populations, including but not limited to markers of stress, senescence, differentiation or protein secretion. As an extended project, further elements of the haematoma microenvironment could be added to the model, such as decreased pH and a three dimensional (3D) substrate.

5.4.3 Summary

hBMSC isolated from elderly OA donors retain immuno-modulatory properties enabling them to regulate lysis by IL-2 activated NK cells in a dose-dependent manner. However, the AUC_{50} values were lower when compared to previously reported values obtained using hBMSC from young adults indicating a possible age-related loss of immuno-modulatory capacity *in vitro*. Further, culture under hypoxic conditions reduced NK cell-mediated hBMSC cytotoxicity in both unstimulated co-cultures, where no influence on hBMSC survival was seen at any ratio, and in stimulated co-cultures compared

to the normoxic conditions. The killing of hBMSC by NK cells was contact-dependent and targeted. Further, the co-cultures elicited very different gene expression profiles, demonstrating that hBMSC interactions with and responses to NK cells are strongly dependent on oxygen level.

Chapter 6

Examining the interactions between hBMSC and monocytes under normoxic and hypoxic conditions

6.1 Abstract

Aim: To characterise the interactions between monocytes and hBMSC under normoxic and hypoxic conditions.

Methods: Expression of Vascular Endothelial Growth Factor A (VEGF-a), SDF-1, and FGF-2 in co-cultures of hBMSC and monocytes were compared with that in monocytes stimulated down M1, M2a, and M2c macrophage lineage under normoxic and hypoxic conditions. Gene expression of key markers of monocyte differentiation were examined by flow cytometry for co-cultures in hypoxic and normoxic conditions. The tube forming stimulating activity of supernatants from normoxic and hypoxic condition hBMSC-monocyte co-cultures was assessed using a HUVEC tube forming assay. Finally, the chemotactic effects of monocytes in normoxic and hypoxic conditions were assessed by real-time migration assays.

Results: SDF-1, FGF-2, and VEGF-a expression were higher in normoxic compared to hypoxic conditions in the co-cultures, and most similar to the M2c differentiated macrophages. However, gene expression showed that a major subpopulation of the co-cultured monocytes in normoxic conditions was (CD209+)(CD16+)(CD163+), with a further subpopulation expressing CD80. Hypoxic conditions appeared to prevent development of this subpopulation. Supernatants from co-cultures under normoxic conditions resulted in increased tube forming activity in HUVECs compared to

control, while no change was seen in the hypoxic conditions. Finally, monocytes appeared to have a chemotactic effect on hBMSC in normoxia, and a more chemokinetic effect in hypoxic conditions.

Conclusion: The oxygen level used in hBMSC isolation and co-culture with monocytes has significant effects on the interaction between the cells. Interaction in normoxic conditions resulted in the development of an immunomodulatory macrophage-like population with pro-angiogenic properties, which was not seen in the hypoxic condition.

6.2 Introduction

Forty-eight hours after fracture occurs, monocytes are among the most numerous cell types within a haematoma (Könnecke et al. 2014; Pence and Woods 2014). These rapidly migrating cells, which comprise between 3 to 8 percent of circulating cells in a healthy adult, are key mediators of repair (Monie 2017). Monocytes mediate repair directly, through phagocytosis, antigen-presentation, and cytokine release, as well as through differentiation into macrophages and dendritic cells (Geissmann et al. 2010). Recent studies in the heart and liver have shown that monocytes / macrophages have an important regulatory role in the development and resolution of fibrosis, an ability of particular interest with regards to surgical bone marrow stimulation techniques, due to the prevalence of fibrocartilage within the repair tissue (Lech and Anders 2013; Pellicoro et al. 2014). The monocyte-derived effector cells, macrophages and dendritic cells, retain features of the monocyte (antigen-presentation, phagocytosis and cytokine release) while also having more specialised roles in repair. For example, monocytes are able differentiate into macrophages which can be polarised towards pro-inflammatory (M1, or classically activated) macrophages, or broadly anti-inflammatory (M2, or alternatively activated) macrophages, depending on the environment (Lech and Anders 2013; Wu et al. 2013). Generally speaking, M1 macrophages have greater phagocytic behaviour and are associated with clearance of debris and the anti-microbial response, while M2 macrophages are more secretory and are associated with the resolution of repair. The M1:M2 balance has profound consequences for repair; following fracture, a skew towards an M1 phenotype is detrimental to bone formation, since a delayed repair is ultimately less problematic than an infected wound, while an M2 skew enhances bone formation as a result of increased osteoblastogenesis (Gu et al. 2017; Lu et al. 2017; Pajarinen et al. 2018; Schlundt, El Khassawna, et al. 2018). Indeed, the increased osteoblastogenesis appears to result from cross-talk between monocytes / macrophages and hBMSC and is an example of one instance where monocytes / macrophages interact with hBMSC to bring about repair.

Interactions between monocytes / macrophages and hBMSC have been studied under normoxic conditions, but the understanding of interactions under hypoxic conditions is incomplete or has been performed using hBMSC isolated and cultured under normoxic conditions (Rosová et al. 2008). In the previous chapters, it was shown that the isolation conditions of the hBMSC have profound consequences for their behaviour, both in mono- and co-cultures. As a result, it was hypothesised that the oxygen conditions of the hBMSC-monocyte co-culture could be critical to the outcome of the interaction, resulting in altered phenotypes in both cell types. In this chapter, the influence of the co-culture on monocyte behaviour was interrogated first. This was examined by considering gene expression, cell surface markers, and functional outputs (angiogenesis) through RT-qPCR, flow cytometry, and tube forming assays. Finally, the chemotactic influence of monocytes on hypoxic and normoxic isolated and cultured hBMSC was explored to demonstrate physical association between the cell types.

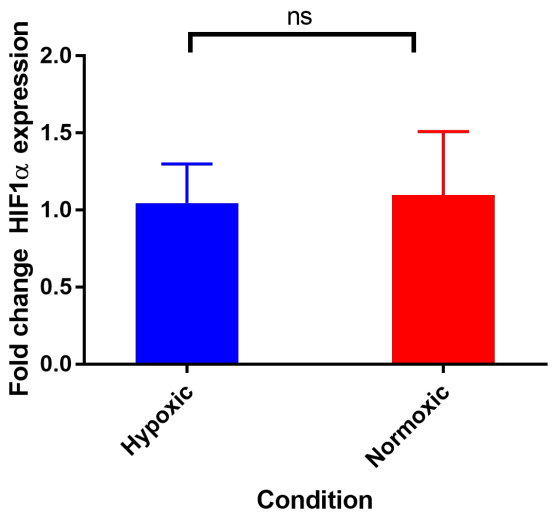

Fig. 6.1 Comparison of gene expression of HIF-1α by co-cultures of monocytes and hBMSC in normoxic and hypoxic culture conditions

Monocytes were isolated from PBMC using the Miltenyi MACS Pan Monocyte kit. Monocytes co-cultured with hBMSC for 7 days under normoxic or hypoxic culture conditions. After 7 days, cells were retrieved and expression of HIF-1α was measured using RT-qPCR. Fold change relative to unstimulated cultures. Student's T-test $p < 0.05$. Error bars show compound standard deviation, as described in section 2.4.1 $N = 3$.

6.3 Results

Monocytes are among the most rapidly infiltrating cell types in the early haematoma, and previous studies have shown that they are able to influence hBMSC migration. To characterise the consequences of hBMSC – monocyte interactions within the haematoma in more detail, monocytes were extracted from buffy coats and characterised by flow cytometry. An example of the population isolated can be found in fig. 4.10a. Co-cultures of monocytes and hBMSC were set up for 7 days under normoxic and hypoxic conditions, and changes in gene expression analysed using RT-qPCR. HIF-1α expression was not altered by co-culturing monocytes with hypoxic isolated hBMSC under hypoxic conditions, or with normoxic isolated hBMSC under normoxic conditions (fig. 6.1). However, the normoxic co-cultures showed significantly higher expression of both IL-6 (fig. 6.2a) and CXCL10 (fig. 6.2b) compared to the hypoxic co-cultures. Further, CXCL10 expression was not increased by co-culturing monocytes and hBMSC under hypoxic conditions, although IL-6 expression was increased. The relative increase in IL-6 expression was also higher than the increase in CXCL10 expression in the normoxic co-culture.

Differences in the expression of pro-angiogenic genes between normoxic and hypoxic co-cultures were also seen (fig. 6.3). Expression of FGF-2 (fig. 6.3a), SDF-1 (fig. 6.3b), and VEGF-a (fig. 6.3c) were all significantly higher in normoxic co-cultures compared to hypoxic. Expression of FGF-2 and

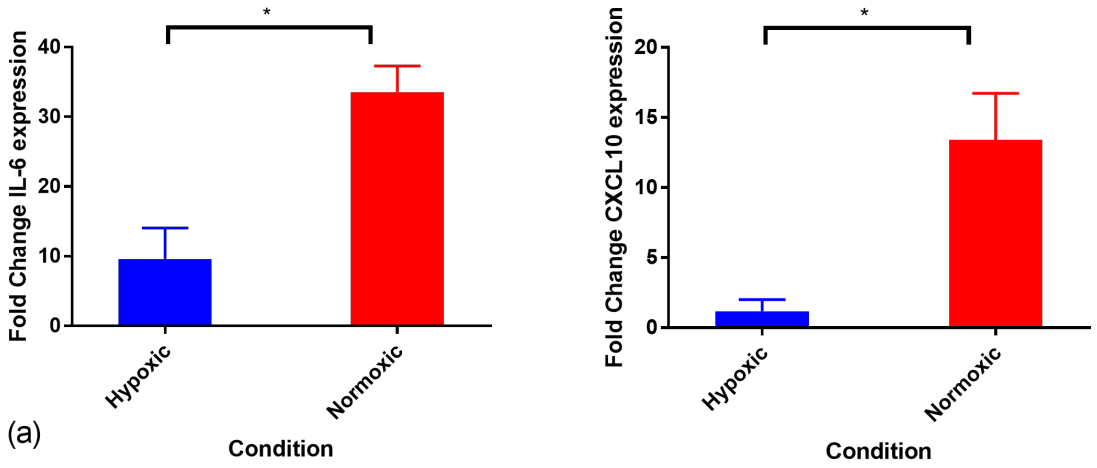

Fig. 6.2 Comparison of gene expression of IL-6 and CXCL10 by co-cultures of monocytes and hBMSC in normoxic and hypoxic culture conditions

Monocytes were isolated from PBMC using the Miltenyi MACS Pan Monocyte kit. Monocytes co-cultured with hBMSC for 7 days under normoxic or hypoxic culture conditions. After 7 days, cells were retrieved and expression of IL-6 (fig. 6.2a), and CXCL10 (fig. 6.2b) were measured using RT-qPCR. Fold change relative to unstimulated cultures. Student's T-test p values: $* < 0.05$. Error bars show compound standard deviation, as described in section 2.4.1 $N = 3$.

VEGF-a were increased in the hypoxic co-cultures relative to controls, but SDF-1 expression was not. As with IL-6 and CXCL10 expression, the fold change increase in expression maintained a similar ratio for FGF-2, SDF-1, and VEGF-a in both the normoxic and hypoxic co-cultures, with the greatest increase in FGF-2, followed by VEGF-a, and SDF-1 showing the lowest increase.

To aid the further characterisation of monocytes co-cultured with hBMSC, macrophage subtypes were produced from monocytes polarised into M1, M2a, and M2c subtypes using cytokine cocktails of GM-CSF + IFNγ + TNFα, M-CSF + IL-4, and M-CSF + IL-10 respectively under normoxic and hypoxic conditions. After monocyte differentiation the expression of the aforementioned pro-angiogenic genes FGF-2 (fig. 6.4a), SDF-1 (fig. 6.4b), and VEGF-a (fig. 6.4c) were measured using RT-qPCR. Under these conditions, the M2c polarised monocytes were the only subtype showing upregulation of these three genes. As in the co-cultures, the upregulation was highest in FGF-2, lowest in SDF-1 with VEGF-a being intermediary. However, unlike the co-cultures, the upregulation was higher in the hypoxic condition compared to the normoxic.

To explore the similarity between the pro-angiogenic gene expression signature of co-cultured monocytes and those differentiated with M-CSF + IL-10 in greater detail, monocytes were either differentiated with M-CSF + IL-10 or co-cultured with hBMSC for 7 days under normoxic or hypoxic culture conditions. A panel of surface antigen markers were used to characterise the monocytes

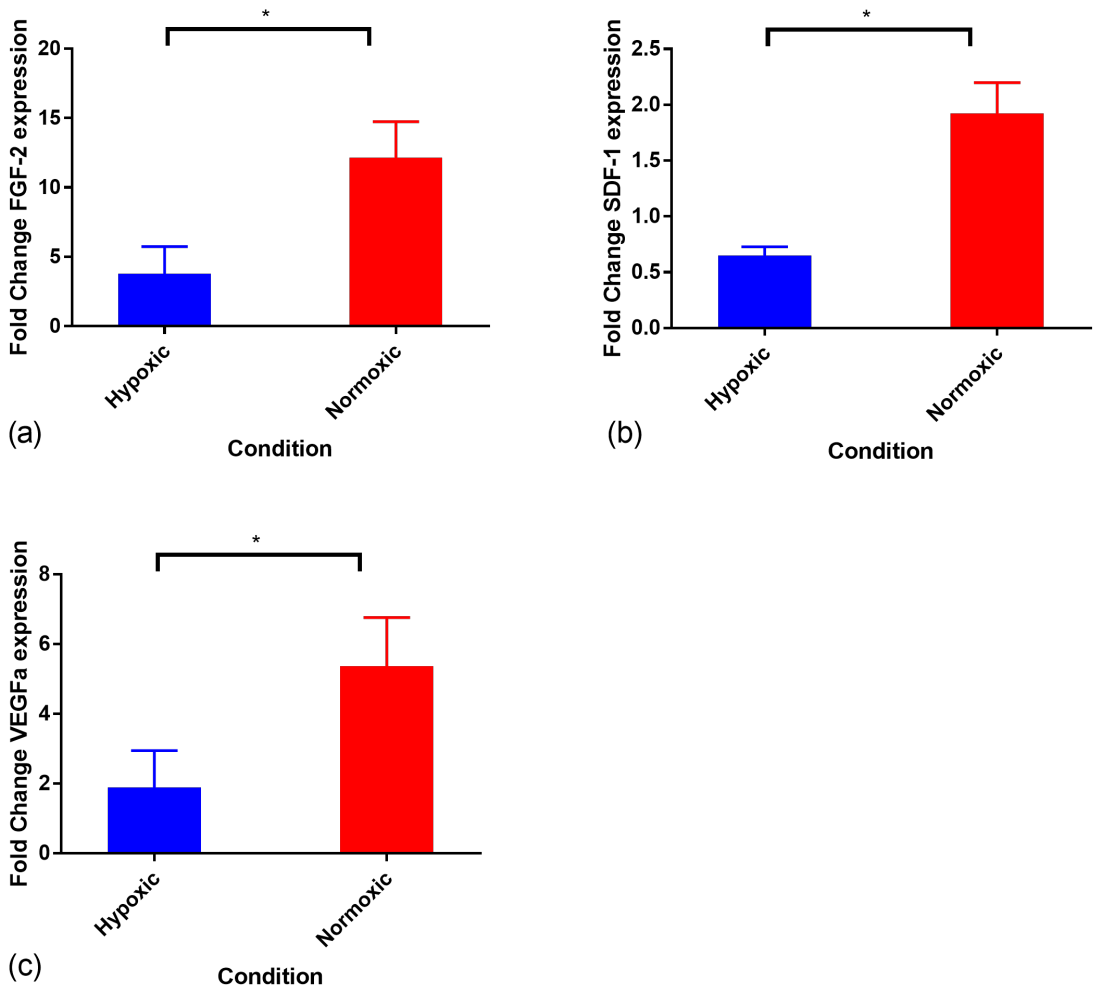

Fig. 6.3 Comparison of gene expression of FGF-2, SDF-1, and VEGF-a by co-cultures of monocytes and hBMSC in normoxic and hypoxic culture conditions

Monocytes were isolated from PBMC using the Miltenyi MACS Pan Monocyte kit. Monocytes co-cultured with hBMSC for 7 days under normoxic or hypoxic culture conditions. After 7 days, cells were retrieved and expression of FGF-2 (fig. 6.3a), SDF-1 (fig. 6.3b), and VEGF-a (fig. 6.3c) were measured using RT-qPCR. Fold change relative to unstimulated cultures. Student's T-test p values: $* < 0.05$. Error bars show compound standard deviation, as described in section 2.4.1. $N = 3$.

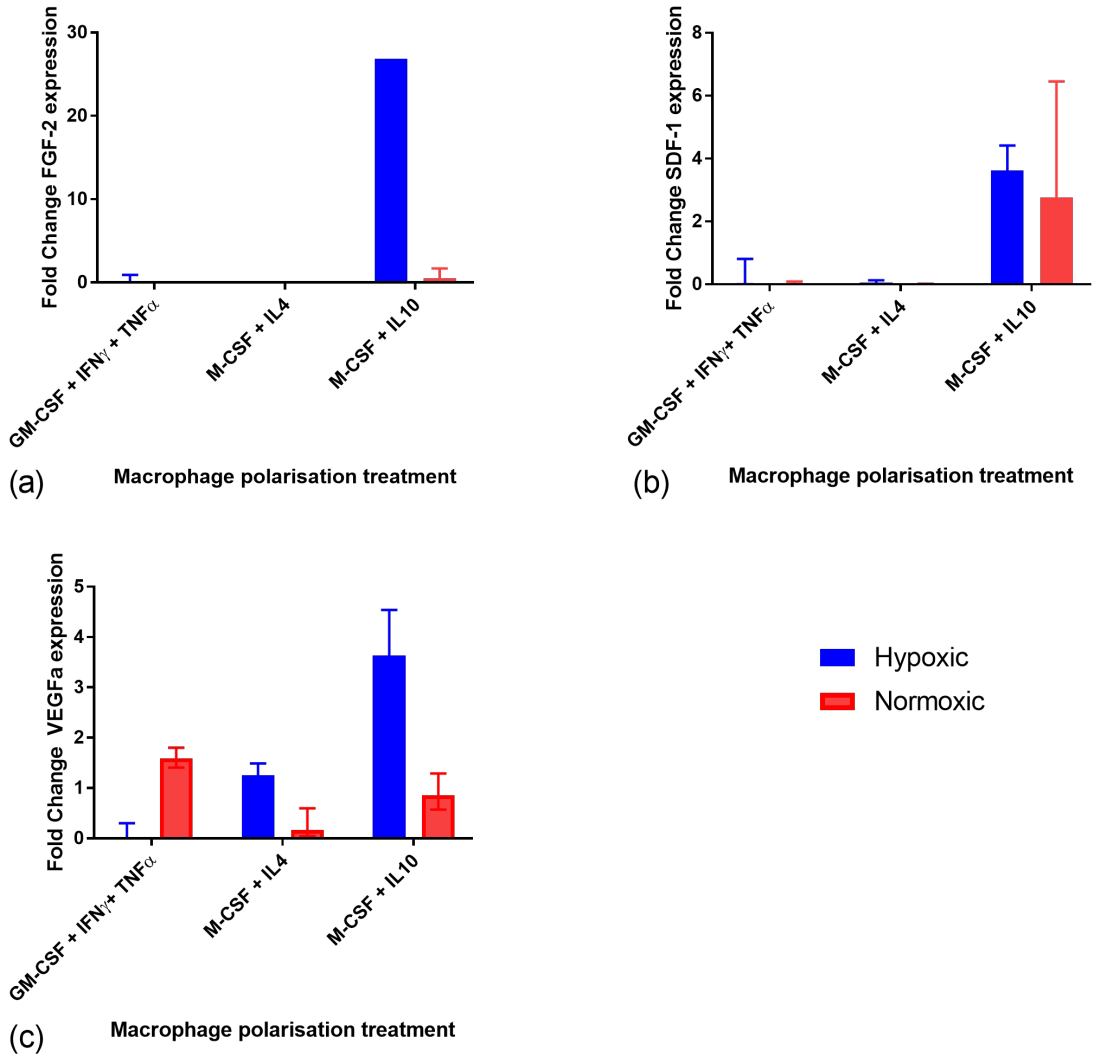

Fig. 6.4 Comparison of gene expression of FGF-2, SDF-1, and VEGF-a by monocytes differentiated using three different cytokine panels in normoxic and hypoxic culture conditions

Monocytes were isolated from PBMC using the Miltenyi MACS Pan Monocyte kit. Monocytes were either differentiated using either GM-CSF + IFNγ + TNFα, or M-CSF + IL-4, or M-CSF + IL-10 for 7 days under normoxic or hypoxic culture conditions. After 7 days, cells were retrieved and expression of FGF-2 (fig. 6.4a), SDF-1 (fig. 6.4b), and VEGF-a (fig. 5.4c) were measured using RT-qPCR. Fold change relative to unstimulated cultures. Error bars show compound standard deviation, as described in section 2.4.1 $N = 3$.

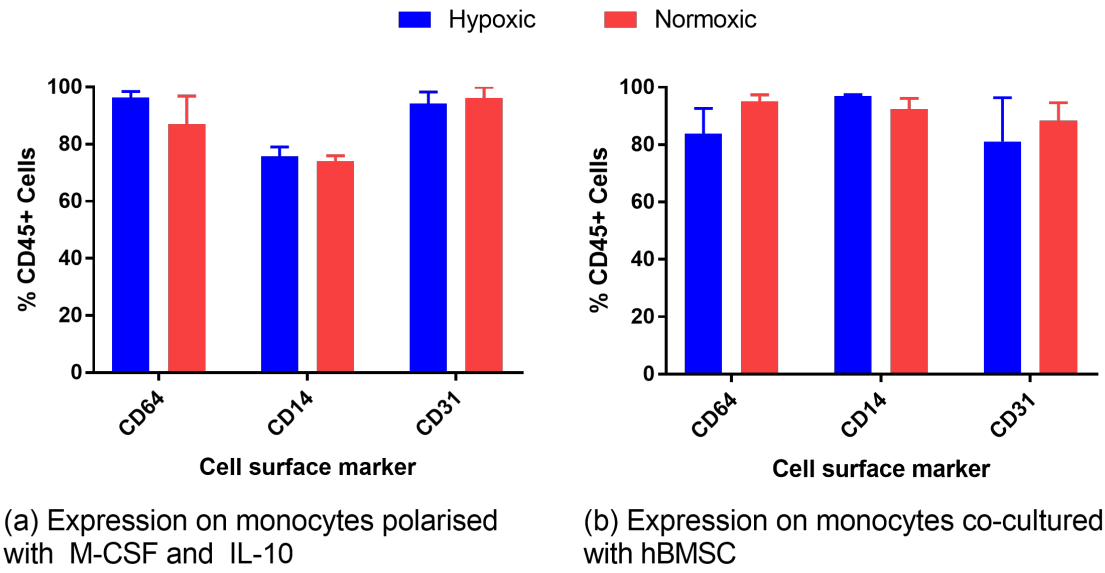

Fig. 6.5 Comparison of CD64, CD14, and CD31 marker expression on differentiated and co-cultured monocytes in normoxic and hypoxic culture conditions

Monocytes were isolated from PBMC using the Miltenyi MACS Pan Monocyte kit. Monocytes were either differentiated using M-CSF and IL-10 (fig. 6.5a, $N = 3$), or co-cultured with hBMSC (fig. 6.5b, $N = 4$) for 7 days under normoxic or hypoxic culture conditions. After 7 days, cells were retrieved and the CD45-positive fraction was characterised by flow cytometry for expression of CD64, CD14, CD31, CD200R, Tie2, CD11b, CD163, CD16, CD209, and CD80. No significance was found between normoxic and hypoxic pairs within a sample. CD14 expression was significantly different in both conditions between the differentiated cells and the co-culture (Multiple T-test, $p < 0.05$).

following the 7 day period. These markers were assessed by both single colour (figs. 6.5 to 6.7) and multiparametric (figs. 6.8 and 6.9) flow cytometer analysis.

Assessment of key monocyte markers CD64, CD14, and CD31 (fig. 6.5) showed that there was no difference between expression levels of any of the markers when cells were cultured under hypoxic or normoxic conditions for both the differentiated (fig. 6.5a) and co-cultured (fig. 6.5b) monocytes. Expression of CD64, and CD31 was the same in the differentiated and co-cultured monocytes. CD14 expression was higher in the co-culture condition in both hypoxic and normoxic conditions (fig. 6.5b) compared to the corresponding hypoxic and normoxic conditions for the differentiated monocytes (fig. 6.5a). Assessment of pro-inflammatory monocyte markers CD200R, CD11b, Tie2, and CD80 (fig. 6.6) showed that levels of markers were expressed at a low level in both differentiated (fig. 6.6a) and co-cultured monocytes (fig. 6.6b). There was no statistical difference between the levels of expression of CD200R, CD11b, or Tie2 in hypoxic and normoxic conditions for either differentiated or co-cultured monocytes, or between paired conditions as before. By contrast, CD80 was significantly higher in normoxic conditions than hypoxic in the co-culture condition, and both were higher in the co-culture than in the differentiated monocytes. The most striking differences were in the expression

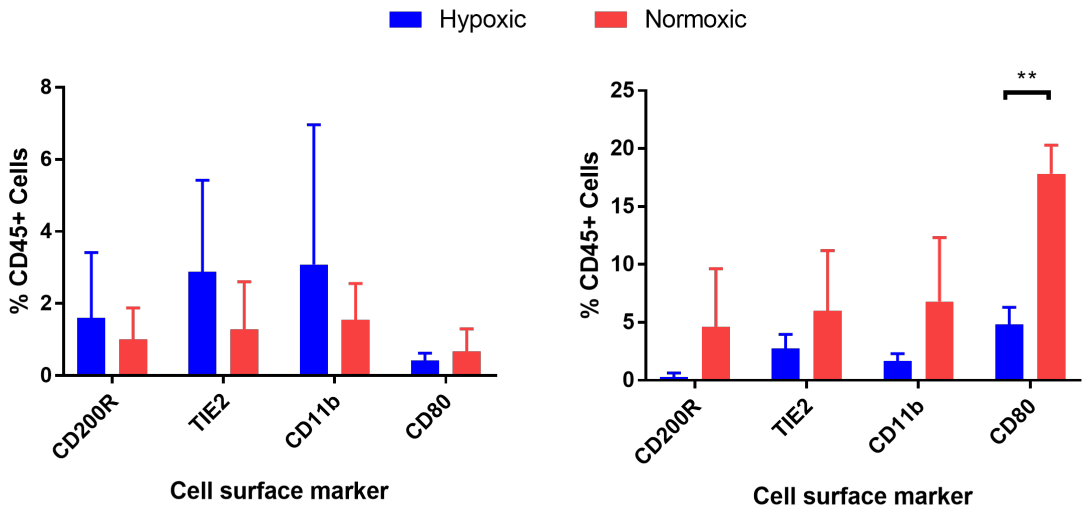

(a) Expression on monocytes polarised with M-CSF and IL-10

(b) Expression on monocytes co-cultured with hBMSC

Fig. 6.6 Comparison of CD200R, Tie2, CD11b, and CD80 marker expression on differentiated and co-cultured monocytes in normoxic and hypoxic culture conditions

Monocytes were isolated from PBMC using the Miltenyi MACS Pan Monocyte kit. Monocytes were either differentiated using M-CSF and IL-10 (fig. 6.6a $N = 3$), or co-cultured with hBMSC (fig. 6.6b $N = 4$) for 7 days under normoxic or hypoxic culture conditions. After 7 days, cells were retrieved and the CD45-positive fraction was characterised by flow cytometry for expression of CD64, CD14, CD31, CD200R, Tie2, CD11b, CD163, CD16, CD209, and CD80. No significance was found between normoxic and hypoxic pairs within a sample, or between conditions in the differentiated and co-culture samples for CD200R, TIE2 or CD11b. Expression of CD80 was significantly different between co-cultured, but not differentiated samples in hypoxic and normoxic conditions (Multiple T-test, p values: $** < 0.005$). Error bars show standard deviation.

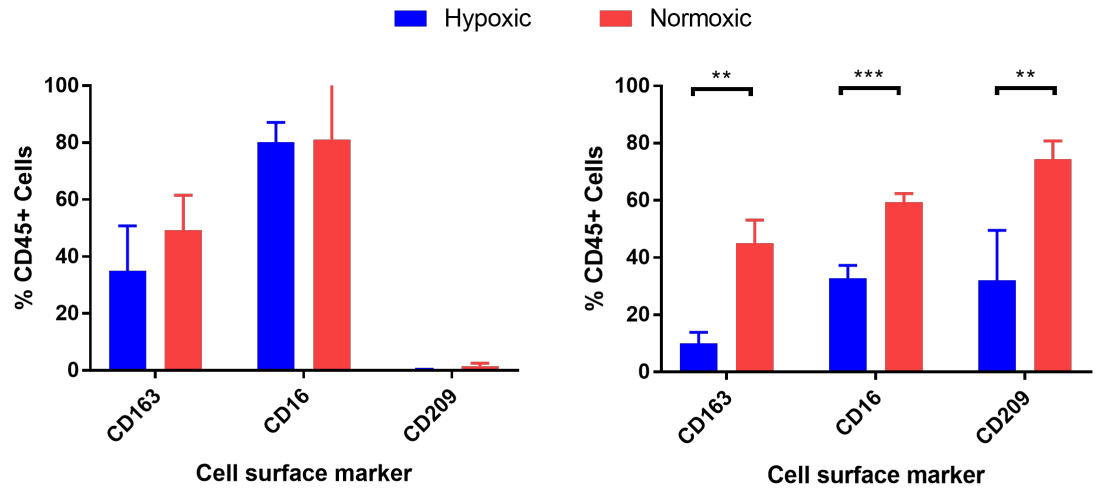

(a) Expression on monocytes polarised with M-CSF and IL-10

(b) Expression on monocytes co-cultured with hBMSC

Fig. 6.7 Comparison of CD163, CD16, and CD209 marker expression on differentiated and co-cultured monocytes in normoxic and hypoxic culture conditions

Monocytes were isolated from PBMC using the Miltenyi MACS Pan Monocyte kit. Monocytes were either differentiated using M-CSF and IL-10 (fig. 6.7a $N = 3$), or co-cultured with hBMSC for 7 days (fig. 6.7b $N = 4$) under normoxic or hypoxic culture conditions. After 7 days, cells were retrieved and the CD45-positive fraction was characterised by flow cytometry for expression of CD64, CD14, CD31, CD200R, Tie2, CD11b, CD163, CD16, CD209, and CD80. No significant difference was seen between expression levels in the differentiated samples. Expression of all markers was significantly different between the normoxic and hypoxic condition in the co-cultured samples. (Multiple T-test, p values: $** < 0.005$, $*** < 0.0005$). Error bars show standard deviation.

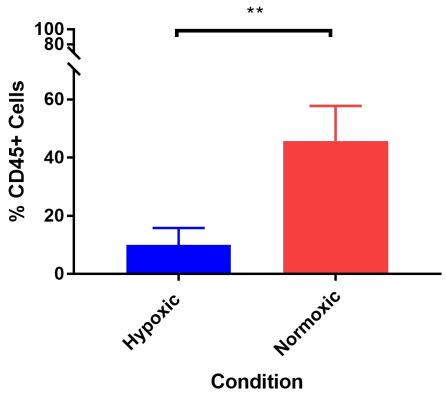

Fig. 6.8 Comparison of multiparametric marker expression of CD163, CD16, and CD209 on co-cultured monocytes in normoxic and hypoxic culture conditions

Monocytes were isolated from PBMC using the Miltenyi MACS Pan Monocyte kit. Monocytes were co-cultured with hBMSC for 7 days under normoxic or hypoxic culture conditions. After 7 days, cells were retrieved and the CD45-positive fraction was characterised by flow cytometry for expression of CD64, CD14, CD31, CD200R, Tie2, CD11b, CD163, CD16, CD209, and CD80. Multiparametric marker expression of CD163, CD16, and CD209 on monocytes co-cultured with hBMSC, $N = 4$. Significant difference between normoxic and hypoxic culture conditions (Student's T-test, p values: $** < 0.005$). Error bars show standard deviation.

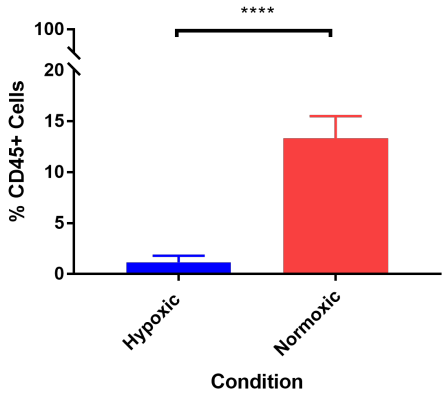

Fig. 6.9 Comparison of multiparametric marker expression of CD163, CD16, CD209, and CD80 on co-cultured monocytes in normoxic and hypoxic culture conditions

Monocytes were isolated from PBMC using the Miltenyi MACS Pan Monocyte kit. Monocytes were co-cultured with hBMSC for 7 days under normoxic or hypoxic culture conditions. After 7 days, cells were retrieved and the CD45-positive fraction was characterised by flow cytometry for expression of CD64, CD14, CD31, CD200R, Tie2, CD11b, CD163, CD16, CD209, and CD80. Multiparametric marker expression of CD163, CD16, CD209, and CD80 on monocytes co-cultured with hBMSC, $N = 4$. Significant difference between normoxic and hypoxic culture conditions (Student's T-test, p values: $**** < 0.0001$). Error bars show standard deviation.

of the more immunoregulatory markers CD163, CD16, and CD209 (fig. 6.7). CD209 was significantly upregulated in both conditions of the co-culture (fig. 6.7b), compared to their paired counterparts in the differentiated monocytes (fig. 6.7a). In the differentiated monocytes (fig. 6.7a), there were no difference between the hypoxic and normoxic condition. However, expression of CD163, CD16, and CD209 were all significantly higher in the normoxic condition than the hypoxic condition in the co-culture (fig. 6.7b). Multiparametric analysis of the data showed that CD163, CD16, and CD209 co-expression was present in over 40 % of co-cultured monocytes in normoxia (fig. 6.8). By contrast, fewer than 10 % of monocytes showed triple-positive co-expression in the hypoxic co-culture condition. Furthermore, around 13 % of co-cultured monocytes in the normoxic condition showed quadruple positive expression of CD163, CD16, CD209, and CD80 (fig. 6.8). As a result of increased pro-angiogenic gene expression and to assess the potential of the monocyte-hBMSC co-cultures to influence blood vessel formation, a tube forming assay was developed and performed. Tube formation assay optimisation was performed to determine the optimal seeding density of HUVECs, concentration of cytokines, and timepoint for endpoint analysis (data not shown). The optimal tube formation as assessed by number of master junctions / segments, mesh size, peak formation time and stability was found to be 1×10^6 HUVECs per ml with high concentration of VEGF-a, SDF, and FGF-2 after 12 hours. Filtered supernatants from one-week cultures of hBMSC or hBMSC and monocytes under normoxic or hypoxic conditions were applied to HUVEC monolayers grown on reduced growth factor basement membrane extract. Tube forming ability was assessed after 12 hours using the Gilles Carpentier Angiogenesis Analyzer (sic) plugin for Image J (fig. 6.10). Since the supernatants from hBMSC alone also induced tube formation activity, the data for hBMSC-monocyte co-cultures were normalised against the paired hBMSC alone data. The number of both master junctions (fig. 6.10a) and master segments (fig. 6.10b) was higher in normoxic conditions than in hypoxic conditions ($p < 0.05$). However, there was no difference between normoxic and hypoxic conditions in terms of total mesh area (fig. 6.10c) or number of extremities (fig. 6.10d).

To understand the influence of monocytes on hBMSC migration, monocytes were used in the Ibidi μ chemotaxis slides as chemotactic agents for hBMSC under both hypoxic and normoxic conditions. When endpoints of the traces corrected to a single origin point are examined, there is a clear difference in behaviour (fig. 6.11). hBMSC isolated and cultured under normoxia show a clear chemotactic response to monocytes with the endpoints tightly clustered towards the chamber containing monocytes (fig. 6.11a). On the other hand, hBMSC from the same patient isolated and cultured under hypoxic conditions have a scattered pattern of endpoints (fig. 6.11b). The majority of cells appear to have migrated towards the monocytes, but the clustering seen in the normoxic condition is not visible. The hypoxic hBMSC have also travelled further than the normoxic hBMSC; there are a large number of normoxic hBMSC clustered near the origin, while most hypoxic hBMSC have migrated away from the origin.

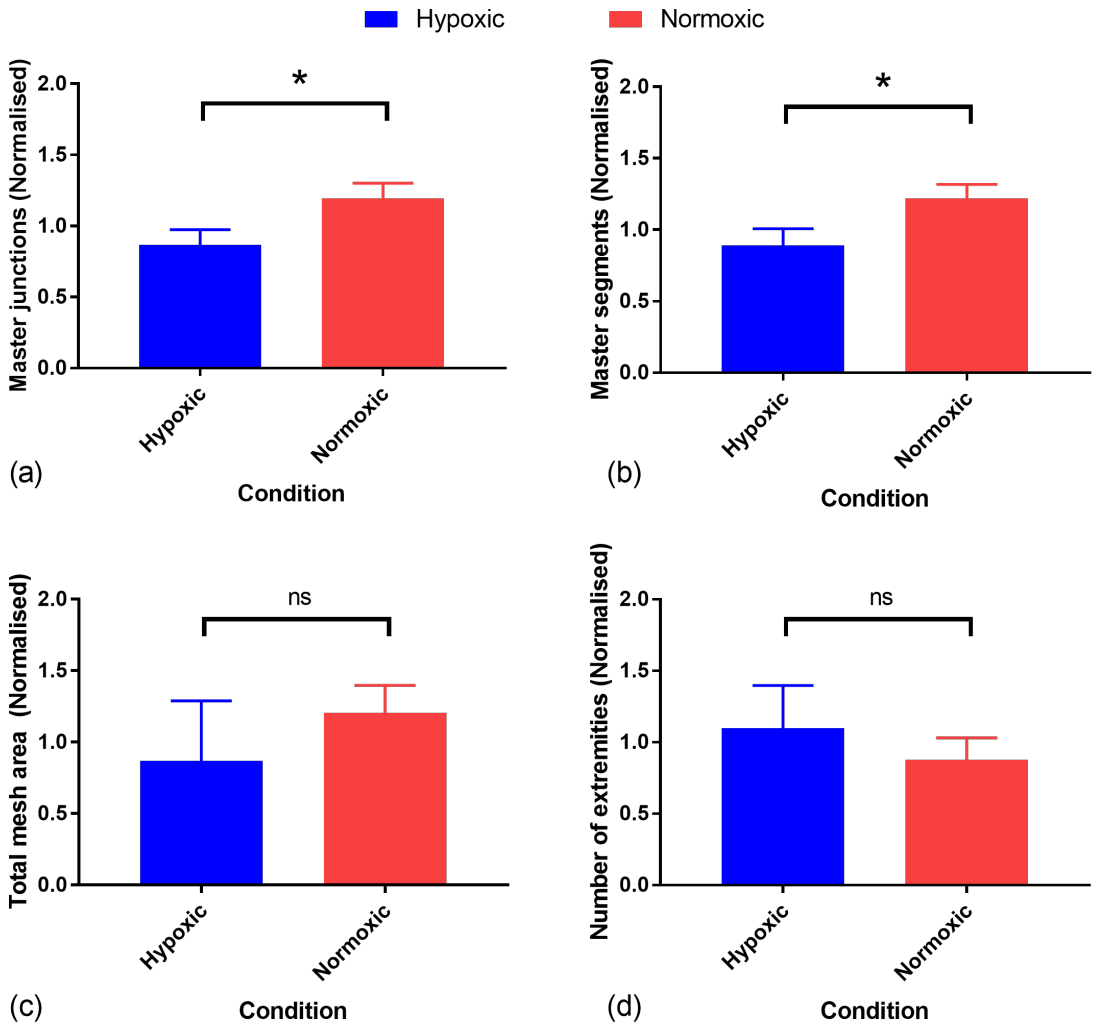

Fig. 6.10 Comparison of tube forming activity stimulated by hBMSC-monocyte co-culture supernatants from hypoxic or normoxic culture conditions

Monocytes were isolated from PBMC using the Miltenyi MACS Pan Monocyte kit. Monocytes co-cultured with hBMSC for 7 days under normoxic or hypoxic culture conditions. After 7 days, supernatants were removed and filtered through a 0.22 µm filter. Supernatants were applied to HUVECs on a BME substrate and incubated for 12 hours under normoxic conditions. Wells were imaged on a bright field microscope and analysed using the Angiogenesis Analyzer plugin for ImageJ. Readouts of the number of master junctions (fig. 6.10a), number of master segments (fig. 6.10b), total mesh area (fig. 6.10c), and number of extremities (fig. 6.10d) were taken. Results were normalised to hBMSC single culture supernatant tube forming ability. Student's T-test p values: $* < 0.05$. Error bars show standard deviation. $N = 3$.

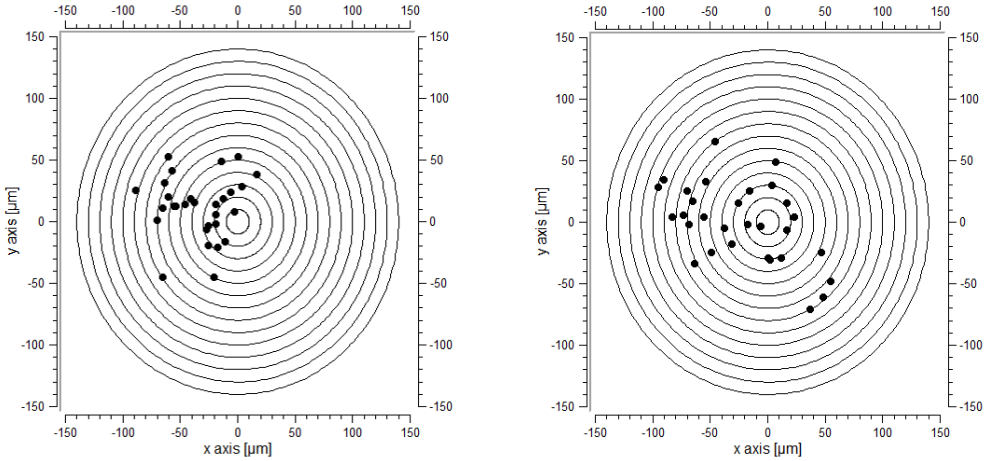

(a) Normoxic hBMSC with monocytes (b) Hypoxic hBMSC with monocytes

Fig. 6.11 Raw traces for hBMSC migrating in response to Pan monocyte isolated subpopulations in normoxic and hypoxic conditions

hBMSC isolated under normoxia or hypoxia were seeded into the central chamber of an Ibidi µ slide 3D. Pan Monocyte isolated PBMC were placed into a side chamber, creating a gradient of secreted factors across the hBMSC. Migration of 30 hBMSC was tracked for 16 hours using MTrackJ plugin for Image J and data analysed in Ibidi Chemotaxis tool. Dots show relative end points of cell movements from a normalized start point (0,0). Location of maximum concentration: (0,−300), minimum: (0,300).

Examining the dynamics of the population movement showed that there was no difference between the velocity of cells in normoxic or hypoxic conditions (fig. 6.12a). However, under hypoxic conditions cell migration was significantly more directed compared to that under normoxic conditions (fig. 6.12b). Further examination of the cell migration showed that the Centre of mass (CoM) of the hBMSC moved towards the monocytes under both the normoxic and hypoxic conditions (fig. 6.13a), with the CoM of both populations moving the same distance (fig. 6.13b).

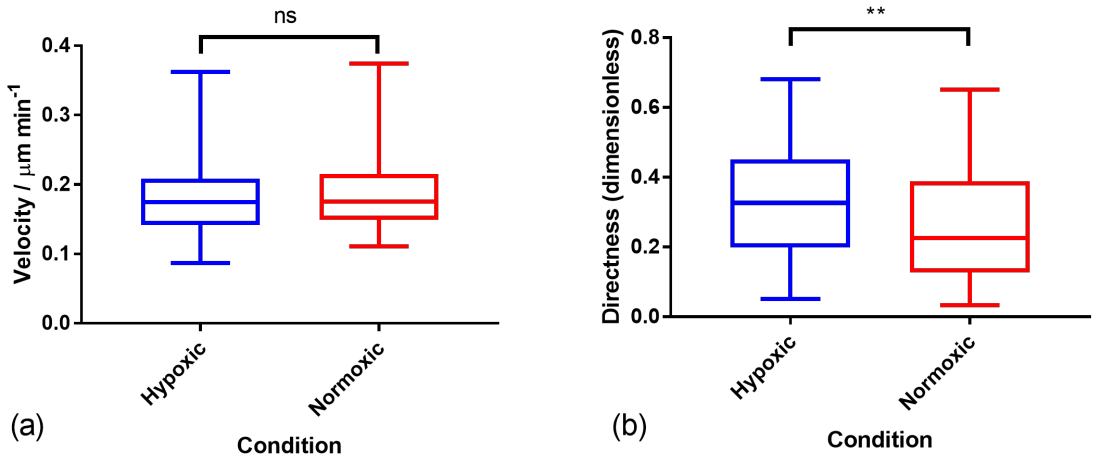

Fig. 6.12 Velocity and directness of hBMSC migrating in response to Pan monocyte isolated subpopulations in normoxic and hypoxic conditions

hBMSC isolated under normoxia or hypoxia were seeded into the central chamber of an Ibidi μ slide 3D. Pan Monocyte isolated PBMC were placed into a side chamber, creating a gradient of secreted factors across the hBMSC. Migration of 30 hBMSC was tracked for 16 hours using MTrackJ plugin for Image J and data analysed in Ibidi Chemotaxis tool. Velocity (fig. 6.12a) and directness (fig. 6.12b) of hBMSC migration was calculated for the hypoxic and normoxic condition. Significant difference between directness in normoxic and hypoxic culture conditions. Error bars show standard deviation. Two-way ANOVA with Tukey's post hoc test, p values: $** < 0.005$. $N = 3$, 30 tracks per replicate.

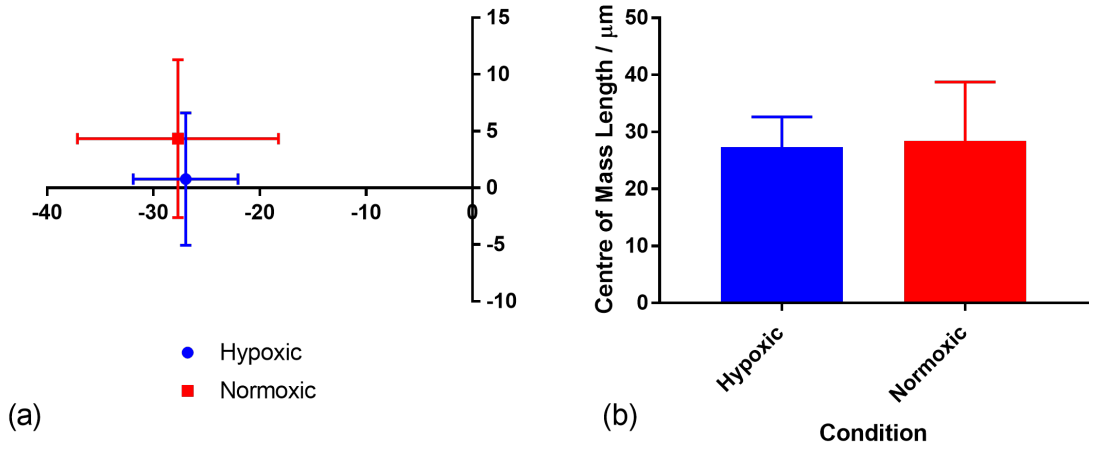

Fig. 6.13 Centre of mass plots of hBMSC migrating in response to Pan monocyte isolated subpopulations in normoxic and hypoxic conditions

hBMSC isolated under normoxia or hypoxia were seeded into the central chamber of an Ibidi µ slide 3D. Pan Monocyte isolated PBMC were placed into a side chamber, creating a gradient of secreted factors across the hBMSC. Migration of 30 hBMSC was tracked for 16 hours using MTrackJ plugin for Image J and data analysed in Ibidi Chemotaxis tool. Centre of mass direction (fig. 6.13a) and centre of mass length (fig. 6.13b) were calculated using the Ibidi Chemotaxis tool. No statistical differences, Student's T-test ($p < 0.05$). $N = 3$. Error bars show standard deviation.

6.4 Discussion

Monocytes are a common cell type in the peripheral blood and accumulate in regions of trauma. They are known to have bi-directional interactions with hBMSC, although the consequences of these interactions in hypoxic conditions have not been completely explored. Greater understanding of how the interactions between monocytes and hBMSC are modified by oxygen level could aid understanding of spatio-temporal regulation of wound healing. Furthermore, there is evidence that monocytes are capable of modifying NK cell cytotoxicity against hBMSC (Jewett et al. 2010).

The aim of this chapter was to characterise how interactions occurring between monocytes and hBMSC were influenced by oxygen level. Initially, the influence of the co-culture on the global behaviour of the co-cultures was examined, followed by more detail work focused on the monocytes. Monocyte-hBMSC co-cultures were set up under normoxic (18.9 % oxygen), and hypoxic (3 % oxygen) conditions. The outcomes of interactions were measured through gene expression, by RT-qPCR, flow cytometry examining cell surface markers, tube forming angiogenesis assays, and real-time migration tracking. As a result, data presented here shows that co-cultures of monocytes and hBMSC exhibit more pro-angiogenic and pro-inflammatory effects under normoxic conditions, compared to hypoxic conditions. This alteration was attributed to monocyte to macrophage differentiation and polarisation within the co-cultures: co-culturing monocytes with hBMSC is known to polarise monocytes towards differentiation into macrophages of the M2 lineage, which are more reparative and pro-angiogenic (Melief et al. 2013; Vasandan et al. 2016). However, this finding was unexpected, since the wider consensus is that both monocytes and hBMSCs are more pro-angiogenic in hypoxic as opposed to normoxic conditions (H. Ding et al. 2013; Jaipersad et al. 2014; Potier et al. 2007; Riboldi et al. 2013). Closer consideration of these hypoxic / normoxic comparison studies shows a critical difference: my study used hBMSC isolated and cultured under hypoxic conditions, while the other studies used hBMSC isolated and cultured under normoxic conditions which then underwent hypoxic preconditioning, or were placed into hypoxic conditions. As a result, the altered outcome of the co-culture in my study is likely attributable to the fundamental difference between the hypoxic and normoxic hBMSC strains. Throughout this thesis, the influence of sustained hypoxic culture dating from the time of isolation on hBMSC has been emphasised, and this finding is another indication of the importance of culture conditions from point of isolation on hBMSC phenotype and behaviour. Supporting the gene expression data was flow cytometry and tube forming data, which also showed a similar pattern, with the normoxic co-cultures having increased pro-angiogenic influences compared to the hypoxic. This was particularly apparent in the tube forming assay: although the hBMSC alone were capable of inducing tube formation, the co-cultures under normoxic conditions showed increased tube formation relative to hBMSC alone, while no change in tube forming capacity was seen in the hypoxic co-cultures. Both hBMSC monocultures, and hBMSC-monocyte co-cultures showed increased tube forming ability compared to monocyte-alone cultures. This increased tube forming ability in the normoxic co-cultures dovetails with the RT-qPCR finding of increased expression of

FGF-2, SDF-1, and VEGF-a in said conditions. However, this finding does not indicate whether the increased pro-angiogenic effects were a result of alterations in the monocytes, hBMSC, or both. Further work could use a CD45 MACS isolation process to separate the hBMSC and monocytes prior to RNA isolation, which would allow the individual contributions of cell type to FGF-2, SDF-1, and VEGF-a expression to be quantified. In addition, the gene expression of hBMSC and monocytes co-cultured in a paracrine system, such as Boyden chambers, under hypoxic and normoxic conditions could also be measured and compared to the direct co-cultures. A study has demonstrated that cell-to-cell interaction is important in polarisation of monocytes when co-cultured with hBMSC, although this work was only done under normoxic conditions (J. Kim and Hematti 2009).

One explanation for the difference in hypoxic and normoxic co-culture RT-qPCR data could have been that the control cultures for the RT-qPCR in hypoxic had higher baseline expression, and therefore while the fold change in secretion was smaller, overall secretion was higher. Examination of the raw data suggests that this was not the case — in fact, the control cultures in normoxic conditions had higher baseline secretion than the hypoxic condition, indicating that the absolute values were even more disparate. At face value, a stronger pro-angiogenic response in a damaged region experiencing hypoxic conditions makes sense; a hypoxic region lacks blood flow, and so vessel formation is required to restore circulation and permit gas and nutrient exchange. However, there are regions of the body such as the bone marrow, where hBMSC are situated, which are hypoxic in a healthy state (Hirao et al. 2006). A blanket pro-angiogenic response to hypoxia would therefore be problematic: further regulatory pathways must be involved. The hBMSC cultured under normoxic conditions may be more pro-angiogenic due to their adaptation to high oxygen levels so that, when placed into hypoxic conditions, they may attempt to compensate by stimulating angiogenesis to restore previous levels of oxygen. It is possible that the hBMSC in this study which were isolated and cultured under hypoxic culture conditions were more quiescent, better adapted to hypoxia, or simply less pro-angiogenic, than those isolated under normoxic conditions. A cross-over experiment, placing the normoxic isolated hBMSC into co-cultures in hypoxic conditions and vice versa might indicate whether this was the case.

Interestingly, the HIF-1α expression levels were unaltered in both the normoxic and hypoxic co-cultures. Consideration of the expression levels, rather than the fold change, showed that the HIF-1α expression was uniformly higher in the hypoxic condition, relative to the normoxic condition. Therefore, although the expression level was not altered by the co-culture, the basal expression was higher in the hypoxic condition. This indicated that the direct co-culture of the hBMSC and monocytes was not influencing the HIF-1α expression. However, gene expression data does not necessarily track to protein levels or activity within the cell. Further, in normoxic conditions HIF-1α degrades rapidly, but is stabilised under hypoxic conditions (Mills et al. 2009). As a result, the higher basal expression of HIF-1α combined with the stabilisation in the hypoxic condition may have led to a much greater HIF-1α protein level in said condition compared to the normoxic. This could be explored through

directly measuring the HIF-1α protein or its modification in the co-cultures via Western Blot or Enzyme-Linked Immunosorbent Assay (ELISA). However, the fact that there was no fold change attributable to the co-cultures in HIF-1α expression does suggest a level of regulation occurring in both conditions.

The IL-6 and CXCL10 expression levels were significantly elevated in normoxic co-cultures, while in the hypoxic co-culture, IL-6 was upregulated to a lesser extent than in normoxia, and CXCL10 was unaltered. Since my model considered only the expression in the cell mixtures, only global changes, rather than changes in the individual cell types, can be examined. There is conflict in the literature regarding how hBMSC-monocyte interactions influence the expression of IL-6 and CXCL10. Findings range from upregulation, through no change, to decreases in gene expression in both the monocytes and hBMSC (Anton et al. 2012; Laranjeira et al. 2015; Melief et al. 2013). However, where changes in expression were shown in these studies, the direction of the change was the same for both genes, which was also seen in my study. Increased IL-6 and CXCL10 secretion is associated with a pro-inflammatory phenotype, as well as increased migration in hBMSC, and with the development of pro-inflammatory M1 macrophage phenotype in monocytes (Anton et al. 2012; Lech and Anders 2013).

Observation of the co-cultures indicated that the monocytes were adhering to the plastic rather than remaining in suspension, indicating that the monocytes were differentiating. Co-culturing monocytes with hBMSC is known to induce differentiation of the monocytes into macrophages, and the pro-angiogenic effects seen could be attributable to a macrophage polarisation (Melief et al. 2013; Vasandan et al. 2016). The use of the macrophage polarisation model is somewhat controversial, since it implies that macrophages lack plasticity and have rigidly, clearly defined terminal differentiation states and, furthermore, is an *in vitro* model which has not necessarily been observed *in vivo*. Indeed, the number of macrophage polarisation subtypes increases with greater research, demonstrating that rather than discrete macrophage identities, there is most likely a continuum of macrophage phenotype and behaviour, with macrophages being able to move within the spectrum (Lech and Anders 2013; Martinez and S. Gordon 2014; Sudan et al. 2015). Despite these drawbacks, this model offers a tool to understand macrophage behaviour at a particular point during culture and allow comparisons between my work and that of other groups.

To further understand the influence of the co-cultures on the monocyte differentiation and macrophage polarisation, the co-cultured monocytes were characterised through comparison of cell surface marker expression, measured by flow cytometry, with that of monocytes differentiated into macrophage subtypes using cytokine mixtures. The chosen subtypes were M1 classically activated, M2a alternatively activated, and M2c immunosuppressive type macrophages (Iqbal and Kumar 2015; Lech and Anders 2013; Stöger et al. 2010; Sudan et al. 2015; L. Xie et al. 2017). The markers selected for comparison (CD64, CD14, CD31, CD200R, TIE2, CD11b, CD80, CD163, CD16, CD209) were chosen due to their common use in defining macrophage subtypes (table A.1). M2b Immunoregulatory-type

Macrophage (M2b) immunoregulatory subtype was not used, since the key activating compounds for this subtype, lipopolysaccharide and immune complexes, are more associated with pathogen responses rather than sterile inflammation as studied in this model. The M2c immunosuppressive macrophage subtype had the most similar pattern of expression to the co-cultures. To confirm this, monocytes driven down the M2c lineage using a cytokine mixture were compared to monocytes co-cultured with hBMSC under both normoxic and hypoxic conditions based on marker expression by flow cytometry. The results showed clearly that there was no difference in cell surface marker expression between monocytes driven to differentiate to the M2c subtype in normoxic or hypoxic culture conditions using cytokine mixtures. However, clear differences were seen between the monocytes co-cultured with hBMSC under normoxic and hypoxic conditions. The co-cultured monocytes were more heterogeneous than the M2c driven monocytes, but both the M2c driven and co-cultured monocytes showed CD14, CD16, and CD163 expression which would seem to indicate that the co-cultured monocytes had an M2c-like phenotype.

However, the biggest difference between the conditions was the expression of CD209 on the co-cultured monocytes compared to the M2c-driven monocytes; CD209 was relatively highly expressed in the co-cultured monocytes, particularly in the normoxic condition, with no expression in the M2c driven monocytes. CD209 was co-expressed with CD16, CD14, and CD163 in over 40 % of normoxic co-cultured monocytes, with fewer than 10 % of the hypoxic co-cultured monocytes showing the same expression pattern. A recent study showed that co-culturing macrophages with BMSC under hypoxic conditions inhibited M1 to M2 transition of macrophages, which supports the decreased expression of M2-like cell surface markers in my study (Faulknor et al. 2017). CD209, along with CD163, CD16 and high CD64, is expressed on a small subset of macrophages with high phagocytic ability and T cell modulation via antigen presentation, suggesting that the co-culture resulted in development of an immuno-modulatory phenotype (Park et al. 2016; Schenk et al. 2014). This subtype appears to be generated through stimulation with IL-1β, IL-15, or Toll Like Receptor 2 / 1 Ligand (TLR-2/-1L). CD209 is also known as Dendritic Cell-Specific Intercellular adhesion molecule-3-Grabbing Non-integrin (DC-SIGN) and was originally considered to be dendritic cell specific, although it has now been identified on multiple different macrophage types, albeit these are primarily at sites of inflammation, or tissue resident especially lymph node macrophages (Ochoa et al. 2008; Park et al. 2016; Schenk et al. 2014). This expression of CD209 in inflammatory conditions indicates that the co-culture in normoxic conditions might have been more stressed or pro-inflammatory than in the hypoxic condition. CD209 expression was not previously observed in co-cultures of monocytes and hBMSC under normoxic conditions (J. Kim and Hematti 2009). However, that particular study used monocytes isolated from whole blood by CD14-positive MACS. While this is commonly done, CD14 is an Lipopolysaccharide (LPS) receptor and monocytes are activated by CD14-LPS complexes (Landmann et al. 1998). LPS itself is used to polarise macrophages *in vitro* (Lech and Anders 2013). It is possible that the selection method in that study could result in pre-conditioning of the monocytes

due to binding of the selection antibody to CD14, while the monocytes used in this study were unlabelled, leading to the difference between the data.

Additionally, a subset of this (CD209+)(CD16+)(CD163+) population also expressed CD80. In both normoxic and hypoxic conditions, this comprised around one third of the (CD209+)(CD16+)(CD163+) cells. These cells were significantly more numerous in the normoxic condition and so the (CD80+) population was proportionately larger compared to the hypoxic condition. CD80 expression is associated with classically activated M1 type macrophages, and is considered a marker of pro-inflammatory macrophages (Lech and Anders 2013; Stöger et al. 2010). CD80, also known as B7-1, is a co-signalling molecule with roles in antigen presentation and T cell activation, similar to CD209 (L. Chen 2004; Park et al. 2016; Schenk et al. 2014). The co-expression of CD209, and CD163 suggest at a dendritic identity, which is further supported by the expression of CD80 by a subpopulation; CD80 expression is upregulated as DC mature (Collin et al. 2013). However, DC do not express CD16, and only a subpopulation of DC (interstitial DC) express CD14. The fact that the proportion of the (CD209+)(CD16+)(CD163+) population expressing CD80 was similar in normoxic and hypoxic conditions suggests that the same interactions were occurring between the hBMSC and monocytes in hypoxic and normoxic conditions, but this was weaker in the hypoxic condition, leading to lower levels of differentiation. Although the CD14/CD16 expression data would suggest at a macrophage identity, further work could use other more specific markers such as CD11c or CD103 for DCs to definitively identify the cell type derived from co-cultured monocytes (Merad et al. 2013).

The migration induced in hBMSC by monocytes was examined under normoxic and hypoxic conditions, to understand whether the populations would have the potential co-localise *in vivo*. This showed that while both monocytes induced migration in hBMSC under both hypoxic and normoxic conditions, the normoxic condition had a stronger chemotactic effect, with the hypoxic condition inducing more chemokinesis, as seen by the greater spread in the migration traces. That being said, the hypoxic traces showed greater directness than the normoxic traces. hBMSC migration has previously been shown to be reduced under hypoxic conditions (Raheja et al. 2011). However, this study used hBMSC which had been isolated from a juvenile donor under normoxic conditions, which were then placed into hypoxic conditions. As discussed previously, this may result in differences in the hBMSC population and correspondingly different behaviours during co-culture.

6.4.1 Limitations

Many of the limitations of this study have already been discussed in previous chapters: the use of allogenic cell sources, the use of elderly hBMSC, and the use of LRS cones have all been covered. In addition, the use of the mixed co-culture for RT-qPCR and lack of protein expression data have been previously discussed.

Like many studies, the tube forming assay was used to provide functional assessment of pro-angiogenic potential. This assay uses HUVECs which have high angiogenic potential and, if treated with pro-angiogenic factors when grown on a gel substrate, will form pseudocapillaries (W. Chen et al. 2018). This assay is widely used, provides quantifiable outputs, and is relatively simple, being a short assay and not requiring animal usage and, as a result, is often used to screen compounds for effects on angiogenesis. This method does have drawbacks: the capillaries formed are non-functional pseudocapillaries, the matrix is only formed in 2 dimensions, and the results may not represent *in vivo* processes. *In vivo* angiogenic assays, such as the chick chorioallantoic membrane assay or the mouse Matrigel plug angiogenesis assay provide more potentially biologically relevant data, but are more complex and less suited for screening or preliminary investigations (D. Xie et al. 2016). Furthermore, the assay used only supernatants from the co-cultures, rather than the cells themselves. Monocytes, for example, are known to support the formation of capillary networks (Dalton et al. 2014; Sidibe et al. 2018). As a result, some elements of the biology of the system have been neglected through the use of supernatants. However, three-cell tube forming systems are extremely rare in the literature due to the challenge in creating and interpreting them. This would be an ideal opportunity for a future study.

6.4.2 Future directions

Some future directions have already been suggested previously within this discussion, albeit mainly adding extra details to the existing work. The aforementioned extension of the tube forming assay work would be a key initial point for development of further work. In addition, performing the assays within a simulated pro-inflammatory environment through the addition of cytokines such as IFNγ, TNFα, or IL-1β, or through the addition of haematoma supernatant could indicate how these interactions were influenced not only by the oxygen level, but also the biochemical environment of the repair. Further, greater in-depth analysis of the hBMSC-monocyte interactions could be performed, perhaps tracking the exchange of microvesicles, mitochondria, or other cellular material, to demonstrate the vector by which the cells communicate when in direct co-culture.

Greater understanding of how monocytes and hBMSC interact within the haematoma following bone marrow stimulation could be obtained by extending the co-culture model. This could be done through addition of pro-inflammatory stimuli, as mentioned within chapter 5, which could include administration of cytokines such as IL-1β, IL-8, or TNFα, or haematoma supernatants (Gerstenfeld et al. 2003). In addition, a greater number of oxygen levels ranging from 1 to 18.9 % oxygen could be used to demonstrate the temporal changes in the oxygen content of a haematoma during the switch from the inflammatory to the re-vascularisation phase. This work could also be used as a prelude to development of a three-cell system to allow development of a more detailed *in vitro* model of trauma induced repair following bone marrow stimulation.

6.4.3 Summary

This study has shown that co-cultures of hBMSC and monocytes develop a pro-angiogenic, immuno-modulatory phenotype under normoxic conditions. However, this is inhibited in hypoxia, likely due to the hBMSC which had been isolated and cultured under hypoxic conditions. In this respect, this study is differentiated from other studies, which used hBMSC isolated under normoxic conditions and then exposed to hypoxia. This difference between the normoxic and hypoxic conditions could represent the temporal influence of oxygen on hBMSC-monocyte interactions during repair; in the early stages of repair, the haematoma lacks a blood supply and is profoundly hypoxic. As repair progresses, the damaged tissue surrounding the haematoma is re-vascularised and the oxygen level at the periphery increases, gradually invading the haematoma and creating an oxygen gradient. The inhibition of the pro-angiogenic, immuno-modulatory phenotype in the hypoxic conditions could represent a mechanism to ensure a controlled repair, by preventing suppression of the inflammatory response and angiogenesis until appropriate clearance and stabilisation of the wound had occurred, indicated by re-vascularisation of the periphery of the damaged site.

Chapter 7

Summary and Conclusion

7.1 Introduction

The aim of this body of work was to extend the present understanding of the consequences of interactions occurring between hBMSCs and PBMCs within the haematoma formed by surgical bone marrow stimulation techniques, as opposed to pharmacological stimulation, for example by Granulocyte Colony Stimulating Factor (G-CSF). To do this, hBMSC which had been isolated and cultured under normoxic and hypoxic conditions were characterised, with the normoxic strains representing the cell populations commonly used in other studies or therapeutically, and the hypoxic strains representing the endogenous hBMSC population. These cells were then used in parallel migration assays with subpopulations of PBMC isolated using sequential magnetic activated cell sorting to identify a population resulting in hBMSC migration. Characterisation of this population showed that it comprised a NK cell population. Co-cultures of NK cells and hBMSC under hypoxic and normoxic conditions showed that under hypoxic conditions, hBMSC were able to modulate the activity of NK cells to a greater degree than the same system under normoxic conditions. Co-cultures of hBMSC and monocytes showed that co-cultures exhibited pro-angiogenic and pro-inflammatory behaviour, attributed in part to monocyte-to-macrophage differentiation under normoxic conditions. This behaviour was significantly reduced under hypoxic conditions. hBMSC recruitment by monocytes was also influenced, with greater chemotaxis seen in the hBMSC under normoxic conditions. As a result, this work has explored some facets of PBMC-hBMSC interactions which are likely to occur within the haematoma formed following bone marrow stimulation techniques and has made novel contributions to the current understanding. This final discussion will summarise the key findings and outlooks for this work.

Table 7.1 Comparison of donor characteristics between this study and a sample of those in the wider literature. (*one study)

	My Work	Wider Literature
Donor Age	64 to 87 years	Paediatric* – 45 years
Donor Health Status	Advanced OA, unknown co-morbidity	Paediatric Spinal Scoliosis* Other: Healthy
Donation Site	Proximal tibial reamings	Paedeatric Spinal Marrow* Other: Iliac Crest

7.2 Key Findings

7.2.1 Donor characteristics and donation site alter hBMSC behaviour *in vitro*

Throughout this thesis, comparisons have been made between my work and that in the wider literature. A constant theme has been the differences seen between the results obtained using hBMSC isolated under normoxic conditions in this work and those in other studies. The key differences between the hBMSC used in the wider literature, and those used in my study, were the age, health status, and site of donation as outlined in table 7.1.

The normoxic hBMSC isolated in my study did show characteristics of hBMSC populations, including osteogenic, adipogenic, and chondrogenic differentiation, the ability to form colonies, and cell surface markers at abundances close to those specified by the ISCT (Dominici et al. 2006). However, the behaviour of the cells did show differences from those reported in the literature. Examples of this include the observation that the colony forming unit activity was significantly lower in the aged hBMSC compared to those from younger donors. Another example is the decreased ability of aged normoxic hBMSC to modulate killing by NK cells, either with or without activation, leading to greater hBMSC death. The immuno-modulatory ability of hBMSC reported in the literature was significantly higher than that seen in my studies (Poggi et al. 2005; Sotiropoulou et al. 2006; Spaggiari et al. 2006).

As a result, this work has shown that while hBMSC can be isolated from the tibia and femur of elderly donors with advanced OA, the hBMSC obtained have decreased proliferative and immuno-modulatory function (in terms of modulating NK cell activity). In addition, far fewer hBMSC were present in the marrow samples received due to the greater reversion of red marrow to yellow marrow in the appendicular compared to the axial skeleton. Although the number of variables present prevents identification of donor site, disease stage, or age as the principle cause of this shift, my work has shown that the hBMSC found within the osteoarthritic knee of elderly patients have lower proliferative and immuno-modulatory potential compared to those from the axial skeleton of younger, healthy donors.

This may provide some insight as to why bone marrow stimulation techniques lose effectiveness in elderly patients.

7.2.2 Isolation and culture of hBMSC under hypoxic conditions results in altered hBMSC phenotype and behaviour, and is different from hypoxic pre-exposure

The use of hypoxic-preconditioning, rather than permanent hypoxic culture, is widespread throughout the current literature. My work has shown that, in terms of hBMSC phenotype and behaviour, the two are not the same. The first indication of this was that hypoxic hBMSC did not shows osteogenic ability, and a preliminary study suggested that moving the cultures to normoxic conditions did not restore osteogenic ability. The colony formation ability of hBMSC was not higher in the hypoxic condition than the normoxic condition, although proliferation was higher in my study, contrasting with the literature which showed increased colony formation in hypoxic preconditioned hBMSC (Ang et al. 2010). In addition, studies using hypoxic preconditioned hBMSC showed that CD90 expression was decreased by hypoxic culture: my study showed the reverse, with CD90 expression higher in the hypoxic hBMSC compared to the normoxic (Adesida et al. 2012). Sustained hypoxic culture and hypoxic preconditioning appeared to result in different hBMSC populations, which may not be functionally equivalent. My work has shown that sustained hypoxic culture results in hBMSC with different phenotypes and behaviours compared to those exposed cells grown in normoxia and then moved to hypoxic conditions. One possibility for the observed variation between the populations may be due to different selection pressures placed upon the hBMSC during the initial adhesion and expansion phase. These observations also hold true for the hBMSC-PBMC co-cultures: as in the published studies discussed in chapter 4, chapter 5, chapter 6, PBMC were used fresh and isolated using similar methods, hence the differences between my work and the studies in the literature were unlikely to have arisen due to the PBMC. The hBMSC niche within the bone marrow is profoundly hypoxic, and so isolation under normoxic conditions would place oxidative stress on the cell population, selecting for a subpopulation with the greatest tolerance to stress. To contrast, hypoxic isolation conditions may more closely recreate niche conditions, which may range from 0.6 to 2.8 % oxygen, leading to a heterogenous population more like the resting, quiescent population (Spencer et al. 2014). This hypothesis is supported by the potent immuno-modulatory influence seen in direct co-cultures of hypoxic hBMSC and non-activated NK cells: no killing was seen, in contrast with normoxic hBMSC and non-activated NK cells where hBMSC death occurred. In fact, this finding would suggest that hBMSC should be isolated and cultured under hypoxic conditions and may have a distinctly different influence in regenerative therapies.

7.2.3 Isolation and culture of hBMSC under hypoxic conditions influences interactions with PBMC

Both direct and paracrine interactions between hBMSC and PBMC were modulated by the oxygen level of the system in a way consistent with events occurring during repair. The lack of non-activated NK cell killing of hBMSC under hypoxic conditions has already been attributed to the immunomodulatory abilities of resting hBMSC within their intact niche. The fact that increased oxygen levels or NK cell activation resulted in hBMSC lysis supports the niche hypothesis: these conditions would not be found within healthy, undamaged bone marrow and so are consistent with conditions and events occurring after trauma, where oxygen levels have been shown to increase from the physoxic 0.6 to 2.8 % as a result of bleeding from ruptured blood vessels (Spencer et al. 2014). In terms of recruitment by NK cells, hBMSC migrated more rapidly, but less directly in response to NK cells under hypoxic conditions compared to normoxic, meaning that a level of co-localisation would occur, and hence only a subpopulation of the hBMSC could co-localise with the NK cells. This partitioning of hBMSC and NK cells in the hypoxic environment may represent regulation of hBMSC immuno-modulatory activity, on the one hand providing a counter-regulatory mechanism to prevent over-suppression of the early inflammatory response by killing hBMSC, and on the other by enhancing expression of immuno-modulatory genes by hBMSC. Moreover, this reduction in hBMSC numbers could represent an anti-tumour-like response or indeed an anti-fibrotic mechanism to prevent excessive accumulation of hBMSC prior to establishment of the repair framework, which otherwise could have negative consequences for restoration of tissue structure and function. The response in normoxic conditions could represent the events occurring during haemostasis, but is more likely to show how NK cells respond to hBMSC under increased metabolic stress, supported by the increased expression of IDO, a cytokine associated with immune evasion, by the co-cultured hBMSC. This NK cell response in normoxic conditions is likely to be strongly related to their anti-tumour role, whereby NK cells preferentially target poorly differentiated or stressed progenitor cells (Tseng et al. 2010).

The monocyte-hBMSC co-cultures showed a similar difference between normoxic and hypoxic conditions. Under normoxic conditions, co-cultures had stronger pro-angiogenic ability and the monocytes within said co-cultures developed a pro-angiogenic, pro-inflammatory, and pro-migratory macrophage-like phenotype. Here again is a point where my research diverged from the literature: my studies found that the hypoxic co-cultures showed less pro-angiogenic ability and the monocyte-to-macrophage differentiation was significantly reduced, while other studies have shown that angiogenesis was enhanced in hBMSC-monocyte co-cultures in hypoxia. However, harking back to the hypoxic isolation versus pre-conditioning point, the difference is likely to be due to the isolation condition of the hBMSC. The hBMSC selected by normoxic isolation may have intrinsically higher pro-angiogenic potential, which was stimulated in the other studies by immediate introduction to an hypoxic environment. In my study, the hBMSC were isolated under an hypoxic environment and so lacked the stimulus of rapid introduction to hypoxia. The lack of HIF-1α upregulation in the hypoxic cultures does support

this fact. *In vivo*, the inhibition of angiogenesis stimulated by hBMSC – monocyte interactions under hypoxic conditions is logical: once again, the hBMSC niche in the bone marrow is hypoxic and so induction of angiogenesis under hypoxic conditions without further stimulation is undesirable. Perturbation of the system by damage would lead to stress, indicating the need for repair and hence stimulating angiogenesis. Moreover, oxygen levels rise as healing progresses as the haematoma / callus is connected to, and invaded by, the vasculature. The induction of a pro-angiogenic response by the rising oxygen level may stimulate monocytes / macrophages and hBMSC embedded within the haematoma to enable vascularisation in a controlled manner. Examination of osteochondral repair shows that repair occurs from the periphery towards the centre of the defect, supporting this hypothesis (Lydon et al. 2017). The stronger chemotaxis in hBMSC responding to monocytes seen under normoxic conditions may indicate a part of this response, as the two cell types co-localise to enable angiogenesis.

7.2.4 Oxygen level during isolation and culture of hBMSC may be a key regulator of immuno-modulatory behaviour and represent a mechanism for spatio-temporal control of healing.

The oxygen level that hBMSC are isolated, established and cultured under makes a significant difference to their interactions with PBMC. As discussed, my studies show multiple divergences with the literature in terms of said interactions, both when compared to those occurring under normoxic conditions and under hypoxic preconditioning. The use of continuous, sustained hypoxic conditions was the critical difference between my studies and those in the literature, and these findings represent a novel contribution to the literature. The paradigm suggested by these findings is as follows: co-cultures of hBMSC and PBMC under hypoxic conditions represent the early phase of healing, covering haemostasis and the initiation of the inflammatory and clearance phase. At this point, recruitment of immune populations is important, as is clearance of debris caused by trauma and the deposition of matrix to stabilise the region and provide a scaffold for later repair. During this phase, balanced immuno-modulation is required to ensure that the inflammatory response is proportionate to the injury. Additionally, uncoordinated osteogenesis and angiogenic activity are detrimental at this stage, due to the debris clearance and lack of structure in the wound. Therefore, under hypoxic conditions, angiogenic and osteogenic activity are curtailed, while interactions between hBMSC and NK cells result in increased hBMSC immuno-modulatory activity and death, and between hBMSC and monocytes significantly decrease the pro-angiogenic activity. Moreover, the hypoxic condition could also represent the endogenous bone marrow niche of the hBMSC, hence the greater immuno-modulatory behaviour particularly seen in the dramatic inhibition of NK cell mediated hBMSC death in the unactivated NK cell-hBMSC co-cultures.

On the other hand, the *in vitro* normoxic condition could represent a less metabolically restricted, more dynamic, later phase of healing such as vascularisation or remodelling of the haematoma, perhaps even extending into hard callus formation. In these conditions, osteogenesis and angiogenesis are enhanced and desirable to progress towards resolution, since initial debris clearance is complete and the provisional matrix laid down in the earlier repair phases is remodelled to provide a scaffold for the repair. In this environment, interactions between hBMSC and monocytes to produce a pro-angiogenic phenotype are upregulated. The increased NK cell mediated hBMSC death in the normoxic condition is likely to be related: while NK cell numbers decrease in the latter phases of repair, their role as anti-tumour cells means that they are likely to target poorly differentiated or stressed hBMSC to protect against adverse events.

Since a region of damage has an oxygen gradient, from profound hypoxia in the centre to increasing oxygen towards the periphery, it is reasonable to assume that the events outlined above will be occurring simultaneously in different regions of the repair. The oxygen gradient may well play a role in co-ordinating the different stages of repair occurring in each specific micro-environment, ensuring an orderly progression through the stages. Moreover, these hypoxic hBMSC appear to have greater immuno-modulatory potential, making them more suitable for regenerative therapies.

7.2.5 Use of hypoxic conditions may improve chondrogenic outcomes

With regards to the specific aim of MF/MD therapies, namely stimulating defect infill with hyaline cartilage via chondrogenesis, maintenance of the hBMSC under hypoxic conditions appears to be preferable to normoxic conditions, either within the wound or during *ex-vivo* culture for later exogenous administration of autologous hBMSC. The hBMSC isolated and cultured under hypoxic conditions appear to generate a more homogeneous cartilage matrix when stimulated down the chondrogenic pathway compared to those in normoxic conditions. Increased matrix homogeneity could indicate improved biomechanical properties and increase the longevity of the the regenerated cartilage. Furthermore, the hypoxic hBMSC show decreased osteogenesis when stimulated, which could mean a reduced risk of mineralisation occurring within the repair tissue.

In addition, the improved immuno-modulatory properties of the hypoxic hBMSC could be beneficial for chondrogenesis. To start with, the hypoxic hBMSC appear to be less susceptible to NK cell-mediated killing, and to stimulate a more immuno-modulatory, less pro-angiogenic phenotype in monocytes. If the 'cell replacement' paradigm of repair is considered, this could mean that the hypoxic hBMSC are less likely to be lost to the action of cytotoxic cell types, and therefore more are present to differentiate into chondrocytes and contribute to repair than the normoxic hBMSC. Alongside direct contribution through differentiation, the immuno-modulatory properties of the hBMSC could be important indirectly; excessive and uncontrolled pro-inflammatory response following trauma is associated with increased scarring. In the case of hyaline cartilage repair, this could take the form of a

repair tissue with a higher proportion of fibrocartilage as opposed to hyaline cartilage. The presence of a more immuno-modulatory cell type, such as hypoxic hBMSC, could increase the regulation of the immune response following surgery, thereby enabling and supporting chondrogenesis and leading to repair tissue which could be primarily hyaline cartilage rather than fibrocartilage scar tissue.

7.3 Barriers to translation

Although this work provides indications that use of hypoxic conditions may be beneficial, significant barriers to translation remain. These can be broken down into three main categories: regulatory, system or organisational, and individual.

7.3.1 Regulatory barriers

Use of hBMSC for regenerative medicine in the UK is regulated by the Medicines and Health Products Regulatory Authority (MHRA), and by other agencies elsewhere (MHRA 2015). As such, the data presented here are insufficient to support immediate clinical translation, for example the isolation and expansion of exogenous hBMSC under hypoxic as opposed to normoxic conditions. While the exact regulatory requirements to introduce such a claim are beyond the scope of this discussion, it is reasonable to believe that at minimum, greater safety and efficacy data would be requested, probably requiring further *in-vitro* and *in-vivo* testing. Should this be deemed satisfactory, clinical trials would be required prior to licensing, necessitating funding and organisation.

7.3.2 System or organisational barriers

Working under hypoxic conditions presents a range of logistical and safety challenges due to the very nature of hypoxia; the extreme reduction of oxygen levels. This requires specialist equipment, such as incubators and laminar flow hoods capable of maintaining an hypoxic environment, as well as gas supplies to provide the nitrogen used to generate the hypoxic environment. This may also necessitate expansion of laboratory space to provide room for the hypoxic equipment. In addition, hypoxic culture work presents health and safety challenges requiring specialist training and safety equipment, such as oxygen monitors. Although these challenges are surmountable, there is a significant up-front cost in terms of both time and resources related to the installation of facilities, as well as on-going costs related to gas supply, maintenance and safety inspections. Particularly with regards to the National Health Service (NHS), a cost-benefit analysis would have to demonstrate significant advantages to the use of these techniques prior to their adoption.

7.3.3 Individual barriers

Should the preceding barriers be cleared, specialist training and ways of working are required to ensure that the hypoxic conditions are maintained correctly during culture and processing. This would affect both the surgical team and any supporting laboratory staff, requiring changes in practice in both the theatre and the tissue culture facility. Adequate training and access to appropriate facilities would be crucial to enabling adoption of these techniques.

7.4 Overall conclusion

This work has shown that the oxygen level used to isolate and culture hBMSC is critical to their behaviour, in particular their immuno-modulatory properties. This suggests that oxygen is a key regulator of the contributions of hBMSC to repair, as outlined in the figure below (fig. 7.1). In addition, this work has shown that hBMSC isolated from elderly donors with OA retain a level of immuno-modulation, albeit lower than that found in younger donors as described previously, which may provide some insight into the decreased efficacy of bone marrow stimulation with increasing age (Muschler et al. 2001; Stiehler et al. 2016). In terms of regenerative therapy, my findings indicate that hBMSC isolated and cultured under hypoxic conditions may have distinct therapeutic effects compared to cells grown under normoxic conditions, with applicability to both surgical bone marrow stimulation techniques and fracture healing in general.

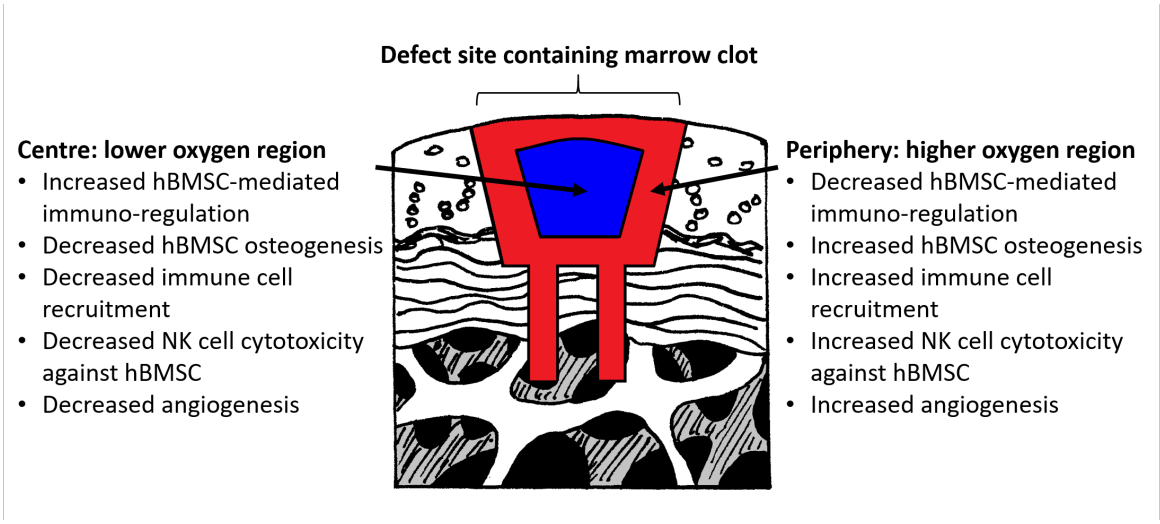

Fig. 7.1 Outline of oxygen-dependent contributions of hBMSC within the clot formed following bone marrow stimulation

hBMSC may contribute differently to repair, depending on the level of oxygen available. At the periphery, the proximity to vasculature results in a higher oxygen level while the centre of the clot remains hypoxic. hBMSC within the lower oxygen regions have a more immunomodulatory phenotype, while those within the higher oxygen regions have a more pro-inflammatory phenotype.

7.5 Further work

Throughout this thesis, various opportunities for developing the research further have been identified. In the short term, the three experiments which should be done next are:

1. Crossing over the hypoxic hBMSC to normoxic conditions and vice versa for characterisation work. This would include the adipogenic, chondrogenic, and osteogenic differentiation, CFU assay and assessment of surface marker expression and cellular stress markers, such as HIF-1α and senescence. In addition, performing transcriptome and epigenome analysis on the hypoxic and normoxic strains in situ, with particular attention paid to genes relating to metabolism and immuno-modulation could indicate whether the population differences were transient and due to adaptation, or more permanent and due to population selection.

2. Performing the NK cell-hBMSC co-cultures using hBMSC isolated under hypoxic and normoxic conditions from the iliac crests of young (under 45 years) donors, using the same ratios to determine whether donor age influences the immuno-modulatory ability of hBMSC towards NK cells.

3. Examining the hBMSC-monocyte interactions in greater detail. This would comprise performing the co-cultures and analysing changes in gene expression and cell surface marker expression in separated populations following the co-culture. This could in particular examine genes related to angiogenesis and immuno-modulation to determine the cell type responsible for the observed phenotype. In addition, the tube forming assay could be extended to use the hBMSC-monocyte mixture, labelled with fluorescent markers, with the HUVECs to identify how the physical contribution of the hBMSC or monocytes to the pseudocapillary network is altered by oxygen level.

In the long term, the following strands could be followed to extend this work further:

1. The model could be refined further to more closely adhere to the conditions within a repair to examine how this influences the hBMSC behaviour and interactions with PBMC, using experiments similar to those laid out within this work. The refinements to the model could include addition of inflammatory stimuli, such as TNFα, IL-1β, or IL-6 to the culture media. Another refinement would be use of a greater range of oxygen levels, based more closely on the oxygen level found within a haematoma during various phases of repair. A final option would be introduction of a 3D environment, perhaps through embedding cells within a fibrin gel and examining how this influences differentiation, gene expression, migration and protein secretion. Use of an explant culture bioreactor, such as that developed by Rocky Tuan (Hang Lin et al. 2014) would be the ultimate goal of the model refinements, allowing interrogation of more complex interactions.

2. Having refined the model, a more complex cell-mixture could be added. Some studies have examined the interactions between hBMSC, monocytes and NK cells, finding that, for example, monocytes reduce NK cell mediated hBMSC death (Jewett et al. 2010). Once again, this work focusses solely on the normoxic environment: use of the three-cell system in the model outlined above would demonstrate greater biological relevance.

References

Abramson, Steven B. and Mukundan Attur (2009). "Developments in the Scientific Understanding of Osteoarthritis". In: *Arthritis Res. Ther.* 11.3, p. 227. ISSN: 1478-6362. DOI: 10.1186/ar2655. pmid: 19519925.

Adams, Francis and Hippocrates (2000).

Adesida, Adetola B, Aillette Mulet-Sierra, and Nadr M Jomha (Mar. 2, 2012). "Hypoxia Mediated Isolation and Expansion Enhances the Chondrogenic Capacity of Bone Marrow Mesenchymal Stromal Cells". In: *Stem Cell Res Ther* 3.2, p. 9. ISSN: 1757-6512. DOI: 10.1186/scrt100. pmid: 22385573.

Agaiby, A. D. and M. Dyson (Nov. 1999). "Immuno-Inflammatory Cell Dynamics during Cutaneous Wound Healing". In: *J. Anat.* 195 (Pt 4), pp. 531–542. ISSN: 0021-8782. pmid: 10634692.

Alexander, Colin J. (Nov. 1, 1999). "Heberden's and Bouchard's Nodes". In: *Annals of the Rheumatic Diseases* 58.11, pp. 675–678. ISSN: 0003-4967, 1468-2060. DOI: 10.1136/ard.58.11.675. pmid: 10531070.

Almeida, Catarina R., Daniela P. Vasconcelos, Raquel M. Gonçalves, and Mário A. Barbosa (Feb. 7, 2012). "Enhanced Mesenchymal Stromal Cell Recruitment via Natural Killer Cells by Incorporation of Inflammatory Signals in Biomaterials". In: *J R Soc Interface* 9.67, pp. 261–271. ISSN: 1742-5689. DOI: 10.1098/rsif.2011.0357. pmid: 21752807.

Alnaeeli, Mawadda, Josef M. Penninger, and Yen-Tung Andy Teng (Sept. 1, 2006). "Immune Interactions with CD4+ T Cells Promote the Development of Functional Osteoclasts from Murine CD11c+ Dendritic Cells". In: *J. Immunol.* 177.5, pp. 3314–3326. ISSN: 0022-1767. pmid: 16920972.

Ang, Sonny et al. (Nov. 19, 2010). "NK Cell Proliferation and Cytolytic Function Are Compromised In the Hypoxic Tumor Microenvironment". In: *Blood* 116.21, pp. 4291–4291. ISSN: 0006-4971, 1528-0020.

Anton, Kevin, Debabrata Banerjee, and John Glod (Apr. 4, 2012). "Macrophage-Associated Mesenchymal Stem Cells Assume an Activated, Migratory, Pro-Inflammatory Phenotype with Increased IL-6 and CXCL10 Secretion". In: *PLOS ONE* 7.4. also zotero-910, e35036. ISSN: 1932-6203. DOI: 10.1371/journal.pone.0035036.

ARUK (2013). *OSTEOARTHRITIS IN GENERAL PRACTICE Data and Perspectives*. Arthritis Research UK.

– (2017). *Arthritis Research UK | Arthritis Research UK*. URL: http://www.arthritisresearchuk.org/ (visited on 12/19/2017).

Bae, Dae Kyung, Kyoung Ho Yoon, and Sang Jun Song (Apr. 2006). "Cartilage Healing after Microfracture in Osteoarthritic Knees". In: *Arthroscopy* 22.4, pp. 367–374. ISSN: 1526-3231. DOI: 10.1016/j.arthro.2006.01.015. pmid: 16581448.

Bailey, K., F. R. Bettelheim, L. Lorand, and W. R. Middlebrook (Feb. 10, 1951). "Action of Thrombin in the Clotting of Fibrinogen". In: *Nature* 167.4241, pp. 233–234. ISSN: 0028-0836. pmid: 14806439.

Bank, I., M. Book, and R. Ware (July 1994). "Functional Role of VLA-1 (CD49A) in Adhesion, Cation-Dependent Spreading, and Activation of Cultured Human T Lymphocytes". In: *Cell. Immunol.* 156.2, pp. 424–437. ISSN: 0008-8749. DOI: 10.1006/cimm.1994.1187. pmid: 8025956.

Barbul, Adrian (Oct. 2008). "Proline Precursors to Sustain Mammalian Collagen Synthesis". In: *J. Nutr.* 138.10, 2021S–2024S. ISSN: 1541-6100. DOI: 10.1093/jn/138.10.2021S. pmid: 18806118.

Bari, Cosimo De, Tobias B. Kurth, and Andrea Augello (2010). "Mesenchymal stem cells from development to postnatal joint homeostasis, aging, and disease". en. In: *Birth Defects Research Part C: Embryo Today: Reviews* 90.4, pp. 257–271. ISSN: 1542-9768. DOI: 10.1002/bdrc.20189.

Bartlett, W., J. A. Skinner, C. R. Gooding, R. W. J. Carrington, A. M. Flanagan, T. W. R. Briggs, and G. Bentley (May 2005). "Autologous Chondrocyte Implantation versus Matrix-Induced Autologous Chondrocyte Implantation for Osteochondral Defects of the Knee: A Prospective, Randomised Study". In: *J Bone Joint Surg Br* 87.5, pp. 640–645. ISSN: 0301-620X. DOI: 10.1302/0301-620X.87B5.15905. pmid: 15855365.

Bastian, Okan W., Leo Koenderman, Jacqueline Alblas, Luke P. H. Leenen, and Taco J. Blokhuis (Mar. 1, 2016). "Neutrophils Contribute to Fracture Healing by Synthesizing Fibronectin+ Extracellular Matrix Rapidly after Injury". In: *Clinical Immunology* 164 (Supplement C), pp. 78–84. ISSN: 1521-6616. DOI: 10.1016/j.clim.2016.02.001.

Bateman, Marjorie E., Amy L. Strong, John A. McLachlan, Matthew E. Burow, and Bruce A. Bunnell (2016). "The Effects of Endocrine Disruptors on Adipogenesis and Osteogenesis in Mesenchymal Stem Cells: A Review". In: *Front Endocrinol (Lausanne)* 7, p. 171. ISSN: 1664-2392. DOI: 10.3389/fendo.2016.00171. pmid: 28119665.

Becher, Christoph, Jan Springer, Sven Feil, Guiliano Cerulli, and Hans H Paessler (Apr. 11, 2008). "Intra-Articular Temperatures of the Knee in Sports – An in-Vivo Study of Jogging and Alpine Skiing". In: *BMC Musculoskelet Disord* 9, p. 46. ISSN: 1471-2474. DOI: 10.1186/1471-2474-9-46. pmid: 18405365.

Beck, M., M. Kalhor, M. Leunig, and R. Ganz (July 2005). "Hip Morphology Influences the Pattern of Damage to the Acetabular Cartilage: Femoroacetabular Impingement as a Cause of Early Osteoarthritis of the Hip". In: *J Bone Joint Surg Br* 87.7, pp. 1012–1018. ISSN: 0301-620X. DOI: 10.1302/0301-620X.87B7.15203. pmid: 15972923.

Bellotti, Chiara, Serena Duchi, Alessandro Bevilacqua, Enrico Lucarelli, and Filippo Piccinini (Dec. 2016). "Long Term Morphological Characterization of Mesenchymal Stromal Cells 3D Spheroids Built with a Rapid Method Based on Entry-Level Equipment". In: *Cytotechnology* 68.6, pp. 2479–2490. ISSN: 0920-9069. DOI: 10.1007/s10616-016-9969-y. pmid: 27023795.

Benedek, T. G. (Mar. 1, 2006). "A History of the Understanding of Cartilage". In: *Osteoarthritis and Cartilage* 14.3, pp. 203–209. ISSN: 1063-4584. DOI: 10.1016/j.joca.2005.08.014.

Bergdolt, Stephanie, Anna Kovtun, Yvonne Hägele, Astrid Liedert, Thorsten Schinke, Michael Amling, Markus Huber-Lang, and Anita Ignatius (June 14, 2017). "Osteoblast-Specific Overexpression of Complement Receptor C5aR1 Impairs Fracture Healing". In: *PLOS ONE* 12.6, e0179512. ISSN: 1932-6203. DOI: 10.1371/journal.pone.0179512.

Berman, M. E., Y. Xie, and W. A. Muller (Feb. 15, 1996). "Roles of Platelet/Endothelial Cell Adhesion Molecule-1 (PECAM-1, CD31) in Natural Killer Cell Transendothelial Migration and Beta 2 Integrin Activation." In: *The Journal of Immunology* 156.4, pp. 1515–1524. ISSN: 0022-1767, 1550-6606. pmid: 8568255.

Billcliff, Peter G., Ruth Rollason, Ian Prior, Dylan M. Owen, Katharina Gaus, and George Banting (Apr. 1, 2013). "CD317/Tetherin Is an Organiser of Membrane Microdomains". In: *J Cell Sci* 126.7, pp. 1553–1564. ISSN: 0021-9533, 1477-9137. DOI: 10.1242/jcs.112953. pmid: 23378022.

Bio, ACEA (2018). *RTCA XCelligence*. URL: https://www.aceabio.com/products/rtca-xcelligence/ (visited on 05/01/2018).

Biologicals, Novus (2011). *CD11b Expression, Leukocyte Adhesion and the Innate Immune System | Antibody News: Novus Biologicals*. URL: https://www.novusbio.com/antibody-news/antibodies/cd11b-expression-and-the-innate-immune-system (visited on 04/22/2019).

– (2015). *Integrin Beta 1/CD29 - a Cell Adhesion and Cell Signaling Protein with Diverse Functions | Antibody News: Novus Biologicals*. URL: https://www.novusbio.com/antibody-news/antibodies/integrin-beta-1-cd29-a-cell-adhesion-and-cell-signaling-protein-with-diverse-functions (visited on 04/22/2019).

Biosciences, BD (2018). *BV421,Mouse,Anti-Human,CD31,L133.1,RUO - 744801 | BD Biosciences-US*. URL: https://www.bdbiosciences.com/us/reagents/research/antibodies-buffers/immunology-reagents/anti-human-antibodies/cell-surface-antigens/bv421-mouse-anti-human-cd31-l1331/p/744801 (visited on 05/13/2018).

Block, Travis J., Milos Marinkovic, Olivia N. Tran, Aaron O. Gonzalez, Amanda Marshall, David D. Dean, and Xiao-Dong Chen (Oct. 27, 2017). "Restoring the Quantity and Quality of Elderly Human Mesenchymal Stem Cells for Autologous Cell-Based Therapies". In: *Stem Cell Res Ther* 8. ISSN: 1757-6512. DOI: 10.1186/s13287-017-0688-x. pmid: 29078802.

Bolontrade, Marcela and Mariana García (Oct. 24, 2016). *Mesenchymal Stromal Cells as Tumor Stromal Modulators*. Academic Press. 644 pp. ISBN: 978-0-12-803103-2.

Bornes, Troy D., Nadr M. Jomha, Aillette Mulet-Sierra, and Adetola B. Adesida (Apr. 23, 2015). "Hypoxic Culture of Bone Marrow-Derived Mesenchymal Stromal Stem Cells Differentially Enhances in Vitro Chondrogenesis within Cell-Seeded Collagen and Hyaluronic Acid Porous Scaffolds". In: *Stem Cell Res Ther* 6, p. 84. ISSN: 1757-6512. DOI: 10.1186/s13287-015-0075-4. pmid: 25900045.

Boulos, K. and B. M. Jolles-Haeberli (Dec. 2008). "[Total knee arthroplasty today: what should we tell our patients?]." In: *Rev Med Suisse* 4.184, pp. 2737–2742. ISSN: 1660-9379. pmid: 19160639.

Boyce, Brendan F. and Lianping Xing (Sept. 2007). "The RANKL/RANK/OPG Pathway". In: *Curr Osteoporos Rep* 5.3, pp. 98–104. ISSN: 1544-1873. pmid: 17925190.

Boyden, Stephen (Feb. 28, 1962). "THE CHEMOTACTIC EFFECT OF MIXTURES OF ANTIBODY AND ANTIGEN ON POLYMORPHONUCLEAR LEUCOCYTES". In: *J Exp Med* 115.3, pp. 453–466. ISSN: 0022-1007. pmid: 13872176.

Brandt, K. D., E. L. Radin, P. A. Dieppe, and L. van de Putte (Oct. 1, 2006). "Yet More Evidence That Osteoarthritis Is Not a Cartilage Disease". In: *Annals of the Rheumatic Diseases* 65.10, pp. 1261–1264. ISSN: 0003-4967, 1468-2060. DOI: 10.1136/ard.2006.058347. pmid: 16973787.

Bridges, Patricia S. (1992). "Prehistoric Arthritis in the Americas". In: *Annual Review of Anthropology* 21.1, pp. 67–91. DOI: 10.1146/annurev.an.21.100192.000435.

Brittberg, M., A. Lindahl, A. Nilsson, C. Ohlsson, O. Isaksson, and L. Peterson (Oct. 6, 1994). "Treatment of Deep Cartilage Defects in the Knee with Autologous Chondrocyte Transplantation". In: *N. Engl. J. Med.* 331.14, pp. 889–895. ISSN: 0028-4793. DOI: 10.1056/NEJM199410063311401. pmid: 8078550.

Broyles, Joseph E. (2017a). "Biologic Augmented Microdrilling Surgery for Multiple and Large Full-Thickness Cartilage Lesions in the Knee: Early Clinical and Radiological Results". In: *Surgical Science* 08.02. In collab. with M. Adaire O'Brien, Stephanie T. Broyles, and M. Patrick Stagg, pp. 102–117. ISSN: 2157-9407, 2157-9415. DOI: 10.4236/ss.2017.82013.

– (Feb. 1, 2017b). "Microdrilling Surgery Augmented With Intra-Articular Bone Marrow Aspirate Concentrate, Platelet-Rich Plasma, and Hyaluronic Acid: A Technique for Cartilage Repair in the Knee". In: *Arthroscopy Techniques* 6.1. In collab. with M. Adaire O'Brien and M. Patrick Stagg, e201–e206. ISSN: 2212-6287. DOI: 10.1016/j.eats.2016.09.024.

Bruderer, M., R. G. Richards, M. Alini, and M. J. Stoddart (Oct. 23, 2014). "Role and Regulation of RUNX2 in Osteogenesis". In: *Eur Cell Mater* 28, pp. 269–286. ISSN: 1473-2262. pmid: 25340806.

Buckwalter, Joseph A. (Oct. 2003). "Sports, Joint Injury, and Posttraumatic Osteoarthritis". In: *J Orthop Sports Phys Ther* 33.10, pp. 578–588. ISSN: 0190-6011. DOI: 10.2519/jospt.2003.33.10.578. pmid: 14620787.

Caldwell, K. L. and J. Wang (Mar. 2015). "Cell-based articular cartilage repair: the link between development and regeneration". eng. In: *Osteoarthritis and Cartilage* 23.3, pp. 351–362. ISSN: 1522-9653. DOI: 10.1016/j.joca.2014.11.004.

Caplan, Arnold I. (1991). "Mesenchymal Stem Cells". In: *Journal of Orthopaedic Research* 9.5, pp. 641–650. ISSN: 1554-527X. DOI: 10.1002/jor.1100090504.

– (June 2017). "Mesenchymal Stem Cells: Time to Change the Name!" In: *Stem Cells Transl Med* 6.6, pp. 1445–1451. ISSN: 2157-6564. DOI: 10.1002/sctm.17-0051. pmid: 28452204.

Caplan, Arnold I. and Diego Correa (July 8, 2011). "The MSC: An Injury Drugstore". In: *Cell Stem Cell* 9.1, pp. 11–15. ISSN: 1934-5909. DOI: 10.1016/j.stem.2011.06.008. pmid: 21726829.

Chakkalakal, D. A., A. A. Mashoof, J. Novak, B. S. Strates, and M. H. McGuire (Dec. 1, 1994). "Mineralization and pH Relationships in Healing Skeletal Defects Grafted with Demineralized Bone Matrix". In: *J. Biomed. Mater. Res.* 28.12, pp. 1439–1443. ISSN: 1097-4636. DOI: 10.1002/jbm.820281209.

Chan, James K et al. (May 2015). "Low-Dose TNF Augments Fracture Healing in Normal and Osteoporotic Bone by up-Regulating the Innate Immune Response". In: *EMBO Mol Med* 7.5, pp. 547–561. ISSN: 1757-4676. DOI: 10.15252/emmm.201404487. pmid: 25770819.

Chaplin, David D. (Feb. 2010). "Overview of the Immune Response". In: *J. Allergy Clin. Immunol.* 125 (2 Suppl 2), S3–23. ISSN: 1097-6825. DOI: 10.1016/j.jaci.2009.12.980. pmid: 20176265.

Charles, Julia F. and Mary C. Nakamura (Mar. 2014). "Bone and the Innate Immune System". In: *Curr Osteoporos Rep* 12.1, pp. 1–8. ISSN: 1544-1873. DOI: 10.1007/s11914-014-0195-2. pmid: 24500569.

Charnley, John (May 27, 1961). "ARTHROPLASTY OF THE HIP: A New Operation". In: *The Lancet*. Originally Published as Volume 1, Issue 7187 277.7187, pp. 1129–1132. ISSN: 0140-6736. DOI: 10.1016/S0140-6736(61)92063-3.

Chen, Lieping (May 2004). "Co-Inhibitory Molecules of the B7–CD28 Family in the Control of T-Cell Immunity". In: *Nature Reviews Immunology* 4.5, pp. 336–347. ISSN: 1474-1741. DOI: 10.1038/nri1349.

Chen, Wenchuan, Xian Liu, Qianmin Chen, Chongyun Bao, Liang Zhao, Zhimin Zhu, and Hockin H. K. Xu (2018). "Angiogenic and Osteogenic Regeneration in Rats via Calcium Phosphate Scaffold and Endothelial Cell Co-Culture with Human Bone Marrow Mesenchymal Stem Cells (MSCs), Human Umbilical Cord MSCs, Human Induced Pluripotent Stem Cell-Derived MSCs and Human Embryonic Stem Cell-Derived MSCs". In: *Journal of Tissue Engineering and Regenerative Medicine* 12.1 (), pp. 191–203. ISSN: 1932-7005. DOI: 10.1002/term.2395.

Chen, Youbin, Jiankun Xu, Zhonglian Huang, Menglei Yu, Yuantao Zhang, Hongjiang Chen, Zebin Ma, Haojie Liao, and Jun Hu (Mar. 8, 2017). "An Innovative Approach for Enhancing Bone Defect Healing Using PLGA Scaffolds Seeded with Extracorporeal-Shock-Wave-Treated Bone Marrow Mesenchymal Stem Cells (BMSCs)". In: *Scientific Reports* 7, p. 44130. ISSN: 2045-2322. DOI: 10.1038/srep44130.

Chijimatsu, Ryota and Taku Saito (June 2019). "Mechanisms of synovial joint and articular cartilage development". en. In: *Cellular and Molecular Life Sciences*. ISSN: 1420-9071. DOI: 10.1007/s00018-019-03191-5.

Chistiakov, Dimitry A., Murry C. Killingsworth, Veronika A. Myasoedova, Alexander N. Orekhov, and Yuri V. Bobryshev (Jan. 2017). "CD68/Macrosialin: Not Just a Histochemical Marker". In: *Lab. Invest.* 97.1, pp. 4–13. ISSN: 1530-0307. DOI: 10.1038/labinvest.2016.116. pmid: 27869795.

Chiu, Ya-Hui and Christopher T. Ritchlin (Nov. 2016). "DC-STAMP: A Key Regulator in Osteoclast Differentiation". In: *J Cell Physiol* 231.11, pp. 2402–2407. ISSN: 0021-9541. DOI: 10.1002/jcp.25389. pmid: 27018136.

Chiu, Ya-Hui, Edward Schwarz, et al. (Sept. 2017). "Dendritic Cell-Specific Transmembrane Protein (DC-STAMP) Regulates Osteoclast Differentiation via the Ca2+ /NFATc1 Axis". In: *J. Cell. Physiol.* 232.9, pp. 2538–2549. ISSN: 1097-4652. DOI: 10.1002/jcp.25638. pmid: 27723141.

Chiu, Ya-Hui, Tzong-Ren Sheu, Jinbo Li, Dongge Li, Michael Thullen, Brendan F. Boyce, Christopher T. Ritchlin, and Javier Rangel-Moreno (Sept. 29, 2015). "Dendritic Cell-Specific Transmembrane Protein (DC-STAMP) Modulates Bone Resorption in Inflammatory Arthritis and Fracture Repair". In: *ACR Meeting Abstracts*. 2015 ACR/ARHP Annual Meeting.

Cho, Sarah K., Annie Bourdeau, Michelle Letarte, and Juan Carlos Zúñiga-Pflücker (Dec. 15, 2001). "Expression and Function of CD105 during the Onset of Hematopoiesis from Flk1+ Precursors". In: *Blood* 98.13, pp. 3635–3642. ISSN: 0006-4971, 1528-0020. DOI: 10.1182/blood.V98.13.3635. pmid: 11739167.

Chu, Constance R., Michal Szczodry, and Stephen Bruno (Feb. 2010). "Animal Models for Cartilage Regeneration and Repair". In: *Tissue Eng Part B Rev* 16.1, pp. 105–115. ISSN: 1937-3368. DOI: 10.1089/ten.teb.2009.0452. pmid: 19831641.

Claes, Lutz, Stefan Recknagel, and Anita Ignatius (Mar. 2012). "Fracture Healing under Healthy and Inflammatory Conditions". In: *Nat Rev Rheumatol* 8.3, pp. 133–143. ISSN: 1759-4790. DOI: 10.1038/nrrheum.2012.1.

ClinicalTrials.Gov (July 2018). URL: https://clinicaltrials.gov/ (visited on 07/24/2018).

Colburn, Nona T., Kristien J. M. Zaal, Francis Wang, and Rocky S. Tuan (June 2009). "A Role for Gamma/Delta T Cells in a Mouse Model of Fracture Healing". In: *Arthritis Rheum.* 60.6, pp. 1694–1703. ISSN: 0004-3591. DOI: 10.1002/art.24520. pmid: 19479830.

Collin, Matthew, Naomi McGovern, and Muzlifah Haniffa (Sept. 2013). "Human Dendritic Cell Subsets". In: *Immunology* 140.1, pp. 22–30. ISSN: 0019-2805. DOI: 10.1111/imm.12117. pmid: 23621371.

Cooper, Megan A, Todd A Fehniger, and Michael A Caligiuri (Nov. 1, 2001). "The Biology of Human Natural Killer-Cell Subsets". In: *Trends in Immunology* 22.11, pp. 633–640. ISSN: 1471-4906. DOI: 10.1016/S1471-4906(01)02060-9.

Croitoru-Lamoury, Juliana, Francois M. J. Lamoury, John J. Zaunders, Laura A. Veas, and Bruce J. Brew (Jan. 2007). "Human Mesenchymal Stem Cells Constitutively Express Chemokines and Chemokine Receptors That Can Be Upregulated by Cytokines, IFN-Beta, and Copaxone". In: *J. Interferon Cytokine Res.* 27.1, pp. 53–64. ISSN: 1079-9907. DOI: 10.1089/jir.2006.0037. pmid: 17266444.

Cundy, T., M. N. Beneton, A. J. Darby, W. J. Marshall, and J. A. Kanis (1987). "Osteopenia in Systemic Mastocytosis: Natural History and Responses to Treatment with Inhibitors of Bone Resorption". In: *Bone* 8.3, pp. 149–155. ISSN: 8756-3282. pmid: 3606906.

Al-Dahiri, Ahmed and Ian Pallister (Jan. 1, 2006). "Arthrodesis for Osteoarthritis of the Manubriosternal Joint". In: *Eur J Cardiothorac Surg* 29.1, pp. 119–121. ISSN: 1010-7940, 1873-734X. DOI: 10.1016/j.ejcts.2005.10.031. pmid: 16337403.

Dalton, Heather J., Guillermo Armaiz-Pena, Vianey Gonzalez-Villasana, Gabriel Lopez-Berestein, Menashe Bar-Eli, and Anil K. Sood (Mar. 1, 2014). "Monocyte Subpopulations in Angiogenesis". In: *Cancer Res* 74.5, pp. 1287–1293. ISSN: 0008-5472. DOI: 10.1158/0008-5472.CAN-13-2825. pmid: 24556724.

Dawes, Ritu, Svetla Petrova, Zhe Liu, David Wraith, Peter C. L. Beverley, and Elma Z. Tchilian (Mar. 15, 2006). "Combinations of CD45 Isoforms Are Crucial for Immune Function and Disease". In: *The Journal of Immunology* 176.6, pp. 3417–3425. ISSN: 0022-1767, 1550-6606. DOI: 10.4049/jimmunol.176.6.3417. pmid: 16517710.

De Vries–van Melle, Marloes L., Roberto Narcisi, Nicole Kops, Wendy J.L.M. Koevoet, P. Koen Bos, J. Mary Murphy, Jan A.N. Verhaar, Peter M. van der Kraan, and Gerjo J.V.M. van Osch (Jan. 1, 2014). "Chondrogenesis of Mesenchymal Stem Cells in an Osteochondral Environment Is Mediated by the Subchondral Bone". In: *Tissue Eng Part A* 20.1-2, pp. 23–33. ISSN: 1937-3341. DOI: 10.1089/ten.tea.2013.0080. pmid: 23980750.

Decker, Rebekah S., Eiki Koyama, and Maurizio Pacifici (Dec. 2015). "Articular cartilage: structural and developmental intricacies and questions". In: *Current osteoporosis reports* 13.6, pp. 407–414. ISSN: 1544-1873. DOI: 10.1007/s11914-015-0290-z.

Decker, Rebekah S., Hyo-Bin Um, et al. (June 2017). "Cell origin, volume and arrangement are drivers of articular cartilage formation, morphogenesis and response to injury in mouse limbs". In: *Developmental Biology* 426.1, pp. 56–68. ISSN: 0012-1606. DOI: 10.1016/j.ydbio.2017.04.006.

Deng, Yinan, Yingcai Zhang, Linsen Ye, Tong Zhang, Jintao Cheng, Guihua Chen, Qi Zhang, and Yang Yang (Dec. 5, 2016). "Umbilical Cord-Derived Mesenchymal Stem Cells Instruct Monocytes Towards an IL10-Producing Phenotype by Secreting IL6 and HGF". In: *Scientific Reports* 6, p. 37566. ISSN: 2045-2322. DOI: 10.1038/srep37566.

Depoix, Christophe Louis, Olivier Flabat, Frédéric Debière, and Corinne Hubinont (Sept. 1, 2016). "HIF1A and EPAS1 mRNA and Protein Expression during in Vitro Culture of Human Primary Term Cytotrophoblasts and Effect of Oxygen Tension on Their Expression". In: *Reproductive Biology* 16.3, pp. 203–211. ISSN: 1642-431X. DOI: 10.1016/j.repbio.2016.05.001.

Dietz, Allan, Peggy Bulur, Richard L Emery, Jeffrey Winters, Dennis E Epps, Abba C Zubair, and Stanimir Vuk-Pavlović (Dec. 1, 2006). "A Novel Source of Viable Peripheral Blood Mononuclear Cells from Leukoreduction System Chamber". In: *Transfusion* 46, pp. 2083–9. DOI: 10.1111/j.1537-2995.2006.01033.x.

DiMarino, Amy M., Arnold I. Caplan, and Tracey L. Bonfield (2013). "Mesenchymal Stem Cells in Tissue Repair". In: *Front. Immunol.* 4. ISSN: 1664-3224. DOI: 10.3389/fimmu.2013.00201.

Ding, Hao, You-Shui Gao, Yang Wang, Chen Hu, Yuan Sun, and Changqing Zhang (Dec. 13, 2013). "Dimethyloxaloylglycine Increases the Bone Healing Capacity of Adipose-Derived Stem Cells by Promoting Osteogenic Differentiation and Angiogenic Potential". In: *Stem Cells and Development* 23.9, pp. 990–1000. ISSN: 1547-3287. DOI: 10.1089/scd.2013.0486.

Ding, Lei and Sean J. Morrison (Mar. 14, 2013). "Haematopoietic Stem Cells and Early Lymphoid Progenitors Occupy Distinct Bone Marrow Niches". In: *Nature* 495.7440, pp. 231–235. ISSN: 0028-0836. DOI: 10.1038/nature11885.

Dominici, M. et al. (2006). "Minimal Criteria for Defining Multipotent Mesenchymal Stromal Cells. The International Society for Cellular Therapy Position Statement". In: *Cytotherapy* 8.4, pp. 315–317. ISSN: 1465-3249. DOI: 10.1080/14653240600855905.

Doolittle, Russell F (2010). "Fibrinogen and Fibrin". In: *eLS*. John Wiley & Sons, Ltd. ISBN: 978-0-470-01590-2. DOI: 10.1002/9780470015902.a0001409.pub2.

Dupont, Kenneth M., Kapil Sharma, Hazel Y. Stevens, Joel D. Boerckel, Andrés J. García, and Robert E. Guldberg (Feb. 23, 2010). "Human Stem Cell Delivery for Treatment of Large Segmental Bone Defects". In: *PNAS* 107.8, pp. 3305–3310. ISSN: 0027-8424, 1091-6490. DOI: 10.1073/pnas.0905444107. pmid: 20133731.

Ebert, J., P. Edwards, M. Fallon, T. Ackland, and D. Wood (Jan. 1, 2017). "A Randomised Trial Investigating an Accelerated Weight Bearing Program after Autologous Chondrocyte Implantation: 2-Year Outcomes". In: *Journal of Science and Medicine in Sport* 20, e29. ISSN: 1440-2440, 1878-1861. DOI: 10.1016/j.jsams.2016.12.069.

Edderkaoui, Bouchra (Mar. 2, 2017). "Potential Role of Chemokines in Fracture Repair". In: *Front Endocrinol (Lausanne)* 8. ISSN: 1664-2392. DOI: 10.3389/fendo.2017.00039. pmid: 28303118.

Einhorn, Thomas A. and Louis C. Gerstenfeld (Jan. 2015). "Fracture Healing: Mechanisms and Interventions". In: *Nat Rev Rheumatol* 11.1, pp. 45–54. ISSN: 1759-4804. DOI: 10.1038/nrrheum.2014.164. pmid: 25266456.

Epari, Devakara R., Jasmin Lienau, Hanna Schell, Florian Witt, and Georg N. Duda (Oct. 2008). "Pressure, Oxygen Tension and Temperature in the Periosteal Callus during Bone Healing—An in Vivo Study in Sheep". In: *Bone* 43.4, pp. 734–739. ISSN: 8756-3282. DOI: 10.1016/j.bone.2008.06.007.

Espinoza, F., F. Aliaga, and P. L. Crawford (Feb. 2016). "[Overview and perspectives of mesenchymal stem cell therapy in intensive care medicine]." In: *Rev Med Chil* 144.2, pp. 222–231. ISSN: 0034-9887. DOI: 10.4067/S0034-98872016000200011. pmid: 27092677.

Farlow, James Orville and M. K. Brett-Surman (1999). *The Complete Dinosaur*. Indiana University Press. 792 pp. ISBN: 978-0-253-21313-6.

Faulknor, Renea A., Melissa A. Olekson, Emmanuel C. Ekwueme, Paulina Krzyszczyk, Joseph W. Freeman, and François Berthiaume (June 2017). "Hypoxia Impairs Mesenchymal Stromal Cell-

Induced Macrophage M1 to M2 Transition". In: *Technology (Singap World Sci)* 5.2, pp. 81–86. ISSN: 2339-5478. DOI: 10.1142/S2339547817500042. pmid: 29552603.

Fauriat, Cyril, Eric O. Long, Hans-Gustaf Ljunggren, and Yenan T. Bryceson (Mar. 18, 2010). "Regulation of Human NK-Cell Cytokine and Chemokine Production by Target Cell Recognition". In: *Blood* 115.11, pp. 2167–2176. ISSN: 0006-4971. DOI: 10.1182/blood-2009-08-238469. pmid: 19965656.

Fellows, Christopher R., Csaba Matta, Roza Zakany, Ilyas M. Khan, and Ali Mobasheri (2016). "Adipose, Bone Marrow and Synovial Joint-Derived Mesenchymal Stem Cells for Cartilage Repair". In: *Frontiers in Genetics* 7. ISSN: 1664-8021. DOI: 10.3389/fgene.2016.00213.

Fink, Trine, Abildtrup Lisbeth, Fogd Kirsten, Abdallah Basem M., Kassem Moustapha, Ebbesen Peter, and Zachar Vladimir (Dec. 23, 2008). "Induction of Adipocyte-Like Phenotype in Human Mesenchymal Stem Cells by Hypoxia". In: *STEM CELLS* 22.7, pp. 1346–1355. ISSN: 1066-5099. DOI: 10.1634/stemcells.2004-0038.

Fox, Sophia Alice J., Asheesh Bedi, and Scott A. Rodeo (Nov. 2009). "The Basic Science of Articular Cartilage". In: *Sports Health* 1.6, pp. 461–468. ISSN: 1941-7381. DOI: 10.1177/1941738109350438. pmid: 23015907.

Frame, Boy and Robert K. Nixon (Sept. 19, 1968). "Bone-Marrow Mast Cells in Osteoporosis of Aging". In: *New England Journal of Medicine* 279.12, pp. 626–630. ISSN: 0028-4793. DOI: 10.1056/NEJM196809192791203. pmid: 5668079.

Franceschi, Renny T. and Bhanumathi S. Iyer (1992). "Relationship between Collagen Synthesis and Expression of the Osteoblast Phenotype in MC3T3-E1 Cells". In: *Journal of Bone and Mineral Research* 7.2, pp. 235–246. ISSN: 1523-4681. DOI: 10.1002/jbmr.5650070216.

Friedenstein, A. J., R. K. Chailakhjan, and K. S. Lalykina (Oct. 1970). "The Development of Fibroblast Colonies in Monolayer Cultures of Guinea-Pig Bone Marrow and Spleen Cells". In: *Cell Tissue Kinet* 3.4, pp. 393–403. ISSN: 0008-8730. pmid: 5523063.

Friedenstein, A. J., R. K. Chailakhyan, and U. V. Gerasimov (May 1987). "Bone Marrow Osteogenic Stem Cells: In Vitro Cultivation and Transplantation in Diffusion Chambers". In: *Cell Tissue Kinet* 20.3, pp. 263–272. ISSN: 0008-8730. pmid: 3690622.

Friedenstein, A. J., R. K. Chailakhyan, N. V. Latsinik, A. F. Panasyuk, and I. V. Keiliss-Borok (Apr. 1974). "Stromal Cells Responsible for Transferring the Microenvironment of the Hemopoietic Tissues. Cloning in Vitro and Retransplantation in Vivo". In: *Transplantation* 17.4, pp. 331–340. ISSN: 0041-1337. pmid: 4150881.

Fritsch, Klaus O et al. (May 22, 2015). "The Orthopedic Diseases of Ancient Egypt". In: *The Anatomical Record* 298.6, pp. 1036–1046. ISSN: 1932-8486. DOI: 10.1002/ar.23136.

Fu, Binqing, Zhigang Tian, and Haiming Wei (Apr. 2014). "Subsets of Human Natural Killer Cells and Their Regulatory Effects". In: *Immunology* 141.4, pp. 483–489. ISSN: 0019-2805. DOI: 10.1111/imm.12224. pmid: 24303897.

Furuta, Taisuke, Shigeru Miyaki, Hiroyuki Ishitobi, Toshihiko Ogura, Yoshio Kato, Naosuke Kamei, Kenji Miyado, Yukihito Higashi, and Mitsuo Ochi (Dec. 2016). "Mesenchymal Stem Cell-Derived Exosomes Promote Fracture Healing in a Mouse Model". In: *Stem Cells Transl Med* 5.12, pp. 1620–1630. ISSN: 2157-6564. DOI: 10.5966/sctm.2015-0285. pmid: 27460850.

Gane, Pierre, Catherine Pecquet, Patrick Lambin, Nissen Abuaf, Francisque Leynadier, and Philippe Rouger (2018). "Flow Cytometric Evaluation of Human Basophils". In: *Cytometry* 14.3 (), pp. 344–348. ISSN: 1097-0320. DOI: 10.1002/cyto.990140316.

Ganguly, Payal, Jehan J. El-Jawhari, Peter V. Giannoudis, Agata N. Burska, Frederique Ponchel, and Elena A. Jones (Sept. 2017). "Age-Related Changes in Bone Marrow Mesenchymal Stromal Cells". In: *Cell Transplant* 26.9, pp. 1520–1529. ISSN: 0963-6897. DOI: 10.1177/0963689717721201. pmid: 29113463.

Gao, Bin and Svetlana Radaeva (July 1, 2013). "Natural Killer and Natural Killer T Cells in Liver Fibrosis". In: *Biochimica et Biophysica Acta (BBA) - Molecular Basis of Disease*. Fibrosis:

Translation of Basic Research to Human Disease 1832.7, pp. 1061–1069. ISSN: 0925-4439. DOI: 10.1016/j.bbadis.2012.09.008.

Gao, Liang, Patrick Orth, Kathrin Müller-Brandt, Lars K. H. Goebel, Magali Cucchiarini, and Henning Madry (Mar. 27, 2017). "Early Loss of Subchondral Bone Following Microfracture Is Counteracted by Bone Marrow Aspirate in a Translational Model of Osteochondral Repair". In: *Sci Rep* 7. ISSN: 2045-2322. DOI: 10.1038/srep45189. pmid: 28345610.

Garcia-Vallejo, Juan J. and Yvette van Kooyk (Oct. 1, 2013). "The Physiological Role of DC-SIGN: A Tale of Mice and Men". In: *Trends in Immunology* 34.10, pp. 482–486. ISSN: 1471-4906, 1471-4981. DOI: 10.1016/j.it.2013.03.001. pmid: 23608151.

Garrod, Alfred Baring (1859). *The Nature and Treatment of Gout and Rheumatic Gout.* In collab. with Francis A. Countway Library of Medicine. London : Walton and Maberly. 658 pp.

Geissmann, Frederic, Markus G. Manz, Steffen Jung, Michael H. Sieweke, Miriam Merad, and Klaus Ley (Feb. 5, 2010). "Development of Monocytes, Macrophages, and Dendritic Cells". In: *Science* 327.5966, pp. 656–661. ISSN: 0036-8075, 1095-9203. DOI: 10.1126/science.1178331. pmid: 20133564.

Gerstenfeld, Louis C., Dennis M. Cullinane, George L. Barnes, Dana T. Graves, and Thomas A. Einhorn (Apr. 1, 2003). "Fracture Healing as a Post-Natal Developmental Process: Molecular, Spatial, and Temporal Aspects of Its Regulation". In: *J. Cell. Biochem.* 88.5, pp. 873–884. ISSN: 0730-2312. DOI: 10.1002/jcb.10435. pmid: 12616527.

Glass, Graeme E., James K. Chan, Andrew Freidin, Marc Feldmann, Nicole J. Horwood, and Jagdeep Nanchahal (Jan. 25, 2011). "TNF- Promotes Fracture Repair by Augmenting the Recruitment and Differentiation of Muscle-Derived Stromal Cells". In: *Proc Natl Acad Sci U S A* 108.4, pp. 1585–1590. ISSN: 0027-8424. DOI: 10.1073/pnas.1018501108. pmid: 21209334.

Goldring, Mary B. and Miguel Otero (Sept. 2011). "Inflammation in Osteoarthritis". In: *Curr Opin Rheumatol* 23.5, pp. 471–478. ISSN: 1531-6963. DOI: 10.1097/BOR.0b013e328349c2b1. pmid: 21788902.

Golledge, Jonathan, Ann Van Campenhout, Shripad Pal, and Catherine Rush (Sept. 1, 2007). "Bone Marrow–Derived Cells and Arterial Disease". In: *Journal of Vascular Surgery* 46.3, pp. 590–600. ISSN: 0741-5214. DOI: 10.1016/j.jvs.2007.04.031.

Goujon, Emile (1869). "Recherches Experimentales Sur Les Proprietes Physiologiques de La Moelle Des Os." In: *J Anat Physiol.* 6, pp. 399–412.

Gracitelli, Guilherme C., Vinícius Y. Moraes, Carlos Es Franciozi, Marcus V. Luzo, and João Carlos Belloti (Sept. 3, 2016). "Surgical Interventions (Microfracture, Drilling, Mosaicplasty, and Allograft Transplantation) for Treating Isolated Cartilage Defects of the Knee in Adults". In: *Cochrane Database Syst Rev* 9, p. CD010675. ISSN: 1469-493X. DOI: 10.1002/14651858.CD010675.pub2. pmid: 27590275.

Granero-Moltó, Froilán et al. (Aug. 1, 2009). "Regenerative Effects of Transplanted Mesenchymal Stem Cells in Fracture Healing". In: *STEM CELLS* 27.8, pp. 1887–1898. ISSN: 1549-4918. DOI: 10.1002/stem.103.

Gray, Henry and Warren H. Lewis (1918). "Fig. 347, Chapter III. Syndesmology. Section 7b. The Knee-Joint." In: *Anatomy of the Human Body.* 20th Edition. Lea & Febiger, p. 1404. ISBN: B000TW11G6.

Green, Jordan D. et al. (Dec. 1, 2015). "Multifaceted Signaling Regulators of Chondrogenesis: Implications in Cartilage Regeneration and Tissue Engineering". In: *Genes & Diseases* 2.4, pp. 307–327. ISSN: 2352-3042. DOI: 10.1016/j.gendis.2015.09.003.

Greenbaum, Adam, Yen-Michael S. Hsu, Ryan B. Day, Laura G. Schuettpelz, Matthew J. Christopher, Joshua N. Borgerding, Takashi Nagasawa, and Daniel C. Link (Mar. 14, 2013). "CXCL12 in Early Mesenchymal Progenitors Is Required for Haematopoietic Stem-Cell Maintenance". In: *Nature* 495.7440, pp. 227–230. ISSN: 0028-0836. DOI: 10.1038/nature11926.

Gross, Catharina C., Andreas Schulte-Mecklenbeck, Heinz Wiendl, Emanuela Marcenaro, Nicole Kerlero de Rosbo, Antonio Uccelli, and Alice Laroni (Dec. 19, 2016). "Regulatory Functions of

Natural Killer Cells in Multiple Sclerosis". In: *Front Immunol* 7. ISSN: 1664-3224. DOI: 10.3389/fimmu.2016.00606. pmid: 28066417.

Gu, Qiaoli, Huilin Yang, and Qin Shi (July 1, 2017). "Macrophages and Bone Inflammation". In: *Journal of Orthopaedic Translation*. Special Issue:Inflammation and the Musculoskeletal System 10, pp. 86–93. ISSN: 2214-031X. DOI: 10.1016/j.jot.2017.05.002.

Guihard, Pierre et al. (2018). "Induction of Osteogenesis in Mesenchymal Stem Cells by Activated Monocytes/Macrophages Depends on Oncostatin M Signaling". In: *STEM CELLS* 30.4 (), pp. 762–772. ISSN: 1549-4918. DOI: 10.1002/stem.1040.

Halioua, Bruno and Bernard Ziskind (2005). *Medicine in the Days of the Pharaohs*. Harvard University Press. 300 pp. ISBN: 978-0-674-01702-3.

Harris, Edward D. and Peter A. McCroskery (Jan. 3, 1974). "The Influence of Temperature and Fibril Stability on Degradation of Cartilage Collagen by Rheumatoid Synovial Collagenase". In: *New England Journal of Medicine* 290.1, pp. 1–6. ISSN: 0028-4793. DOI: 10.1056/NEJM197401032900101. pmid: 4357162.

Hartigan, B. J., P. J. Stern, and T. R. Kiefhaber (Oct. 2001). "Thumb Carpometacarpal Osteoarthritis: Arthrodesis Compared with Ligament Reconstruction and Tendon Interposition". In: *J Bone Joint Surg Am* 83-A.10, pp. 1470–1478. ISSN: 0021-9355. pmid: 11679595.

Hatherley, Deborah, Susan M. Lea, Steven Johnson, and A. Neil Barclay (May 7, 2013). "Structures of CD200/CD200 Receptor Family and Implications for Topology, Regulation, and Evolution". In: *Structure* 21.5, pp. 820–832. ISSN: 0969-2126. DOI: 10.1016/j.str.2013.03.008. pmid: 23602662.

Hayat, M. A. (Mar. 31, 1993). *Stains and Cytochemical Methods*. Springer Science & Business Media. 458 pp. ISBN: 978-0-306-44294-0.

Hazeldine, Jon and Janet M. Lord (Sept. 2013). "The Impact of Ageing on Natural Killer Cell Function and Potential Consequences for Health in Older Adults". In: *Ageing Res Rev* 12.4, pp. 1069–1078. ISSN: 1568-1637. DOI: 10.1016/j.arr.2013.04.003. pmid: 23660515.

Heberden, William (1818). *Commentaries on the History and Cure of Diseases*. Boston. ISBN: ISBN: 9781151989864.

Herter, S., M. C. Birk, C. Klein, C. Gerdes, P. Umana, and M. Bacac (Mar. 1, 2014). "Glycoengineering of Therapeutic Antibodies Enhances Monocyte/Macrophage-Mediated Phagocytosis and Cytotoxicity". In: *The Journal of Immunology* 192.5, pp. 2252–2260. ISSN: 0022-1767, 1550-6606. DOI: 10.4049/jimmunol.1301249.

Hill, John (1812). *The Family Herbal;or, An Account of All Those English Plants, Which Are Remarkable for Their Virtues, and of the Drugs Which Are Produced by Vegetables of Other Countries; with Their Descriptions and Their Uses, as Proved by Experience /by Sir John Hill*. In collab. with Missouri Botanical Garden. London, George Virtue. 478 pp.

Hirao, Makoto, Noriyuki Tamai, Noriyuki Tsumaki, Hideki Yoshikawa, and Akira Myoui (Oct. 13, 2006). "Oxygen Tension Regulates Chondrocyte Differentiation and Function during Endochondral Ossification". In: *J. Biol. Chem.* 281.41, pp. 31079–31092. ISSN: 0021-9258, 1083-351X. DOI: 10.1074/jbc.M602296200. pmid: 16905540.

Histopathologic Techniques (2006). Goodwill Trading Co., Inc. 372 pp. ISBN: 978-971-12-0270-5.

Hoff, Paula, T. Gaber, et al. (Dec. 1, 2016). "Immunological Characterization of the Early Human Fracture Hematoma". In: *Immunol Res* 64.5-6, pp. 1195–1206. ISSN: 0257-277X, 1559-0755. DOI: 10.1007/s12026-016-8868-9.

Hoff, Paula, Patrick Maschmeyer, et al. (Mar. 2013). "Human Immune Cells' Behavior and Survival under Bioenergetically Restricted Conditions in an in Vitro Fracture Hematoma Model". In: *Cell Mol Immunol* 10.2, pp. 151–158. ISSN: 1672-7681. DOI: 10.1038/cmi.2012.56. pmid: 23396474.

Hoogduijn, Martin, Anneke Van den Beukel, Lidewij Wiersma, and Jooske Ijzer (Dec. 12, 2013). "CHRISTMAS 2013: RESEARCH Morphology and Size of Stem Cells from Mouse and Whale: Observational Study". In: *BMJ (Clinical research ed.)* 347, f6833. DOI: 10.1136/bmj.f6833.

Hu, Lei, Ying Wen, Junji Xu, Tingting Wu, Chunmei Zhang, Jinsong Wang, Jie Du, and Songlin Wang (Oct. 12, 2016). "Pretreatment with Bisphosphonate Enhances Osteogenesis of Bone Marrow

Mesenchymal Stem Cells". In: *Stem Cells and Development* 26.2, pp. 123–132. ISSN: 1547-3287. DOI: 10.1089/scd.2016.0173.

Huang, Ngan F, Amy Lam, Qizhi Fang, Richard E Sievers, Song Li, and Randall J Lee (July 1, 2009). "Bone Marrow-Derived Mesenchymal Stem Cells in Fibrin Augment Angiogenesis in the Chronically Infarcted Myocardium". In: *Regenerative Medicine* 4.4, pp. 527–538. ISSN: 1746-0751. DOI: 10.2217/rme.09.32.

Huang, Wei-Hua, Hen-Li Chen, Po-Hsun Huang, Tu-Lai Yew, Ming-Wei Lin, Shing-Jong Lin, and Shih-Chieh Hung (Feb. 1, 2014). "Hypoxic Mesenchymal Stem Cells Engraft and Ameliorate Limb Ischaemia in Allogeneic Recipients". In: *Cardiovasc. Res.* 101.2, pp. 266–276. ISSN: 1755-3245. DOI: 10.1093/cvr/cvt250. pmid: 24220639.

Hung, Shun-Pei, Jennifer H. Ho, Yu-Ru V. Shih, Ting Lo, and Oscar K. Lee (Feb. 2012). "Hypoxia Promotes Proliferation and Osteogenic Differentiation Potentials of Human Mesenchymal Stem Cells". In: *J. Orthop. Res.* 30.2, pp. 260–266. ISSN: 1554-527X. DOI: 10.1002/jor.21517. pmid: 21809383.

Hunziker, E. B. (Jan. 1999). "Articular cartilage repair: are the intrinsic biological constraints undermining this process insuperable?" eng. In: *Osteoarthritis and Cartilage* 7.1, pp. 15–28. ISSN: 1063-4584. DOI: 10.1053/joca.1998.0159.

Hunziker, E. B. and L. C. Rosenberg (May 1996). "Repair of partial-thickness defects in articular cartilage: cell recruitment from the synovial membrane". eng. In: *The Journal of Bone and Joint Surgery. American Volume* 78.5, pp. 721–733. ISSN: 0021-9355. DOI: 10.2106/00004623-199605000-00012.

Hwang, Ilwoong, Tianxiang Zhang, Jeannine M. Scott, Ae Ra Kim, Taehyung Lee, Tejaswi Kakarla, Ahrom Kim, John B. Sunwoo, and Sungjin Kim (Dec. 1, 2012). "Identification of Human NK Cells That Are Deficient for Signaling Adaptor FcR and Specialized for Antibody-Dependent Immune Functions". In: *Int Immunol* 24.12, pp. 793–802. ISSN: 0953-8178. DOI: 10.1093/intimm/dxs080.

Iqbal, Salma and Ashok Kumar (Dec. 28, 2015). "Characterization of In Vitro</Em> Generated Human Polarized Macrophages". In: *Journal of Clinical & Cellular Immunology* 6.6, pp. 1–8. ISSN: 2155-9899. DOI: 10.4172/2155-9899.1000380.

Ishikawa, Masahiro et al. (2014). "MCP/CCR2 Signaling Is Essential for Recruitment of Mesenchymal Progenitor Cells during the Early Phase of Fracture Healing". In: *PLoS ONE* 9.8, e104954. ISSN: 1932-6203. DOI: 10.1371/journal.pone.0104954. pmid: 25133509.

Jaipersad, Anthony S., Gregory Y. H. Lip, Stanley Silverman, and Eduard Shantsila (2014). "The Role of Monocytes in Angiogenesis and Atherosclerosis". In: *J. Am. Coll. Cardiol.* 63.1, pp. 1–11. ISSN: 1558-3597. DOI: 10.1016/j.jacc.2013.09.019. pmid: 24140662.

James, Sally et al. (June 9, 2015). "Multiparameter Analysis of Human Bone Marrow Stromal Cells Identifies Distinct Immunomodulatory and Differentiation-Competent Subtypes". In: *Stem Cell Reports* 4.6, pp. 1004–1015. ISSN: 2213-6711. DOI: 10.1016/j.stemcr.2015.05.005. pmid: 26070611.

Jameson, Julie, Karen Ugarte, Nicole Chen, Pia Yachi, Elaine Fuchs, Richard Boismenu, and Wendy L. Havran (Apr. 26, 2002). "A Role for Skin T Cells in Wound Repair". In: *Science* 296.5568, pp. 747–749. ISSN: 0036-8075, 1095-9203. DOI: 10.1126/science.1069639. pmid: 11976459.

El-Jawhari, Jehan J., Elena Jones, Dennis McGonagle, and Peter V. Giannoudis (2016). "Interactions Between Multipotential Stromal Cells (MSCs) and Immune Cells During Bone Healing". In: *Recent Advances in Stem Cells*. Stem Cell Biology and Regenerative Medicine. Humana Press, Cham, pp. 179–211. ISBN: 978-3-319-33268-0 978-3-319-33270-3. DOI: 10.1007/978-3-319-33270-3_9.

Jeltsch, Michael, Veli-Matti Leppänen, Pipsa Saharinen, and Kari Alitalo (Sept. 2013). "Receptor Tyrosine Kinase-Mediated Angiogenesis". In: *Cold Spring Harb Perspect Biol* 5.9. ISSN: 1943-0264. DOI: 10.1101/cshperspect.a009183. pmid: 24003209.

Jewett, Anahid, Aida Arasteh, Han-Ching Tseng, Armin Behel, Hobie Arasteh, Wendy Yang, Nicholas A. Cacalano, and Avina Paranjpe (Mar. 31, 2010). "Strategies to Rescue Mesenchymal Stem Cells

(MSCs) and Dental Pulp Stem Cells (DPSCs) from NK Cell Mediated Cytotoxicity". In: *PLoS ONE* 5.3, e9874. ISSN: 1932-6203. DOI: 10.1371/journal.pone.0009874. pmid: 20360990.

Jiang, Yangzi and Rocky S. Tuan (Apr. 2015). "Origin and Function of Cartilage Stem/Progenitor Cells in Osteoarthritis". In: *Nat Rev Rheumatol* 11.4, pp. 206–212. ISSN: 1759-4804. DOI: 10.1038/nrrheum.2014.200. pmid: 25536487.

Johnstone, B., T. M. Hering, A. I. Caplan, V. M. Goldberg, and J. U. Yoo (Jan. 10, 1998). "In Vitro Chondrogenesis of Bone Marrow-Derived Mesenchymal Progenitor Cells". In: *Exp. Cell Res.* 238.1, pp. 265–272. ISSN: 0014-4827. DOI: 10.1006/excr.1997.3858. pmid: 9457080.

Julier, Ziad, Anthony J. Park, Priscilla S. Briquez, and Mikaël M. Martino (Apr. 2017). "Promoting tissue regeneration by modulating the immune system". In: *Acta Biomaterialia* 53, pp. 13–28. ISSN: 1742-7061. DOI: 10.1016/j.actbio.2017.01.056.

Kagemna and Ptahhotep (Nov. 20, 2009). *The Instruction of Ptah-Hotep and the Instruction of Ke'GemniThe Oldest Books in the World*. Trans. by Battiscombe G. (Battiscombe George) Gunn.

Karahuseyinoglu, Sercin, Cetin Kocaefe, Deniz Balci, Esra Erdemli, and Alp Can (Mar. 2008). "Functional Structure of Adipocytes Differentiated from Human Umbilical Cord Stroma-Derived Stem Cells". In: *Stem Cells* 26.3, pp. 682–691. ISSN: 1549-4918. DOI: 10.1634/stemcells.2007-0738. pmid: 18192234.

Kean, Walter F., Shannon Tocchio, Mary Kean, and K. D. Rainsford (Feb. 2013). "The Musculoskeletal Abnormalities of the Similaun Iceman ("ÖTZI"): Clues to Chronic Pain and Possible Treatments". In: *Inflammopharmacology* 21.1, pp. 11–20. ISSN: 1568-5608. DOI: 10.1007/s10787-012-0153-5. pmid: 23096483.

Keppel, Molly P., Nermina Topcagic, Annelise Y. Mah, Tiphanie P. Vogel, and Megan A. Cooper (Feb. 15, 2015). "Activation-Specific Metabolic Requirements for NK Cell IFN- Production". In: *J Immunol* 194.4, pp. 1954–1962. ISSN: 0022-1767. DOI: 10.4049/jimmunol.1402099. pmid: 25595780.

Khalilpourfarshbafi, Manizheh, Fatemeh Hajiaghaalipour, Kesavanarayanan Krishnan Selvarajan, and Aishah Adam (June 1, 2017). "Mesenchymal Stem Cell-Based Therapies against Podocyte Damage in Diabetic Nephropathy". In: *Tissue Eng Regen Med* 14.3, pp. 201–210. ISSN: 1738-2696, 2212-5469. DOI: 10.1007/s13770-017-0026-5.

Kim, Jaehyup and Peiman Hematti (Dec. 1, 2009). "Mesenchymal Stem Cell–Educated Macrophages: A Novel Type of Alternatively Activated Macrophages". In: *Experimental Hematology* 37.12, pp. 1445–1453. ISSN: 0301-472X. DOI: 10.1016/j.exphem.2009.09.004.

Kim, Yoon-Chung, Young-Hoon Kim, Jang-Woon Kim, and Kee-Yong Ha (Sept. 2016). "Transplantation of Mesenchymal Stem Cells for Acute Spinal Cord Injury in Rats: Comparative Study between Intralesional Injection and Scaffold Based Transplantation". In: *J Korean Med Sci* 31.9, pp. 1373–1382. ISSN: 1011-8934. DOI: 10.3346/jkms.2016.31.9.1373. pmid: 27510379.

Kisselbach, Lynn, Michael Merges, Alexis Bossie, and Ann Boyd (2009). "CD90 Expression on Human Primary Cells and Elimination of Contaminating Fibroblasts from Cell Cultures". In: *Cytotechnology* 59.1, pp. 31–44. ISSN: 0920-9069. DOI: 10.1007/s10616-009-9190-3. pmid: 19296231.

Kliche, S. and J. Waltenberger (July 2001). "VEGF Receptor Signaling and Endothelial Function". In: *IUBMB Life* 52.1-2, pp. 61–66. ISSN: 1521-6543. DOI: 10.1080/15216540252774784. pmid: 11795595.

Knutsen, Gunnar, Jon Olav Drogset, Lars Engebretsen, Torbjørn Grøntvedt, Tom C. Ludvigsen, Sverre Løken, Eirik Solheim, Torbjørn Strand, and Oddmund Johansen (Aug. 17, 2016). "A Randomized Multicenter Trial Comparing Autologous Chondrocyte Implantation with Microfracture: Long-Term Follow-up at 14 to 15 Years". In: *J Bone Joint Surg Am* 98.16, pp. 1332–1339. ISSN: 1535-1386. DOI: 10.2106/JBJS.15.01208. pmid: 27535435.

Kolar, Paula, Timo Gaber, Carsten Perka, Georg N. Duda, and Frank Buttgereit (Mar. 16, 2011). "Human Early Fracture Hematoma Is Characterized by Inflammation and Hypoxia". In: *Clin Orthop Relat Res* 469.11, pp. 3118–3126. ISSN: 0009-921X, 1528-1132. DOI: 10.1007/s11999-011-1865-3.

Komatsu, D. E and M Hadjiargyrou (Apr. 2004). "Activation of the Transcription Factor HIF-1 and Its Target Genes, VEGF, HO-1, iNOS, during Fracture Repair". In: *Bone* 34.4, pp. 680–688. ISSN: 8756-3282. DOI: 10.1016/j.bone.2003.12.024.

Konan, S., F. Rayan, G. Meermans, J. Witt, and F. S. Haddad (Mar. 2011). "Validation of the Classification System for Acetabular Chondral Lesions Identified at Arthroscopy in Patients with Femoroacetabular Impingement". In: *The Journal of Bone and Joint Surgery. British volume* 93-B.3, pp. 332–336. ISSN: 0301-620X, 2044-5377. DOI: 10.1302/0301-620X.93B3.25322.

Könnecke, Ireen et al. (July 1, 2014). "T and B Cells Participate in Bone Repair by Infiltrating the Fracture Callus in a Two-Wave Fashion". In: *Bone* 64, pp. 155–165. ISSN: 8756-3282. DOI: 10.1016/j.bone.2014.03.052.

Kovach, Tracy K., Abhijit S. Dighe, Peter I. Lobo, and Quanjun Cui (2015). "Interactions between MSCs and Immune Cells: Implications for Bone Healing". In: *Journal of Immunology Research* 2015. DOI: 10.1155/2015/752510. pmid: 26000315.

Kovtun, Anna, S. Bergdolt, R. Wiegner, P. Radermacher, M. Huber-Lang, and A. Ignatius (2016). "The Crucial Role of Neutrophil Granulocytes in Bone Fracture Healing". In: *Eur Cell Mater* 32, pp. 152–162. ISSN: 1473-2262. pmid: 27452963.

Kreuz, P. C., M. R. Steinwachs, C. Erggelet, S. J. Krause, G. Konrad, M. Uhl, and N. Südkamp (Nov. 2006). "Results after microfracture of full-thickness chondral defects in different compartments in the knee". eng. In: *Osteoarthritis and Cartilage* 14.11, pp. 1119–1125. ISSN: 1063-4584. DOI: 10.1016/j.joca.2006.05.003.

Kroner, Jochen, Anna Kovtun, Julia Kemmler, et al. (Dec. 1, 2017). "Mast Cells Are Critical Regulators of Bone Fracture–Induced Inflammation and Osteoclast Formation and Activity". In: *Journal of Bone and Mineral Research* 32.12, pp. 2431–2444. ISSN: 1523-4681. DOI: 10.1002/jbmr.3234.

Kroner, Jochen, Anna Kovtun, Joanna Messmann, Gudrun Strauss, Sebastian Seitz, Thorsten Schinke, Anne Dudeck, and Anita Ignatius (Apr. 21, 2016). "Mast Cells Regulate Inflammation and Bone Regeneration in Fracture Healing". In: 43rd Annual European Calcified Tissue Society Congress. BioScientifica. DOI: 10.1530/boneabs.5.P45.

Kuhns, Michael S., Mark M. Davis, and K. Christopher Garcia (Feb. 2006). "Deconstructing the Form and Function of the TCR/CD3 Complex". In: *Immunity* 24.2, pp. 133–139. ISSN: 1074-7613. DOI: 10.1016/j.immuni.2006.01.006. pmid: 16473826.

Kuri-Harcuch, Walid, Leigh S. Wise, and Howard Green (May 1, 1978). "Interruption of the Adipose Conversion of 3T3 Cells by Biotin Deficiency: Differentiation without Triglyceride Accumulation". In: *Cell* 14.1, pp. 53–59. ISSN: 0092-8674, 1097-4172. DOI: 10.1016/0092-8674(78)90300-8. pmid: 667936.

Labek, G., M. Thaler, W. Janda, M. Agreiter, and B. Stöckl (Mar. 2011). "Revision Rates after Total Joint Replacement: Cumulative Results from Worldwide Joint Register Datasets". In: *J Bone Joint Surg Br* 93.3, pp. 293–297. ISSN: 2044-5377. DOI: 10.1302/0301-620X.93B3.25467. pmid: 21357948.

Lacey, David L., William J. Boyle, W. Scott Simonet, Paul J. Kostenuik, William C. Dougall, John K. Sullivan, Javier San Martin, and Roger Dansey (May 2012). "Bench to Bedside: Elucidation of the OPG–RANK–RANKL Pathway and the Development of Denosumab". In: *Nature Reviews Drug Discovery* 11.5, pp. 401–419. ISSN: 1474-1784. DOI: 10.1038/nrd3705.

Laird, S. M., R. Widdowson, M. El-Sheikhi, A. J. Hall, and T. C. Li (May 1, 2011). "Expression of CXCL12 and CXCR4 in Human Endometrium; Effects of CXCL12 on MMP Production by Human Endometrial Cells". In: *Hum Reprod* 26.5, pp. 1144–1152. ISSN: 0268-1161. DOI: 10.1093/humrep/der043.

Lalu, Manoj M. et al. (Nov. 17, 2016). "Evaluating Mesenchymal Stem Cell Therapy for Sepsis with Preclinical Meta-Analyses Prior to Initiating a First-in-Human Trial". In: *Elife* 5. ISSN: 2050-084X. DOI: 10.7554/eLife.17850. pmid: 27870924.

Landmann, Regine, Susanne Link, Sebastiano Sansano, Zarko Rajacic, and Werner Zimmerli (May 1998). "Soluble CD14 Activates Monocytic Cells Independently of Lipopolysaccharide". In: *Infect Immun* 66.5, pp. 2264–2271. ISSN: 0019-9567. pmid: 9573116.

Langenbach, Fabian and Jörg Handschel (Sept. 30, 2013). "Effects of Dexamethasone, Ascorbic Acid and -Glycerophosphate on the Osteogenic Differentiation of Stem Cells in Vitro". In: *Stem Cell Research & Therapy* 4.5, p. 117. ISSN: 1757-6512. DOI: 10.1186/scrt328.

Laranjeira, Paula et al. (2015). "Human Bone Marrow-Derived Mesenchymal Stromal Cells Differentially Inhibit Cytokine Production by Peripheral Blood Monocytes Subpopulations and Myeloid Dendritic Cells". In: *Stem Cells Int* 2015. ISSN: 1687-966X. DOI: 10.1155/2015/819084. pmid: 26060498.

Lardner, Anne (Jan. 4, 2001). "The Effects of Extracellular pH on Immune Function". In: *J Leukoc Biol* 69.4, pp. 522–530. ISSN: 0741-5400, 1938-3673. pmid: 11310837.

Le Blanc, Katarina and Lindsay C. Davies (Mar. 1, 2018). "MSCs—Cells with Many Sides". In: *Cytotherapy* 20.3, pp. 273–278. ISSN: 1465-3249. DOI: 10.1016/j.jcyt.2018.01.009.

Lebert-Ghali, Charles-Etienne, Carole Bonkoungou, Marilaine Fournier, Aditi Sood, and Heather J. Melichar (May 1, 2017). "Modulation of T Cell Function by CD271". In: *The Journal of Immunology* 198 (1 Supplement), pp. 80.17–80.17. ISSN: 0022-1767, 1550-6606.

Lech, Maciej and Hans-Joachim Anders (July 1, 2013). "Macrophages and Fibrosis: How Resident and Infiltrating Mononuclear Phagocytes Orchestrate All Phases of Tissue Injury and Repair". In: *Biochimica et Biophysica Acta (BBA) - Molecular Basis of Disease*. Fibrosis: Translation of Basic Research to Human Disease 1832.7, pp. 989–997. ISSN: 0925-4439. DOI: 10.1016/j.bbadis.2012.12.001.

Lee, Kevin B. L., Victor T. Z. Wang, Yiong Huak Chan, and James H. P. Hui (Nov. 2012). "A Novel, Minimally-Invasive Technique of Cartilage Repair in the Human Knee Using Arthroscopic Microfracture and Injections of Mesenchymal Stem Cells and Hyaluronic Acid–a Prospective Comparative Study on Safety and Short-Term Efficacy". In: *Ann. Acad. Med. Singap.* 41.11, pp. 511–517. ISSN: 0304-4602. pmid: 23235728.

Lee, Kevin, James H.P. Hui, Im Chim Song, Lenny Ardany, and Eng Hin Lee (Nov. 1, 2007). "Injectable Mesenchymal Stem Cell Therapy for Large Cartilage Defects—A Porcine Model". In: *STEM CELLS* 25.11, pp. 2964–2971. ISSN: 1549-4918. DOI: 10.1634/stemcells.2006-0311.

Li, Junhong et al. (June 2017). "Pro-Inflammatory Effects of the Th1 Chemokine CXCL10 in Acquired Aplastic Anaemia". In: *Cytokine* 94, pp. 45–51. ISSN: 1096-0023. DOI: 10.1016/j.cyto.2017.04.010. pmid: 28411045.

Li, Shu-Hong et al. (May 1, 2009). "Tracking Cardiac Engraftment and Distribution of Implanted Bone Marrow Cells: Comparing Intra-Aortic, Intravenous, and Intramyocardial Delivery". In: *The Journal of Thoracic and Cardiovascular Surgery* 137.5, 1225–1233.e1. ISSN: 0022-5223. DOI: 10.1016/j.jtcvs.2008.11.001.

Li, Yan, Gianluca Toraldo, Aimin Li, Xiaoying Yang, Hongying Zhang, Wei-Ping Qian, and M. Neale Weitzmann (May 1, 2007). "B Cells and T Cells Are Critical for the Preservation of Bone Homeostasis and Attainment of Peak Bone Mass in Vivo". In: *Blood* 109.9, pp. 3839–3848. ISSN: 0006-4971. DOI: 10.1182/blood-2006-07-037994. pmid: 17202317.

Li, Zhong (2013). "CD133: A Stem Cell Biomarker and Beyond". In: *Exp Hematol Oncol* 2, p. 17. ISSN: 2162-3619. DOI: 10.1186/2162-3619-2-17. pmid: 23815814.

Lin, Hang, Thomas P. Lozito, Peter G. Alexander, Riccardo Gottardi, and Rocky S. Tuan (July 7, 2014). "Stem Cell-Based Microphysiological Osteochondral System to Model Tissue Response to Interleukin-1". In: *Mol Pharm* 11.7, pp. 2203–2212. ISSN: 1543-8384. DOI: 10.1021/mp500136b. pmid: 24830762.

Lin, Haotian et al. (Mar. 2016). "Lens Regeneration Using Endogenous Stem Cells with Gain of Visual Function". In: *Nature* 531.7594, pp. 323–328. ISSN: 1476-4687. DOI: 10.1038/nature17181.

Lipinksi, Michael J. and Stephen E. Epstein (Aug. 29, 2016). "Mesenchymal Stem Cells Grown under Chronic Hypoxia Traffic to Regions of Myocardial Infarction, Suppress Splenic Natural

Killer Cells, and Attenuate Adverse Remodeling in Mice with Large Acute MI". In: *Mesenchymal Stem Cells Grown under Chronic Hypoxia Traffic to Regions of Myocardial Infarction, Suppress Splenic Natural Killer Cells, and Attenuate Adverse Remodeling in Mice with Large Acute MI*. European Society of Cardiology (ESC) Congress. In collab. with Dror Luger, Peter C. Westman, David K. Glover, Julien Dimastromatteo, Juan Carlos Frias, M. Teresa Albelda, Sergey Sikora, and Ron Waksman.

Liu, Mingli, Shanchun Guo, Jacqueline M. Hibbert, Vidhan Jain, Neeru Singh, Nana O. Wilson, and Jonathan K. Stiles (June 2011). "CXCL10/IP-10 in Infectious Diseases Pathogenesis and Potential Therapeutic Implications". In: *Cytokine Growth Factor Rev* 22.3, pp. 121–130. ISSN: 1359-6101. DOI: 10.1016/j.cytogfr.2011.06.001. pmid: 21802343.

Loeffler, David A., Gloria H. Heppner, and Paul L. Juneau (July 30, 1991). "Natural Killer-Cell Activity under Conditions Reflective of Tumor Micro-Environment". In: *International Journal of Cancer* 48.6, pp. 895–899. ISSN: 1097-0215. DOI: 10.1002/ijc.2910480617.

Loi, Florence, Luis A. Córdova, Jukka Pajarinen, Tzu-hua Lin, Zhenyu Yao, and Stuart B. Goodman (May 2016). "Inflammation, Fracture and Bone Repair". In: *Bone* 86, pp. 119–130. ISSN: 8756-3282. DOI: 10.1016/j.bone.2016.02.020. pmid: 26946132.

Lonza (2018). *Fresh Unprocessed Bone Marrow*. URL: https://www.lonza.com/products-services/bio-research/primary-cells/hematopoietic-cells/unprocessed-bone-marrow.aspx (visited on 05/13/2018).

Lu, Laura Y. et al. (Nov. 2017). "Pro-Inflammatory M1 Macrophages Promote Osteogenesis by Mesenchymal Stem Cells via the COX-2-Prostaglandin E2 Pathway". In: *J. Orthop. Res.* 35.11, pp. 2378–2385. ISSN: 1554-527X. DOI: 10.1002/jor.23553. pmid: 28248001.

Luckheeram, Rishi Vishal, Rui Zhou, Asha Devi Verma, and Bing Xia (2012). *CD4*. URL: https://www.hindawi.com/journals/jir/2012/925135/ (visited on 04/22/2019).

Lydon, Helen, Alan Getgood, and Frances M. D. Henson (June 1, 2017). "Healing of Osteochondral Defects via Endochondral Ossification in an Ovine Model". In: *Cartilage*, p. 1947603517713818. ISSN: 1947-6043. DOI: 10.1177/1947603517713818. pmid: 28629234.

Magnusson, K. et al. (June 1, 2017). "Genetic Factors Contribute More to Hip than Knee Surgery Due to Osteoarthritis – a Population-Based Twin Registry Study of Joint Arthroplasty". In: *Osteoarthritis and Cartilage* 25.6, pp. 878–884. ISSN: 1063-4584. DOI: 10.1016/j.joca.2016.12.015.

Małkiewicz, Agata and Magdalena Dziedzic (2012). "Bone Marrow Reconversion – Imaging of Physiological Changes in Bone Marrow". In: *Pol J Radiol* 77.4, pp. 45–50. ISSN: 1733-134X. pmid: 23269936.

Marędziak, Monika, Krzysztof Marycz, Krzysztof A. Tomaszewski, Katarzyna Kornicka, and Brandon Michael Henry (2016). "The Influence of Aging on the Regenerative Potential of Human Adipose Derived Mesenchymal Stem Cells". In: *Stem Cells Int* 2016. ISSN: 1687-966X. DOI: 10.1155/2016/2152435. pmid: 26941800.

Margo, Bradley J., Craig S. Radnay, and Giles R. Scuderi (Feb. 1, 2010). "Anatomy of the Knee". In: *The Knee*. 0 vols. WORLD SCIENTIFIC, pp. 1–17. ISBN: 978-981-4282-03-1. DOI: 10.1142/9789814282048_0001.

Martin, Elizabeth (Sept. 17, 2015). *Concise Medical Dictionary*. Oxford University Press. ISBN: 978-0-19-968781-7.

Martinez, Fernando O. and Siamon Gordon (Mar. 3, 2014). "The M1 and M2 Paradigm of Macrophage Activation: Time for Reassessment". In: *F1000Prime Rep* 6. ISSN: 2051-7599. DOI: 10.12703/P6-13. pmid: 24669294.

Massicotte, Frédéric (2011). "Epidemiology of Osteoarthritis". In: *Martel-Pelletier J, Pelletier J-P, eds. Understanding Osteoarthritis From Bench to Bedside. Kerala, India: Research Signpost*, p. 26.

McKeown, S R (Mar. 2014). "Defining Normoxia, Physoxia and Hypoxia in Tumours—Implications for Treatment Response". In: *Br J Radiol* 87.1035. ISSN: 0007-1285. DOI: 10.1259/bjr.20130676. pmid: 24588669.

Mehrotra, Meenal, Christopher R. Williams, Makio Ogawa, and Amanda C. LaRue (Jan. 2013). "Hematopoietic Stem Cells Give Rise to Osteo-Chondrogenic Cells". In: *Blood Cells, Molecules, and Diseases* 50.1, pp. 41–49. ISSN: 1079-9796. DOI: 10.1016/j.bcmd.2012.08.003.

Melief, Sara M., Sacha B. Geutskens, Willem E. Fibbe, and Helene Roelofs (June 1, 2013). "Multipotent Stromal Cells Skew Monocytes towards an Anti-Inflammatory Interleukin-10-Producing Phenotype by Production of Interleukin-6". In: *Haematologica* 98.6, pp. 888–895. ISSN: 0390-6078, 1592-8721. DOI: 10.3324/haematol.2012.078055. pmid: 23349310.

Méndez-Ferrer, Simón et al. (Aug. 12, 2010). "Mesenchymal and Haematopoietic Stem Cells Form a Unique Bone Marrow Niche". In: *Nature* 466.7308, pp. 829–834. ISSN: 0028-0836. DOI: 10.1038/nature09262. pmid: 20703299.

Menti, C., M. Beltrami, A. L. Possan, S. T. Martins, J. A. P. Henriques, A. D. Santos, F. P. Missell, and M. Roesch-Ely (July 1, 2016). "Biocompatibility and Degradation of Gold-Covered Magneto-Elastic Biosensors Exposed to Cell Culture". In: *Colloids and Surfaces B: Biointerfaces* 143, pp. 111–117. ISSN: 0927-7765. DOI: 10.1016/j.colsurfb.2016.03.034.

Merad, Miriam, Priyanka Sathe, Julie Helft, Jennifer Miller, and Arthur Mortha (2013). "The Dendritic Cell Lineage: Ontogeny and Function of Dendritic Cells and Their Subsets in the Steady State and the Inflamed Setting". In: *Annu Rev Immunol* 31. ISSN: 0732-0582. DOI: 10.1146/annurev-immunol-020711-074950. pmid: 23516985.

MHRA (2015). *Advanced Therapy Medicinal Products: Regulation and Licensing*. URL: https://www.gov.uk/guidance/advanced-therapy-medicinal-products-regulation-and-licensing (visited on 06/16/2019).

Milgram, James W. (July 1991). "Nonunion and Pseudarthrosis of Fracture Healing: A Histopathologic Study of 95 Human Specimens." In: *Clinical Orthopaedics and Related Research* 268, p. 203.

Millis, Darryl L. (2014). "7 - Responses of Musculoskeletal Tissues to Disuse and Remobilization". In: *Canine Rehabilitation and Physical Therapy (Second Edition)*. St. Louis: W.B. Saunders, pp. 92–153. ISBN: 978-1-4377-0309-2. DOI: 10.1016/B978-1-4377-0309-2.00007-7.

Mills, Caroline N, Sandeep S Joshi, and Richard M Niles (Nov. 17, 2009). "Expression and Function of Hypoxia Inducible Factor-1 Alpha in Human Melanoma under Non-Hypoxic Conditions". In: *Mol Cancer* 8, p. 104. ISSN: 1476-4598. DOI: 10.1186/1476-4598-8-104. pmid: 19919690.

Milosavljevic, Neda, Marina Gazdic, Bojana Simovic Markovic, Aleksandar Arsenijevic, Jasmin Nurkovic, Zana Dolicanin, Valentin Djonov, Miodrag L. Lukic, and Vladislav Volarevic (Aug. 2017). "Mesenchymal Stem Cells Attenuate Acute Liver Injury by Altering Ratio between Interleukin 17 Producing and Regulatory Natural Killer T Cells". In: *Liver Transpl.* 23.8, pp. 1040–1050. ISSN: 1527-6473. DOI: 10.1002/lt.24784. pmid: 28481005.

Mithoefer, Kai, Vivek Venugopal, and Moiz Manaqibwala (Aug. 1, 2016). "Incidence, Degree, and Clinical Effect of Subchondral Bone Overgrowth After Microfracture in the Knee , Incidence, Degree, and Clinical Effect of Subchondral Bone Overgrowth After Microfracture in the Knee". In: *Am J Sports Med* 44.8, pp. 2057–2063. ISSN: 0363-5465. DOI: 10.1177/0363546516645514.

Moffett, John R. and Ma Aryan Namboodiri (Aug. 2003). "Tryptophan and the Immune Response". In: *Immunol. Cell Biol.* 81.4, pp. 247–265. ISSN: 0818-9641. DOI: 10.1046/j.1440-1711.2003.t01-1-01177.x. pmid: 12848846.

Moioli, Eduardo K., Paul A. Clark, Mo Chen, James E. Dennis, Helaman P. Erickson, Stanton L. Gerson, and Jeremy J. Mao (Dec. 15, 2008). "Synergistic Actions of Hematopoietic and Mesenchymal Stem/Progenitor Cells in Vascularizing Bioengineered Tissues". In: *PLOS ONE* 3.12, e3922. ISSN: 1932-6203. DOI: 10.1371/journal.pone.0003922.

Monie, Tom P. (Jan. 1, 2017). "Section 1 - A Snapshot of the Innate Immune System". In: *The Innate Immune System*. Ed. by Tom P. Monie. Academic Press, pp. 1–40. ISBN: 978-0-12-804464-3. DOI: 10.1016/B978-0-12-804464-3.00001-6.

Moniri, Mani, Ada Young, Kelsey Reinheimer, Jarrett Rayat, Long-jun Dai, and Garth Warnock (Jan. 19, 2014). "Dynamic Assessment of Cell Viability, Proliferation and Migration Using Real Time Cell Analyzer System (RTCA)". In: *Cytotechnology* 67. DOI: 10.1007/s10616-014-9692-5.

Moodley, Kriebashne, Catherine E. Angel, Michelle Glass, and E. Scott Graham (Sept. 15, 2011). "Real-Time Profiling of NK Cell Killing of Human Astrocytes Using xCELLigence Technology". In: *J. Neurosci. Methods* 200.2, pp. 173–180. ISSN: 1872-678X. DOI: 10.1016/j.jneumeth.2011.07.005. pmid: 21781988.

Morrison, Sean J. and David T. Scadden (Jan. 16, 2014). "The Bone Marrow Niche for Haematopoietic Stem Cells". In: *Nature* 505.7483, pp. 327–334. ISSN: 0028-0836. DOI: 10.1038/nature12984.

Mountziaris, Paschalia M. and Antonios G. Mikos (June 2008). "Modulation of the Inflammatory Response for Enhanced Bone Tissue Regeneration". In: *Tissue Eng Part B Rev* 14.2, pp. 179–186. ISSN: 1937-3368. DOI: 10.1089/ten.teb.2008.0038. pmid: 18544015.

Moussa, Mayssam, Daniel Lajeunesse, George Hilal, Oula El Atat, Gaby Haykal, Rim Serhal, Antonio Chalhoub, Charbel Khalil, and Nada Alaaeddine (Mar. 1, 2017). "Platelet Rich Plasma (PRP) Induces Chondroprotection via Increasing Autophagy, Anti-Inflammatory Markers, and Decreasing Apoptosis in Human Osteoarthritic Cartilage". In: *Experimental Cell Research* 352.1, pp. 146–156. ISSN: 0014-4827. DOI: 10.1016/j.yexcr.2017.02.012.

Mukherjee, Ratnadeep, Pijus Kanti Barman, Pravat Kumar Thatoi, Rina Tripathy, Bidyut Kumar Das, and Balachandran Ravindran (Sept. 11, 2015). "Non-Classical Monocytes Display Inflammatory Features: Validation in Sepsis and Systemic Lupus Erythematous". In: *Scientific Reports* 5, p. 13886. ISSN: 2045-2322. DOI: 10.1038/srep13886.

Murphy, Evelyn P., Christopher Fenelon, Niall P. McGoldrick, and Stephen R. Kearns (Mar. 26, 2018). "Bone Marrow Aspirate Concentrate and Microfracture Technique for Talar Osteochondral Lesions of the Ankle". In: *Arthrosc Tech* 7.4, e391–e396. ISSN: 2212-6287. DOI: 10.1016/j.eats.2017.10.011. pmid: 29868410.

Muschler, G. F., H. Nitto, C. A. Boehm, and K. A. Easley (Jan. 2001). "Age- and Gender-Related Changes in the Cellularity of Human Bone Marrow and the Prevalence of Osteoblastic Progenitors". In: *J. Orthop. Res.* 19.1, pp. 117–125. ISSN: 0736-0266. DOI: 10.1016/S0736-0266(00)00010-3. pmid: 11332607.

Narbona-Carceles, Javier, Javier Vaquero, Susana Suárez-Sancho B.s, Francisco Forriol, and Maria Eugenia Fernández-Santos (Oct. 1, 2014). "Bone Marrow Mesenchymal Stem Cell Aspirates from Alternative Sources Is the Knee as Good as the Iliac Crest?" In: *Injury* 45, S42–S47. ISSN: 0020-1383, 1879-0267. DOI: 10.1016/S0020-1383(14)70009-9.

NCBI (2019). *HLA-DRA Major Histocompatibility Complex, Class II, DR Alpha [Homo Sapiens (Human)] - Gene - NCBI*. URL: https://www.ncbi.nlm.nih.gov/gene/3122 (visited on 04/22/2019).

Néron, Sonia, Louis Thibault, Nathalie Dussault, Geneviève Côté, Éric Ducas, Nicolas Pineault, and Annie Roy (June 1, 2007). "Characterization of Mononuclear Cells Remaining in the Leukoreduction System Chambers of Apheresis Instruments after Routine Platelet Collection: A New Source of Viable Human Blood Cells". In: *Transfusion* 47.6, pp. 1042–1049. ISSN: 1537-2995. DOI: 10.1111/j.1537-2995.2007.01233.x.

Newman, R. J., M. J. Francis, and R. B. Duthie (Mar. 1987). "Nuclear Magnetic Resonance Studies of Experimentally Induced Delayed Fracture Union". In: *Clin. Orthop. Relat. Res.* 216, pp. 253–261. ISSN: 0009-921X. pmid: 3815955.

Ni, Maoshing (May 10, 1995). *The Yellow Emperor's Classic of Medicine: A New Translation of the Neijing Suwen with Commentary*. Shambhala Publications. 339 pp. ISBN: 978-0-8348-2576-5.

NICE (2014). *NICE CG177*. URL: https://www.nice.org.uk/guidance/CG177/chapter/Key-priorities-for-implementation (visited on 10/16/2015).

– (Oct. 4, 2017). *Autologous Chondrocyte Implantation for Treating Symptomatic Articular Cartilage Defects of the Knee*. URL: https://www.nice.org.uk/guidance/ta477/chapter/1-Recommendations (visited on 08/28/2018).

– (2018). *Mosaicplasty for Symptomatic Articular Cartilage Defects of the Knee | Guidance and Guidelines | NICE*. URL: https://www.nice.org.uk/guidance/ipg607 (visited on 08/12/2018).

Nicolaidou, Vicky, Mei Mei Wong, Andia N. Redpath, Adel Ersek, Dilair F. Baban, Lynn M. Williams, Andrew P. Cope, and Nicole J. Horwood (2012). "Monocytes Induce STAT3 Activation in Human

Mesenchymal Stem Cells to Promote Osteoblast Formation". In: *PLoS ONE* 7.7, e39871. ISSN: 1932-6203. DOI: 10.1371/journal.pone.0039871. pmid: 22802946.

Niu, Ping et al. (July 14, 2015). "Transcriptional Profiling of Interleukin-2-Primed Human Adipose Derived Mesenchymal Stem Cells Revealed Dramatic Changes in Stem Cells Response Imposed by Replicative Senescence". In: *Oncotarget* 6.20, pp. 17938–17957. ISSN: 1949-2553. pmid: 26255627.

Noulin, Florian, Céline Borlon, Peter van den Eede, Luc Boel, Catherine M. Verfaillie, Umberto D'Alessandro, and Annette Erhart (Feb. 20, 2013). *Expression of Reticulocyte Surface Markers by Flow Cytometry*. DOI: 10.1371/journal.pone.0040798.g003.

Obregon, Maria-Jesus (Feb. 2008). "Thyroid Hormone and Adipocyte Differentiation". In: *Thyroid* 18.2, pp. 185–195. ISSN: 1050-7256. DOI: 10.1089/thy.2007.0254. pmid: 18279019.

Ochoa, Maria Teresa, Anya Loncaric, Stephan R. Krutzik, Todd C. Becker, and Robert L. Modlin (Sept. 1, 2008). ""Dermal Dendritic Cells" Comprise Two Distinct Populations: CD1+ Dendritic Cells and CD209+ Macrophages". In: *Journal of Investigative Dermatology* 128.9, pp. 2225–2231. ISSN: 0022-202X. DOI: 10.1038/jid.2008.56.

Ohnishi, Shunsuke, Takeshi Yasuda, Soichiro Kitamura, and Noritoshi Nagaya (May 2007). "Effect of Hypoxia on Gene Expression of Bone Marrow-Derived Mesenchymal Stem Cells and Mononuclear Cells". In: *Stem Cells* 25.5, pp. 1166–1177. ISSN: 10665099, 15494918. DOI: 10.1634/stemcells.2006-0347.

Ono, Takehito, Kazuo Okamoto, Tomoki Nakashima, Takeshi Nitta, Shohei Hori, Yoichiro Iwakura, and Hiroshi Takayanagi (Mar. 11, 2016). "IL-17-Producing T Cells Enhance Bone Regeneration". In: *Nature Communications* 7, p. 10928. ISSN: 2041-1723. DOI: 10.1038/ncomms10928.

Ono, Takehito and Hiroshi Takayanagi (Aug. 1, 2017). "Osteoimmunology in Bone Fracture Healing". In: *Curr Osteoporos Rep* 15.4, pp. 367–375. ISSN: 1544-1873, 1544-2241. DOI: 10.1007/s11914-017-0381-0.

Onofre, Gabriela, Martina Kolácková, Karolina Jankovicová, and Jan Krejsek (2009). "Scavenger Receptor CD163 and Its Biological Functions". In: *Acta Medica (Hradec Kralove)* 52.2, pp. 57–61. ISSN: 1211-4286. pmid: 19777868.

Orr, Mark T. and Lewis L. Lanier (Sept. 17, 2010). "Natural Killer Cell Education and Tolerance". In: *Cell* 142.6, pp. 847–856. ISSN: 0092-8674. DOI: 10.1016/j.cell.2010.08.031. pmid: 20850008.

Pajarinen, Jukka, Tzuhua Lin, Emmanuel Gibon, Yusuke Kohno, Masahiro Maruyama, Karthik Nathan, Laura Lu, Zhenyu Yao, and Stuart B. Goodman (Jan. 2, 2018). "Mesenchymal Stem Cell-Macrophage Crosstalk and Bone Healing". In: *Biomaterials*. ISSN: 0142-9612. DOI: 10.1016/j.biomaterials.2017.12.025.

Pan, Tianhong, Biao Huang, Weiping Zhang, Stephan Gabos, Dorothy Yu Huang, and Vignesh Devendran (Feb. 18, 2013). "Cytotoxicity Assessment Based on the AUC50 Using Multi-Concentration Time-Dependent Cellular Response Curves". In: *Analytica Chimica Acta* 764, pp. 44–52. ISSN: 0003-2670. DOI: 10.1016/j.aca.2012.12.047.

Pang, Jian, Hai-Ling Guo, Dao-Fang Ding, Yu-Yun Wu, Yong-Fang Zhao, Xin-Feng Gu, and Yu-Xin Zheng (2015). "Changes of Mesenchymal Stromal Cells Mobilization and Bone Turnover in an Experimental Bone Fracture Model in Ovariectomized Mice". In: *Int J Clin Exp Pathol* 8.9, pp. 10228–10238. ISSN: 1936-2625. pmid: 26617731.

Panteli, Michalis, Ippokratis Pountos, Elena Jones, and Peter V. Giannoudis (Apr. 1, 2015). "Biological and Molecular Profile of Fracture Non-Union Tissue: Current Insights". In: *J. Cell. Mol. Med.* 19.4, pp. 685–713. ISSN: 1582-4934. DOI: 10.1111/jcmm.12532.

Papke, Björn et al. (Apr. 20, 2016). "Identification of Pyrazolopyridazinones as PDE Inhibitors". In: *Nature Communications* 7, p. 11360. ISSN: 2041-1723. DOI: 10.1038/ncomms11360.

Park, Kun Taek, Mahmoud M. ElNaggar, Gaber S. Abdellrazeq, John P. Bannantine, Victoria Mack, Lindsay M. Fry, and William C. Davis (Oct. 20, 2016). "Phenotype and Function of CD209+ Bovine Blood Dendritic Cells, Monocyte-Derived-Dendritic Cells and Monocyte-Derived Macrophages". In: *PLOS ONE* 11.10, e0165247. ISSN: 1932-6203. DOI: 10.1371/journal.pone.0165247.

Paul, Gregory S. (Dec. 1, 2016). *The Princeton Field Guide to Dinosaurs*. 2nd. ISBN: 978-0-691-16766-4.

Pellicoro, Antonella, Prakash Ramachandran, John P. Iredale, and Jonathan A. Fallowfield (Mar. 2014). "Liver Fibrosis and Repair: Immune Regulation of Wound Healing in a Solid Organ". In: *Nat Rev Immunol* 14.3, pp. 181–194. ISSN: 1474-1733. DOI: 10.1038/nri3623.

Pence, Brandt D. and Jeffrey A. Woods (Jan. 1, 2014). "Exercise, Obesity, and Cutaneous Wound Healing: Evidence from Rodent and Human Studies". In: *Adv Wound Care (New Rochelle)* 3.1, pp. 71–79. ISSN: 2162-1918. DOI: 10.1089/wound.2012.0377. pmid: 24761347.

Petri, Maximilian et al. (Nov. 2013). "Repair of Segmental Long-Bone Defects by Stem Cell Concentrate Augmented Scaffolds: A Clinical and Positron Emission Tomography - Computed Tomography Analysis". In: *Int Orthop* 37.11, pp. 2231–2237. ISSN: 0341-2695. DOI: 10.1007/s00264-013-2087-y. pmid: 24013459.

Phinney, Donald G. and Mark F. Pittenger (2018). "Concise Review: MSC-Derived Exosomes for Cell-Free Therapy". In: *STEM CELLS* 35.4 (), pp. 851–858. ISSN: 1549-4918. DOI: 10.1002/stem.2575.

Pittenger, Mark F. et al. (Apr. 2, 1999). "Multilineage Potential of Adult Human Mesenchymal Stem Cells". In: *Science* 284.5411, pp. 143–147. ISSN: 0036-8075, 1095-9203. DOI: 10.1126/science.284.5411.143. pmid: 10102814.

Poggi, Alessandro, Claudia Prevosto, Anna-Maria Massaro, Simone Negrini, Serena Urbani, Ivana Pierri, Riccardo Saccardi, Marco Gobbi, and Maria Raffaella Zocchi (Nov. 15, 2005). "Interaction between Human NK Cells and Bone Marrow Stromal Cells Induces NK Cell Triggering: Role of NKp30 and NKG2D Receptors". In: *J. Immunol.* 175.10, pp. 6352–6360. ISSN: 0022-1767. pmid: 16272287.

Poli, Aurélie, Tatiana Michel, Maud Thérésine, Emmanuel Andrès, François Hentges, and Jacques Zimmer (Apr. 2009). "CD56bright Natural Killer (NK) Cells: An Important NK Cell Subset". In: *Immunology* 126.4, pp. 458–465. ISSN: 0019-2805. DOI: 10.1111/j.1365-2567.2008.03027.x. pmid: 19278419.

Potier, Esther, Elisabeth Ferreira, Rina Andriamanalijaona, Jean-Pierre Pujol, Karim Oudina, Delphine Logeart-Avramoglou, and Hervé Petite (Apr. 2007). "Hypoxia Affects Mesenchymal Stromal Cell Osteogenic Differentiation and Angiogenic Factor Expression". In: *Bone* 40.4, pp. 1078–1087. ISSN: 8756-3282. DOI: 10.1016/j.bone.2006.11.024. pmid: 17276151.

Prasanna, S. Jyothi, Divya Gopalakrishnan, Shilpa Rani Shankar, and Anoop Babu Vasandan (Feb. 2, 2010). "Pro-Inflammatory Cytokines, IFN and TNF, Influence Immune Properties of Human Bone Marrow and Wharton Jelly Mesenchymal Stem Cells Differentially". In: *PLOS ONE* 5.2, e9016. ISSN: 1932-6203. DOI: 10.1371/journal.pone.0009016.

Pridie, KH and G Gordon (Jan. 1959). "A Method of Resurfacing Osteoarthritic Knee Joints". In: *Journal of Bone and Joint Surgery* 41.3, pp. 618–619.

Pritzker, K. P. H., S. Gay, S. A. Jimenez, K. Ostergaard, J. -P. Pelletier, P. A. Revell, D. Salter, and W. B. van den Berg (Jan. 1, 2006). "Osteoarthritis Cartilage Histopathology: Grading and Staging". In: *Osteoarthritis and Cartilage* 14.1, pp. 13–29. ISSN: 1063-4584. DOI: 10.1016/j.joca.2005.07.014.

Promega (2018). *Celltox-Green-Cytotoxicity-Assay-Protocol.Pdf*. URL: https://www.promega.com/-/media/files/resources/protocols/technical-manuals/101/celltox-green-cytotoxicity-assay-protocol.pdf (visited on 06/25/2018).

Puchtler, Holde, Susan N. Meloan, and Mary S. Terry (Feb. 1969). "ON THE HISTORY AND MECHANISM OF ALIZARIN AND ALIZARIN RED S STAINS FOR CALCIUM". In: *Journal of Histochemistry & Cytochemistry* 17.2, pp. 110–124. ISSN: 0022-1554, 1551-5044. DOI: 10.1177/17.2.110.

Qian, Li-Wu, Andrea B. Fourcaudot, Kazuyoshi Yamane, Tao You, Rodney K. Chan, and Kai P. Leung (Jan. 1, 2016). "Exacerbated and Prolonged Inflammation Impairs Wound Healing and Increases Scarring". In: *Wound Repair and Regeneration* 24.1, pp. 26–34. ISSN: 1524-475X. DOI: 10.1111/wrr.12381.

Quevedo, Henry C. et al. (Aug. 18, 2009). "Allogeneic Mesenchymal Stem Cells Restore Cardiac Function in Chronic Ischemic Cardiomyopathy via Trilineage Differentiating Capacity". In: *Proc Natl Acad Sci U S A* 106.33, pp. 14022–14027. ISSN: 0027-8424. DOI: 10.1073/pnas.0903201106. pmid: 19666564.

Quinlan, Elaine, Adolfo López-Noriega, Emmet Thompson, Helena M. Kelly, Sally Ann Cryan, and Fergal J. O'Brien (Jan. 28, 2015). "Development of Collagen–Hydroxyapatite Scaffolds Incorporating PLGA and Alginate Microparticles for the Controlled Delivery of rhBMP-2 for Bone Tissue Engineering". In: *Journal of Controlled Release* 198, pp. 71–79. ISSN: 0168-3659. DOI: 10.1016/j.jconrel.2014.11.021.

Raheja, Leah F., Damian C. Genetos, Alice Wong, and Clare E. Yellowley (2011). "Hypoxic Regulation of Mesenchymal Stem Cell Migration: The Role of RhoA and HIF-1". In: *Cell Biology International* 35.10, pp. 981–989. ISSN: 1095-8355. DOI: 10.1042/CBI20100733.

Ramirez-GarciaLuna, Jose Luis et al. (Mar. 28, 2017). "Defective Bone Repair in Mast Cell-Deficient Cpa3Cre/+ Mice". In: *PLoS One* 12.3. ISSN: 1932-6203. DOI: 10.1371/journal.pone.0174396. pmid: 28350850.

Rapp, Anna E., Ronny Bindl, Stefan Recknagel, Annika Erbacher, Ingo Müller, Hubert Schrezenmeier, Christian Ehrnthaller, Florian Gebhard, and Anita Ignatius (Feb. 5, 2016). "Fracture Healing Is Delayed in Immunodeficient NOD/Scid- IL2R Cnull Mice". In: *PLOS ONE* 11.2, e0147465. ISSN: 1932-6203. DOI: 10.1371/journal.pone.0147465.

Rasmusson, Ida, Olle Ringdén, Berit Sundberg, and Katarina Le Blanc (Oct. 27, 2003). "Mesenchymal Stem Cells Inhibit the Formation of Cytotoxic T Lymphocytes, but Not Activated Cytotoxic T Lymphocytes or Natural Killer Cells". In: *Transplantation* 76.8, pp. 1208–1213. ISSN: 0041-1337. DOI: 10.1097/01.TP.0000082540.43730.80. pmid: 14578755.

Rees, Peter Adam, Nicholas Stuart Greaves, Mohamed Baguneid, and Ardeshir Bayat (Nov. 1, 2015). "Chemokines in Wound Healing and as Potential Therapeutic Targets for Reducing Cutaneous Scarring". In: *Adv Wound Care (New Rochelle)* 4.11, pp. 687–703. ISSN: 2162-1918. DOI: 10.1089/wound.2014.0568. pmid: 26543682.

Reinke, Simon et al. (Mar. 20, 2013). "Terminally Differentiated CD8+ T Cells Negatively Affect Bone Regeneration in Humans". In: *Science Translational Medicine* 5.177, 177ra36–177ra36. ISSN: 1946-6234, 1946-6242. DOI: 10.1126/scitranslmed.3004754. pmid: 23515078.

Riboldi, Elena, Chiara Porta, Sara Morlacchi, Antonella Viola, Alberto Mantovani, and Antonio Sica (Feb. 1, 2013). "Hypoxia-Mediated Regulation of Macrophage Functions in Pathophysiology". In: *Int Immunol* 25.2, pp. 67–75. ISSN: 0953-8178. DOI: 10.1093/intimm/dxs110.

Ridiandries, Anisyah, Joanne T. M. Tan, and Christina A. Bursill (Oct. 18, 2018). "The Role of Chemokines in Wound Healing". In: *Int J Mol Sci* 19.10. ISSN: 1422-0067. DOI: 10.3390/ijms19103217. pmid: 30340330.

Rio, Donald C., Manuel Ares, Gregory J. Hannon, and Timothy W. Nilsen (Jan. 6, 2010). "Purification of RNA Using TRIzol (TRI Reagent)". In: *Cold Spring Harb Protoc* 2010.6, pdb.prot5439. ISSN: 1940-3402, 1559-6095. DOI: 10.1101/pdb.prot5439. pmid: 20516177.

Rodrigues, Natacha, Matthew Benning, Ana M. Ferreira, Luke Dixon, and Kenny Dalgarno (Jan. 1, 2016). "Manufacture and Characterisation of Porous PLA Scaffolds". In: *Procedia CIRP*. The Second CIRP Conference on Biomanufacturing 49, pp. 33–38. ISSN: 2212-8271. DOI: 10.1016/j.procir.2015.07.025.

Rodríguez-Merchán, E. Carlos and Alexander D. Liddle (Nov. 15, 2016). *Joint Preservation in the Adult Knee*. Springer. 182 pp. ISBN: 978-3-319-41808-7.

Roemeling-Van Rhijn, M. et al. (2013). "Effects of Hypoxia on the Immunomodulatory Properties of Adipose Tissue-Derived Mesenchymal Stem Cells". In: *Front. Immunol.* 4. ISSN: 1664-3224. DOI: 10.3389/fimmu.2013.00203.

Rosová, Ivana, Mo Dao, Ben Capoccia, Daniel Link, and Jan A. Nolta (Aug. 2008). "Hypoxic Preconditioning Results in Increased Motility and Improved Therapeutic Potential of Human

Mesenchymal Stem Cells". In: *Stem Cells* 26.8, pp. 2173–2182. ISSN: 1066-5099. DOI: 10.1634/stemcells.2007-1104. pmid: 18511601.

Rothschild, Bruce M., Zheng Xiaoting, and Larry D. Martin (June 1, 2012). "Osteoarthritis in the Early Avian Radiation: Earliest Recognition of the Disease in Birds". In: *Cretaceous Research* 35 (Supplement C), pp. 178–180. ISSN: 0195-6671. DOI: 10.1016/j.cretres.2011.12.008.

Russell, Keith A., Natalie H. C. Chow, David Dukoff, Thomas W. G. Gibson, Jonathan LaMarre, Dean H. Betts, and Thomas G. Koch (2016). "Characterization and Immunomodulatory Effects of Canine Adipose Tissue- and Bone Marrow-Derived Mesenchymal Stromal Cells". In: *PLOS ONE* 11.12, e0167442. ISSN: 1932-6203. DOI: 10.1371/journal.pone.0167442.

Sacchetti, Benedetto et al. (Oct. 19, 2007). "Self-Renewing Osteoprogenitors in Bone Marrow Sinusoids Can Organize a Hematopoietic Microenvironment". In: *Cell* 131.2, pp. 324–336. ISSN: 0092-8674, 1097-4172. DOI: 10.1016/j.cell.2007.08.025. pmid: 17956733.

Samadelli, Marco, Marcello Melis, Matteo Miccoli, Eduard Egarter Vigl, and Albert R. Zink (Sept. 1, 2015). "Complete Mapping of the Tattoos of the 5300-Year-Old Tyrolean Iceman". In: *Journal of Cultural Heritage* 16.5, pp. 753–758. ISSN: 1296-2074. DOI: 10.1016/j.culher.2014.12.005.

Sarkar, Subhashis, Wilfred T. V. Germeraad, Kasper M. A. Rouschop, Elisabeth M. P. Steeghs, Michel van Gelder, Gerard M. J. Bos, and Lotte Wieten (May 28, 2013). "Hypoxia Induced Impairment of NK Cell Cytotoxicity against Multiple Myeloma Can Be Overcome by IL-2 Activation of the NK Cells". In: *PLOS ONE* 8.5, e64835. ISSN: 1932-6203. DOI: 10.1371/journal.pone.0064835.

Saudemont, Aurore, Nathalie Jouy, Dominique Hetuin, and Bruno Quesnel (Mar. 15, 2005). "NK Cells That Are Activated by CXCL10 Can Kill Dormant Tumor Cells That Resist CTL-Mediated Lysis and Can Express B7-H1 That Stimulates T Cells". In: *Blood* 105.6, pp. 2428–2435. ISSN: 0006-4971. DOI: 10.1182/blood-2004-09-3458. pmid: 15536145.

Saw, Khay-Yong (Apr. 2011). "Articular Cartilage Regeneration With Autologous Peripheral Blood Progenitor Cells and Hyaluronic Acid After Arthroscopic Subchondral Drilling: A Report of 5 Cases With Histology". In: *Arthroscopy: The Journal of Arthroscopic & Related Surgery* 27.4. In collab. with Adam Anz, Shahrin Merican, Yong-Guan Tay, Kunaseegaran Ragavanaidu, Caroline S. Y. Jee, and David A. McGuire, pp. 493–506. ISSN: 0749-8063. DOI: 10.1016/j.arthro.2010.11.054.

– (Apr. 2013). "Articular Cartilage Regeneration With Autologous Peripheral Blood Stem Cells Versus Hyaluronic Acid: A Randomized Controlled Trial". In: *Arthroscopy: The Journal of Arthroscopic & Related Surgery* 29.4. In collab. with Caroline Siew-Yoke Jee, Shahrin Merican, Reza Ching-Soong Ng, Sharifah A. Roohi, and Kunaseegaran Ragavanaidu, pp. 684–694. ISSN: 0749-8063. DOI: 10.1016/j.arthro.2012.12.008.

Saw, Khay-Yong, Paisal Hussin, Seng-Cheong Loke, Mohd Azam, Hui-Cheng Chen, Yong-Guan Tay, Sharon Low, Keng-Ling Wallin, and Kunaseegaran Ragavanaidu (Dec. 2009). "Articular Cartilage Regeneration With Autologous Marrow Aspirate and Hyaluronic Acid: An Experimental Study in a Goat Model". In: *Arthroscopy: The Journal of Arthroscopic & Related Surgery* 25.12, pp. 1391–1400. ISSN: 0749-8063. DOI: 10.1016/j.arthro.2009.07.011.

Schäfer, Matthias and Sabine Werner (Aug. 2008). "Cancer as an Overhealing Wound: An Old Hypothesis Revisited". In: *Nature Reviews Molecular Cell Biology* 9.8, pp. 628–638. ISSN: 1471-0080. DOI: 10.1038/nrm2455.

Schell, H., G. N. Duda, A. Peters, S. Tsitsilonis, K. A. Johnson, and K. Schmidt-Bleek (Feb. 7, 2017). "The Haematoma and Its Role in Bone Healing". In: *Journal of Experimental Orthopaedics* 4, p. 5. ISSN: 2197-1153. DOI: 10.1186/s40634-017-0079-3.

Schenk, Mirjam, Mario Fabri, Stephan R Krutzik, Delphine J Lee, David M Vu, Peter A Sieling, Dennis Montoya, Philip T Liu, and Robert L Modlin (Feb. 2014). "Interleukin-1 Triggers the Differentiation of Macrophages with Enhanced Capacity to Present Mycobacterial Antigen to T Cells". In: *Immunology* 141.2, pp. 174–180. ISSN: 0019-2805. DOI: 10.1111/imm.12167. pmid: 24032597.

Schlundt, Claudia, Thaqif El Khassawna, et al. (Jan. 1, 2018). "Macrophages in Bone Fracture Healing: Their Essential Role in Endochondral Ossification". In: *Bone* 106, pp. 78–89. ISSN: 8756-3282. DOI: 10.1016/j.bone.2015.10.019.

Schlundt, Claudia, Hanna Schell, Alessandro Serra, Andreas Radbruch, Hans-Dieter Volk, and Georg N Duda (2013). "B Cells Regulate Bone Formation During Fracture Healing". In: p. 3.

Schmidt-Bleek, Katharina, Hanna Schell, Norma Schulz, Paula Hoff, Carsten Perka, Frank Buttgereit, Hans-Dieter Volk, Jasmin Lienau, and Georg N. Duda (July 26, 2011). "Inflammatory Phase of Bone Healing Initiates the Regenerative Healing Cascade". In: *Cell Tissue Res* 347.3, pp. 567–573. ISSN: 0302-766X, 1432-0878. DOI: 10.1007/s00441-011-1205-7.

Schneider, David F., Jessica L. Palmer, Julia M. Tulley, John T. Speicher, Elizabeth J. Kovacs, Richard L. Gamelli, and Douglas E. Faunce (June 15, 2011). "A Novel Role for NKT Cells in Cutaneous Wound Repair". In: *J Surg Res* 168.2, 325–33.e1. ISSN: 0022-4804. DOI: 10.1016/j.jss.2009.09.030. pmid: 20089261.

Scott, Michelle A., Virginia T. Nguyen, Benjamin Levi, and Aaron W. James (Oct. 2011). "Current Methods of Adipogenic Differentiation of Mesenchymal Stem Cells". In: *Stem Cells Dev* 20.10, pp. 1793–1804. ISSN: 1547-3287. DOI: 10.1089/scd.2011.0040. pmid: 21526925.

Sefati, Niloofar, Mohsen Norouzian, Hojjat-Allah Abbaszadeh, Mohammad-Amin Abdollahifar, Abdollah Amini, Mohammad Bagheri, Arefeh Aryan, and Fatemeh Fadaei Fathabady (Mar. 2018). "Effects of Bone Marrow Mesenchymal Stem Cells-Conditioned Medium on Tibial Partial Osteotomy Model of Fracture Healing in Hypothyroidism Rats". In: *Iran Biomed J* 22.2, pp. 90–98. ISSN: 1028-852X. DOI: 10.22034/ibj.22.2.90. pmid: 28755654.

Sellam, Jérémie and Francis Berenbaum (Dec. 2013). "Is Osteoarthritis a Metabolic Disease?" In: *Joint Bone Spine* 80.6, pp. 568–573. ISSN: 1297319X. DOI: 10.1016/j.jbspin.2013.09.007.

Serra, Alessandro, Ireen Könnecke, Katharina Schmidt-Bleek, Hanna Schell, Andreas Radbruch, and Georg Duda (Feb. 2012). "Lymphocytes Control Bone Fracture Healing by Programming the Mineralisation Capacity of Migratory Osteogenic Precursors". In: *Annals of the Rheumatic Diseases* 71 (Suppl 1), A63.1–A63. ISSN: 0003-4967, 1468-2060. DOI: 10.1136/annrheumdis-2011-201237.6.

Shaw, Albert C., Daniel R. Goldstein, and Ruth R. Montgomery (Dec. 2013). "Age-Dependent Dysregulation of Innate Immunity". In: *Nat Rev Immunol* 13.12, pp. 875–887. ISSN: 1474-1733. DOI: 10.1038/nri3547. pmid: 24157572.

Sheehy, Eamon J., Conor T. Buckley, and Daniel J. Kelly (Jan. 6, 2012). "Oxygen Tension Regulates the Osteogenic, Chondrogenic and Endochondral Phenotype of Bone Marrow Derived Mesenchymal Stem Cells". In: *Biochemical and Biophysical Research Communications* 417.1, pp. 305–310. ISSN: 0006-291X. DOI: 10.1016/j.bbrc.2011.11.105.

Sheng, Guojun (Nov. 2015). "The developmental basis of mesenchymal stem/stromal cells (MSCs)". In: *BMC Developmental Biology* 15. ISSN: 1471-213X. DOI: 10.1186/s12861-015-0094-5.

Shi, Z., A. E. Wakil, and D. C. Rockey (Sept. 30, 1997). "Strain-Specific Differences in Mouse Hepatic Wound Healing Are Mediated by Divergent T Helper Cytokine Responses". In: *Proc. Natl. Acad. Sci. U.S.A.* 94.20, pp. 10663–10668. ISSN: 0027-8424. pmid: 9380692.

Shimomura, Kazunori, Hiromichi Fujie, David A. Hart, Hideki Yoshikawa, and Norimasa Nakamura (2017). "Osteochondral Repair Using a Hybrid Implant Composed of Stem Cells and Biomaterial". In: *Bio-Orthopaedics*. Springer, Berlin, Heidelberg, pp. 671–682. ISBN: 978-3-662-54180-7 978-3-662-54181-4. DOI: 10.1007/978-3-662-54181-4_53.

Shintani, N. and E. B. Hunziker (Nov. 24, 2011). "Differential Effects of Dexamethasone on the Chondrogenesis of Mesenchymal Stromal Cells: Influence of Microenvironment, Tissue Origin and Growth Factor". In: *Eur Cell Mater* 22, 302–319, discussion 319–320. ISSN: 1473-2262. pmid: 22116649.

Sidibe, Adama, Patricia Ropraz, Stéphane Jemelin, Yalin Emre, Marine Poittevin, Marc Pocard, Paul F. Bradfield, and Beat A. Imhof (Jan. 24, 2018). "Angiogenic Factor-Driven Inflammation Promotes

Extravasation of Human Proangiogenic Monocytes to Tumours". In: *Nature Communications* 9.1, p. 355. ISSN: 2041-1723. DOI: 10.1038/s41467-017-02610-0.

Sidney, Laura E, Matthew J Branch, Siobhán E Dunphy, Harminder S Dua, and Andrew Hopkinson (June 2014). "Concise Review: Evidence for CD34 as a Common Marker for Diverse Progenitors". In: *Stem Cells* 32.6, pp. 1380–1389. ISSN: 1066-5099. DOI: 10.1002/stem.1661. pmid: 24497003.

Sîrbulescu, Ruxandra F. et al. (Sept. 2017). "Mature B Cells Accelerate Wound Healing after Acute and Chronic Diabetic Skin Lesions". In: *Wound Repair Regen* 25.5, pp. 774–791. ISSN: 1524-475X. DOI: 10.1111/wrr.12584. pmid: 28922523.

Smyth, Mark J. et al. (Feb. 2005). "Activation of NK Cell Cytotoxicity". In: *Mol. Immunol.* 42.4, pp. 501–510. ISSN: 0161-5890. DOI: 10.1016/j.molimm.2004.07.034. pmid: 15607806.

Sneath, R J and D C Mangham (1998). "The Normal Structure and Function of CD44 and Its Role in Neoplasia." In: *Mol Pathol* 51.4, pp. 191–200. ISSN: 1366-8714. pmid: 9893744.

Söderstjerna, Erika, Fredrik Johansson, Birgitta Klefbohm, and Ulrica Englund Johansson (2013). "Gold- and Silver Nanoparticles Affect the Growth Characteristics of Human Embryonic Neural Precursor Cells". In: *PLOS ONE* 8.3, e58211. ISSN: 1932-6203. DOI: 10.1371/journal.pone.0058211.

Söderström, Kalle, Emily Stein, Paula Colmenero, Ulrich Purath, Ulf Müller-Ladner, Cristina Teixeira de Matos, Ingo H. Tarner, William H. Robinson, and Edgar G. Engleman (July 20, 2010). "Natural Killer Cells Trigger Osteoclastogenesis and Bone Destruction in Arthritis". In: *Proc Natl Acad Sci U S A* 107.29, pp. 13028–13033. ISSN: 0027-8424. DOI: 10.1073/pnas.1000546107. pmid: 20615964.

Soliman, Hatem, Melanie Mediavilla-Varela, and Scott Antonia (2010). "Indoleamine 2,3-Dioxygenase". In: *Cancer J* 16.4. ISSN: 1528-9117. DOI: 10.1097/PPO.0b013e3181eb3343. pmid: 20693847.

Son, Min-Sun, Edmund Lau, Javad Parvizi, Michael A. Mont, Kevin J. Bozic, and Steven Kurtz (Dec. 1, 2017). "What Are the Frequency, Associated Factors, and Mortality of Amputation and Arthrodesis After a Failed Infected TKA?" In: *Clin Orthop Relat Res* 475.12, pp. 2905–2913. ISSN: 0009-921X, 1528-1132. DOI: 10.1007/s11999-017-5285-x.

Sotiropoulou, Panagiota A., Sonia A. Perez, Angelos D. Gritzapis, Constantin N. Baxevanis, and Michael Papamichail (Jan. 2006). "Interactions between Human Mesenchymal Stem Cells and Natural Killer Cells". In: *Stem Cells* 24.1, pp. 74–85. ISSN: 1066-5099. DOI: 10.1634/stemcells.2004-0359. pmid: 16099998.

Spaggiari, Grazia Maria, Andrea Capobianco, Stelvio Becchetti, Maria Cristina Mingari, and Lorenzo Moretta (Feb. 15, 2006). "Mesenchymal Stem Cell-Natural Killer Cell Interactions: Evidence That Activated NK Cells Are Capable of Killing MSCs, Whereas MSCs Can Inhibit IL-2-Induced NK-Cell Proliferation". In: *Blood* 107.4, pp. 1484–1490. ISSN: 0006-4971, 1528-0020. DOI: 10.1182/blood-2005-07-2775. pmid: 16239427.

Spencer, Joel A. et al. (Apr. 10, 2014). "Direct Measurement of Local Oxygen Concentration in the Bone Marrow of Live Animals". In: *Nature* 508.7495, pp. 269–273. ISSN: 0028-0836. DOI: 10.1038/nature13034.

Spender, John Kent (Apr. 14, 1888). "On Some Hitherto Undescribed Symptoms in the Early History of Osteoarthritis: The So-Called Rheumatoid Arthritis". In: *Br Med J* 1.1424, pp. 781–783. ISSN: 0007-1447, 1468-5833. DOI: 10.1136/bmj.1.1424.781.

Starlinger, Patrick et al. (Oct. 2011). "Discrimination between Circulating Endothelial Cells and Blood Cell Populations with Overlapping Phenotype Reveals Distinct Regulation and Predictive Potential in Cancer Therapy". In: *Neoplasia* 13.10, pp. 980–990. ISSN: 1522-8002. pmid: 22028623.

Steadman, Richard J, William G. Rodkey, Steven Singleton, and Karen Briggs (Oct. 1, 1997). "Microfracture Technique for Full-Thickness Chondral Defects: Technique and Clinical Results". In: *Operative Techniques in Orthopaedics* 7, pp. 300–304. DOI: 10.1016/S1048-6666(97)80033-X.

Steen, Kay H., Astrid E. Steen, and Peter W. Reeh (May 1995). "A Dominant Role of Acid pH in Inflammatory Excitation and Sensitization of Nociceptors in Rat Skin, in Vitro". In: *The Journal of Neuroscience.*

Stiehler, Maik, Juliane Rauh, Cody Bünger, Angela Jacobi, Corina Vater, Theresa Schildberg, Cornelia Liebers, Klaus-Peter Günther, and Henriette Bretschneider (May 2016). "In Vitro Characterization of Bone Marrow Stromal Cells from Osteoarthritic Donors". In: *Stem Cell Res* 16.3, pp. 782–789. ISSN: 1876-7753. DOI: 10.1016/j.scr.2016.03.013. pmid: 27155399.

Stöger, J. Lauran, Pieter Goossens, and Menno P. J. de Winther (Mar. 2010). "Macrophage Heterogeneity: Relevance and Functional Implications in Atherosclerosis". In: *Curr Vasc Pharmacol* 8.2, pp. 233–248. ISSN: 1875-6212. pmid: 20180776.

Styner, Maya, Buer Sen, Zhihui Xie, Natasha Case, and Janet Rubin (Nov. 1, 2010). "Indomethacin Promotes Adipogenesis of Mesenchymal Stem Cells Through a Cyclooxygenase Independent Mechanism". In: *J Cell Biochem* 111.4, pp. 1042–1050. ISSN: 0730-2312. DOI: 10.1002/jcb.22793. pmid: 20672310.

Sudan, Bayan, Mark A. Wacker, Mary E. Wilson, and Joel W. Graff (2015). "A Systematic Approach to Identify Markers of Distinctly Activated Human Macrophages". In: *Front. Immunol.* 6. ISSN: 1664-3224. DOI: 10.3389/fimmu.2015.00253.

Sung, J. H., H.-M. Yang, J. B. Park, G.-S. Choi, J.-W. Joh, C. H. Kwon, J. M. Chun, S.-K. Lee, and S.-J. Kim (Oct. 2008). "Isolation and Characterization of Mouse Mesenchymal Stem Cells". In: *Transplant. Proc.* 40.8, pp. 2649–2654. ISSN: 0041-1345. DOI: 10.1016/j.transproceed.2008.08.009. pmid: 18929828.

Suzuki, Y., K. J. Kim, S. Kotake, and T. Itoh (2001). "Stromal Cell Activity in Bone Marrow from the Tibia and Iliac Crest of Patients with Rheumatoid Arthritis". In: *J. Bone Miner. Metab.* 19.1, pp. 56–60. ISSN: 0914-8779. pmid: 11156475.

Swenson, Orvar and C. Lloyd Claff (Jan. 2, 1946). "Changes in the Hydrogen Ion Concentration of Healing Fractures". In: *Exp Biol Med (Maywood)* 61.2, pp. 151–154. ISSN: 1535-3702, 1535-3699. DOI: 10.3181/00379727-61-15256. pmid: 21017603.

Szpaderska, A. M., J. D. Zuckerman, and L. A. DiPietro (Aug. 2003). "Differential Injury Responses in Oral Mucosal and Cutaneous Wounds". In: *J. Dent. Res.* 82.8, pp. 621–626. ISSN: 0022-0345. DOI: 10.1177/154405910308200810. pmid: 12885847.

Tada, Hiroyuki, Eiji Nemoto, Brian L. Foster, Martha J. Somerman, and Hidetoshi Shimauchi (June 1, 2011). "Phosphate Increases Bone Morphogenetic Protein-2 Expression through cAMP-Dependent Protein Kinase and ERK1/2 Pathways in Human Dental Pulp Cells". In: *Bone* 48.6, pp. 1409–1416. ISSN: 8756-3282. DOI: 10.1016/j.bone.2011.03.675.

Tajbakhsh, Shahragim (June 25, 2009). "Stem Cell: What's in a Name?" In: *Nature Reports Stem Cells*. ISSN: false. DOI: 10.1038/stemcells.2009.90.

Takakura, Y., Y. Tanaka, K. Sugimoto, K. Akiyama, and S. Tamai (Apr. 1999). "Long-Term Results of Arthrodesis for Osteoarthritis of the Ankle". In: *Clin. Orthop. Relat. Res.* 361, pp. 178–185. ISSN: 0009-921X. pmid: 10212611.

Tan Ai Lyn, Grainger Andrew J., Tanner Steven F., Shelley David M., Pease Colin, Emery Paul, and McGonagle Dennis (July 28, 2005). "High-resolution Magnetic Resonance Imaging for the Assessment of Hand Osteoarthritis". In: *Arthritis & Rheumatism* 52.8, pp. 2355–2365. ISSN: 0004-3591. DOI: 10.1002/art.21210.

Taniguchi, H. (Oct. 1990). "Mast Cells in Fracture Healing: An Experimental Study Using Rat Model". In: *Nippon Seikeigeka Gakkai Zasshi* 64.10, pp. 949–957. ISSN: 0021-5325. pmid: 2266303.

Tavassoli, M. and W. H. Crosby (July 5, 1968). "Transplantation of Marrow to Extramedullary Sites". In: *Science* 161.3836, pp. 54–56. ISSN: 0036-8075. pmid: 4871792.

Tavella, S., P. Raffo, C. Tacchetti, R. Cancedda, and P. Castagnola (Dec. 1994). "N-CAM and N-Cadherin Expression during in Vitro Chondrogenesis". In: *Exp. Cell Res.* 215.2, pp. 354–362. ISSN: 0014-4827. DOI: 10.1006/excr.1994.1352. pmid: 7982473.

Tay, Kae Sian, Ngai Nung Lo, Seng Jin Yeo, Shi Lu Chia, Darren K. J. Tay, and Pak Lin Chin (Apr. 2013). "Revision Total Knee Arthroplasty: Causes and Outcomes". In: *Ann. Acad. Med. Singap.* 42.4, pp. 178–183. ISSN: 0304-4602. pmid: 23677212.

Thiagarajan, Lalitha, Hosam Al-Deen M. Abu-Awwad, and James E. Dixon (2017). "Osteogenic Programming of Human Mesenchymal Stem Cells with Highly Efficient Intracellular Delivery of RUNX2". In: *STEM CELLS Translational Medicine* 6.12, pp. 2146–2159. ISSN: 2157-6580. DOI: 10.1002/sctm.17-0137.

Thomas, Shane R., Andrew C. Terentis, Hong Cai, Osamu Takikawa, Aviva Levina, Peter A. Lay, Mohammed Freewan, and Roland Stocker (Aug. 17, 2007). "Post-Translational Regulation of Human Indoleamine 2,3-Dioxygenase Activity by Nitric Oxide". In: *J. Biol. Chem.* 282.33, pp. 23778–23787. ISSN: 0021-9258, 1083-351X. DOI: 10.1074/jbc.M700669200. pmid: 17535808.

Tian, Hong-tao, Bo Zhang, Qing Tian, Yong Liu, Shu-hua Yang, and Zeng-wu Shao (Oct. 20, 2013). "Construction of Self-Assembled Cartilage Tissue from Bone Marrow Mesenchymal Stem Cells Induced by Hypoxia Combined with GDF-5". In: *J. Huazhong Univ. Sci. Technol. [Med. Sci.]* 33.5, pp. 700–706. ISSN: 1672-0733, 1993-1352. DOI: 10.1007/s11596-013-1183-y.

Toben, Daniel et al. (Jan. 1, 2011). "Fracture Healing Is Accelerated in the Absence of the Adaptive Immune System". In: *J Bone Miner Res* 26.1, pp. 113–124. ISSN: 1523-4681. DOI: 10.1002/jbmr.185.

Tocantins, Leandro M. (Jan. 31, 1936). "Platelets and the Structure and Physical Properties of Blood Clots". In: *American Journal of Physiology-Legacy Content* 114.3, pp. 709–715. ISSN: 0002-9513. DOI: 10.1152/ajplegacy.1936.114.3.709.

Tomer, Aaron (Nov. 1, 2004). "Human Marrow Megakaryocyte Differentiation: Multiparameter Correlative Analysis Identifies von Willebrand Factor as a Sensitive and Distinctive Marker for Early (2N and 4N) Megakaryocytes". In: *Blood* 104.9, pp. 2722–2727. ISSN: 0006-4971, 1528-0020. DOI: 10.1182/blood-2004-02-0769. pmid: 15198950.

Tosello-Trampont, Annie, Fionna A. Surette, Sarah E. Ewald, and Young S. Hahn (Mar. 20, 2017). "Immunoregulatory Role of NK Cells in Tissue Inflammation and Regeneration". In: *Front Immunol* 8. ISSN: 1664-3224. DOI: 10.3389/fimmu.2017.00301. pmid: 28373874.

Toupadakis, Chrisoula A., Jennifer L. Granick, Myrrh Sagy, Alice Wong, Ehssan Ghassemi, Dai-Jung Chung, Dori L. Borjesson, and Clare E. Yellowley (Sept. 2013). "Mobilization of Endogenous Stem Cell Populations Enhances Fracture Healing in a Murine Femoral Fracture Model". In: *Cytotherapy* 15.9, pp. 1136–1147. ISSN: 1477-2566. DOI: 10.1016/j.jcyt.2013.05.004. pmid: 23831362.

Trebše, Rihard and Anže Mihelič (2012). "Chapter 2 Joint Replacement: Historical Overview". In: *Infected Total Joint Arthroplasty*. 1st Edition. Springer-Verlag. ISBN: ISBN 978-1-4471-2482-5.

Trudnowski, Raymond J. and Rodolfo C. Rico (May 1, 1974). "Specific Gravity of Blood and Plasma at 4 and 37 °C". In: *Clinical Chemistry* 20.5, pp. 615–616. ISSN: 0009-9147, 1530-8561. pmid: 4826961.

Tseng, Han-Ching et al. (July 16, 2010). "Increased Lysis of Stem Cells but Not Their Differentiated Cells by Natural Killer Cells; De-Differentiation or Reprogramming Activates NK Cells". In: *PLoS One* 5.7. ISSN: 1932-6203. DOI: 10.1371/journal.pone.0011590. pmid: 20661281.

Ulstein, Svend, Asbjørn Årøen, Jan Harald Røtterud, Sverre Løken, Lars Engebretsen, and Stig Heir (2014). "Microfracture Technique versus Osteochondral Autologous Transplantation Mosaicplasty in Patients with Articular Chondral Lesions of the Knee: A Prospective Randomized Trial with Long-Term Follow-Up". In: *Knee Surg Sports Traumatol Arthrosc* 22.6, pp. 1207–1215. ISSN: 0942-2056. DOI: 10.1007/s00167-014-2843-6. pmid: 24441734.

Uniprot (2019). *ALCAM - CD166 Antigen Precursor - Homo Sapiens (Human) - ALCAM Gene & Protein*. URL: https://www.uniprot.org/uniprot/Q13740 (visited on 04/22/2019).

Urist, M. R., R. Mazet, and F. C. Mclean (2017). "The Pathogenesis and Treatment of Delayed Union and Non-Union; a Survey of Eighty-Five Ununited Fractures of the Shaft of the Tibia and One Hundred Control Cases with Similar Injuries." In: *J Bone Joint Surg Am* 36-A.5 (). ISSN: 0021-9355. pmid: 13211690.

Van Acker, Heleen H., Anna Capsomidis, Evelien L. Smits, and Viggo F. Van Tendeloo (July 24, 2017). "CD56 in the Immune System: More Than a Marker for Cytotoxicity?" In: *Front Immunol* 8. ISSN: 1664-3224. DOI: 10.3389/fimmu.2017.00892. pmid: 28791027.

Vasandan, Anoop Babu, Sowmya Jahnavi, Chandanala Shashank, Priya Prasad, Anujith Kumar, and S. Jyothi Prasanna (Dec. 2, 2016). "Human Mesenchymal Stem Cells Program Macrophage Plasticity by Altering Their Metabolic Status *via* a PGE_2-Dependent Mechanism". In: *Scientific Reports* 6, p. 38308. ISSN: 2045-2322. DOI: 10.1038/srep38308.

Versus Arthritis (2017). URL: https://www.versusarthritis.org/.

Vertelov, Grigory, Ludmila Kharazi, M G Muralidhar, Givon Sanati, Timothy Tankovich, and Alex Kharazi (Jan. 7, 2013). "High Targeted Migration of Human Mesenchymal Stem Cells Grown in Hypoxia Is Associated with Enhanced Activation of RhoA". In: *Stem Cell Res Ther* 4.1, p. 5. ISSN: 1757-6512. DOI: 10.1186/scrt153. pmid: 23295150.

Vivier, Eric, Elena Tomasello, Myriam Baratin, Thierry Walzer, and Sophie Ugolini (May 2008). "Functions of Natural Killer Cells". In: *Nat. Immunol.* 9.5, pp. 503–510. ISSN: 1529-2916. DOI: 10.1038/ni1582. pmid: 18425107.

Vos, Barber, and Bell (Aug. 2015). "Global, Regional, and National Incidence, Prevalence, and Years Lived with Disability for 301 Acute and Chronic Diseases and Injuries in 188 Countries, 1990–2013: A Systematic Analysis for the Global Burden of Disease Study 2013". In: *The Lancet* 386.9995, pp. 743–800. ISSN: 01406736. DOI: 10.1016/S0140-6736(15)60692-4.

Wagegg, Markus et al. (Feb. 2, 2012). "Hypoxia Promotes Osteogenesis but Suppresses Adipogenesis of Human Mesenchymal Stromal Cells in a Hypoxia-Inducible Factor-1 Dependent Manner". In: *PLOS ONE* 7.9, e46483. ISSN: 1932-6203. DOI: 10.1371/journal.pone.0046483.

Wakkach, Abdelilah, Anna Mansour, Romain Dacquin, Emmanuel Coste, Pierre Jurdic, Georges F. Carle, and Claudine Blin-Wakkach (Dec. 15, 2008). "Bone Marrow Microenvironment Controls the in Vivo Differentiation of Murine Dendritic Cells into Osteoclasts". In: *Blood* 112.13, pp. 5074–5083. ISSN: 1528-0020. DOI: 10.1182/blood-2008-01-132787. pmid: 18768394.

Walenda, Thomas, Simone Bork, Patrick Horn, Frederik Wein, Rainer Saffrich, Anke Diehlmann, Volker Eckstein, Anthony D. Ho, and Wolfgang Wagner (Jan. 1, 2010). "Co-Culture with Mesenchymal Stromal Cells Increases Proliferation and Maintenance of Haematopoietic Progenitor Cells". In: *Journal of Cellular and Molecular Medicine* 14.1-2, pp. 337–350. ISSN: 1582-4934. DOI: 10.1111/j.1582-4934.2009.00776.x.

Wang, Kemeng, Guoqing Wei, and Delong Liu (Nov. 29, 2012). "CD19: A Biomarker for B Cell Development, Lymphoma Diagnosis and Therapy". In: *Exp Hematol Oncol* 1, p. 36. ISSN: 2162-3619. DOI: 10.1186/2162-3619-1-36. pmid: 23210908.

Wang, Weiguang, Diana Rigueur, and Karen M. Lyons (Mar. 2014). "TGF Signaling in Cartilage Development and Maintenance". In: *Birth Defects Res C Embryo Today* 102.1, pp. 37–51. ISSN: 1542-975X. DOI: 10.1002/bdrc.21058. pmid: 24677722.

Wang, Xiaoqin, Omar Omar, Forugh Vazirisani, Peter Thomsen, and Karin Ekström (2018). "Mesenchymal Stem Cell-Derived Exosomes Have Altered microRNA Profiles and Induce Osteogenic Differentiation Depending on the Stage of Differentiation". In: *PLOS ONE* 13.2, e0193059. ISSN: 1932-6203. DOI: 10.1371/journal.pone.0193059.

Wang, XingYun et al. (Mar. 28, 2018). "Evaluation and Optimization of Differentiation Conditions for Human Primary Brown Adipocytes". In: *Sci Rep* 8. ISSN: 2045-2322. DOI: 10.1038/s41598-018-23700-z. pmid: 29593245.

Wang, Ying, Xiaodong Chen, Wei Cao, and Yufang Shi (Nov. 2014). "Plasticity of Mesenchymal Stem Cells in Immunomodulation: Pathological and Therapeutic Implications". In: *Nat Immunol* 15.11, pp. 1009–1016. ISSN: 1529-2908. DOI: 10.1038/ni.3002.

Wang, Yongji and Nader Sheibani (2002). "Expression Pattern of Alternatively Spliced PECAM-1 Isoforms in Hematopoietic Cells and Platelets". In: *Journal of Cellular Biochemistry* 87.4, pp. 424–438. ISSN: 1097-4644. DOI: 10.1002/jcb.10321.

Wang, Zhaoqing and Xiyun Yan (Apr. 28, 2013). "CD146, a Multi-Functional Molecule beyond Adhesion". In: *Cancer Lett.* 330.2, pp. 150–162. ISSN: 1872-7980. DOI: 10.1016/j.canlet.2012.11.049. pmid: 23266426.

Wei, Xin, Xue Yang, Zhi-peng Han, Fang-fang Qu, Li Shao, and Yu-fang Shi (June 2013). "Mesenchymal Stem Cells: A New Trend for Cell Therapy". In: *Acta Pharmacologica Sinica* 34.6, pp. 747–754. ISSN: 1745-7254. DOI: 10.1038/aps.2013.50.

Wenger, Roland H, Vartan Kurtcuoglu, Carsten C Scholz, Hugo H Marti, and David Hoogewijs (Sept. 18, 2015). "Frequently Asked Questions in Hypoxia Research". In: *Hypoxia (Auckl)* 3, pp. 35–43. ISSN: 2324-1128. DOI: 10.2147/HP.S92198. pmid: 27774480.

Widuchowski, W., J. Widuchowski, R. Faltus, P. Lukasik, G. Kwiatkowski, K. Szyluk, and B. Koczy (Feb. 2011). "Long-Term Clinical and Radiological Assessment of Untreated Severe Cartilage Damage in the Knee: A Natural History Study". In: *Scand J Med Sci Sports* 21.1, pp. 106–110. ISSN: 1600-0838. DOI: 10.1111/j.1600-0838.2009.01062.x. pmid: 20136756.

Wiencke, John. K., Rondi Butler, George Hsuang, Melissa Eliot, Stephanie Kim, Manuel A. Sepulveda, Derick Siegel, E. Andres Houseman, and Karl T. Kelsey (Mar. 11, 2016). "The DNA Methylation Profile of Activated Human Natural Killer Cells". In: *Epigenetics* 11.5, pp. 363–380. ISSN: 1559-2294. DOI: 10.1080/15592294.2016.1163454. pmid: 26967308.

Worthley, Daniel L. et al. (Jan. 15, 2015). "Gremlin 1 Identifies a Skeletal Stem Cell with Bone, Cartilage, and Reticular Stromal Potential". In: *Cell* 160.1-2, pp. 269–284. ISSN: 1097-4172. DOI: 10.1016/j.cell.2014.11.042. pmid: 25594183.

Wu, Andy C., Liza J. Raggatt, Kylie A. Alexander, and Allison R. Pettit (June 26, 2013). "Unraveling Macrophage Contributions to Bone Repair". In: *BoneKEy Reports* 2. ISSN: xxxx-xxxx. DOI: 10.1038/bonekey.2013.107.

Xiao, Guozhi, Rajaram Gopalakrishnan, Di Jiang, Elizabeth Reith, M. Douglas Benson, and Renny T. Franceschi (2009). "Bone Morphogenetic Proteins, Extracellular Matrix, and Mitogen-Activated Protein Kinase Signaling Pathways Are Required for Osteoblast-Specific Gene Expression and Differentiation in MC3T3-E1 Cells". In: *Journal of Bone and Mineral Research* 17.1, pp. 101–110. ISSN: 1523-4681. DOI: 10.1359/jbmr.2002.17.1.101.

Xie, Daniel, Donghong Ju, Cecilia Speyer, David Gorski, and Mary A. Kosir (Aug. 14, 2016). "Strategic Endothelial Cell Tube Formation Assay: Comparing Extracellular Matrix and Growth Factor Reduced Extracellular Matrix". In: *J Vis Exp* 114. ISSN: 1940-087X. DOI: 10.3791/54074. pmid: 27585062.

Xie, Linglin, Ke Zhang, Dane Rasmussen, Junpeng Wang, Dayong Wu, James N. Roemmich, Amy Bundy, W. Thomas Johnson, and Kate Claycombe (Jan. 31, 2017). *Identification Markers Used in Our Study to Classify Macrophage Phenotypes*. DOI: 10.1371/journal.pone.0169581.t004.

Xu, Chong, Jinhan He, Hongfeng Jiang, Luxia Zu, Wenjie Zhai, Shenshen Pu, and Guoheng Xu (Aug. 2009). "Direct Effect of Glucocorticoids on Lipolysis in Adipocytes". In: *Mol Endocrinol* 23.8, pp. 1161–1170. ISSN: 0888-8809. DOI: 10.1210/me.2008-0464. pmid: 19443609.

Yang, Der-Chih, Muh-Hwa Yang, Chih-Chien Tsai, Tung-Fu Huang, Yau-Hung Chen, and Shih-Chieh Hung (2011). "Hypoxia Inhibits Osteogenesis in Human Mesenchymal Stem Cells through Direct Regulation of RUNX2 by TWIST". In: *PLOS ONE* 6.9, e23965. ISSN: 1932-6203. DOI: 10.1371/journal.pone.0023965.

Yeap, Wei Hseun et al. (Sept. 27, 2016). "CD16 Is Indispensable for Antibody-Dependent Cellular Cytotoxicity by Human Monocytes". In: *Scientific Reports* 6, p. 34310. ISSN: 2045-2322. DOI: 10.1038/srep34310.

Yu, Yan Yiu, Theodore Miclau, and Ralph Marcucio (2012). "Functional Roles of Macrophages during Fracture Repair". In: ORS 2012 Annual Meeting, p. 1.

Yu, Yang et al. (Oct. 26, 2016). "Mesenchymal Stem Cells with Sirt1 Overexpression Suppress Breast Tumor Growth via Chemokine-Dependent Natural Killer Cells Recruitment". In: *Scientific Reports* 6, p. 35998. ISSN: 2045-2322. DOI: 10.1038/srep35998.

Zanoni, Ivan, Renato Ostuni, Lorri R. Marek, Simona Barresi, Roman Barbalat, Gregory M. Barton, Fancesca Granucci, and Jonathan C. Kagan (Nov. 11, 2011). "CD14 Controls the LPS-Induced Endocytosis of Toll-like Receptor 4". In: *Cell* 147.4, pp. 868–880. ISSN: 0092-8674. DOI: 10.1016/j.cell.2011.09.051. pmid: 22078883.

Zengini, Eleni et al. (Apr. 2018). "Genome-Wide Analyses Using UK Biobank Data Provide Insights into the Genetic Architecture of Osteoarthritis". In: *Nat. Genet.* 50.4, pp. 549–558. ISSN: 1546-1718. DOI: 10.1038/s41588-018-0079-y. pmid: 29559693.

Zevenbergen, L., W. Gsell, D. D. Chan, J. Vander Sloten, U. Himmelreich, C. P. Neu, and I. Jonkers (2018). "Functional assessment of strains around a full-thickness and critical sized articular cartilage defect under compressive loading using MRI". In: *Osteoarthritis and Cartilage* 26.12, pp. 1710–1721. ISSN: 1522-9653. DOI: 10.1016/j.joca.2018.08.013.

Zhai, G., D. J. Hart, B. S. Kato, A. MacGregor, and T. D. Spector (Feb. 2007). "Genetic Influence on the Progression of Radiographic Knee Osteoarthritis: A Longitudinal Twin Study". In: *Osteoarthr. Cartil.* 15.2, pp. 222–225. ISSN: 1063-4584. DOI: 10.1016/j.joca.2006.09.004. pmid: 17045816.

Zhang, Bin (Aug. 15, 2010). "CD73: A Novel Target for Cancer Immunotherapy". In: *Cancer Res* 70.16, pp. 6407–6411. ISSN: 0008-5472. DOI: 10.1158/0008-5472.CAN-10-1544. pmid: 20682793.

Zhang, Jingru, Daoxin Ma, Jingjing Ye, Shaolei Zang, Fei Lu, Meixiang Yang, Xun Qu, Xiulian Sun, and Chunyan Ji (Oct. 1, 2012). "Prognostic Impact of -like Ligand 4 and Notch1 in Acute Myeloid Leukemia". In: *Oncology Reports* 28.4, pp. 1503–1511. ISSN: 1021-335X. DOI: 10.3892/or.2012.1943.

Zhang, Lijie, Jerry Hu, and Kyriacos A. Athanasiou (2009). "The role of tissue engineering in articular cartilage repair and regeneration". eng. In: *Critical Reviews in Biomedical Engineering* 37.1-2, pp. 1–57. ISSN: 0278-940X.

Zhang, Nu and Michael J. Bevan (Aug. 26, 2011). "CD8+ T Cells: Foot Soldiers of the Immune System". In: *Immunity* 35.2, pp. 161–168. ISSN: 1074-7613. DOI: 10.1016/j.immuni.2011.07.010. pmid: 21867926.

Zhao, Qi, Xijie Wang, Shuyan Wang, Zheng Song, Jiaxian Wang, and Jing Ma (Mar. 9, 2017). "Cardiotoxicity Evaluation Using Human Embryonic Stem Cells and Induced Pluripotent Stem Cell-Derived Cardiomyocytes". In: *Stem Cell Research & Therapy* 8, p. 54. ISSN: 1757-6512. DOI: 10.1186/s13287-017-0473-x.

Appendix A

Supplementary Tables

A.1 Markers Used For Flow Cytometry

Table A.1 Markers used for flow cytometry

Marker used	**Other names**	**Function**	**Reference**
CD3	T3 complex	T cell activation	Kuhns et al. 2006
CD4	T3, L3T4, Ly1, Leu3	Differentiation and activation of T helper cells	Luckheeram et al. 2012
CD8	T8, Leu2, Ly2/Ly3	Differentiation, activation and mediation of direct cytotoxicity by cytotoxic T-cells	N. Zhang and Bevan 2011
CD11b	Integrin alpha M (ITGAM), macrophage antigen-1 (MAC-1), Complement receptor 3 (CR3)	Cellular adhesion and migrationof leukocytes	Biologicals 2011
CD14	Myeloid cell-specific leucine-rich glycoprotein.	Endotoxin co-receptor binding lipopolysaccharides	Zanoni et al. 2011

Marker used	Other names	Function	Reference
CD16	Type III Fc-gamma receptor (FcγRIII)	Low affinity antibody Fc receptor. Activation and control of antibody-dependent cell-mediated cytoxicity (ADCC) and antibody-dependent cell-mediated phagocytosis (ADCP). Required for NK cell ADCC.	Yeap et al. 2016
CD19	B-lymphocyte antigen	Control and mediation of B-cell signalling and activity	K. Wang et al. 2012
CD29	Integrin beta-1 (ITGB1)	Diverse roles in cell adhesion and signalling	Biologicals 2015
CD34	Haematopoietic progenitor cell antigen	Unknown role, possibly related to adhesion. Associated with progenitor cells, particularly HSPCs	Sidney et al. 2014
CD44	Multiple including: Chondroitin, Sulphate Proteoglycan, Homing cell adhesion molecule (HCAM), Hermes antigen, Hyaluronate Receptor	Diverse functions related to cellular adhesion including angiogenesis, cytokine release, and cellular homing to lymph nodes	Sneath and Mangham 1998
CD45	Leukocyte common antigen, Protein tyrosine phosphatase, receptor type C	Diverse roles in lymphocyte function and development	Dawes et al. 2006
CD49alpha	Very late antigen-1 (VLA-1), alpha-1 beta-1 integrin	Extracellular matrix receptor with roles in ahdesion and activation of T cells	Bank et al. 1994
CD56	Neural cell adhesion molecule (NCAM)	Activation of signalling pathways leading to immunostimulation. Natural Killer cell marker.	Van Acker et al. 2017
CD64	Type I Fc-gamma receptor (FcγRI)	High affinity antibody Fc receptor. Activation and control of ADCC and ADCP	Herter et al. 2014
CD68	Macrosialin	Putative scavenger receptor, possible involvement with antigen presentation	Chistiakov et al. 2017

Marker used	Other names	Function	Reference
CD73	Lymphocyte differentiation antigen, Ecto-5'-nucleotidase (ecto-5'-NT, EC 3.1.3.5)	Diverse roles including ion and fluid transport, cell-cell, and cell-matrix interactions	B. Zhang 2010
CD80	B7-1	Co-signalling molecule with roles in antigen presentation and T cell activation	Schenk et al. 2014
CD90	Thymocyte differentiation antigen-1 (Thy-1)	Diverse roles including cell-cell and cell-matrix interactions, and release of factors in response to tissue damage	Kisselbach et al. 2009
CD105	Endoglin	Support of early haematopoiesis and angiogenesis	Cho et al. 2001
CD133	Prominin-1	Unknown role, possible involvement with proliferation. Strongly associated with stem and tumour cells	Z. Li 2013
CD146	Melanoma cell adhesion molecule (MCAM)	Diverse functions, most commonly associated with adhesion, but also including angiogenesis, migration and differentiation of MSCs	Z. Wang and Yan 2013
CD163	Scavenger receptor cysteine-rich type 1 protein M130, Hemoglobin scavenger receptor	Scavenger receptor involved with tolerance, haemoglobin clearance, and adhesion	Onofre et al. 2009
CD166	Activated leukocyte cell adhesion molecule (ALCAM)	Diverse roles related to adhesion	Uniprot 2019
CD200R	Cell surface glycoprotein CD200 receptor 1	Negative regulation of myeloid cell activity through binding to CD200	Hatherley et al. 2013
CD209	Dendritic cell-specific intercellular adhesion molecul-3-Grabbing non-integrin (DC-SIGN)	Pattern recognition receptor with roles in tercellular adhesion and antigen processing	Garcia-Vallejo and Kooyk 2013

Marker used	Other names	Function	Reference
CD271	Nerve growth factor receptor, p75 neurotrophin receptor	Immunomodulation, particularly of T cells	Lebert-Ghali et al. 2017
CD309	Vascular endothelial growth factor receptor-2 (VEGFR2)	Binds and mediates downstream responses to VEGF, including angiogenesis	Kliche and Waltenberger 2001
CD317	Tetherin, Bone marrow stromal antigen 2	Diverse roles in cell membrane, including lipid raft organisation and inhibition of viral release	Billcliff et al. 2013
HLA-DR	MHC Class II receptor	Antigen presentation and immune cell activation	NCBI 2019
Tie2	Angiopoietin receptor	Regulation of angiogenesis, and vascular remodelling and stability	Jeltsch et al. 2013

A.2 Equipment Used

Table A.2 Table of equipment used

Equipment	Details
Category 2 certified biological safety cabinet	Thermo Scientific MSC Advantage
Water bath	Grant OLS 200
Tissue culture Centrifuge	Thermo Scientific Sorvall ST16R
Normoxic incubator	Sanyo CO2 incubator
Hypoxic incubator	Thermo Scientific Heracell Vios 160i
Pipettes	Various Eppendorf
Pipetboy	Integra Biosciences pipetboy
Multi-dispense pipette	Eppendorf Multipette E3X
Light microscope	Leica DMIRB
Camera	Q Imaging micropublisher 3.3RTV
Fluorescent microscope	Nikon Eclipse TDI
Camera	Hamamatsu ORCA-05G
Stage and control	Nikon TI-S-EJOY and Nikon TI-SH-U
Automated shutter	Nikon NI-SH-CON
Temperature control	OKO Lab Control Unit

Equipment	Details
Light	Nikon Intensilight C-HGFI
Xcelligence	ACEA Biosciences Xcelligence RTCA DP
Vortex mixer	Various
Quadromacs	Miltenyi Quadromacs
RNA centrifuge	Eppendorf Centrifuge 5471R
DNA centrifuge	Eppendorf MiniSpin Plus
Ice machine	Scotsman AF-80
qPCR reader	Applied Biosystems StepOnePlus Real-time PCR analyser
Heat blocks	VWR digital heatblock / Techne
Fume cabinet	Mach-Aire
Fluorescent platereader	BMG Labtech Fluostar Optima
Densitometer	Thermo Scientific GS-800 Calibrated Densitometer
RNA quantification	Thermo Scientific Nanodrop 2000
Fridge 2 to 8 °C	Various
Freezer −20 °C	Various
−70 °C Freezer	New Brunswick U725-G Innova Freezer
Liquid nitrogen storage system	Arpege 110
Distilled water dispenser	Millipore ELIX / Synergy UV
Digital Scale	Sartorius CPA224S
Rocking stage	VWR Stage Rocker
Magnetic stirring platform	Stuart Heat Stir CB162
Flow cytometer	Becton Dickenson LSR Fortessa Analyser and Sampler
X-ray developing cassette	Hypercassette Amersham Pharmacia Biotech
Automatic X-ray film processing machine	MSL MSLXF01

A.3 Reagents Used

Table A.3 Table of reagents used

Reagent	Catalogue number	Company
Alcian Blue 8GX	A5268	Sigma Aldrich Company Ltd
Alizarin red, 2 % solution	42746	Alfa Aesar
Amphotericin B	A9528	Sigma Aldrich Company Ltd

Reagent	Catalogue number	Company
autoMACS rinsing solution	130-091-222	Miltenyi Biotec Ltd.
B Cell Isolation Kit II, human	130-091-151	Miltenyi Biotec Ltd.
Beta-mercaptoethanol	M6250	Sigma Aldrich Company Ltd
BGP, TC grade	G9422-50G	Sigma Aldrich Company Ltd
Bovine Serum Albumin	130-091-376	Miltenyi Biotec Ltd.
Calcein-AM	425201	Biolegend
CD146 microbeads, human	130-093-593	Miltenyi Biotec Ltd.
CD31 microbead kit, human	130-091-935	Miltenyi Biotec Ltd.
CD34 microbeads, human	130-046-702	Miltenyi Biotec Ltd.
CD45 microbeads, human	130-045-801	Miltenyi Biotec Ltd.
CellTox Green	G8742	Promega
Crystal Violet	PL.8000	Pro-Lab Diagnostics
Cultrex PathClear Reduced Growth Factor BME	3433-005-01	R&D systems
Custom primers (as listed)	Custom order	Integrated DNA Technologies
DAPI	D9542	Sigma Aldrich Company Ltd
Dexamethasone	D4902	Sigma Aldrich Company Ltd
Dimethyl sulphoxide	D8418	Sigma Aldrich Company Ltd
Direct-zol RNA MiniPrep Plus kit	R2061	Zymo Research
Distel	TM305	Star Lab Group
Distilled Water DNase/RNase free	10977049	ThermoFisher Scientific
DMEM with Glutamax	21885108	Gibco Laboratories
DMEM with high glucose and GlutaMAX	10566016	Gibco Laboratories
EDTA	15575-020	Life Technologies
Endothelial Cell Growth Supplement	E2759-15MG	Sigma Aldrich Company Ltd
Ethanol Absolute	32221-2.5L	Sigma Aldrich Company Ltd
Ethanol, BioUltra, for molecular biology, $\geq$99.8 %	51976	Sigma Aldrich Company Ltd
FcR block	130-059-901	Miltenyi Biotec Ltd.
Fetal Bovine Serum	02-00-850	First Link (UK) Ltd.
Fibroblast Growth Factor 2	100-18C	Peprotech
Formalin solution 10 % neutral buffered	HT501320	Sigma Aldrich Company Ltd

Reagent	Catalogue number	Company
Gelatin 2 % solution for tissue culture	G1393-20ML	Sigma Aldrich Company Ltd
Gentamicin solution	G1272	Sigma Aldrich Company Ltd
Heparin for tissue culture	H3149-25KU	Sigma Aldrich Company Ltd
Hs_B2M_1_SG QuantiTect Primer Asssay	QT00088935	Qiagen
Hs_FGF2_1_SG QuantiTect Primer Assay	QT00047579	Qiagen
Human Chemokine Antibody Array kit	ARY017	R&D Systems
HUVEC-Umbil Vein, pooled cells, EGM-2, cryo amp	C2519A	Lonza
Hydrocholoric acid	H1758-500mL	Sigma Aldrich Company Ltd
Isopropyl alcohol	W292907	Sigma Aldrich Company Ltd
ITS+ Premix Universal Culture Supplement	354352	Corning
L-Ascorbic Acid Phosphate Sesquimagnes	A8960	Sigma Aldrich Company Ltd
Leukocyte Cone	NC24	National Blood & Transplant
L-GlutaMAX	35050038	Life Technologies
Lymphoprep	11114544	Axis Shield POC AS
Medium 199 with HEPES	M7528-500ml	Sigma Aldrich Company Ltd
NK Cell Isolation Kit, human	130-092-657	Miltenyi Biotec Ltd.
OneComp eBeads	01-1111-42	eBioscience
Pan Monocyte Isolation Kit, human	130-096-537	Miltenyi Biotec Ltd.
PBS	10010056	Gibco Laboratories
Proline	P5607	Sigma Aldrich Company Ltd
Proteome profiler human chemokine array kit	ARY017	R&D systems
QuantiTect Reverse Transcription Kit	205311	Qiagen
Recombinant human GM-CSF	300-03	Peprotech
Recombinant human IL-10	200-10b	Peprotech
Recombinant Human IL4	200-04	Peprotech
Recombinant human M-CSF	300-25	Peprotech
Recombinant human SDF1	300-28B	Peprotech

Reagent	Catalogue number	Company
Recombinant Human TGFβ1	100-21-50	Peprotech
Recombinant Human TNF-α	300-01a	Peprotech
Recombinant human VEGF	100-20B	Peprotech
RPMI-1640	31870-025	Life Technologies
Sodium Pyruvate, 1 mmol	S8636	Sigma Aldrich Company Ltd
B-glycerol phosphate	G9422	Sigma Aldrich Company Ltd
Stempro Adipogenesis Differentiation Kit	A10070-01	Life Technologies
Sterile mineral oil	M5310-100ml	Sigma Aldrich Company Ltd
Triton x100	T8787-50ML	Sigma Aldrich Company Ltd
TRIzol reagent	15596026	ThermoFisher Scientific
TryplE Express (No Phenol Red)	12604021	Invitrogen
Trypsin EDTA	T3924	Sigma Aldrich Company Ltd
αMEM without nucleosides	22561054	Gibco Laboratories